Synthesis and Studies of Novel Polybenzimidazoles with Improved Properties for Proton Exchange Membrane

Newly Synthesized Py-PBI

Conventional PBI

FA solution of Py-PBI   Membrane of Py-PBI   FA solution of PBI   Membrane of PBI

Membrane casting at 60 °C

A Thesis Submitted for the Degree of

DOCTOR OF PHILOSOPHY

BY

Sudhangshu Maity

School of Chemistry

University of Hyderabad

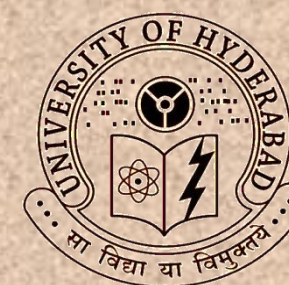**Hyderabad-500 046**

INDIA

December 2013

Synthesis and Studies of Novel Polybenzimidazoles with Improved Properties for Proton Exchange Membrane

A Thesis Submitted for the Degree of

DOCTOR OF PHILOSOPHY

BY

Sudhangshu Maity

School of Chemistry
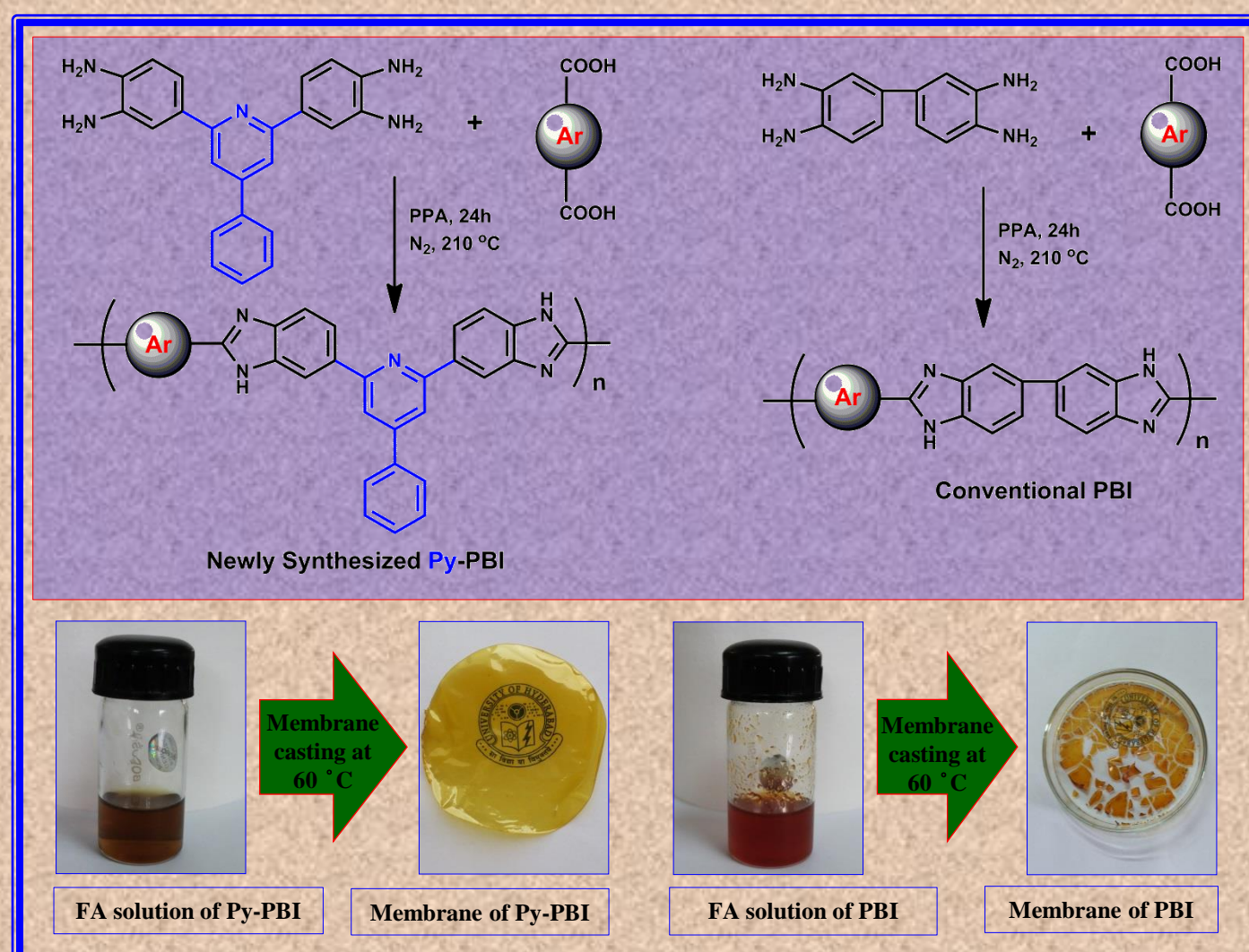## University of Hyderabad
Hyderabad-500 046
INDIA

December 2013

Dedicated
To
মা ও বাবা

DECLARATION

I hereby declare that the matter embodied in the thesis entitled *"Synthesis and Studies of Novel Polybenzimidazoles with Improved Properties for Proton Exchange Membrane"* is the result of investigations carried out by me in the School of Chemistry, University of Hyderabad, Hyderabad, India under the supervision of **Professor Tushar Jana** and it has not been submitted elsewhere for the award of any degree or diploma or membership, etc.

In keeping with the general practice of reporting scientific investigations, due acknowledgements have been made wherever the work described is based on the findings of other investigators. Any omission or error that might have crept in is regretted.

December, 2013   **Sudhangshu Maity**

UNIVERSITY OF HYDERABAD
Central University (P.O.), Hyderabad-500046, INDIA

Professor Tushar Jana
School of Chemistry
University of Hyderabad

Web: *http://chemistry.uohyd.ernet.in/~tj/*

Tel: 91-40-23134808 (Office)
        91-40-65555187 (Home)
        91-9440127016 (Mobile)
Fax: 91-40-23012460
 E-mail: *tusharjana@uohyd.ac.in*
           tjscuoh@gmail.com

CERTIFICATE

This is to certify that the work described in this thesis entitled ***"Synthesis and Studies of Novel Polybenzimidazoles with Improved Properties for Proton Exchange Membrane"*** has been carried out by Mr. Sudhangshu Maity under my supervision and the same has not been submitted elsewhere for any degree.

Dean
School of Chemistry
University of Hyderabad
Hyderabad-500 046
India

Professor Tushar Jana
(Thesis supervisor)

PREFACE

The present thesis entitled ***"Synthesis and Studies of Novel Polybenzimidazoles with Improved Properties for Proton Exchange Membrane"*** has been divided into seven chapters. ***Chapter 1*** explains a brief introduction of aromatic heterocyclic polybenzimidazoles polymers, common synthesis procedure for different types structures, their various properties and applications. Also the most advanced application of phosphoric acid doped polybenzimidazole membrane as a polymer electrolyte membrane in high temperature PEM fuel cell is discussed. ***Chapter 2*** deals with the details of materials source, synthesis and brief experimental procedure for characterization of all synthesized polymers. Several experimental methods used for investigations of the varieties of properties of polybenzimidazoles are also discussed. ***Chapter 3*** explores the N-alkyl chain length effect on solubility and flexibility of N-substituted polybenzimidazoles (N-PBIs) which in turn allow the ready processability of N-PBIs. ***Chapter 4*** describes the synthesis of highly soluble and readily processable pyridine based polybenzimidazoles (Py-PBIs) from an alternative, inexpensive and readily accessible novel tetramine monomer called 2,6-bis(3',4'-diaminophenyl)-4-phenylpyridine (Py-TAB). The newly synthesized Py-PBIs show improved properties as PEM compared to conventional PBI. ***Chapter 5*** deals with copolymer structural effect on the properties of polybenzimidazole copolymers synthesized from an unconventional monomer Py-TAB and the conventional 3,3',4,4'-tetraminobiphenyl (TAB) which in turn affects to proton conductivity and the other properties of PEM. ***Chapter 6*** describes synthesis of *meta* and *para* diblock PBI (*m*-PBI-*b*-*p*-PBI) copolymers and studies of the effect of block length on the properties of PEM which obtained from these block copolymers. ***Chapter 7*** summarizes the findings of the present investigations, presents a concluding remark and the future scopes and upcoming challenges.

December, 2013   **Sudhangshu Maity**
School of Chemistry
University of Hyderabad
Hyderabad 500 046
India

ACKNOWLEDGEMENT

December, 2013   **Sudhangshu Maity**
University of Hyderabad
  Hyderabad-500 046
         India

COMMON ABBREVIATIONS

AB-PBI--------Poly(2,5-benzimidazole)
AFML------------Air Force Material Laboratory
BDA-------------------Biphenyl 4,4'-dicarboxylic acid
BPDA--------------------4,4'-Dicarboxy benzophenone
DMA-------------------------N,N-Dimethyl acetamide
DMSO------------------------Dimethyl sulfoxide
DMF--------------------------------N,N-Dimethyl formamide
DMA------------------------------------Dynamic mechanical analyzer
DCA---------------------------------------Dicarboxylic acid
DSC---Differential scanning calorimeter
DPIP---Diphenyl isophthalate
DMIP---Dimethyl isophthalate
DFX--α,α'-Difurfuryloxy-p-xylene
FA--Formic acid
FTIR---Fourier transform infrared spectroscopy
GP---Graphene
GPC--Gel permeable chromatography
HFIPA--4,4'-(Hexafluoroisopropylidene)bis(benzoic acid)
IPA--Isophthalic acid
IV--Inherent viscosity
MW--Molecular weight
MEA--Membrane electrode assembly
MWNT---Multiwalled carbon nanotube
MSA--Methane sulfonic acid
MEA---Membrane electrode assembly
N-PBI---N-substituted polybenzimidazole
NMR--Nuclear magnetic resonance
NMP-- N-Methyl-2-pyrrolidone
NASA---National Aeronautics and Space Administration
OBA--4,4'-Oxybis(benzoic acid)
OPBI---Poly(4,4'-diphenylether-5,5'-bibenzimidazole)
PA--Phosphoric acid
PI---Polyimides
PPA--Polyphosphoric acid
PBI--------------------------------------Polybenzimidazole
Py-PBI--------------------------------------Pyridine based polybenzimidazole
PEMFC----------------------------------Polymer electrolyte membrane fuel cell
Py-TAB--------------------------------2,6-Bis(3',4'-diaminophenyl)-4-phenylpyridine
TPA----------------------------------Terephthalic acid
T_g---------------------------------Glass transition temperature
TAB----------------------------3,3',4,4'-Tetraaminobiphenyl
TGA-------------------------Thermogravimetric analyzer
TMC---------------------Total monomer concentration
TMBP----------------4,4'-Diglycidyl(3,3',5,5'-tetramethylbiphenyl)
WAXD----------Wide angle X-ray diffraction

CONTENTS

CHAPTER–2 *Materials and Experimental Methods* *39-47*

CHAPTER–3 *N-alkyl Polybenzimidazole: Effect of Alkyl Chain Length* *48-68*

CHAPTER–4   *Soluble Polybenzimidazoles for PEM: Synthesized from Efficient, Inexpensive, Readily Accessible Alternative Tetraamine Monomer*   *69-92*

CHAPTER 1

Introduction

1.1. HISTORY OF POLYBENZIMIDAZOLE (PBI):

Polybenzimidazoles are a class of thermally and chemically stable aromatic heterocyclic polymer. The concept of polybenzimidazole reported for the first time in a Patent (US Patent 2, 895, 948) in 1959 by Brinker and Robinson.[1] Polybenzimidazole was first synthesized by Marvell and Vogel from Illinois University in 1961 just to obtain the material without any target.[2-5] But later it was revealed that PBI has marvellous properties like high stability; especially thermally and chemically in drastic conditions. Due to demands of NASA scientists for fire and heat proof material; NASA and Air Force Material Laboratory (AFML) worked on several types of polybenzimidazole to fulfil their requirements and to get extensive properties to manufacture the flake and the fibre.[6-8] They have explored and synthesized polybenzimidazoles for many good properties like flame retardation property, stable from radiation, excellent mechanical, thermal stabilities and strength retention over wide range of temperatures, toughness, chemically resistance and adhesion characteristics. After the discovery of these properties of the polybenzimidazole; NASA was collaborated with Celanese Company so that they (Celanese) could produce large amounts of PBI which NASA could use as fire resistance jackets and make adhesive foams and fibre for their requirements. In the 1980's, low molecular weight polybenzimidazoles were marketed under the name of "**Celazole**" as moulding resins. Then 20 years later, in 1983 Celanese Company marketed polybenzimidazole with meta phenylene linkage, poly[2,2'-(*m*-phenylene)-5,5'-bibenzimidazole] as "**PBI**" for the use in wide range of textile fibers. Thereafter, Celanese Company started production of large amount of PBI and they have marketed PBI world-wide. Due to high performance fibres, PBI has been used for several decades for high comfort, non-flammable fabrics and used as flight suits, fireproof clothing and hand gloves for astronauts and pilots. Due to its outstanding fibre, film or membranes formation capability; it has been used in numerous industrial applications. To enhance the properties of PBI, several research groups have made their efforts and the reviews of such have come out in literature.[6-8,9-15]
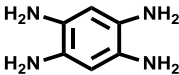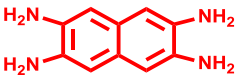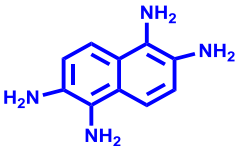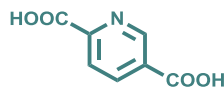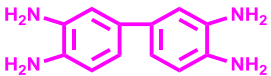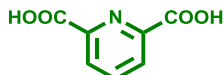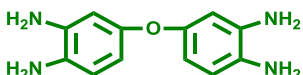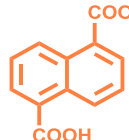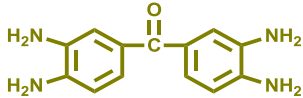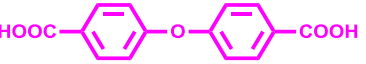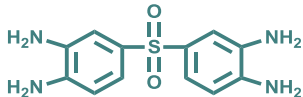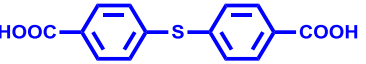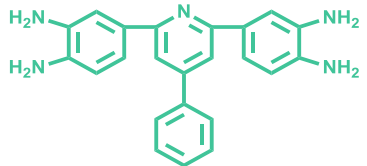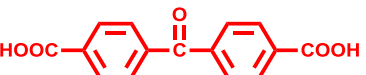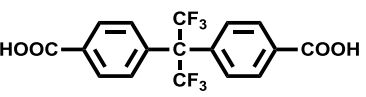
1.2. SYNTHESIS OF POLYBENZIMIDAZOLES:

After the synthesis of polybenzimidazole by Marvell and Vogel in 1961, the polymerization techniques to make PBI have been explored in different ways. The general synthetic procedure of PBI is the polycondensation reaction of aromatic tetramines (bis-*o*-diamines) and aromatic dicarboxylates (acid, ester or amides).[2,3,6,10] Although different types of techniques are available in literature; the most popular and well known technique is solution medium polycondensation using polyphosphoric acid (PPA). Different types of monomers (tetramines and dicarboxylates) which have been used are tabulated in the Table 1.1. This is a representative list of monomers which were used very often, there are several other monomer, are also known in the literature. All the different techniques are carried out at higher heating condition and

under nitrogen atmosphere. These varieties of polycondensation techniques are briefly discussed in the following sections:

Table 1.1. *Different types of aromatic tetramine and dicarboxylic acid monomers along with their melting points (MP) for the synthesis of polybenzimidazole (PBI).*

Tetramine Monomer	MP (°C)	Dicarboxylic Monomer	MP (°C)
1,2,4,5-Tetraminobenzene	275	Benzene-1,3-(dicarboxylicacid)	342
2,3,6,7-Tetraminonaphthaline	178	Benzene-1,4-(dicarboxylicacid)	>300
1,2,5,6-Tetraminonaphthaline	—	Pyridine-2,5-(dicarboxylicacid)	245
3,3',4,4'-Tetraminobiphenyl	—	Pyridine-2,6-(dicarboxylicacid)	249
3,3',4,4'-Tetraminodiphenylether	150	Naphthalene-1,5-(dicarboxylicacid)	>300
3,3',4,4'-Tetraminodiphenylsulfide	102	Biphenyl-4,4'-(dicarboxylicacid)	>300
3,3',4,4'-Tetraminobenzophenone	174	4,4'-Oxybis(benzoicacid)	—
3,3',4,4'-Tetraminodiphenylsulfone	217	4,4'-Thiobis(benzoicacid)	—
2,6-bis(3,4-diaminophenyl)-4-phenylpyridine	221	Benzophenone-4,4'-(dicarboxylicacid)	—
		4,4'-(Hexafluoroisopropylidene)bis(benzoicacid)	272

1.2.1. Melt Polymerization:

The melt polymerization technique[2-4] is mainly carried out between the tetramine and diacid or their ester derivative at higher temperature and under nitrogen atmosphere. This is a two stage process; in the first step equimolecular mixture of tetramine (TAB) and the dicarboxylates [like (isophthalic acid (IPA), diphenyl isophthalate (DPIP) or dimethyl isophthalate (DMIP)] are mixed at 200 °C to 300 °C and in the second step melted and solidified reaction mixture is pulverized at a reduced atmosphere and further increased the temperature to 350-400 °C. The reaction technique and the condition are shown in the Scheme 1.1. The main disadvantage of the two stage melt polymerization is the making of foam due to the formation of phenol or water as a by-product.
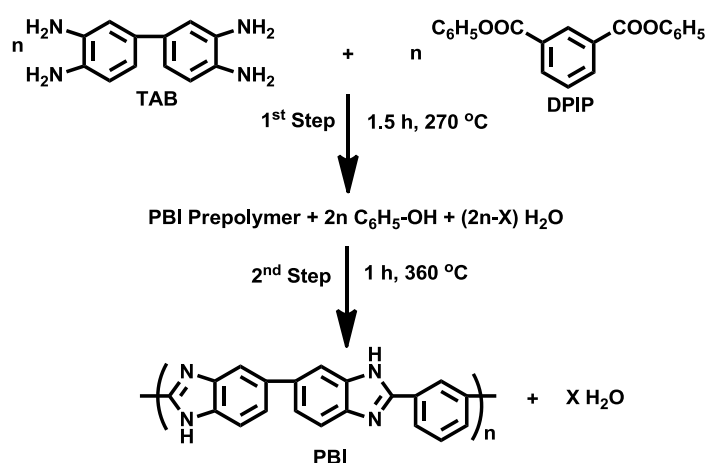
Scheme 1.1. *Two steps melt polycondensation for polybenzimidazole (PBI) synthesis.*

1.2.2. Solution Polymerization:

In solution polymerization, high boiling solvents such as *N,N*-dimethyl acetamide (DMAc), *N,N*-dimethyl formamide (DMF) were used.[16-18] But the main drawbacks of these methods are the resulting PBI has low molecular weight as evident from low inherent viscosity (IV) of the polymer solution. The higher molecular weight (MW) can be obtained at higher temperature, but at that temperature (more than 200 °C) the solvents evaporates from the reaction medium and the reaction mixture turns into a melted and solidified product which is quite difficult to remove from the process. Iwakura et al.[19] reported first time in 1964, the solution polymerization of PBI using PPA, where PPA was used as solvent and as well as catalyst for polyheterocyclization reactions.[20-22] In this procedure equimolecular tetraamine and the dicarboxylic acid were taken in the polyphosphoric acid (PPA) medium and the reaction mixture was keep under continuous flow of nitrogen gas at 180-210 °C for 24 h. When diamine have counter acid salts then at first tetramines are kept at 140 °C for complete removal of the hydrochloride (HCl)[6] gas and then add

the equal moles of dicarboxylic acid. The continuous nitrogen flow is required for the removal of by product like water or phenol from the reaction mixture. The main advantages of the PPA medium is high MW PBI can be synthesized and the polymer product can be easily processed from the reaction mixture at the hot condition. The reaction procedure and the condition for PPA based solutions polycondensation of PBI are shown in the Scheme 1.2.
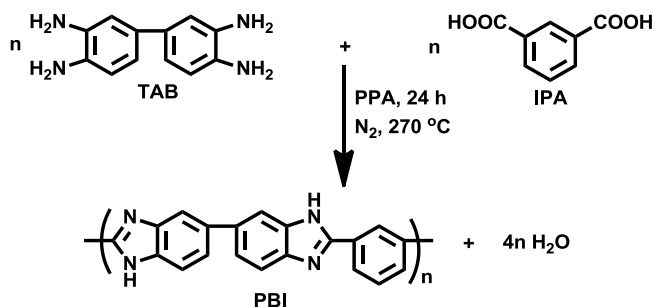
Scheme 1.2. *Solution polymerization process for synthesis of polybenzimidazole (PBI) in polyphosphoric acid (PPA) medium.*

1.2.3. Use of Catalyst for PBI Synthesis:

In catalytic polymerization technique several research groups have put in their efforts.[6,23-28] In this technique 3,3',4,4'-tetraminobiphenyl (TAB) as well as isophthalic acid as monomer and diphenyl isophthalate, dichlorophenylphosphine, chlorophenylphosphine, triphenyl phosphite, diphenylphosphine oxide, diphenyl chlorophosphate, triphenyl phosphate, dimethoxyphenylphosphine, dibutoxyphenylphosphine, *o*-phenyl phosphorochloridate, phenyl and dichlorodimethylsilane are used as a catalyst for the production of PBI. By these catalysts, PBI with IV > 0.7dL/g can be easily produced.[29] It has also been demonstrated and reported in the literature that with the increase of catalyst concentration upto 1 wt% the MW gradually increases. The reaction procedure is shown in the Scheme 1.3.
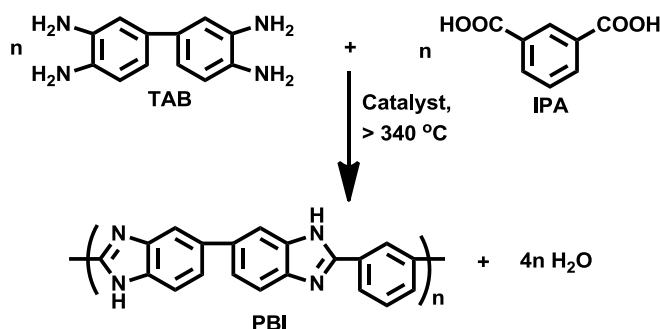
Scheme 1.3. *Catalytic polymerization process for polybenzimidazole (PBI) synthesis.*

1.3. STRUCTURAL VARIATION OF POLYBENZIMIDAZOLES:

After 1961 synthesis of polybenzimidazoles by Marvell et al. without any specific target, till now several research groups have modified the structure of high temperature resistance PBI. Commercially available PBI has been well explored since 1980 which is mostly used in different advanced fields. PBI has some different unique properties and difficulties that have been discussed in the next few sections. To improve the properties of PBI according to the requirements; scientist have made varieties of PBI. The varieties of PBI include poly[2,2'-(1,4-phenylene)-5,5'-bibenzimidazole] (known as *p*-PBI),[30] poly(4,4'-diphenylether-5,5'-bibenzimidazole) (OPBI),[31-33] poly(2,5-benzimidazole) (AB-PBI),[34] pyridine based PBI (Py-PBI),[35-37] sulfonated PBI,[38] cross-linked and hyperbranched PBI,[39-42] naphthalene based PBI,[43] fluorinated PBI,[44] N-substituted PBI (N-PBI),[45-47] meta-para random PBI copolymer,[48] PBI with sulfone or sulfonic acid groups in the backbone[49] and many others. Due to highly rigid rod structure and strong inter-molecular and intra-molecular chain hydrogen bonding; its solubility is poor in common organic solvents. Varieties of PBI have been synthesized to monitor the properties. To improve the solubility of PBIs researchers have incorporated hetero atoms[46,50] in the polymer main chain or by N-substitution post polymerization with sulfonic or the aliphatic groups.[38,45] PBIs have acid uptake capability and hence incorporation of hetero atom in the polymer main chain can increase the acid doping level which is useful for fuel cell application. To increase the flexibility; PBI have been modified with main or side chain by incorporation of flexor group like para linkage monomer or aliphatic group or bulky group containing hetero atom.[35,48] Sulfonated acid group containing PBI can play an important role to increasing the water and acid uptake capacity. To improve the membrane quality, especially thermal and mechanical properties, many modifications have been explored. Recently our group has modified PBI with side[45] and the main chain[35] which increases solubility, flexibility and acid doping capability. The classification of PBI as shown in the next following sections is based on main chain repeat unit order, structures.

1.3.1. Polybenzimidazole Block Copolymer:

Monitor and control of extensive properties of PBI modifications have been carried out by changing the crucial structure. It is well known that polymer architecture has an influence on final polymer properties. The block copolymers can change morphology and the properties. In block copolymer (Figure 1.1) can make multiphase separation morphology observed due to the blocky nature and it reflects to the entire properties of the whole polymer. Sulfonic acid group containing PBI can absorb more amount of acid and water.[51,52] For this reason Mader et al.[53] has produced an alternative segmented block copolymer of PBI with one block part containing the sulfonic acid group. Lee et al.[54] has made block PBI with sulfone containing poly (arylene ether) polymer which shows more acid loading and mechanical properties. Our group has successfully made the *meta-para* block PBI which shows excellent proton conductivity as well

as thermomechanical properties (discussed in Chapter 6).[55] The multi block copolymer can make hydrophilic and hydrophobic phase separation which can make the entire ionic domain connected. Ng et al.[56] prepared multi block poly arylene ether and PBI block copolymer, also.
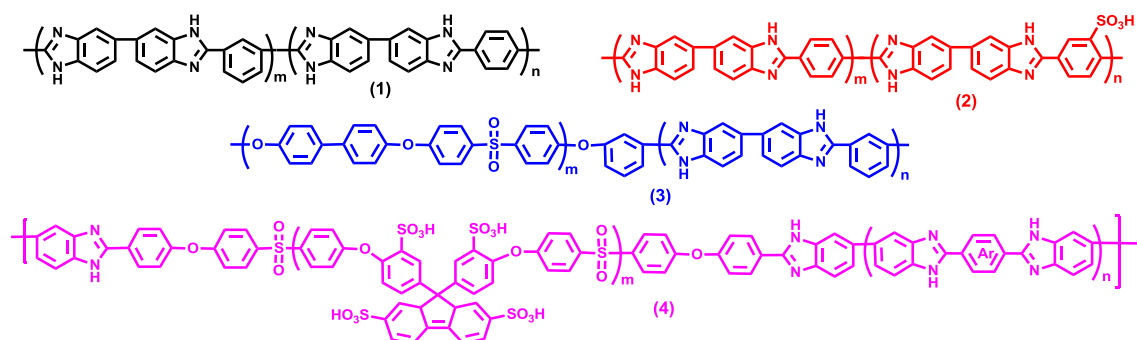
Figure 1.1. *Different types of polybenzimidazole (PBI) block copolymer.*

1.3.2. Polybenzimidazole Random Copolymer:

It has been well reported and documented that the structural architecture can affect the several properties of polymer. Incorporation of hetero atom to the polymer back bone can change the mechanical, thermal and solubility of PBI polymer.[35,57,58] To increase the solubility ether linkage can easily be introduced to the PBI backbone by random copolymerization.[51,59] The incorporation of the hetero atom and bulky group to the polymer back bone increases the flexibility as well as the proton conductivity of the PBI.[35] The sulfonic acid group containing PBI can alter the proton conductivity and the crucial physical properties as well. Sulfonic acid group can be incorporated into the polymer backbone by random copolymerization by introducing monomers which have the sulfonic acid group and it is the best technique to incorporate the sulfonic acid group in PBI backbone. The fluorine containing PBI[35,44] shows the excellent thermal and mechanical properties that can be easily prepared by random copolymerization by opting fluorine containing monomers. Recently, our group has done three types random copolymers of PBI (a) *meta* and *para* PBI,[48] (b) pyridine based *meta* and *para* PBI[37] and (c) phenylene containing pyridine based *meta* and *para* PBI.[60] In literature different type PBI have been explored to change the properties of PBI. Some of the representative random PBI copolymers are listed in the Figure 1.2.

1.3.3. Polybenzimidazole Homo Polymer:

Even though PBI shows good proton conductivity, thermal and mechanical stabilities but it has some limitation such as, it is soluble only in highly polar aprotic solvents like DMSO, DMAc and *N*-methyl pyrrolidone (NMP) etc.[35,37,45] due to high rigid rod structure. To overcome this limitation, modifications have been done by incorporation of hetero atoms like N, S, O to the main chain or by incorporation of different

groups like hydroxyl, sulfonate, imidazole groups etc.[33,35,58] Recently our group has done a series of pyridine based PBI which enhances the solubility as well as proton conductivity.[35] Flexibility of PBI can be increased by introducing para linkage in the synthesized PBI.[61] The glass transition temperature (T_g) of *p*-PBI decreased by around 60 °C in comparison to *m*-PBI. Fluorine containing PBI can be prepared by using different monomers which exhibits high thermal and chemical stability when compared to *m*-PBI. Few representative homopolymers are shown in the following Figure 1.3.
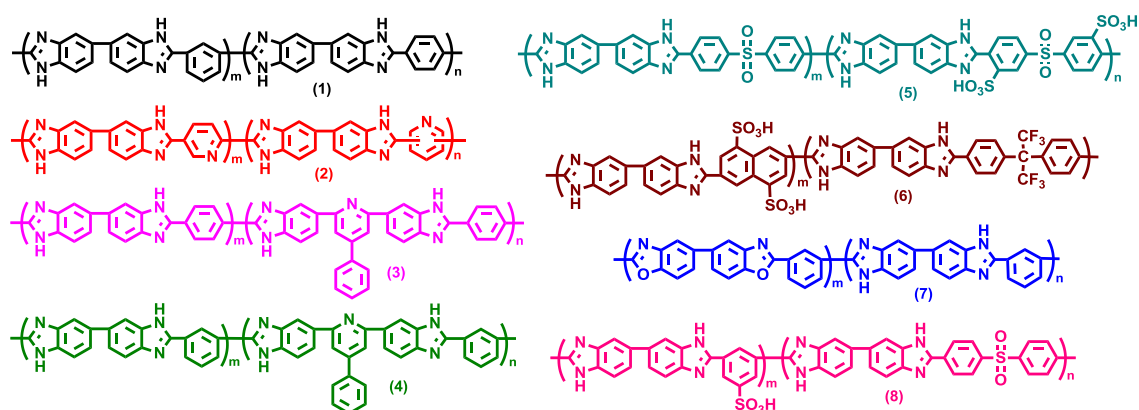
Figure 1.2. Different types of polybenzimidazole (PBI) random copolymer.
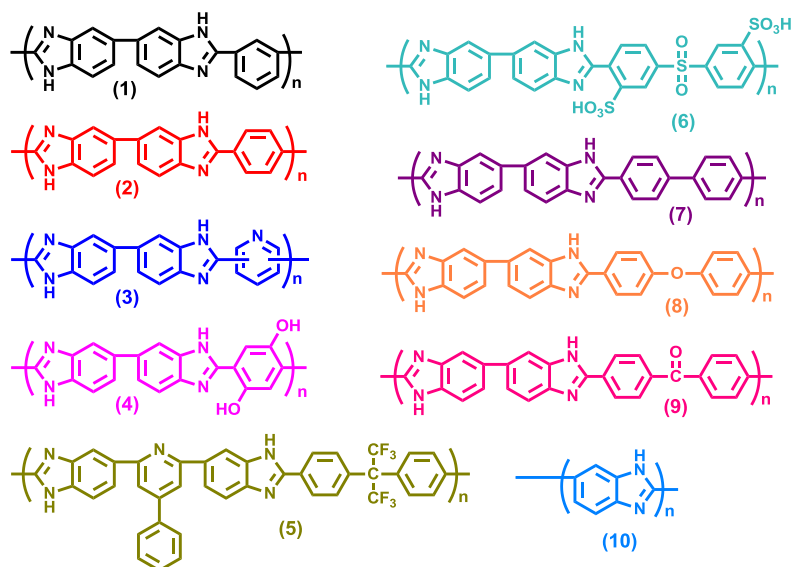
Figure 1.3. Different types of polybenzimidazole (PBI) homo copolymer.

1.3.4. N-substituted PBI:

Polybenzimidazole has amine (-NH-) group which is responsible for 'nucleophilic substitution reaction.' The -NH proton can be easily substituted by less reactive hydroxyethyl,[62] sulfoalkyl,[63]

cyanoethyl,[64] phenyl,[65] alkyl, alkenyl or aryl[66] groups. Sansone et al.[63-67] developed the methods of N-substitution in DMAc or NMP solution. Generally in the beginning PBI is dissolved in solvents and then a strong base like NaH is added for the replacement of hydrogen at higher temperature under inert atmosphere. After that, electrophiles are added to the reaction medium to get the N-substituted PBI. Klaehn et al.[46] recently prepared the alkenyl organosilane (with -CH_2SiMe_2R where R = methyl, vinyl, allyl, hexyl, phenyl, and decyl) substituted PBI which are more and easily soluble in common organic solvents. Pu et al.[50] have made methyl and ethyl substituted PBI which improves the solubility and conductivity as well as decreases the glass transition (T_g). The general procedure of N-substitution of PBI is shown in the next chapter (Chapter 3). We have studied a series of N-alkyl (ethyl to hexadecyl)[45] substituted PBI which enhances the solubility in low boiling solvent like formic acid (FA) and decrease the rigidity and thermal stability (Chapter 3). Few representatives N-substituted PBI presented in the Figure 1.4.
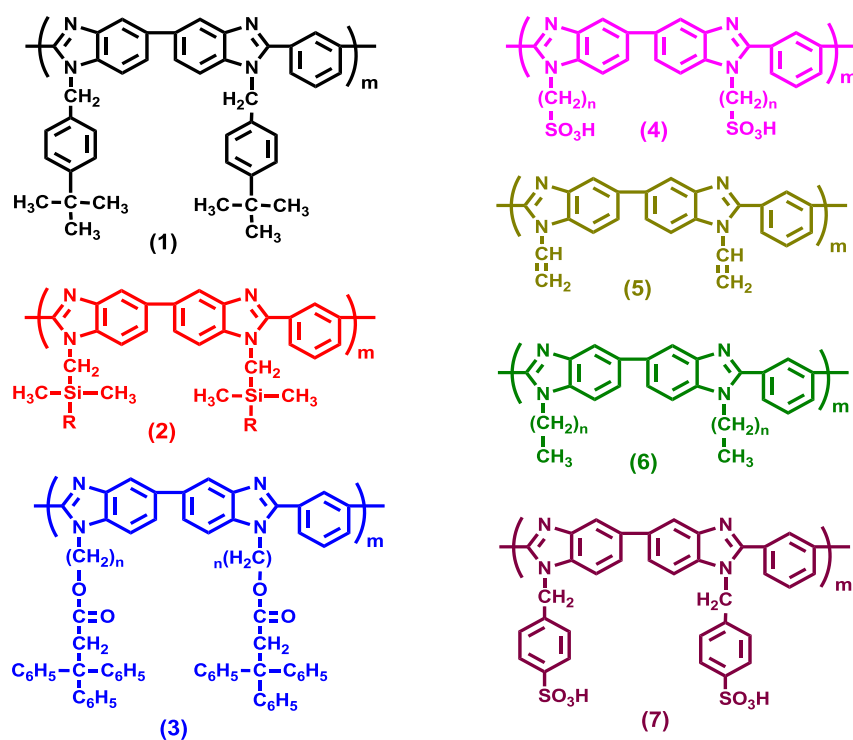
Figure 1.4. *Different types of N-substituted polybenzimidazole (N-PBI) polymer.*

1.3.5. Pyridine Based PBI:

Pyridine dicarboxylic acid containing PBIs have been synthesized by different groups.[35-37] The polar pyridine ring containing (Figure 1.5) polybenzimidazole was first introduced Kalistus et al.[68] by incorporation of meta and para connection to the polymer main chain. The incorporation of extra hetero nitrogen atom to the polymer backbone changes the physical along with chemical properties. Xiao et

al.[21,36] proved that extra nitrogen atom containing pyridine group changes the solubility and the acid doping level with increase in the chemical stability. Recently our group has developed the pyridine ring containing PBI which shows high thermal stability. Our group[35] has recently reported a series of pyridine ring containing phenylene group which increases flexibility, chemical stability, acid doping level in addition to proton conductivity.
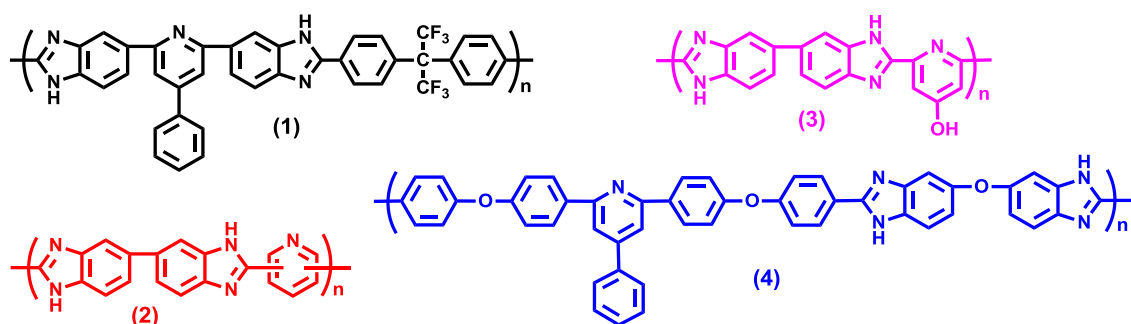
Figure 1.5. *Different types of pyridine based polybenzimidazole (Py-PBI) polymer.*

1.3.6. Cross-linked PBI:

In literature,[39-42] cross-linked or hyperbranched PBIs are synthesized to increase thermal, chemical and mechanical stability. Generally three types of cross-links happen in case of PBI and these are:

(i) Covalent cross-linking: This happens when a covalent chemical bond is formed among polymer.

(ii) Ionic cross-linking: This takes place when the polymer chains are interacting by electrostatic or hydrogen bonding. This type generally observed in acid-base blend or acid-blend ionomers.

(iii) Mixed ionic-covalent cross-linking: This occurs when a mixture of the above two are found.

Kim et al.[69] demonstrated that cross-linked PBI by 3-phenyl-3,4-dihydro-6-tert-butyl-2H-1,3-benzoxazine (pBUa) in DMAc at 220 °C shows high proton conductivity (0.12 Scm^{-1}) at 150 °C under anhydrous conditions. Aili et al.[70] prepared cross-linked PBI by post-treatment with divinylsulfone which are more stable chemically as well as mechanically when compared to linear PBI. Han et al.[71] obtained cross-linked PBI membranes by using 4,4'-diglycidyl(3,3',5,5'-tetramethylbiphenyl)epoxy resin (TMBP) as an cross-linker at 160 °C. They showed that the resulting PBI is chemically, mechanically stable with increase proton conductivity and decreased swelling in H_3PO_4. Luo et al.[72] have prepared cross-linked PBI via a Diels-Alder reaction between vinylbenzyl functionalized PBI (PBI-VB) and α,α'-difurfuryloxy-p-xylene (DFX). They have shown the crosslinked PBI membrane improved mechanical strength, chemical stability as well as higher H_3PO_4 retention ability. Fang's[42,73] group made the hyperbranched PBI by using tetramine benzidine and benzene tricarboxylic acid which have more tensile strength in the region 4.1-4.9

GPa comparable to PBI membranes. Sheratte[74] reported a cross-linked PBI and they have also obtained mechanically and chemically stable PBI. Few representative Cross-linked PBI structures are shown in Figure 1.6.
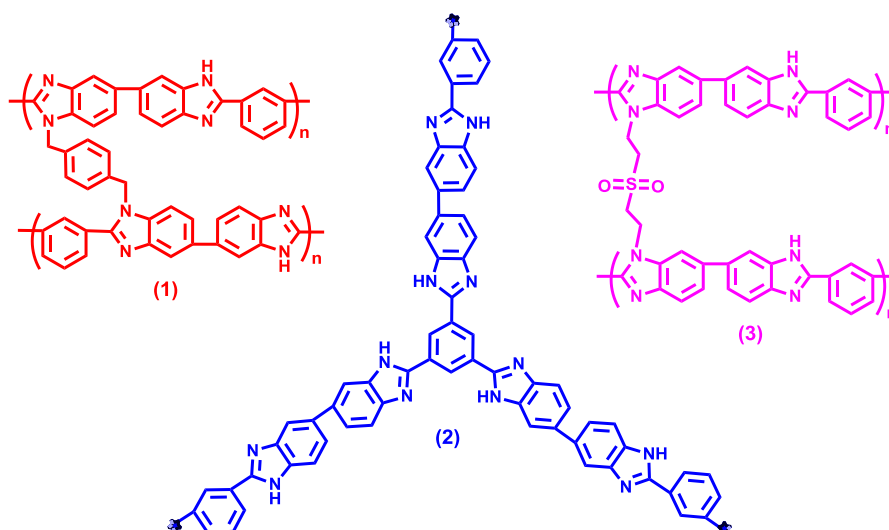
Figure 1.6. *Different types of cross-linked polybenzimidazole (PBI) polymer.*

1.4. PHYSICAL PROPERTIES OF POLYBENZIMIDAZOLE:

Polybenzimidazole (PBI) is an amorphous aromatic heterocyclic polymer which has a highly rigid rod structure. It has strong tendency to form intra and inter molecular hydrogen bonding through the imine (-N=) and amine (-NH-) group which are represent in the imidazole group of the polymer main chain.[58,75-77] Due to highly rigid rod structure it shows high thermal, mechanical and chemically, radiative stability.[6-8] Due to these excellent properties it has numerous applications in different areas like chemical, aerospace, electrical industries, as a membrane and the most recent one is as a polymer electrolyte membrane (PEM) for application in the fuel cell. PBI has proton donor and acceptor side and for this reason it can consume acid via hydrogen bonding. The acid doped membranes are used as PEM in fuel cell.[35,45] Due to highly rigid rod structure, PBIs are soluble only in few highly polar aprotic solvents like DMAc, DMF, dimethyl sulfoxide (DMSO), NMP.[35,37,45] PBI shows higher glass transition temperature (T_g) around 400 °C.[2,35] The PBI are absorbs light and very active as florescence molecules due to presence of non-bonding electron in the imidazole ring. Generally PBI shows only one absorption peak in DMAc dilute solution for $\pi \rightarrow \pi^*$ transition with certain conformation in the chain.[10,75,77] But recently, we have observed that at room temperature phenylated pyridine ring containing PBI (Py-PBIs)[35] are showing two different absorption peaks due to the two different conformation of the phenyl group in the polymer chain. The absorption spectra in DMAc solution of PBI polymers shows distinct $\pi \rightarrow \pi^*$ transition at 344 and 394 nm for meta (*m*)

and para (*p*) PBI, respectively.[48] The emission spectra of PBI in DMAc solution shows two distinct fluorescence bands at 398 and 416 nm which are due to ^1L_b state in the benzimidazole ring of PBI assigned to the 0 - 0 and 0 - 1 transitions from the excited state.[75] Recently, our group has demonstrated that PBI forms aggregated structure in the solution like DMAc and formic acid.[58,77] Literature also discussed the formation of gels of PBI in an appropriate concentration in different solvents.[78,79]

1.4.1. Solubility:

The solubility of PBIs are restricted to only few highly polar aprotic solvents and few strong organic, inorganic acids due to presence of highly rigid rod structure for imidazole ring and formation of strong inter and intra hydrogen bonding. It is soluble only in DMAc, DMF, DMSO, NMP solvents which are highly polar and aprotic solvents.[19,35,37,45,80] PBI are soluble in sulfuric acid (H_2SO_4), methane sulfonic acid (CH_3SO_3H), formic acid (FA) and in phosphoric acid (H_3PO_4).[35,45] Recently, solubility in ionic liquid medium has been reported and fabrication of membrane from this solution was discussed.[81-83] The solubility of PBI polymer depends upon the structure and still now many modifications have been found to increase solubility. N-substituted alkylated organosilane PBIs[46] are soluble in organic medium. Recently, we have explored a series of N-alkylated PBI which are soluble in low boiling solvent like FA.[45] Incorporation of hetero atom like N, S, O to the polymer main chain increases the solubility as well the flexibility.[35,37,84,85] Recently we reported that phenylene pyridine ring incorporation to the PBI[35] main chain increases the d-spacing of inter molecular chain distance and for this reason the solvents molecules goes to the inside of the polymer chain and hence the solubility increases. The other modification whereby incorporation of different groups to the polymer chain increases the solubility and processability such as the nitro,[86] silane,[87] hexafluoroisopropylidene,[44,88] etc.

1.4.2. Viscosity and Molecular Weight:

The solubility of PBI is restricted to few solvents and hence most of the viscosity measurements are done extensively in DMAc, CH_3SO_3H, H_2SO_4.[19,35,37,45,80] The viscosity of PBI depends upon the solvents due to the orientation of polymer chain in solution. According to the nature of solvent and the interaction between solvent and PBI, the dynamic radius of chains can alter and this affect the resulting viscosity. Most often viscosity measurement carried in conc. H_2SO_4 (96-98%) medium. Marvel had shown that the viscosity is 2 to 3 times more in FA and H_2SO_4 medium in comparison to DMSO.[2,3,5] The inherent viscosity (IV) depends upon the moisture, temperature, solvent and the polymer character. The molecular weight (MW) can be calculated from the viscosity. Kozima et al.[89] studied the molecular weight of OPBI in DMAc by light scattering and intrinsic viscometric study. Kozima also studied the molecular weight of OPBI in FA with the help of Mark-Houwink equation ($[\eta] = K \overline{M_w^a}$) where 'a' and 'k' are the constant and

depend on the character of polymer backbone and solvent. Recently our group has made an effort to measure the MW of PBI with the help of iso-ionic dilution method and by applying Mark-Houwink equation in formic acid in case of OPBI. The other well known technique to calculate the MW is by applying end group analysis with the help of ^{1}H NMR analysis.[54] This method can be applied in case of oligomeric PBI species. Several group have utilized gel permeable chromatography (GPC) and light scattering technique to measure the MW. However, the poor solubility and tendency to form aggregates, interferes these measurements and hence often the measured MW by these methods are found to be overestimated. All these measurement are carried out at 60-70 °C in presence of LiCl in the PBI in DMAc/DMSO solution.[90]

1.4.3. Thermal Properties:

PBI is an ideal candidate as a high performance polymer owing to its high thermal stability. Marvel et al. at first experienced that at higher temperature PBI are stable and hence it can be used as a fire retardant material. To determine the thermal stability thermogravimetric analyzer (TGA) is the most reliable instrument and used very often to determine the PBI thermal stability. Literature reports conclude that PBI polymers are stable upto 600 °C under nitrogen (Figure 1.7) atmosphere[91a] and beyond this temperature degradation of PBIs backbone start with the release of carbon dioxide. The initial weight loss happens upto 5 wt% below 150 °C due to the loss of loosely bounded water molecules.[2] It is well reported in literature that PBIs are hygroscopic in nature and it absorbs moisture from the atmosphere. The exceptionally high thermal stability of PBI polymers are mainly due to the following reasons:

(A) Strong inter and intra molecular hydrogen bonding.
(B) High extend of conjugation via imidazole ring to whole polymer chain.
(C) Highly rigid rod structure.
(D) "Bond healing" capabilities.

The thermal stability is less in an oxidative condition compared to inert atmosphere. The hetero atom containing -O- and -SO_2- linkage reduces the thermal stability of PBI due to the increase in flexibility and unsymmetrical structure.[10] The introduction of methyl group into the imidazole ring of PBI causes the thermal stability to decrease. Recently we have studied a series of N-alkyl substituted PBIs and observed that with increase of alkyl chain length, the thermal stability gradually decreases.[45] Our group has observed that the thermal stability of *p*-PBI is more than the *m*-PBI due to the presence of more symmetrical nature of para phenylene linkage in *p*-PBI.[5,48,91b]

PBIs are amorphous, thermo plastic in nature and they show high T_g in between 350-450 °C.[10] The T_g can well be monitored by differential scanning calorimeter (DSC) and dynamical mechanical analysis (DMA) techniques. The T_g truly depends on the internal chemical structure of the PBI chain. The crystallinity can be increase by introduce the hetero atoms like S, N, O, F etc. to the polymer

backbone.[10,35,92] The T_g also depends on the symmetrical nature of the polymer backbone. Recently, our group has demonstrated that the T_g of *m*-PBI (420 °C) is more than *p*-PBI (361 °C) owing to para phenylene linkage presence in the *p*-PBI chain which is more symmetrical in nature.[48] Menczel observed that T_g of *m*-PBI by DSC and DMA that the T_g of the *m*-PBI polymer is 387 °C and calculated the *β*-relaxation at 290 °C associated with loss of water while the *γ*-transition at 20 °C which is not similar and he assign *δ*-transition at 90 °C due to the rotation of the *m*-phenylene ring. Recently we have demonstrated the T_g gradually decreases with the increase in the alkyl chain length in imidazole ring due to the incorporating flexible alkyl chain.[93] We have also demonstrated the incorporation of the extra nitrogen atom to the PBI backbone increases thermal transition temperature.[35]
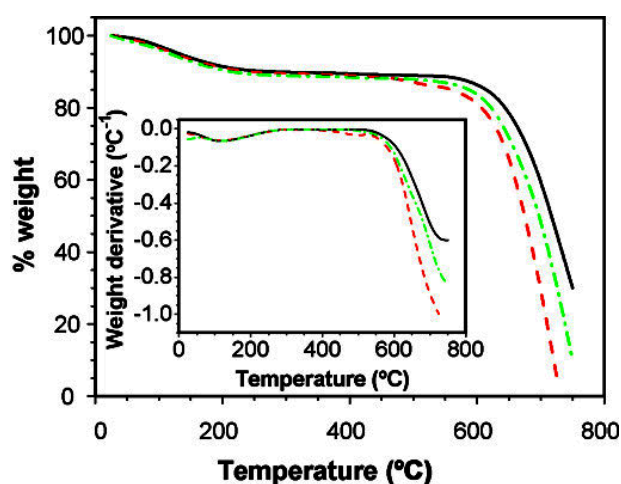
Figure 1.7. Thermal stability of polybenzimidazole (PBI) polymer (adapted from reference 91a).

1.4.4. Mechanical Properties:

PBIs has a highly rigid rod structure and has strong hydrogen bond formation tendency because of the presence of imine (-N=) and amine (-NH-) groups which helps in forming close packed structures and resulting in good mechanical stability (Figure 1.8).[58,75-77] The mechanical strength of PBI is one of key parameters for application in fuel cell. The acid loaded PBI membranes show low mechanical properties which is not good for fuel cell. Below 2 moles of phosphoric acid (PA) loaded membrane decreases the cohesion force of PBI chains due to interaction of PA and imidazole group of PBI chains.[94] If more acid loading in the PBI chain happens it further decreases the intermolecular interaction of PBI and hence the mechanical stability decreases. From DMAc casted membranes which have acid doping level, ~ 5-6 mole/ repeat unit is the optimum acid loading to maintain good mechanical stability.[95] The mechanical stability depends on the internal chemical structure of PBI.[31,37,38,43,96] To improve the mechanical stability of the PBI membranes researchers have made cross-linked and hyperbranched PBI.[69-73] Li et al. made the

crosslinked PBI vie *p*-xylene connection between the PBI chain molecules which shows 21-23 MPa more tensile in strength when compared to the parent PBI.[97] The molecular weight of polymer also controls the mechanical stability of PBI, for example, from 20000 to 55000 gmol^{-1} the tensile strength increases from 4 to 12 MPa of acid doped PBI membranes.[98]
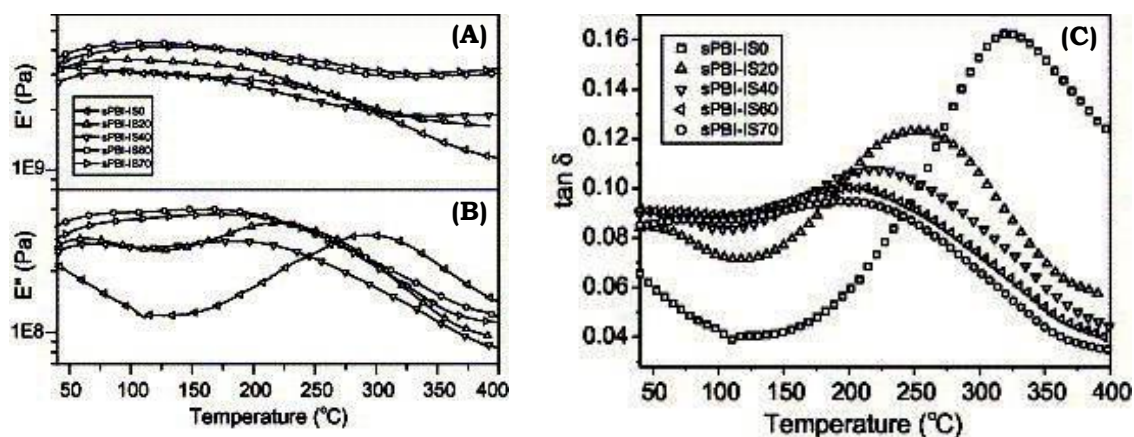
Figure 1.8. *Temperature dependent various thermo-mechanical properties (A) storage modulus (E'), (B) loss modulus (E") and (C) tan δ of polybenzimidazole (PBI) polymer (adapted from reference 49).*

1.4.5. Oxidative Stability:

In fuel cell application one of the most important parameters is the chemical stability of the membranes at drastic chemical environment. The oxidative stability (Figure 1.9) of PBI membranes has been extensively studied by the application of Fenton's solution technique which is made from 3% H_2O_2 solution in water containing the Fe^{2+} ion.[35,99,100] Gaudiana and Conley[101] show that in Fenton's test, the produced hydroxyl (OH·) and hydroperoxyl (OOH·) radical attack the PBI weakest part, the nitrogen atom of imidazole ring in the polymer chain. The FT-IR study also has been studied to know the degradation procedure. Musto et al.[102] shown that two new absorption peaks are formed which indicate that the degradation of PBI has taken place and the stretching vibrations of the product or intermediate of the polymer are identified. The oxidative stability depends on the chemical structure of the PBI backbone. The wt% loss varies during Fenton's test and it can show 10-40 wt% degradation. The cross-linked PBI shows high oxidative stability rather than the mother PBI which is well reported in literature.[71,97,103] To improve the chemical stability in drastic chemical condition, composite membranes of PBI have been reported.[104-106] Recently our group has demonstrated that the amine functionalized silica nano particle enhances oxidative stability in case of OPBI polymer.[104] The hetero atom F containing PBI polymers are chemically more stable than the normal PBI.[103,107] Our group has recently reported that hetero nitrogen atom can also improve the chemical oxidative stability.[35]
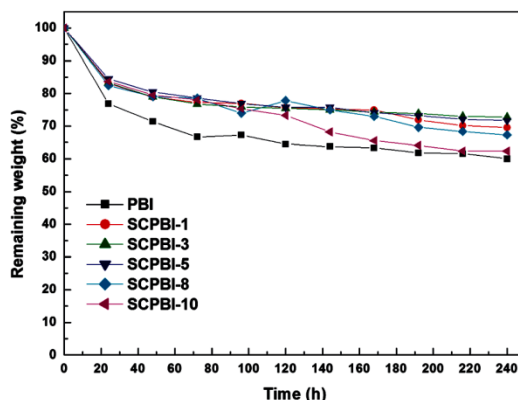
Figure 1.9. *Thermochemical stability (Fenton test) of polybenzimidazole (adapted from reference 106).*

1.4.6. Photophysical Properties:

PBI shows absorption (Figure 1.10A) and fluorescence (Figure 1.10B) properties both in solution and solid state. In literature, photophysical studies have been extensively studied to understand inter and intra molecular interaction with a particular solvent and the chain conformation, aggregation and gelation properties. Till now only very few reports have explored the chain conformation of PBI in solution due to the solubility problem of PBIs.[10,75,77] The absorption as well as the emission depend on the internal structure of PBI and the solvents.[35,48] PBI shows two different absorption peak at 340 nm and 440 nm due to π-π^* and n-π^* transition of imidazole moiety, respectively in *N,N*-dimethyl acetamide (DMAc) solution.[10,58,75,77] Recently, Sannigrahi et al.[48] observed that absorption spectra of PBI in DMAc solution shows distinct $\pi \rightarrow \pi^*$ transition at 344 and 394 nm for meta (*m*) and para (*p*) PBI, respectively due to enhancement of the conjugation of *p*-phenylene linkage into the polymer backbone. Recently, our group has demonstrated that the absorption maxima of PBI alters due to the different chemical environment of PBI backbone structure.[33,35,37,48,58,77]
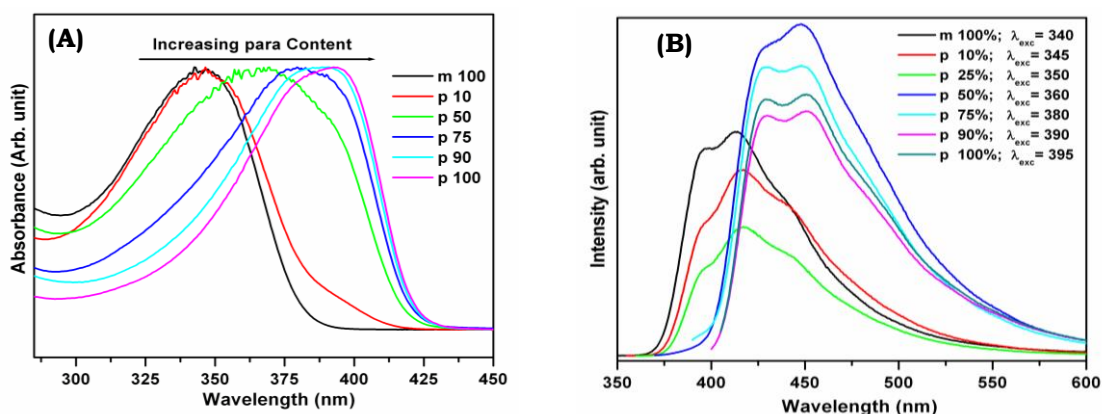
Figure 1.10. *(A) Absorption and (B) fluorescence emission spectra of meta (m)-para (p) random copolymers of PBI in DMAc solution (concentration is 2 × 10^{-5} M) (adapted from reference 48).*

PBI is fluorescence active and the quantum yield is also high (>0.5).[48] The emission spectra of PBI also depends on the polymer backbone structure and the solvent. The emission spectra are obtained in both solution and solid state condition. The emission spectra of PBI in DMAc solution shows two distinct fluorescence bands at 398 and 416 nm due to ^1L_b state in the benzimidazole ring assigned to the 0-0 and 0-1 transitions from the excited state.[75] Recently, our group has demonstrated that PBIs are showing the aggregation properties in the solution like PBI in DMAc and OPBI in FA and the aggregation properties depends on the excitation wavelength .[58,77]

1.4.7. Solution Properties:

Due to limitation of solubility of PBI, the solution properties have not been thoroughly investigated in literature. But few literatures, reported by us and others indicate that different solvents and different structures of PBI show the aggregation, gel and polyelectrolyte nature at varied concentration and temperature.[47,58,77-79] From the solution properties we can understand the conformation and structural behavior of PBI chain easily. The following sections will briefly discuss the solutions properties:

1.4.7.1. Aggregation Properties:

Aggregation in solution can happen due to covalent, hydrogen bonding, electrostatic attraction or Van der Waals force, hydrophobic and hydrophilic interaction of the polymer chains. The aggregation depends on solubility, concentration, polymer backbone structure, molecular weight, solvent and the temperature.[58,75,77] Ogata et al.[108] have studied the aggregation behaviour of polystyrene-*b*-poly(ethylene/butylene)-*b*-polystyrene triblock and Nuopponen et al.[109] have studied poly(*N*-isopropylacrylamide-*b*-styrenes) diblock copolymer. They have tried to explore the aggregation behaviour of copolymer as it depends on solvent polarity. They have also explored the connection between solvent polarity and aggregation behaviour of the copolymer by comparing the aggregations in several solvents. PBI has one major problem which is solubility and due this the aggregation properties have not been explored much. Generally, the solubility decreases with increasing the molecular weight (MW). Kojima et al.[75] have studied the aggregation of PBI and concluded that the overlapping of PBI chains as the cause of aggregation. Recently our group has explored the aggregation of PBI in DMAc by using viscosity, steady state and time dependent fluorescence techniques and our study revealed that the concentration dependent PBI chains make orientation from compact coil to an extended helical rod like structure. Our group has also demonstrated the aggregation behavior of poly(4,4′-diphenylether-5,5′-bibenzimidazole) (OPBI) in polar aprotic DMAc and protic FA solvents which depends on the polymer concentration and solution temperature.[58] This study reveals that the swelling of OPBI happens in case of aprotic solvent but not in protic solvent. The temperature study shows the aggregation destabilizes when temperature is increased and the aggregation behavior is dependent on the solvent character as shown in Figure 1.11.
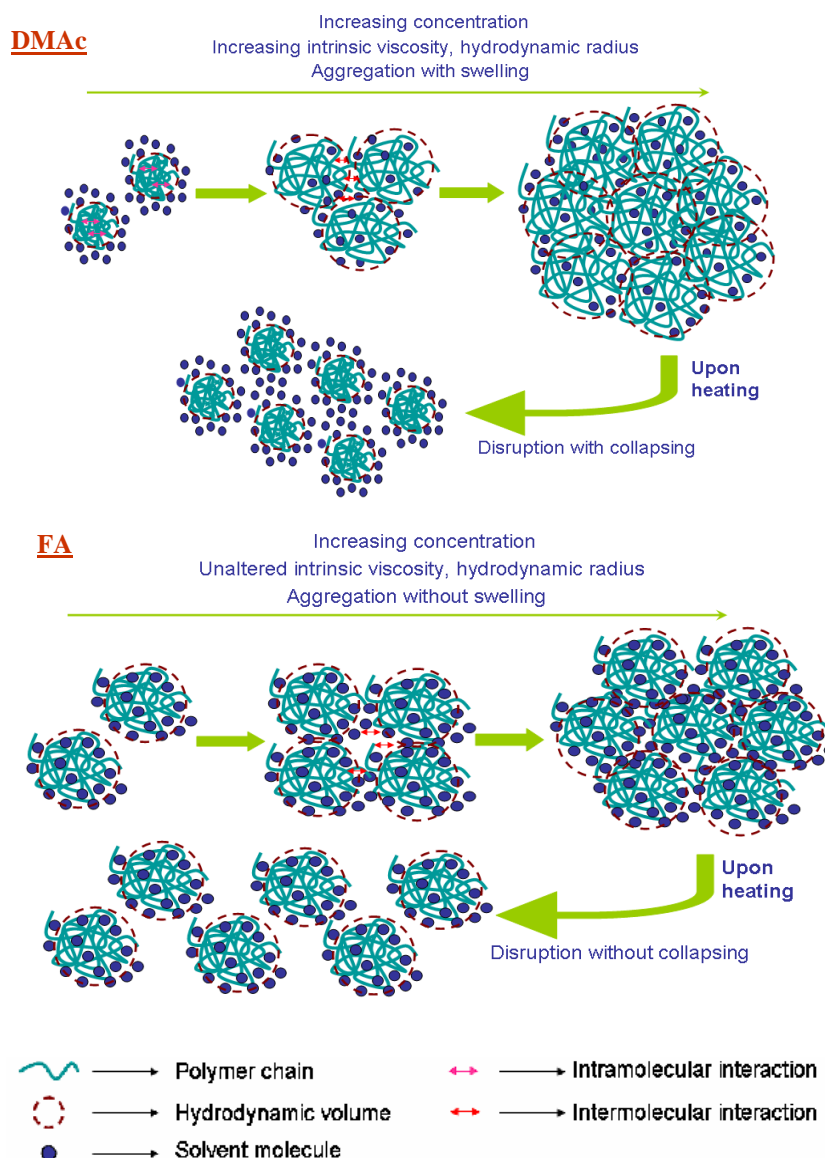
Figure 1.11. *Schematic representation of the aggregation behavior of OPBI in DMAc and FA solvent with increasing concentration. Also, the stability of aggregated structures upon heating is shown (adapted from reference 159c).*

1.4.7.2. Gel Properties:

Polymers form gel in solutions and has great importance in bio and the other application.[110,111] Gel formation happens either physically or chemically which exhibit the reversible or the irreversible nature of the gel, respectively. Gel formation depends on many factors like temperature, solvent polarity, polymer backbone structure, temperature, concentration and MW.[110-113] Chemical gel formation happens due to the covalent bond of the polymer chain or by interchain cross-link or by the hyperbranched polymer chain.

Physical gel formation can happened due to the weak interaction with solvents and polymer chain hydrogen bonding, Van der Waals force or by electrostatic attraction of charged species of polymer backbone structure.[114-118] The main attraction of the gel formation study reveals that (i) the crystal structure and morphology, (ii) the mechanism of gel formation and gel kinetics and (iii) the relation between structure and thermal study in order to understand several physical properties of the gel. Our group has demonstrated experimentally the formation of thermoreversible gel of PBI in H_3PO_4 and FA. The nature and the structure of the gel vary depending on the PBI structure and the solvent. The formation of PBI gel is found to be very attractive alternative to fabricates proton conducting membrane as described in Figure 1.12.
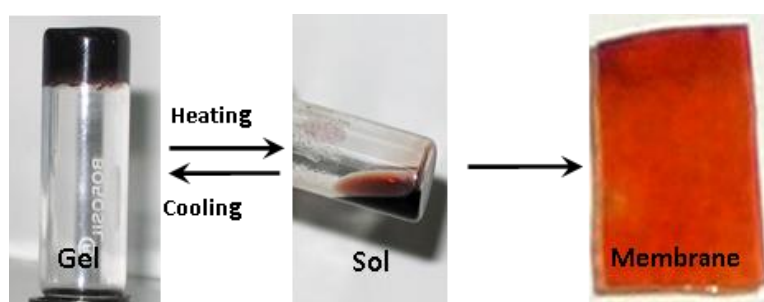
Figure 1.12. *Thermoreversible gelation of polybenzimidazole (PBI) in phosphoric acid (PA) (adapted from reference 79).*

1.5. APPLICATION OF PBI:

Since the discovery of polybenzimidazole by Vogel in 1960, numerous applications of PBI have been explored in several technologically important areas owing to its high thermal, chemical, mechanical stability and inflammable nature. PBIs is used in aerospace, aircraft, electrical, textile and chemical industries.[6,8,11,119,120] It is being used in the air force as a fire proof jacket due to high thermal stability. Due to its good membrane forming property, these membranes have been used in reverse osmosis, gas permeation and water desolation. Most recently, as an advanced application, acid doped PBI membrane has been used in the fuel cell as a polymer electrolyte membrane (PEM).[34-36] The following sections will discuss in details the applications of the PBI:

1.5.1. Conventional Application:

1.5.1.1. Structural Engineering Materials:

PBI is used in structural engineering application like aerospace, aircraft and electrical engineering industries because of thermo-mechanical and chemical stabilities.[6]

1.5.1.2. Insulating Material Applications:

PBI can resist heat conduction and act as an insulator. Hence PBI is used as fire proof jacket and the material in aircraft and aerospace at lower and higher temperatures. PBI is not electrically conducting and therefore can be used as good electrical insulator, especially it is being use in cable and wire covers for electrical purpose.[10-13,119,120]

1.5.1.3. Adhesive Materials:

PBIs are used as adhesive materials from the last decade in industry and aerospace. PBI adhesive shears tress at 550 °C and at room temperature is 2500 and 3000 psi, respectively. For this reason PBI can be used in airspace at higher and lower temperature as adhesive due to retard the atmospheric solar orientation. PBI is also used as a cryogenic adhesive materials at various temperatures.[10,11,13]

1.5.1.4. Fiber Materials:

PBI polymer forms good fibre which is mechanically, chemically and thermally stable.[10-13] Due to fibre formation property it is used in different industries like textile, electrical, aeronautical and chemical. The thermal stability is as high as 300 °C and at that temperature it shrinks upto 3% and it does not form smoke and melt at above 500 °C only.[10-13] It does not form any kind of smoke or flame and has the capability to maintain mechanical stability constantly at higher temperature, resists form chemicals, stable at high humidity condition etc.,[150,151] hence PBI is found to be an important material for use as fibre.

1.5.1.5. PBI Membranes:

PBI polymers have excellent capability to form membranes which are highly stable mechanically, chemically and thermally.[6,10,121,122] The PBI membranes are used as semipermeable membranes for reverse osmosis, nano filtration and some medical applications. PBI membranes are used as ion exchange membrane for both cation and anion like phosphate, arsenate, arsenite, sulphate, chromate, phosphate, cupper etc.[121,122,123-125] PBI has proton donor and proton accepter site because of the presence of imidazole ring which chelate the different ions and make hydrogen bond with the electrolyte. PBI membrane can be made as porous in nature and used as gas separator membrane.[126] Recently, acid doped PBI membranes are being used in the high temperature polymer electrolyte membrane fuel cell application as a polyelectrolyte membrane.[34-36] Wang et al.[127] fabricated PBI hollow fibre membranes for nanofiltration by chemically modified crosslinker using *p*-xylene dichloride. The next section discusses in detail about the application of acid doped PBI membrane in the fuel cell.

1.5.2. Advanced Application:

1.5.2.1. Fuel Cell:

Fuel cell (Figure 1.13) is an electrochemical energy conversion device which converts chemical energy to electrical energy.[128-132] Sir William Grove first introduced the concept of a fuel cell in 1839, after that now fuel cell is the most promising technology for power source. But it was first commercialized and demonstrated by NASA in the 1960's with the usage of fuel cells on the Gemini and Apollo space flights. As electrical power source device in stationary or mobile purpose; fuel cell is the most dedicated and the most eco-friendly device due to the formation of water as a product. A fuel cell consists of positively charged anode electrode, negatively charged cathode electrode, electrolyte and external load.[129-131] In anode electrode surface oxidation and cathode surface reduction of the fuels takes place in between two electrode, electrolytes used for separation of the fuels and also passes it ions. The fuel cell (Figure 1.13) can be divided depending upon the type of electrolyte is used in the cell. Different types of fuel cells are known and these fuel cells electrolytes, operating temperature and the catalyst are shown in the Table 1.2.

Table 1.2. *An Overview of different types of Fuel Cells. (Adapted from google image).*

U.S. DEPARTMENT OF ENERGY | Energy Efficiency & Renewable Energy

FUEL CELL TECHNOLOGIES PROGRAM

Comparison of Fuel Cell Technologies

Fuel Cell Type	Common Electrolyte	Operating Temperature	Typical Stack Size	Efficiency	Applications	Advantages	Disadvantages
Polymer Electrolyte Membrane (PEM)	Perfluoro sulfonic acid	50-100°C 122-212° typically 80°C	< 1kW–100kW	60% transportation 35% stationary	• Backup power • Portable power • Distributed generation • Transporation • Specialty vehicles	• Solid electrolyte reduces corrosion & electrolyte management problems • Low temperature • Quick start-up	• Expensive catalysts • Sensitive to fuel impurities • Low temperature waste heat
Alkaline (AFC)	Aqueous solution of potassium hydroxide soaked in a matrix	90-100°C 194-212°F	10–100 kW	60%	• Military • Space	• Cathode reaction faster in alkaline electrolyte, leads to high performance • Low cost components	• Sensitive to CO_2 in fuel and air • Electrolyte management
Phosphoric Acid (PAFC)	Phosphoric acid soaked in a matrix	150-200°C 302-392°F	400 kW 100 kW module	40%	• Distributed generation	• Higher temperature enables CHP • Increased tolerance to fuel impurities	• Pt catalyst • Long start up time • Low current and power
Molten Carbonate (MCFC)	Solution of lithium, sodium, and/or potassium carbonates, soaked in a matrix	600-700°C 1112-1292°F	300 kW-3 MW 300 kW module	45-50%	• Electric utility • Distributed generation	• High efficiency • Fuel flexibility • Can use a variety of catalysts • Suitable for CHP	• High temperature corrosion and breakdown of cell components • Long start up time • Low power density
Solid Oxide (SOFC)	Yttria stabilized zirconia	700-1000°C 1202-1832°F	1 kW–2 MW	60%	• Auxiliary power • Electric utility • Distributed generation	• High efficiency • Fuel flexibility • Can use a variety of catalysts • Solid electrolyte • Suitable for CHP & CHHP • Hybrid/GT cycle	• High temperature corrosion and breakdown of cell components • High temperature operation requires long start up time and limits

For More Information
More information on the Fuel Cell Technologies Program is available at *http://www.hydrogenandfuelcells.energy.gov*.
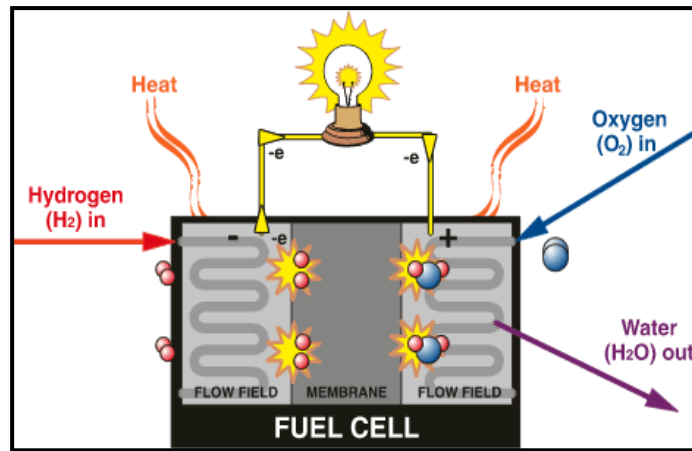
Figure 1.13. *Polymer Electrolyte Membrane Fuel Cell (PEMFC) (adapted from google image).*

1.5.2.2. Proton Exchange Membrane Fuel Cell:

Polymer electrolyte membrane fuel cell is the most promising and dedicated electrochemical device for stationary as well as the mobile purposes due to its simplicity, low cost, long lasting, small size, high efficient, low as well as high operating temperature and for being pollution free among all the other type fuel cell.[133-139] The main construction of the fuel cell is by the two electrode, cathode and anode and a polymer electrolyte membrane which is placed in between the electrodes. In cathode side reduction happens where oxygen fuel is used and anode side oxidation happens where hydrogen fuel is used. The electrodes have platinum surface for the oxidation and the reduction. The protons move from the anode side to the cathode side via the polymer electrolyte membranes. The produced electrons are passed through the external circuit and there loads are applied. The all reaction of hydrogen PEM fuel cell is as follows:

Cell Reactions

$$\text{Anode: } H_2 \longrightarrow 2H^+ + 2e^-$$

$$\text{Cathode: } 1/2\ O_2 + 2H^+ + 2e^- \longrightarrow H_2O$$

$$\text{Overall reaction: } H_2 + 1/2\ O_2 \longrightarrow H_2O + \text{Electrical Energy} + \text{Heat}$$
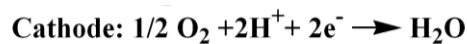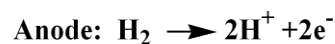
1.5.2.3. Requirement for Proton Exchange Membrane:

To get the efficient and high-performance PEMFC, the polymer membranes should satisfy following requirements:[135,138,139]

(a)   High proton conductivity

(b)   High mechanical stability

(c)   High thermal and chemical stability

(d)   Low reactant permeability

(e)   Good film-formation capacity

(f)   Low cost

(g)   Capability of fabrication into membrane electrode assembly (MEA)

(h)   Negligible electronic conductivity.

1.5.2.4. Reputed Proton Exchange Membranes:

The efficiency of a fuel cell largely depends on polymer electrolyte membranes, which needs to be economical, long lasting and high performance.[20,133,138,140] The polymer electrolyte membranes are the highly charged species which can carry the ions through the membranes in between the two electrodes. Till now many membranes have been explored, but among all the membranes perfluoro sulfonated acid membrane commonly known as the Nafion (Figure 1.14) is most prominent since it was first marketed in 1966 by the USA based DuPont and Dow company.[138,140] Nafion are easily available, has high proton conductive efficiency, and is thermally, chemically and mechanically stable. It can work upto 80 °C for 50,000 hours[137,138,141] and conductivity shown at this temperature 10^{-2} S.cm^{-1}. But the major drawbacks of the Nafion is that it can work upto only 100 °C and does not work beyond this temperature due to dehydration at this temperature, is high in cost, need continuous humidity.[137,138,141] So as an alternative to Nafion many polymers have come to the market as polymer electrolyte membranes and these are polystyrene sulfonic acids,[142] sulfonated polyimides,[143] sulfonated poly(ether ketone)s,[144,145] sulfonated poly(arylene ether sulfone)s,[146] sulfonated poly(phenylene sulfide),[133] sulfonated polyphosphazenes,[147,148] acid doped polybenzimidazoles[35,45,55,58] etc. In the following Figure 1.15 few representative proton exchange membranes molecular structures are shown.
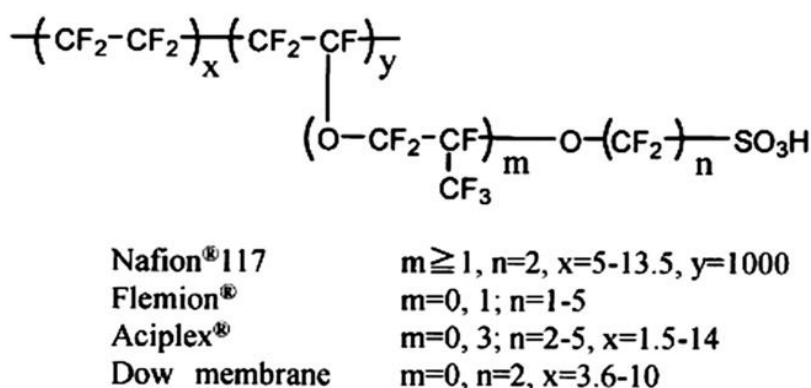
Figure 1.14. *The chemical structures of perfluorosulfonic acid based PEM (adapted from reference 132).*

Figure 1.15. *Examples of proton conducting polymers currently under investigation as PEM materials: (a) sulfonated poly(arylene ether sulfone); (b) sulfophenylated polysulfone; (c) sulfopropylated PBI; (d) sulfonated poly(arylene-co-arylene sulfone); (e) sulfonated naphthalenic polyimide (Ar, various aromatic moieties); (f) poly(aryloxyphosphazene) having sulfonimide units; (g) imidazole-terminated ethylene oxide oligomers ; and (h) Nafion^R marketed by the DuPont company (adapted from reference 146b).*

1.5.2.5. Phosphoric Acid (PA) Doped PBI Membranes as PEM:

As discussed above, there is a used of proton conductivity membranes which can operate at higher temperature so that the process associated with Nafion can be avoided. Although there are many ion conducting polymer are reported in the literature (some of them are shown in Figure 1.15), however each of them have many disadvantages. To solve this problem PA doped PBI based PEM membrane has

been developed. Membrane formation capability of polybenzimidazole is one of the most important parameter of PBI and which has been utilized very successfully in advanced applications like PEM fuel cell and osmosis. PBI form stable and strong hydrogen bond with protic solvents due to presence of imidazole ring which has proton donor amine (-NH-) and proton acceptor imine (-N=) bond.[94,128,182,183] The acid doped PBI can act as a polymer electrolyte membrane is first reported by Savinell.
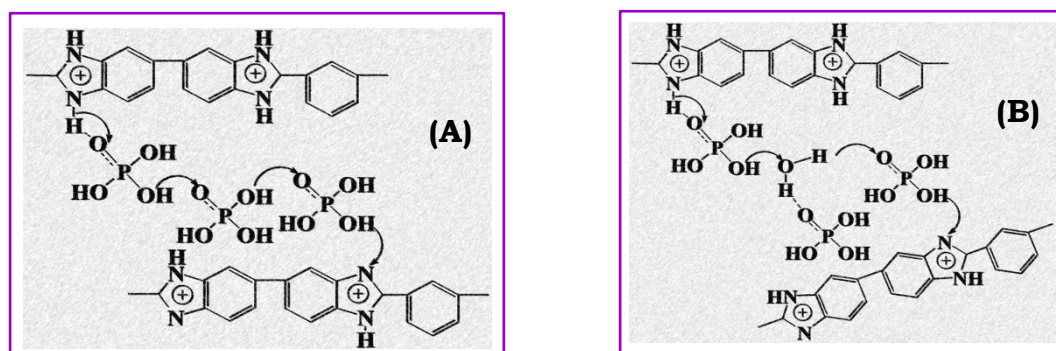
Figure 1.16. *Proton transfer process (A) acid- PBI- acid (B) acid- water-acid PBI (adapted from reference 190b).*

The acid doped PBI especially PA doped PBI is found to be very efficient polymer electrolyte membrane for use in fuel cell. The PA doping level of the PBIs vary from 3-20 moles per repeat unit. The mechanical stability of PBI gradually decreases with the increasing acid doping level.[149,150,151] The mechanical stability decreases due to acid molecules which go to the inside of polymer chains and form hydrogen bonding between acid and imidazole ring. The proton conductivity of PBI increases with the increase of acid doping level. But mechanical stability decreases which is not favourable and the excess acid leach out from the membrane, so the cell voltage decreases. For one PBI repeat unit 4 moles PA can be consumed via hydrogen bonding which is called bonded acid and the excess acid is known as the free acid. The free acids normally come out from the membrane. In order to maintain the mechanical as well as the acid doping level several many efforts have been made. The acid doping level depends on the time, acid concentration, temperature, molecular weight and the internal structure of PBI. The acid doped PBI is the most promising polymer electrolyte membrane due to the properties like mechanical stability, high proton conductivity upto 200 °C, low cost, almost zero water drag coefficient, chemically stable etc.[151,152] Wainright[94,151] reported that, the acid doped PBI (IV = 0.6 dL/g) shows proton conductivity of 2.5×10^{-2} Scm^{-1} with 5 moles PA per repeating unit at 150 °C. The proton conductivity of PBI membranes increases with the increase in temperature. The proton conductivity of acid doped PBI depends upon the water molecules associated. Two types of proton conduction mechanism of PA doped PBI is suggested and these are: (i) Grotthuss mechanics[153] which shows the phosphoric acid and the imidazole ring via hydrogen bonding and (ii) Vehicle mechanism[150] which proposes that the water molecules associated with acid and imidazole

ring via hydrogen bonding which sometimes called diffusion mechanism. Savagado[154] shows that proton conductivity of PBI depends on the acid types and the trends is as follows H_3PO_4 > $HClO_4$ > HNO_3 > HCl. Kawahara et el.[155] show that PA making a strong hydrogen bonding with imidazole ring which is proved by the FT-R spectra. The acid doped membrane swells after acid loading and hence decreases the gas permeability.[97,156] The Figure 1.16 shows the mechanisms of proton transfer in case of acid doped PBI.

1.5.2.6. Phosphoric Acid Doped PBI Membranes Fabrication Methods:

Different approaches have been developed for the fabrication of acid doped PBI membranes till today. We have tried to summarize most of these methods in detail in the following section:

(i) **Sol-gel process:** Sol-gel process is one popular method for fabrication of the membranes. This process was first introduced by Xiao et al.[36] as an in situ process. In this process membrane fabrication is carried out from the reaction mixture of PBI in polyphosphoric acid (PPA). The hot reaction mixture (~200 °C) is poured into the petridis and the membrane cast by doctor knives. In this method the membranes are thicker in comparison to the imbibing process. The PPA gets hydrolysed by atmospheric moisture (>50%) to form the PA loaded membrane. In this method more amounts of acid is consumed in comparison to the imbibing process. A schematic diagram of this is shown in Figure 1.17. This process can produce PA doped membrane with very high PA loading and hence very proton conduction. However, there are several limitation to this method as well.
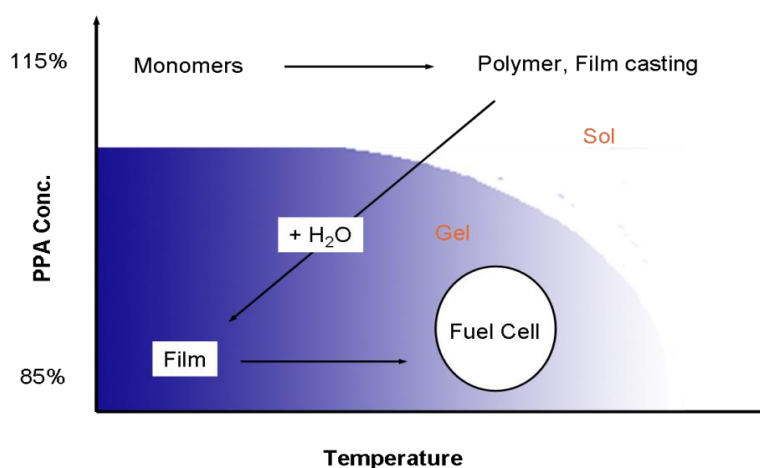
Figure 1.17. Fabrication of PA doped PBI membrane by PPA process (adapted from reference 21).

(ii) **Imbibing process:** Savinell et al.[157] first developed acid doped PBI membranes which is popularly called as imbibing method. In this method PBI is dissolved into the DMAc solvent with lithium chloride (LiCl) as a stabilizer at higher temperature. Then the solution is poured into petridis to fabricate the

membrane at a particular temperature. Then the fabricated membrane is boiled and soaked into deionized water to remove the LiCl and trace amount of the solvent. Then the dried membrane is soaked into the PA for few days and it is then removed from the acid. This process is good for proton conductivity and mechanical stability due to control of the acid doping level of the membranes. In this method the acid loading varies from 5 to 16 moles per repeat unit.[158] However. This method is very tedious and time consuming and moreover owing to the low PA loading, the proton conductivity is not high enough to get efficient fuel cell.

(iii) **Gel process:** Gel process is the easiest process to fabricate the acid loaded PBI membrane. In this process a reversible gel is formed at a particular concentration and temperature. In this process the polymers are dissolved into the PA medium at higher temperature (~180 °C) for 1 to 2 hours. Then the gel solution of the polymer poured into the petridis and the membrane casting takes place. In this process the acid doping level of the PA doped membranes are high and the mechanical properties also high.[159] Recently, our lab has developed this gel method which consumes 40 mole PA per repeat unit. The overall gel formation method is shown in the Figure 1.18. Till now in the literature, the highest PA loading is reported using this gel process. Among several advantages this process can offer, one of the major drawback of this is that the process is highly dependent on the PBI backbone structure and its solubility.
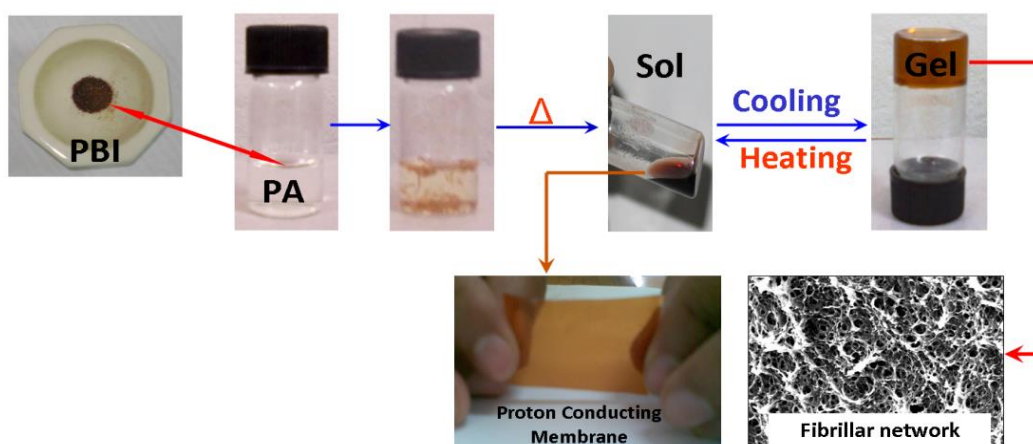
Figure 1.18. *Thermoreversible gelation of polybenzimidazole (PBI) in phosphoric acid (PA) (adapted from reference 190c).*

(iv) **Porogen process:** Porogen process is beneficial over other process for developing acid doped membranes. In the process the porogens like diphthalate (e. g. dimethyl, diethyl, dibutyl and diphenyl, as well as triphenyl phosphate) are mixed with the polymer solution at variable temperature. The well mixture solution is then casted onto the petridis and then the solvent is evaporated at a particular temperature according to the solvent boiling point. The dried membranes are boiled at high temperature with organic

solvent or water to remove porogens from the membrane. After removing the porogens, there is a formation of micro porosity in the membrane and then the membranes are soaked into the PA.[160] This method (Figure 1.19) has advantages that the loaded acid does not come out of the membranes so easily.
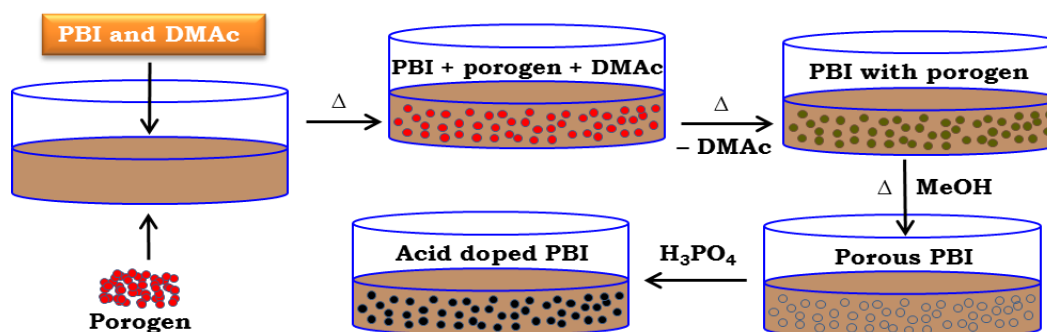
Figure 1.19. *Fabrication of PA doped PBI membrane by porous PBI process.*

(v) **Nanocomposite and blend membranes:** Polymer nanocomposites are two component mixtures which contain nano size filler in the polymer matrix and nano filler tare embedded to the polymer matrix. Recently, nano composites is a very attractive field for research due to the hi-performance and energy application to industrial as well as daily life.[104-106,161-167] The nano fillers are nano in size and highly affect the polymer backbone due to the interaction between polymer matrix and the nanofillers for their fictional groups presence. Till now various nano fillers have come to the market like carbon nanotube,[134,135] graphene,[138] chemically modified silica particles,[105,166] clay,[104,165] fullerene[131,162] etc. Among all, carbon nanotube, graphene and chemically modified silica have been great attraction due to high energy and performance applications. The polymer properties change hugely by adding small amount of the nano materials to the polymer matrix which does not disturb the polymer backbone and the processability of the polymer. A small amount of the nano filler changes the polymer properties like performances such as increased strength and heat resistance, decreased gas permeability and flammability, increased biodegradability of biodegradable polymers, mechanical properties, increase thermal and oxidative stability and acid loading capacity as well as proton conductivity. Nano fillers affect the polymer properties due to properties of nano fillers, such as, (i) low percolation threshold, (ii) arising a low volume fraction due to particle-particle correlation (orientation and position), (iii) extensive interfacial area (communication between matrix and filler) per volume of particles, (iv) short distances between the particles and (v) comparable size scales among the rigid nanoparticles inclusion. According to the dimension of nano fillers can be divided into three different types: (i) one dimension (i.e., clay), (ii) two dimension (i.e., carbon nanotube, graphene) and (iii) three dimension (i.e., silica). Recently, several PBI nanocomposite membrane have been made by using different type nano fillers.[156,168-172] Silicotungstic acid[169] and

phosphotungstic acid[168] increases the phosphoric acid doping level as well as the proton conductivity and the mechanical stability. Carbon nanotube and graphene have also increased the several properties of PBI.[171,172] Our group demonstrated that the ammine modified silica particle and the montmorillonite (Scheme 1.4 and Scheme 1.5) can improve several important properties of the OPBI. The multiwall carbon nanotubes (MWNTs) nanofillers in OPBI nanocomposites containing 0.1-1 wt% are synthesized by Shao et.al.[171]
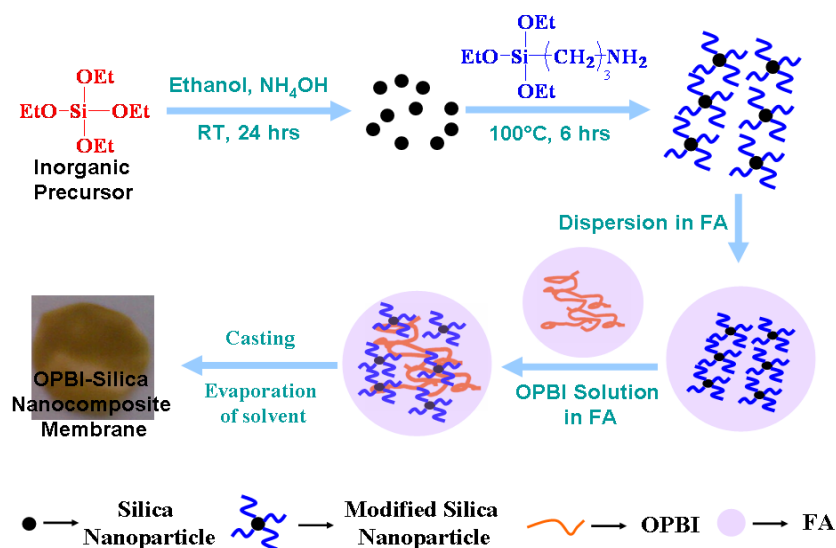
Scheme 1.4. *Schematic representation of OPBI nanocomposites preparation with amine modified silica nanoparticles (AMS) by solution blending process (adapted from reference 105).*
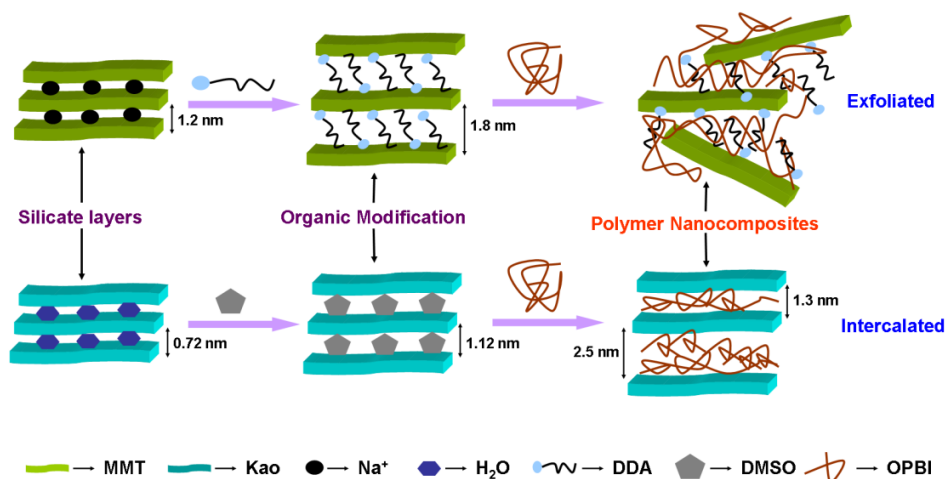
Scheme 1.5. *Schematic representation of OPBI nanocomposite with the organoclay (adapted from reference 104).*

PBI has a good capability to form a blend due to the presence of both proton donor (-NH-) and proton acceptor (-N=) hydrogen bonding sites which interact with other polymer functional groups.[173] PBI blends are extensively studied for their increasing processability, thermal stability, proton conductivity, mechanical properties etc. Different type blends have been prepared like polyimides (PI),[174] polyamide-imide (PAI),[175] polyarylate (PAr),[175] high-modulus aramide (HMA),[176] Poly(ether-imide),[177] poly(4-vinyl-pyridine) (PVP),[121,122] sulfonated poly sulfone,[121,122] aromatic polyethers.[121,122] Our group has demonstrated the formation of PBI with variation of fluorinated polymer like poly(vinylidene fluoride) (PVDF) polymer, polystyrene (Figure 1.20) and PVDF-HFP.[173,178] Several other polymers like sulfonated polymers, PVT are blended with PBI to improve the properties (Figure 1.21). We have observed significant enhancement in proton conduction upon blending.[179] Our group has recognized that presence of hydrophobic PVDF polymer with PBI which decreases the water uptake but increases the acid loading which affects proto conductivity.[173]
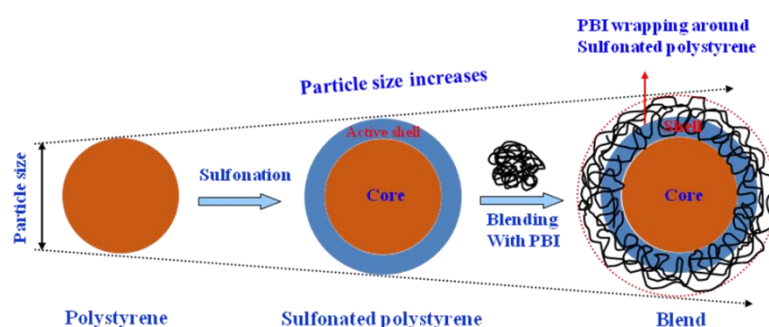
Figure 1.20. *Formation of core (polystyrene)-shell (polybenzimidazole) nanoparticles. (adapted from reference 173b).*

Figure 1.21. *Schematic representation of bled formation with polybenzimidazole (PBI) and poly(1-vinyl-1,2,4-triazole) (PVT) (adapted from reference 179).*

1.6. AIMS OF THE THESIS:

From the above discussion in this chapter, we can convincingly conclude the importance of PBI polymer in the different applications and most recently, especially in the field of PEM for fuel cell. Till now more than 5800 articles, patents and reviews have been published on PBI polymer which confirms the importance of PBI polymer. Despite of large number of literature known to us; till several problems and difficulties like solubility, flexibility and the proton conductivity are not addressed upto the satisfaction. Therefore we have explored the structurally different types of PBIs to tackle the above problems. Therefore the primary aim of this thesis is develop of new PBI structural varieties to solve the problems which are limiting the use of PBI. In Chapter 3 we have attempted to derivatize the PBI by attaching long alkyl chain with an aim that the synthesized PBI will be soluble and hence easily processable. Since most of the reported PBIs are synthesized from only one type of tetramine monomer called TAB, we aims to replace this with a new, easily synthesizable, alternative, efficient tetramine monomer called Py-TAB in Chapter 4. We also aim to prepare the PBI from this new Py-TAB in a way that the new PBI must be soluble, easily processable and should have better proton conductivity behaviour when doped with acid. We have noticed that, almost all the copolymers reported in the literature are made by altering the mole ratio of two dicarboxylic acids with a tetramine. Since we have successful in finding a new tetramine in Chapter 4, hence in Chapter 5, we aim to made new copolymer of PBI where tetramine mole fraction alters with a fixed dicarboxylic acid. This allows us to control the several important properties of PBI copolymer. In Chapter 6 we aim to prepare block copolymer of PBI with three different structures and alter the block length. We also aim to study the effect of these block length on the properties especially conducting properties of doped PBI membranes. The aims and objectives of each chapter of this thesis are explained in more details at the end of the introductory part of the individual chapters.

REFERENCES:

(1)   Brinker, K. C.; Robinson, I. M. U. S. Patent 2,895,948, 1959.

(2)   Vogel, H. A.; Marvel, C. S. *J. Polym. Sci.* **1961**, *50*, 511.

(3)   Vogel, H.; Marvel, C. S. *J. Polym. Sci. A* **1963**, *1*, 1531.

(4)   Plummer. L.; Marvel, C. S. *J. Polym. Sci. A* **1964**, *2*, 2559.

(5)   Marvel, C. S.; Ariz, T.; Vogel, H. A. U. S. Patent 3,174,947, 1965.

(6)   Choe, E. W.; Choe, D. D. *In Polymeric Materials Encyclopedia*; Salamone, J. C.; CRC Press: New York, **1996,** 5619.

(7)   Lee, H.; Stoffey, D.; Neville, K. *New Linear Polymers;* McGraw-Hill, New York, **1967**, Chapter 9.

(8)   Frazerr, A. H. High *Temperature Resistant Polymers;* Interscience: New York, **1968**, 138.

(9)   Critchley, J. P. *Prog. Polym. Sci.* **1970**, *2*, 47.

(10) Neuse, E. W. *Adv. Polym. Sci.* **1982**, *47*, 1.

(11) Power, E. D.; Serad, G. A. *High Performance Polymer: Their origin and Development,* Elesevier, New York, **1986**, 355.

(12) Buckley, A.; Stuetz, D.; Serad, G. A. *Encyclopedia of Polymer Science and Engineering,* Wiley, New York, **1987**, 572.

(13) Critchley, J. P.; Knight, G. J.; Wright, W. W. *Heat-resistant Polymers,* Plenum Press, New York, **1983**, 259.

(14) Prince A. E. U. S. Patent 3,509,108, 1970.

(15) Eguchi, T.; Ohfuji, Y. U. S. Patent 3,655,632, 1972.

(16) Neuse, E.W.; Loonat, M. S. *Macromolecules* **1983**, *16*, 128.

(17) Brand, R. A.; Bruma, M.; Kellman, R.; Marvel, C. S. J. Polym. Sci., Polym. Chem. Ed. **1978**, *16*, 2275.

(18) Higgins, J.; Marvel, C. S. *J. Polym. Sci.* **1970**, *A-1*, 171.

(19) Iwakura,Y.; Uno, K.; Imai, Y. *J. Polym. Sci.* **1964**, *A2*, 2605.

(20) Li, Q.; He, R.; Jensen, J. Q.; Bjerrum, N. J. *Chem. Mater.* **2003**, *15*, 4896.

(21) Xiao, L.; Zhang, H.; Scanlon, E.; Ramanathan, L. S.; Choe, E. W.; Rogers, D.; Apple, T.; Benicewicz, B. C. *Chem. Mater.* **2005**, *17*, 5328.

(22) Li ,Q.; Jensena, J. O.; Savinell, R. F.; Bjerrum, N. J. *Prog. Polym. Sci.* **2009**, *34*, 449.

(23) Choe, E. W.; Conciatori, A. B. U. S. Patent 4,452,972, 1984.

(24) Choe, E. W.; Conciatori, A. B.; Ward, B. C. U. S. Patent 4,463,167, 1984.

(25) Choe, E. W.; Conciatori, A. B. U. S. Patent 4,485,232, 1984.

(26) Choe, E. W.; Conciatori, A. B. ; Ward, B. C. U. S. Patent 4,506,068, 1985.

(27) Choe, E. W.; Conciatori, A. B. U. S. Patent 4,533,725, 1985.

(28)   Choe, E. W.; Conciatori, A. B. U. S. Patent 4,535,144, 1985.

(29)   Choe, E. W. *J. Appl. Polym. Sci.* **1994**, *53*, 497.

(30)   Lobato, J.; Caenizares, P.; Rodrigo, M. A.; Linares, J. J.; Manjavacas, G. *J. Membr. Sci.* **2006**, *280*, 351.

(31)   Xu, H.; Chen, K.; Guo, X.; Fang, J. *Polymer* **2007**, 48, 5541.

(32)   Chen, C. C.; Wang, L. F.; Wang, J. J.; Hsu, T. C.; Chen, C. F. *J. Mater. Sci.* **2002**, *37*, 4109.

(33)   Sannigrahi, A.; Ghosh, S.; Lalnuntluanga, J.; Jana, T. *J. Appl. Polym. Sci.* **2009**, *111*, 2194.

(34)   Asensio, J. N.; Borros, S.; Gomez-Romero, P. *J. Electrochem. Soc.* A **2004**, *151*, 304.

(35)   Maity, S.; Jana, T. *Macromolecules* **2013**, *46*, 6814.

(36)   Xiao, L.; Zhang, H.; Jana, T.; Scanlon, E.; Chen, R.; Choe, E. W.; Ramanathan, L. S.; Yu, S.; Benicewicz, B. C. *Fuel Cells* **2005**, *5*, 287.

(37)   Sannigrahi, A.; Ghosh, S.; Maity, S.; Jana, T. *Polymer* **2010**, *51*, 5929.

(38)   Jouanneau, J.; Mercier, R.; Gonon, L.; Gebel, G. *Macromolecules* **2007**, *40*, 983.

(39)   Sansone, M. J. U. S Patent 4,666,996, 1987.

(40)   Jorgensen, B. S.; Young, J. S.; Espinoza, B. F. U. S Patent 6,946,015, 2004.

(41)   Wang, K. Y.; Xiao, Y. C. Chung, T. S. *Chem. Eng. Sci.* **2006**, *61*, 5807.

(42)   Xu, H.; Chen, K.; Guo, X.; Fang, J.; Yin, J. *J. Membr. Sci.* **2007**, *288*, 255.

(43)   Carollo, A.; Quartarone, E.; Tomasi, C.; Mustarelli, P.; Belotti, F.; Magistris, A.; Maestroni, F.; Parachini, M.; Garlaschelli, L.; Righetti, P. P. *J. Power Sources* **2006**, *160*, 175.

(44)   Chuang, S. W.; Hsu, S. L. C. *J. Polym. Sci., Part A: Polym. Chem.* **2006**, *44*, 4508.

(45)   Maity, S.; Sannigrahi, A.; Ghosh, S.; Jana, T. *Euro. Polym. J.* **2013**, *49*, 2280.

(46)   Klahen, J. R.; Luther, T. A.; Orme, C. J.; Jones, M. G.; Wertsching, A. K.; Peterson, E. S. *Macromolecules* **2007**, *40*, 7487.

(47)   Gieselman, M. B.; Reynolds, J. R. *Macromolecules* **1992**, 25, 4832.

(48)   Sannigrahi, A.; Arunbabu, D.; Sankar, R. M.; Jana, T. *J. Phys. Chem. B* **2007**, *111*, 12124.

(49)   Qing, S.; Huang, W.; Yan, D. *Euro. Poly. J.* **2005**, *41*,1589.

(50)   Pu, H. T.; Liu, Q. Z. ; Liu, G. H. *J. Membr. Sci.* **2004**, *241*,169.

(51)   Qing, S.; Huang W.; Yan, D. *Chemical J. Chinese Universities Chinese* **2005**, *26*, 2145.

(52)   Qing, S.; Huang W.; Yan, D. *Acta Chimica Sinica* **2005**, *63*, 667.

(53)   Mader, J. A.; Benicewicz, B. C. *Fuel Cells* **2011**, *11*, 222.

(54)   Lee, H. S.; Roy, A.; Lane, O.; McGrath, J. E. *Polymer* **2008**, *49*, 5387.

(55)   Maity, S.; Jana, T. (*Chapter 6*).

(56)   Ng, F.; Bae, B.; Miyatake, K.; Watanabe, M. *Chem. Commun.* **2011**, *47*, 8895.

(57) Kang, Y.; Zou, J.; Sun, Z.; Wang, F.; Zhu, H.; Han, K.; Yang, W.; Song, H.; Meng, Q. *Int. J. Hydrogen Energy* **2013**, *38*, 6494.

(58) Ghosh, S.; Sannigrahi, A.; Maity, S.; Jana, T. *J. Phys. Chem. B* **2010**, *114*, 3122.

(59) Kim, T. H.; Kim, S. K.; Lim T. W.; Lee, J. C. *J. Membr. Sci.* **2008**, *323*, 362.

(60) Maity, S.; Jana, T. (*Chapter 5*).

(61) Kim, T. H.; Lim, T. W.; Lee, J. C. *J. Power Sources* **2007**, *172*, 172.

(62) Bower, E. A.; Rafalko, J. J. U. S. Patent 4,599,388, 1986.

(63) Sansone, M. J.; Gupta, B.; Stackman, R. W. U. S. Patent 4,814,399, 1989.

(64) Sansone, M. J. U. S. Patent 4,868,249, 1989.

(65) Sansone, M. J.; Kwiatek, M. S. U. S. Patent 4,933,397, 1990.

(66) Sansone, M. J. U. S. Patent 4,898,917, 1990.

(67) Sansone, M. J.; Gupta, B.; Forbes, C. E.; Kwiatek, M. S. U. S. Patent 4,997,892, Mar 5, 1991.

(68) Kallitsis, J. K.; Gourdoupi, N. *J. New Mater Electrochem. Sys.* **2003**, *6*, 217.

(69) Kim, S. K.; Choi, S. W.; Jeon, W. S.; Park, J. O.; Ko, T.; Chang, H.; Lee, J. C. *Macromolecules* **2012**, *45*, 1438.

(70) Aili, D.; Li, Q.; Christensen, E.; Jensen, J. O.; Bjerrum, N. J. *Polym. Int.* **2011**, *60*, 1201.

(71) Han, M.; Zhang, G.; Liu, Z.; Wang, S.; Li, M.; Zhu, J.; Li, H.; Zhang, Y.; Lew, C. M.; Na, H. *J. Mater. Chem.* **2011**, *21*, 2187.

(72) Luo, H.; Pu, H.; Chang, Z.; Wan D.; Pan, H. *J. Mater. Chem.* **2012**, *22*, 20696.

(73) Xu, H. J.; Chen, K. C.; Guo, X. X.; Fang, J. H.; Yin, J. *J. Polym. Sci. A: Polym. Chem.* **2007**, *45*, 1150.

(74) Sheratte, M. B. U. S. Patent 4,154,919, 1979.

(75) Kojima, T. *J. Polym. Sci. Polym. Phys. Ed.* **1980**, *8*, 1685.

(76) Shogbon, C. B.; Brousseau, J. L.; Zhang, H.; Benicewicz, B. C.; Akpalu, Y. *Macromolecules* **2006**, *36*, 9409.

(77) Sannigrahi, A.; Arunbabu, D.; Sankar, R. M.; Jana, T. *Macromolecules* **2007**, *40*, 2844.

(78) Sannigrahi, A.; Ghosh, S.; Maity, S.; Jana, T. *Polymer* **2011**, *52*, 4319.

(79) Sannigrahi, A.; Arunbabu, D.; Jana, T. *Macromol. Rapid Commun.* **2006**, *27*, 1962.

(80) Kulkarni, M.; Potrekar, R.; Kulkarni, R. A.; Vernekar, S. P. *J. Polym. Sci., Part A: Polym. Chem.* **2008**, *46*, 5776.

(81) Wang, J. T. W.; Hsu, S. L. C. *Electrochim. Acta* **2011**, *56*, 2842.

(82) Wang, B.; Tang, Y.; Wen, Z.; Wang, H. *Euro. Polym. J.* **2009**, *45*, 2962.

(83) Ye, H.; Huang, J.; Xu, J. J.; Kodiweera, N. K. A. C.; Jayakody, J. R. P.; Greenbaum, S. G. *J. Power Sources* **2008**, *178*, 651.

(84) Varma, I. K.; Veena. *J. Polym. Sci., Polym. Chem. Ed.* **1976**, *14*, 973.

(85) Varma, I. K.; Veena. *J. Macromol. Sci., Chem.* **1977**, *11*, 845.

(86) Lyoo, W. S.; Choi, J. H.; Han, S. S.; Yoon, W. S.; Park, M. S.; Ji, B. C. *J. Appl. Polym. Sci.* **2000**, *78*, 438.

(87) Kovacs, H. N.; Delman, A. D.; Simms, B. B. *J. Polym. Sci., Part A: Polym. Chem.* **1968**, *6*, 2103.

(88) Saegusa, Y.; Horikiri, M.; Nakurmura, S. *Macromol. Chem. Phys.* **1997**, *198*, 619.

(89) Kojima, T.; Yokota, R.; Kochi, M.; Kambe, H. *J. Polym. Sci.: Polym. Phys. Ed.* **1980**, *18*, 1673.

(90) (a) Lin, H. L.; Hu, C. R.; Lai, S. W.; Yu, T. L. *J. Membr. Sci.* **2012**, *389*, 399. (b) Yuan, Y.; Johnson, F.; Cabasso, I. *J. Appl. Polym. Sci.* **2009**, *112*, 3436. (c) Lin, H. L.; Chou, Y. C.; Yu, T. L.; Lai, S. W. *Int. J. Hydrog. Energy* **2012**, *37*, 383.

(91) (a) Lobato, J.; Canizares, P.; Rodrigo, M. A.; Linares, J. J.; Aguilar, J. A. *J. Membr. Sci.* **2007**, *306,* 47. (b) Ehlers, G.F. L.; Fisch, K. R.; Powell, W. R. *J. Polym. Sci. A* **1969**, *1,* 2931.

(92) Qian, G.; Benicewicz, B. C. *J. Polym. Sci., Part A: Polym. Chem.* **2009**, *47*, 4064.

(93) Menczel, J. D. *J. Them. Analys. Calmetry* **2000**, *59*, 1023.

(94) Litt, M.; Ameri, R.; Wang, Y.; Savinell, R.; Wainwright, *J. Mater. Res. Soc. Symp. Proc.* **1999**, *548*, 313.

(95) Li, Q. F.; He, R. H.; Jensen, J. O.; Bjerrum, N. J. *Fuel Cells* **2004**, *4*, 147.

(96) Li, Z. X.; Liu, J. H.; Yang, S. Y.; Huang, S. H.; Lu, J. D.; Pu, J. L. *J. Polym. Sci., Part A: Polym. Chem.* **2006**, *44*, 5729.

(97) Li, Q.; He, R.; Jensen, J. Q.; Bjerrum, N. *J. Chem. Mater.* **2007**, *19*, 350.

(98) He, R. H.; Li, Q. F.; Bach, A.; Jensen, J. O.; Bjerrum, N. J. *J. Membr. Sci.* **2006**, *277*, 38.

(99) Kim, T. A.; Jo, W. H. *Chem. Mater.* **2010**, *22*, 3646.

(100) Hubner, G.; Roduner, E. *J. Mater. Chem.* **1999**, *9*, 409.

(101) Gaudiana, R. A.; Conley, R. T. *J. Polym. Sci.* **1969**, *B7*, 793.

(102) Musto, P.; Karasz, F. E.; Macknight, W. J. *Polymer* **1993**, *34*, 2934.

(103) Li, Q.; Jensen, J. O.; Pan, C.; Bandur, V.; Nilsson, M. S.; Schönberger, F.; Chromik, A.; Hein, M.; Häring, T.; Kerres, J.; Bjerrum, N. J. *Fuel Cells* **2008**, *8*, 188.

(104) Ghosh, S.; Sannigrahi, A.; Maity, S.; Jana, T. *J. Phys. Chem. C* **2011**, *115*, 11474.

(105) Ghosh, S.; Maity, S.; Jana, T. *J. Mater. Chem.* **2011**, *21*, 14897.

(106) Wang, S.; Zhao, C.; Ma, W.; Zhang, N.; Zhang, Y.; Zhang , G.; Liu, Z.; Na, H. *J. Mater. Chem. A* **2013**, *1*, 621.

(107) Kerres, J.; Schonberger, F.; Chromik, A.; Haring, T.; Li, Q.; Jensen, J. O.; Pan, C.; Noye, P.; Bjerrum, N. J. *Fuel Cells* **2008**, *8,* 175.

(108) Ogata, Y.; Mogi, T.; Makita, Y. *J. Polym. Sci., Part B: Polym. Phys.* **2010**, *48*, 588.

(109) Nuopponen, M.; Ojala, J.; Tenhu, H. *Polymer* **2004**, *45*, 3643.

(110) Russo, P. S. *Reversible Polymeric Gels and Related Systems; Ed, ACS Symposium Series, American Chemical Society:* New York, **1986**.

(111) Guenet, J. M. *Thermoreversible Gelation of Polymers and Biopolymers; Academic Press:* London, **1992**.

(112) Paul, D. R. *J. Appl. Polym. Sci.* **1967**, *11*, 439.

(113) Kawanishi, K.; Komatsu, M.; Inoue, T. *Polymer* **1987**, *28*, 980.

(114) Mal, S.; Maiti, P.; Nandi, A. K. *Macromolecules* **1995**, *28*, 2371.

(115) Mal, S.; Nandi, A. K. *Polymer* **1998**, *30*, 6301.

(116) Dikshit, A. K.; Nandi, A. K. *Macromolecules* **2000**, *33*, 2616.

(117) Dasgupta, D.; Nandi, A. K. *Macromolecules* **2005**, *38*, 6504.

(118) Dikshit, A. K.; Nandi, A. K. *Langmuir* **2001**, *17*, 3607.

(119) Cassidy, P. E. *Thermally stable Polymers; Dekker,* New York, **1980**.

(120) Sillion, B. *High Perform. Polym.* **1999**, *11*, 417.

(121) Chang, T. S. *Polym. Rev.* **1997**, 37, 277.

(122) Chang, T. S. *Handbook of Thermoplastics; Marcel Dekker, Inc.* **1997**, *703*.

(123) Chung, T. S.; Xu, Z. L. *J. Membr. Sci.* **1998**, *147*, 38.

(124) Wang, K. Y.; Chung, T. S.; Rajagopalan, R. *Ind. Eng. Chem. Res.* **2007**, 46, 1572.

(125) Lv, J.; Wang, K. Y.; Chung, T. S. *J. Membr. Sci.* **2008**, 310, 557.

(126) Bhavsar, R. S.; Nahire, S. B.; Kale, M. S.; Patil, S. G.; Aher, P. P.; Bhavsar, R. A.; Kharul, U. K. *J. Appl. Polym. Sci.* **2011**, *120*, 1090.

(127) Wang, K. Y.; Y, Q.; Chung, T. S.; Rajagopalan, R. *Chem. Eng. Sci.* **2009**, *64*, 1577.

(128) Yeager, E. *Science* **1961**, *134*, 1178.

(129) *Fuel Cell Handbook, 6th Edition, EG & G Technical Services, Inc. U. S. Department of Energy;* November*,* **2002**.

(130) Mench, M. M. *Fuel Cell Engines, John Wiley & Sons, Inc.;* **2008**.

(131) Blomen, L. J. M. J. *Fuel Cell Systems; Plenum Press,* New York, **1993**.

(132) Rikukawa, M.; Sanui, K. *Prog. Polym. Sci.* **2000**, *25*, 1463.

(133) Hickner, M. A.; Ghassemi, H.; Kim, S. Y.; Einsla, B. R.; McGrath, J. E. *Chem. Rev.* **2004**, *104*, 4587.

(134) Basu, S*. Recent Trends in Fuel Cell Science and Technology, Springer,* New York, **2007**.

(135) Kerres, J. A. *J. Membr. Sci.* **2001**, *185*, 3.

(136) Roziere, J.; Jones, D. J. *Annu. Rev. Mater. Res.* **2003**, 33, 503.

(137) Xiao, L. *Ph.D. Thesis, Rensselaer Polytechnic Institute,* Troy*,* New York, **2003**.

(138) Einsla, B. R. *Ph.D. Thesis, Virginia Polytechnic,* Blackburg, Virginia, **2005**.

(139) Sukumar, P. R.; *Ph.D. Thesis, Max-Planck-Institute for Polymer Science,* Mainz, **2006**.

(140) Mauritz, K. A.; Moore, R. B. *Chem. Rev.* **2004**, *104*, 4535.

(141) Mehta, V.; Cooper, J. S. *J. Power. Sources* **2003**, *114*, 32.

(142) Gubler, L.; Scherer, G. G. *Adv. Polym. Sci.* **2008**, 215, 1.

(143) Marestin, C.; Gebel, G.; Diat, O.; Mercie, R. *Adv. Polym. Sci.* **2008**, *216*, 185.

(144) Gasa, J. V.; Weiss, R. A.; Shaw, M. T. *J. Polym. Sci.: Part B: Polym. Phys.* **2006**, *44*, 2253.

(145) Zaidi, S. M. J.; Mikhailenko, S. D.; Robertson, G. P.; Guiver, M. D.; Kaliaguine, S. *J. Membr Sci.* **2000**, *173*, 7.

(146) (a) Wang, F.; Hickner, M.; Kim, Y. S.; Zawodzinski. T. A.; McGrath, J. E. *J. Membr. Sci.* **2002**, *197*, 231. (b) Jannasch, P. *Curr. Opin. Colloid In. Sci.* **2003**, *8*, 96.

(147) Allcock, H. R.; Wood, R. M. *J. Polym. Sci.: Part B: Polym. Phys.* **2006**, *44*, 2358.

(148) Wycisk, R.; Pintauro, P. N. *Adv. Polym. Sci.* **2008**, *216*, 157.

(149) Pals, D. T. E.; Hermans, J. J. *J. Polym. Sci.* **1950**, *5*, 773.

(150) Pu, H.; Meyer, W.; Wegner, G. *J. Polym. Sci., Part B: Polym. Phys.* **2002**, *40*, 663.

(151) Weng, D.; Wainright, J. S.; Landau, U.; Savinell, R. F. *J. Electrochem. Soc.* **1996**, *143*, 1260.

(152) Samms, S. R.; Wusmus, S.; Savinell, R. F. *J. Electrochem. Soc.* **1996**, *143*, 1225.

(153) Bouchet, R.; Siebert, E. *Solid State Ionics* **1999**, *118*, 287.

(154) Xing, B.; Savadogo, O. *J. New. Mater. Electrochem. Syst.* **1999**, *2*, 95.

(155) Kawahara, M.; Morita, J.; Rikukawa, M.; Sanui, K.; Ogata, N. *Electrochim. Acta* **2000**, *45*, 1395.

(156) He, R.; Li, Q.; Xiao, G.; Bjerrum, N. J. *J. Membr. Sci.* **2003**, *226*, 169.

(157) Schechter, A.; Savinell, R. F. *Solid State Ionics* **2002**, *147*, 181.

(158) Mader, J.; Xiao, L.; Schmidt, T, J.; Benicewicz, B, C. *Adv. Polym. Sci.* **2008**, *216*, 63.

(159) (a) Emsley, J.; Reza, N. M.; Dawes, H. M.; Hursthouse, M. B.; Kuroda, R. *Phosphorus & Sulphur*, **1988**, *35*, 141, (b) Sannigrahi, A. *Ph.D. Thesis; University of Hyderabad:* Hyderabad, India, **2010**, (c) Ghosh, S. *Ph.D. Thesis; University of Hyderabad:* Hyderabad, India, **2011**.

(160) Yu, S.; Benicewicz, B. C. *Macromolecules* **2009**, *42*, 8640.

(161) Cao, T.; Webber, S. E. *Macromolecules* **1995**, *28*, 3826.

(162) Loy, D. A.; Assink, R. A. *J. Am. Chem. Soc.* **1992**, *114*, 3977.

(163) Ajayan, P. M.; Stephen, O.; Colliex, C.; Trauth, D. *Science* **1994**, *265*, 1212.

(164) Ajayan, P. M.; Schadler, L. S.; Giannaris, C.; Rubio, A. *Adv. Mater.* **2000**, *12*, 750.

(165) Vaia, R. A.; Krishnamoorti, R. *In Polymer Nanocomposites: Synthesis Characterization and Modeling; American Chemical Society:* Washington, DC, **2001**, *1*.

(166) (a) Althues, H.; Henle, J.; Kaskel, S. *Chem. Soc. Rev.* **2007**, *36*, 1454, (b) Kickelbick, G. *Prog. Polym. Sci.* **2003**, *28*, 83. (c) Antonucci, P. L.; Arico, A. S.; Creti, P.; Ramunni, E.; Antonucci, V. *Solid State Ionics* **1999**, *125*, 431, (d) Akcora, P.; Liu, H.; Kumar, S. K.; Moll, J.; Li, Y.; Benicewicz, B. C.; Schadler, L. S.; Acehan, D.; Panagiotopoulos, A. Z.; Pryamitsyn, V.; Ganesan, V.; Ilavsky, J.; Thiyagarajan, P.; Colby, R. H.; Douglas, J. F. *Nat. Mater.* **2009**, *8*, 354.

(167) Verdejo, R.; Bernal, M. M.; Romasanta, L. J.; Lopez-Manchado, M. A. *J. Mater. Chem*. **2011**, *21*, 3301.

(168) Staiti, P.; Minutoli, M.; Hocevar, S. *J. Power Sources* **2000**, 90, 231.

(169) Staiti, P. *Mater. Lett.* **2001**, *47*, 241.

(170) Javaid Zaidi, S.M. *Electrochem. Acta.* **2005**, *50*, 4771.

(171) Shao, H.; Shi, Z.; Fang, J.; Yin, J. *Polymer* **2009**, 50, 5987.

(172) Kang, J. Y.; Eo, S. M.; Jeon, I. Y.; Choi, Y. S.; Tan, L. S.; Baek, J. B. *J . Polym. Sci.: Part A: Polym. Chem.* **2010**, *48*, 1067.

(173) (a) Arunbabu, D.; Sannigrahi, A.; Jana, T. *J. Phys. Chem. B* **2008**, *112*, 5305. (b) Hazarika, M.; Arunbabu, D.; Jana, T. *J. Colloid Interf. Sci.* **2010**, *351*, 374.

(174) Guerra; G.; Cheo, S.; Williams, D. J.; Karasz, F. E.; Macknight, W. J. *Macromolecules* **1988**, *21*, 231.

(175) Jaffe, M.; Chen, P.; Choe, E. W.; Chang, T. S.; Makhija, S. *Adv. Polym. Sci.* **1994**, *117*, 297.

(176) Chang, T. S.; Herold, F. K. *Polym. Eng. Sci.* **1991**, *31*, 1950.

(177) Musto, P.; Karasz, F. E.; MacKnight, W. J. *Macromolecules* **1991**, *24*, 4762.

(178) Hazarika, M.; Jana, T. *Euro. Polym, J.* **2013**, *49*, 1564.

(179) Hazarika, M.; Jana, T. *ACS Appl. Mater. Interfaces* **2012**, *4*, 5256.

CHAPTER 2

Materials and Experimental Methods

This chapter describes the experimental procedures, characterization techniques and the source of all the materials used for the Chapter 3 to 6. Also in this chapter we have described the instruments details and the corresponding methods used throughout the work of this thesis. These are briefly discussed below.

2.1. MATERIALS:

Benzaldehyde (99%) and 4-amino acetophenone were purchased from Acros Organic, India. Ammonium acetate (96%), acetic acid (99.5%), acetic anhydride (97%) and *N,N*-dimethyl acetamide (DMAc, HPLC grade, 99.8%) were obtained from Fisher Scientific, India. Methane sulfonic acid (MSA) and N-methyl-2-pyrrilidone (NMP) were procured from SRL, India. Sulfuric acid (H_2SO_4, 99.8%), *N*-methyl-2-pyrrilidone (NMP), orthophosphoric acid (H_3PO_4, 85%), KOH were procured from Merck, India. Hydrazine monohydrate, 1-bromopentane, 1-bromohexane, 1-bromooctane and 1-iodoethane were obtained from Avra Synthesis Pvt. Ltd., India. Fuming nitric acid was purchased from Faiz chemicals, India. Isophthalic acid (IPA) and terephthalic acid (TPA), formic acid (FA) 1-bromoheptane, 1-bromodecane, 1-bromododecane, 1-bromotetradecane and 1-bromohexadecane were procured from SRL, India. NaH was received from Finar Chemicals India Pvt. Ltd. The NMR solvent dimethyl sulfoxide (DMSO-d_6), 3,3',4,4'-tetraaminobiphenyl (TAB), biphenyl-4,4'-dicarboxylicacid (BDA), 4,4'-oxybis(benzoicacid) (OBA), 4,4'-dicarboxybenzophenone (BPDA), 4,4'-(hexafluoroisopropylidene)bis(benzoicacid) (HFIPA), polyphosphoric acid (PPA, 115%) were procured from Sigma-Aldrich. 2,6-bis(3',4'-diaminophenyl)-4-phenylpyridine (abbreviated as Py-TAB) monomer was synthesized in the laboratory in 100 g scale using previously reported method after some modification.[1] The reaction sequence for synthesis of Py-TAB is shown in Scheme 2.1. All chemicals were used without further purification.
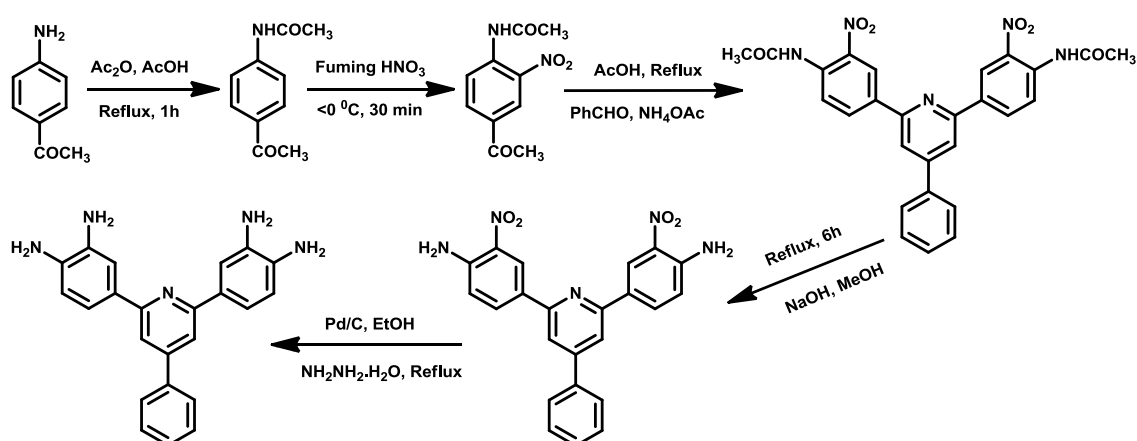
Scheme 2.1. *Synthesis procedure of 2,6-bis(3',4'-diaminophenyl)-4-phenylpyridine(Py-TAB)*

2.2. CHRACTERIZATION METHODS:

2.2.1. Molecular Weight Measurements:

2.2.1.1 Viscosity:

The viscosity measurements of the polymer solutions in H_2SO_4 were carried out at 30 °C in a constant temperature water bath using a Cannon Ubbelohde capillary dilution viscometer (model F725) (Figure 2.1). The inherent viscosity (IV) values were calculated from the flow time data. For all the flow time measurements, 0.2 g/dL polymer solution in H_2SO_4 (98%) were used. The molecular weight of PBI in the related literature has been expressed in terms of IV measured from sulfuric acid solution.
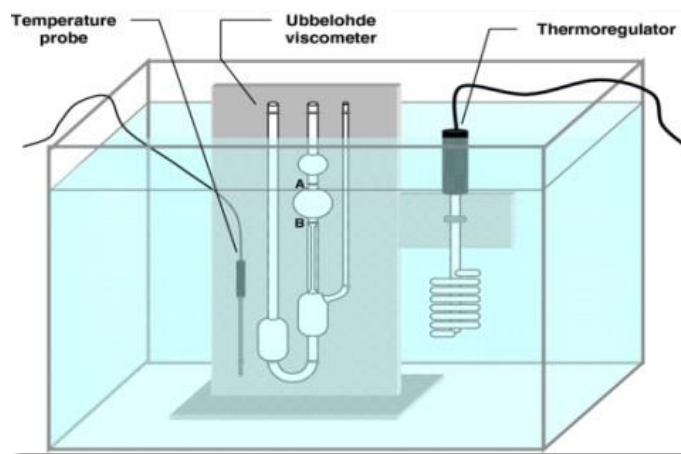
Figure 2.1. *Cannon Ubbelohde capillary dilution viscometer with visco bath (adapted from google image).*

2.2.1.2. Gel Permeable Chromatography:

The molecular weights of pyridine bridge polybenzimidazoles (Py-PBIs; Chapter 4) and Py-PBI copolymers (PBI-*co*-Py-PBI; Chapter 5) were measured at 65 °C using a gel permeation chromatography (GPC, Waters 515 HPLC) with an RI detector (Waters 2414). DMAc with LiCl (1mg/ml) was used as mobile phase. Py-PBIs and copolymers solutions in DMAc of concentration 1.0 mg/ml were prepared. To avoid aggregation of polymers, 1.0 mg/ml of LiCl was mixed into the polymer/DMAc solutions. Then these polymer solutions were filtered through 0.45 μm PTFE filter paper. Then 20 μL of these filtered polymer solutions (in DMAc with LiCl) were injected as samples in the GPC column (Styragel HMW 6E DMF) which was kept at 65 °C. The solution flow rate was 0.5 ml/min. Narrow molecular weight distribution polystyrene standards (Polymer Standards Service) with polydispersity index ≤ 1.1 were used in the GPC molecular weight calibration.

2.2.2. Membrane Fabrication:

All the different types of PBIs (parent PBI, N-PBI, Py-PBI, PBI-*co*-Py-PBI and *m*PBI-*block-p*PBI) were dissolved in DMAc solvent (used for Chapter 3, 4 and 5 work) and methane sulfonic acid (MSA, used for Chapter 6 work) at 2% (w/v) concentration by continuous stirring for 12 h (Figure 2.2). Then clear solutions were filtered through 0.5 µm PTFE filter paper. The filtered solutions were poured into flat glass petridis and solvents were evaporated from the solution at 80 °C for 12 h (for DMAc solvent) and 100 °C for 24 h (for MSA solvent) in a hot air oven. Homogeneous membranes were obtained, taken out from glass petridis, soaked and boiled de-ionized water for three times to remove trace amount of solvents. Finally these membranes were kept in vacuum oven at 120 °C for two days for complete removal of solvent. The obtained membranes thickness was approximately 30 to 40 µm. These membranes were stored in the desiccator for further study.
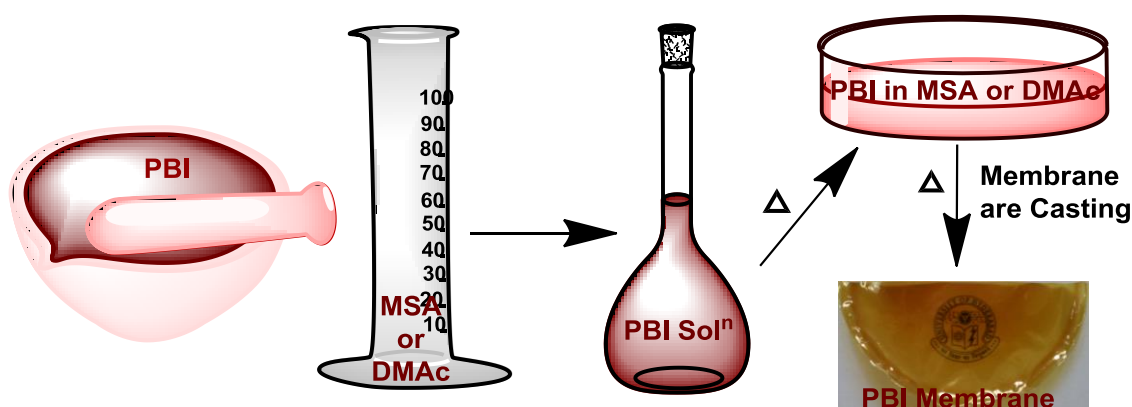
Figure 2.2. Fabrication of polybenzimidazole (PBI) membrane in MSA/DMAc solvent.

2.2.3. Spectroscopic Studies:

2.2.3.1. FT-IR Study:

The FT-IR spectra of all the PBI films were recorded on a (Nicolet 5700 FTIR) FT-IR spectrometer. The PBI films of thickness 30-40 µm were made from DMAc and MSA solutions (2% w/v) of polymers. The resolution of the IR spectrometer is about 4 cm^{-1}.

2.2.3.2. ^{1}H NMR Study:

All the NMR spectra were recorded using Bruker AV 400 MHz NMR spectrometer at room temperature using DMSO-d_6 as NMR solvent.

2.2.3.3. UV-visible Study:

Electronic absorption spectra were recorded on a Cary-100Bio (VARIAN) UV-visible spectrometer. The photophysical studies of all the different types PBIs (for Chapter 4 and 5) were carried out by using dilute solution of polymer in DMAc. The concentrations of the solution for all the PBI samples were kept at 2×10^{-5} M, where molarity is calculated by considering repeat unit as 1 mol.

2.2.3.3. Fluorescence Study:

Steady-state fluorescence emission spectra were recorded on a Jobin Yvon Horiba spectrofluorimeter (Model Fluoromax-4). All the different kinds of PBIs (for Chapter 4 and 5) samples were dissolved in DMAc and the spectra were recorded. The concentration of solutions were 2×10^{-5} M considering PBIs repeat unit molecular weight was consider as 1 mole.

2.2.4. Solubility Test:

The solubility of all structurally different kinds PBIs polymers were checked in common organic solvents like DMAc, NMP, FA, MSA, H_2SO_4, dichloromethane (CH_2Cl_2), chloroform ($CHCl_3$), and tetrahydrofuran (THF). The solubility was carried out up to 3 wt%. The solubility was first carried out in room temperature and then at heating condition.

2.2.5. Thermal Study:

The thermal stability of structurally different PBIs were recorded on a thermo-gravimetric and differential thermal analysis (TG-DTA) (model no: Netzsch STA 409PC) instrument from 30-800 °C and 900 °C with a scanning rate of 10 °C/min in presence of continuous nitrogen flow. All times ~ 8-10 mg samples were used.

2.2.6. Mechanical Study:

The temperature dependent dynamical mechanical properties of all PBI polymers dried films were measured using a dynamic mechanical analyzer (DMA) (TA Instruments, model Q-800). Films of 25 mm × 5 mm × 0.04 mm (L × W × T) dimensions were cut and clamped on the films tension clamp in the pre-calibrated instrument. The samples were annealed at 100 ° C for 30 minutes and then scanned from 100 °C to 450 °C at the heating rate of 4 °C/min. The storage modulus (E), loss modulus (E') and tan δ values were measured at a constant linear frequency of 10 Hz with preload force of 0.01N.

2.2.7. X-ray Diffraction:

The wide angle X-ray diffraction (WAXD) patterns of the dry PBI polymers powders were collected in Philips powder diffraction apparatus (model PW 1830). The powders were taken in a glass

slide and the diffractograms were recorded using nickel-filtered Cu Kα radiation at a scanning rate of 0.6° 2θ/min. The temperature dependent WAXD recorded upto 400 °C from powder sample of N-PBI and PBI.

2.2.8. H_3PO_4 Doping Level:

All the dried membranes obtained from DMAc solution were immersed in H_3PO_4 solution of various concentrations (30, 40, 50 and 60, 70 and 85 wt%) for 7 days. After that the membranes were taken out from the acid bath and extra acid from membrane sample were wiped by filter paper and stored in air tight packet. The H_3PO_4 (PA) doping level of membranes were determined by titrating the membrane samples with pre standardized 0.1(N) sodium hydroxide solutions using a Metrohm Titrino Titrator (model 702). The dry weight of the polymer was obtained by washing the samples with de-ionized water and then drying in vacuum oven at 100 °C for 24 hours. The acid doping levels are expressed as mols of phosphoric acid per mole of PBI repeat unit. The acid doping level was calculated as following equation:

$$\text{Acid (PA) doping level} \quad = \frac{W_{PA}}{W_{dry}} \times \frac{M_{PBI}}{M_{PA}} \qquad \text{-------------- (2.1)}$$

Where W_{PA} and W_{dry} are the weight of acid and dry membrane respectively and M_{PBI} and M_{PA} are the repeating unit molecular weight of the polymer and molecular weight of the phosphoric acid respectively. For each sample, three similar size pieces of sample were titrated and the reported acid doping level data are the average of these three values. In case of Chapter 3, PA doping calculated by using repeat unit molecular weight as, $M_{PBI} = M_{PBI} (1-F_{N-PBI}) + M_{N-PBI} \times F_{N-PBI}$. Where, M_{N-PBI} and F_{N-PBI} are the repeat unit molecular weight of N-PBI and the fraction of repeat unit respectively. In case of Chapter 5, PA doping calculated as Chapter 3 like repeat unit molecular weight of PBI and the fraction of Py-PBI repeat unit.

2.2.9. Water uptake, Swelling Ratio and Swelling Volume:

Water uptake and swelling ratio of the membranes were obtained by immersing the membranes in water for seven days. The PBIs membranes were thoroughly vacuum dried for 24 h at 100 °C before experiment. Then membranes were immersed in de-ionized water for seven days at room temperature. The weight and dimensions of membranes were measured before and after immersion into the water. The water uptake was measured gravimetrically. The wet membranes were quickly wiped to remove the surface water. The water uptake and swelling ratio measurements of the membranes were carried out in triplicate independently with different pieces of membranes to check the reproducibility of the results and finally the average values were taken. Water uptake, swelling ratio and swelling volume of the membranes were calculated using following equations:

$$\text{Water Uptake} = \frac{W_w - W_d}{W_d} \times 100\% \qquad \text{------------- (2.2)}$$

$$\text{Swelling Ratio} = \frac{L_w - L_d}{L_d} \times 100\% \qquad \text{------------- (2.3)}$$

$$\text{Swelling Volume} = \frac{V_w - V_d}{V_d} \times 100\% \qquad \text{------------- (2.4)}$$

Where W_w, V_w, L_w are wet membranes weight, volume, length respectively and W_d, V_d, L_d are dry membranes weight, volume, length respectively.

2.2.10. Oxidative Stability:

The oxidative stability of Py-PBI and PBI-*co*-Py-PBI samples were investigated by Fenton's reagent. Five pieces of sample with the approximate size 2 cm × 1 cm × 0.003 cm were taken for Fenton test. The samples were immersed in 3% H_2O_2 containing of 4 ppm Fe^{2+} solutions. All the Fenton solutions were prepared freshly for the experiments. Samples were kept at 60 °C up to 120 h. Samples were removed every 24 h interval and their weight were measured after washing and drying in vacuum oven for 24 h. We have calculated the degradation amount of membrane from the weight difference between before and after dipping in the Fenton reagent.

2.2.11. Conductivity Study:

We have measured the proton conductivities with the help of a four-probe impedance method by using a Zahner Impedance spectrometer (ZENNIUM PP211) over a frequency range from 1 Hz to 100 KHz. We have also used Metrohm Autolab Impedance spectra (PGSTAT302N) over frequency range1 Hz to 100 KHz for samples of Chapter 5 & 6. A rectangular size PA doped PBI membrane (1.5 cm × 4.0 cm) and four platinum wires were set in a homemade Teflon cell Figure 2.3.[2,3] Two outer electrodes (1.5 cm apart) supply current to the cell, while the two inner electrodes 0.5 cm apart on opposite sides of the membrane measure the potential drop. For the temperature dependence proton conductivity measurement the cell was placed in an oven. The membranes were dried at 100 °C for 2 h. Then membrane samples were then cooled in a vacuum oven and taken out just before conductivity measurement to keep the samples dry. The conductivities of the membranes were measured from room temperature to 160 °C at 20 °C intervals. Before measuring the conductivity, the samples were kept in the oven at each temperature for 30 minutes to reach the temperature equilibrium. Results obtained using the above temperature profile and testing procedure was found reproducible. A two-component model (Figure 2.4) with an Ohmic resistance in parallel with a capacitor was employed to fit the experimental curve of the membrane resistance across the frequency range (the Nyquist plot)[4-8]. The conductivities of the membrane at different temperatures

were calculated from the membrane resistance obtained from the Ohmic resistance. Proton conductivity was then calculated from the following equation:

$$\sigma = \frac{D}{LBR} \qquad \text{-------------} \quad (2.5)$$

Where, D is the distance between the two current electrodes 0.5 cm apart, L and B are the thickness and width, respectively, and R is the measured resistance value.
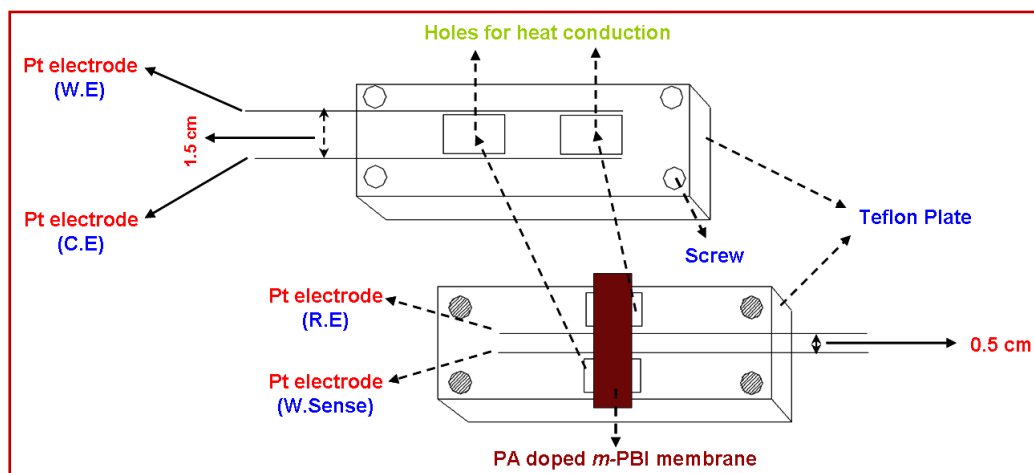
Figure 2.3. *Home made conductivity cell used to measure the proton conductivity of PA doped m-PBI gel membrane. Two parts as shown in the figure are clamped together by the screw and the cell was kept inside a programmable oven to control the temperature (adapted from reference 2)*
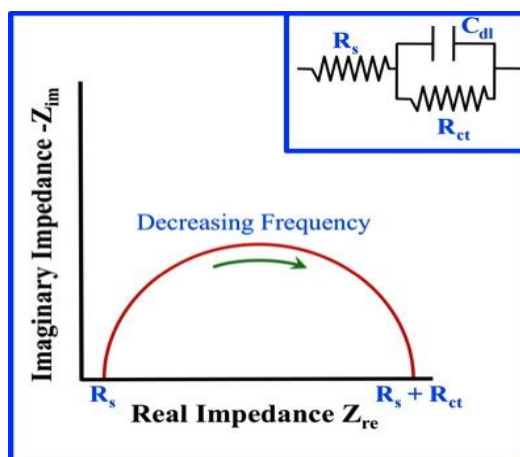
Figure 2.4. *Electrochemical two component impedance spectral diagram (Nyquist plot) (adapted from google image).*

REFERENCES:

(1)   Liu, J. G.; Wang, L. F.; Yang, H. X.; Li, H. S.; Li, Y. F.; Fan, L.; Yang, S. Y. *J. Polym. Sci., Part A: Polym. Chem.* **2004**, *42*, 1845.

(2)   Sannigrahi, A. *Ph.D. Thesis; University of Hyderabad:* Hyderabad, India, **2010**.

(3)   Sannigrahi, A.; Ghosh, S.; Maity, S.; Jana, T. *Polymer* **2011**, *52*, 4319.

(4)   Bouchet, R.; Siebert, E. *Solid State Ion.* **1999**, *118*, 287.

(5)   He, R.; Li, Q.; Xiao, G.; Bjerrum, N. J. *J. Membr. Sci.* **2003**, *226*, 169.

(6)   Pu, H. *Polym. Int.* **2003** *52*, 1540.

(7)   Verma, A.; Scott, K. J. *Solid State Electrochem.* **2010**, *14*, 213.

(8)   Shen, C. H.; Jheng, L. C.; Hsu, S. L. C.; Wang, J. T. W. J. *Mater. Chem.* **2011**, *21*, 15660.

CHAPTER 3

N-Alkyl Polybenzimidazole: Effect of Alkyl Chain Length

Maity, S.; Sannigrahi, A.; Ghosh, S.; Jana, T. *Euro. Polym. J.* **2013**, *49*, 2280-2292.
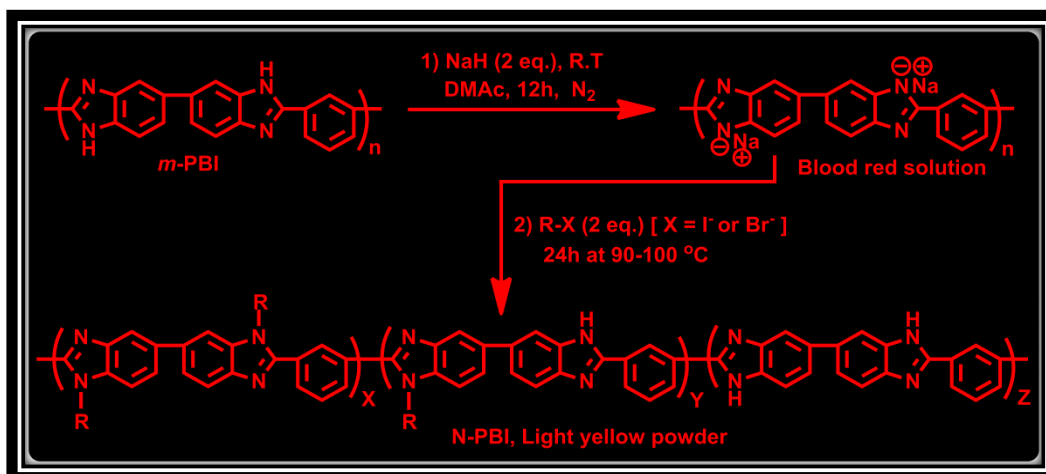
3.1. INTRODUCTION:

Due to large demand of efficient, powerful and eco-friendly source of energy devices, polymer electrolyte membrane fuel cell (PEMFC) has become the one of the most promising candidate for mobile and as well as stationary applications. Although varieties of PEMs are known in the literature, till today the perfluoro sulfonic acid based membrane (Nafion)[1] is mostly used despite of many drawbacks like its high cost and relatively low stability at high temperature etc. As an alternative of Nafion, recently phosphoric acid (PA) doped polybenzimidazole (PBI) membrane[2] has been used and found to be the best alternative because of unique properties such as excellent thermochemical and mechanical stability,[3] high proton conductivity up to 180 °C, zero water osmotic drag coefficient etc.[4-6] However, one of the major drawbacks of PBI is its poor solubility in common organic solvents. It is soluble in only highly polar solvents like *N,N*-dimethyl acetamide (DMAc), *N,N*-dimethyl formamide (DMF), *N*-methyl-2-pyrrolidone (NMP), dimethyl sulfoxide (DMSO) at higher temperature.[7-9] Hence, structural modification of the PBI polymer to increase the solubility and processability in common organic solvents and low boiling solvents is one of the key challenge to be addressed for the development of PBI based PEMFC.

Till today many research groups made efforts to produce different types of PBI structure like poly(2,5-benzimidazole) (AB-PBI),[10] sulfonated PBI,[11-13] hyperbranched polybenzimidazole,[14] crosslinked polybenzimidazole,[15] pyridine based polybenzimidazole[16] N-substituted polybenzimidazole etc.[17-31] Unfortunately, the solubility and processability of PBI as discussed above are not resolved very satisfactorily. Among various efforts, it has been noticed that substitution on the -N atoms of the imidazole rings of the PBI backbone by appropriate functionalities resulted better solubility and processability of PBI in common organic solvents. Synthetically, PBI can be modified in two ways either by modification of monomers or substitution (grafting) to the -N atoms of mother PBI. PBI backbone has highly rigid rod aromatic structure which influences and controls the crucial physical properties of PBI. Upon grafting the PBI chain rigid structure might get affected which in turn may alters the mechanical strength, thermal stability and other physical properties. The chain flexibility which enhances the solubility of polymer can be adjusted by introducing the flexible group[32,33] in the polymer backbone or by substitution in the -N atoms with alkyl,[30] alkyl sulfonated[34] or benzene sulfonate[24] groups. However, a careful optimization has to be made between the chain flexibility and thermomechanical stability. Imidazolium hydrogens are acidic in nature; in each repeat unit backbone has two substitutable hydrogen atoms. So, when DMAc solution of PBI treated with alkali hydride like NaH at higher temperature, it forms a polyanion and then one can do substitution reaction with electrophile like R-CH$_2$-X.

Earlier, it has been reported that the degree of substitution does not depend on the concentration of alkali hydride and electrophile.[23] However, the effect of electrophile molecular size or other words the effect of alkyl chain length in case the electrophile is alkyl halide on the degree of substitution has not been

studied. PBI has very high glass transition temperature (T_g > 400 °C) attributing the rigid structure which resulting poor solubility. The very small free volume because of intra and inter hydrogen bonding in PBI are found to be the main reason for high T_g and less solubility. It can be hypothesized that grafting of long alkyl chain in the PBI backbone may decrease the packing density and thereby increase the free volume by disrupting the hydrogen bonding which in turns decrease the T_g and increase the flexibility of PBI. Earlier, in few reports it was observed that T_g can be decrease with grafting,[25] unfortunately no systematic study has been carried out to understand the effect alkyl chain length size on the T_g and other physical properties. Also it will be interesting to analyze the effect of alkyl chain length on the properties of PA doped N-PBI.

In this Chapter, we have synthesized a series of N-alkyl grafted (ethyl, pentyl, hexyl, heptyl, octyl, decyl, dodecyl, tetradecyl and hexadecyl) polybenzimidazoles. The chemical modification of polybenzimidazole established by ^{1}H NMR and FT-IR technique. The thermal stability, mechanical property and the glass transition temperature (T_g) are measured by thermogravimetric analyzer (TGA), dynamic mechanical analyzer (DMA), respectively. Efforts have been made to prepare PA doped membranes and all types of essential characterization were carried out to evaluate the potential of these acid doped membranes for their use as PEM in fuel cell. In this present work, our goal is to improve the flexibility and solubility of PBI by grafting alkyl chain in the backbone.

3.2. SYNTHESIS:

3.2.1. PBI Synthesis:

The synthetic procedure (Scheme 3.1) for PBI was similar to our earlier reports.[35,36] Briefly the process was as follows: equal moles of TAB and IPA were taken into a three neck flask with PPA (115%) and the reaction mixture continuously stirred by mechanical stirrer in nitrogen atmosphere at 190-210 °C for 24 h. After completion of the reaction PBI was poured into water, then neutralized by sodium bicarbonate ($NaHCO_3$) and thoroughly washed with water. The PBI was dried in vacuum oven at 120 °C for 24 h. The inherent viscosity (IV) of polymer was measured to evaluate the molecular weight of the synthesized polymer. The measured IV of PBI was 1.02 dL/g at 30 °C in H_2SO_4 (98%).
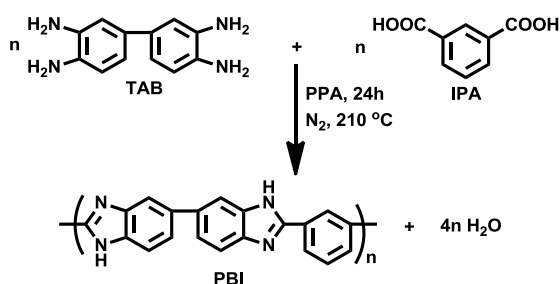
Scheme 3.1. *Synthesis of meta polybenzimidazole (m-PBI).*

3.2.2. Synthesis of N-Alkyl Substituted PBI:

The different chain lengths (from C_2 to C_{16}) alkyl groups were substituted to the imidazole -NH functional group of the PBI backbone (Scheme 3.2). The reactions were carried out as follows: firstly 250 mL 0.5% (w/v) PBI (4.06 mmol) solution in DMAc solvent was prepared and the solution was filtered through 0.5 µm PTFE membrane. This PBI solution in DMAc was stirred in 500 mL three neck flask for 1 h at 30 °C in nitrogen atmosphere. Then 0.195 g (8.12 mmol) NaH was added and then stirring was continued for another 12 h. The PBI in DMAc solution became red in colour after addition of NaH. Then alkyl halide (8.12 mmol) was added to this solution and reflux at 100 °C for overnight (12 h). Then this solution was poured into ice-water mixture and filtered. The residue was thoroughly washed with water which was light brown colour. The N-substituted PBIs (N-PBIs) were kept in vacuum at 120 °C for 48 h to remove the moisture and other solvents.
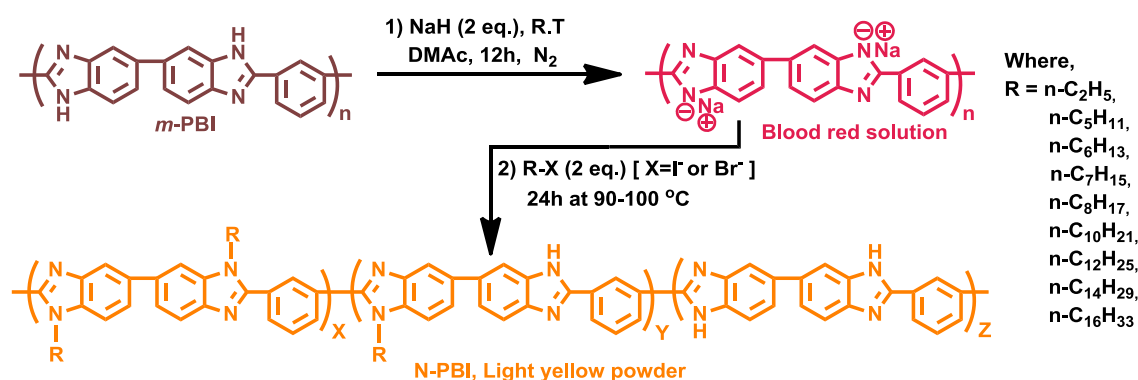
Scheme 3.2. *Synthesis of N-substituted PBI (N-PBI).*

3.3. CHARACTERISATION:

All the information about the materials used in this study and solubility test, membrane fabrication method from the synthesized N-PBIs and the experimental methods of all the characterization techniques which include viscosity, spectroscopic characterization by Fourier transform infrared spectroscopy (FT-IR) and proton NMR, X-ray diffraction (WAXD), thermogravimetric analysis (TGA) and dynamic mechanical analysis (DMA), H_3PO_4 doping level, water uptake, swelling ratio, swelling volume and the proton conductivity measurements for all the N-PBI polymers are discussed in the Chapter 2.

3.4. RESULTS AND DISCUSSION:

3.4.1. FT-IR and ¹H NMR Characterization:

The linear alkyl chains of different chain lengths (C_2-C_{16}) are grafted to the backbone of PBI using reaction conditions as presented in Scheme 3.2. FT-IR and ¹H NMR spectroscopy were used to

characterize the grafting of alkyl chains in the backbone. The FT-IR spectra of parent PBI and alkyl grafted PBI (N-PBI) membranes are shown in Figure 3.1. PBI is hygroscopic in nature and can absorb moisture up to 5-15% of its weight.[37] The presence of O-H stretching frequency at 3620 cm^{-1} is confirmed the hygroscopic nature of parent PBI and N-PBIs. Figure 3.1 shows that with increasing alkyl chain length, the intensity of O-H stretching frequency gradually decreases which indicates the hydrophilic nature of alkyl grafted PBI decreases owing to the hydrophobic character of alkyl chain. The broad peak at 3415 cm^{-1} because of free N-H stretching frequency of benzimidazole is present in N-PBIs with almost negligible intensity indicating that partial alkyl substitution has taken place in imidazole group. The bands at ~2943 cm^{-1} and ~2865 cm^{-1} are the C-H stretching frequency of methyl and methylene (near to N atom of benzimidazole) group of long alkyl chain, respectively. A characteristic absorption band near at ~3063 cm^{-1} is attributing to aromatic C-H stretching frequency. The presence of both imidazole -NH group and long alkyl chain in the N-PBIs indicates that 100% alkyl substitution did not take place and therefore the molecular structure of the N-PBIs is as shown in Scheme 3.2. Hence it becomes necessary to estimate the % of N-alkylation in N-PBIs and we have utilized NMR spectroscopy as described in the following section.
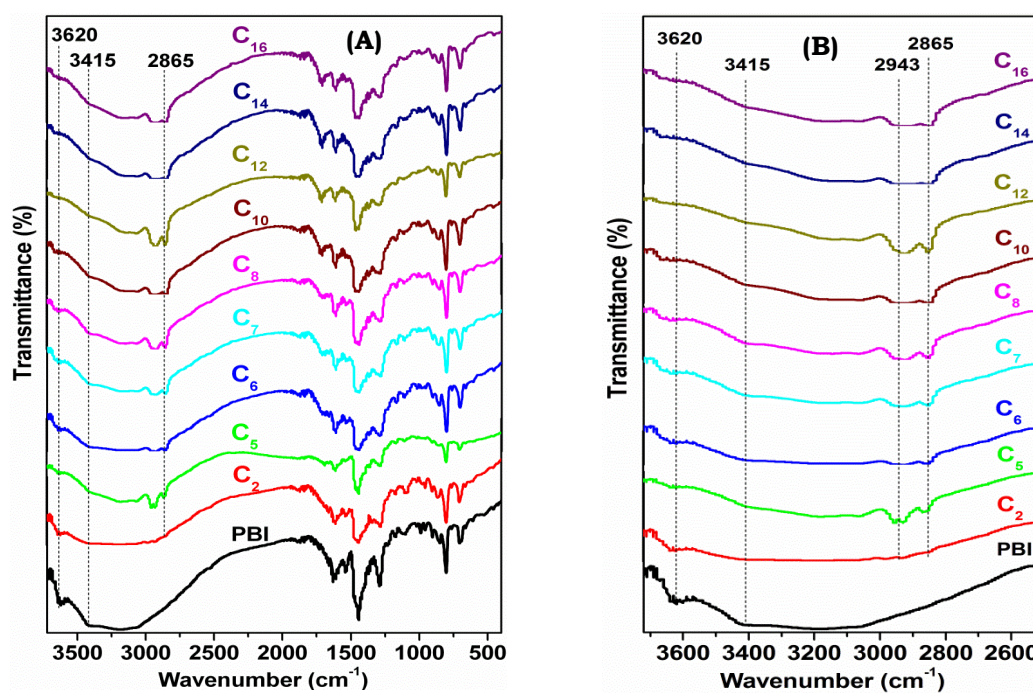
Figure 3.1. *FT-IR spectra of N-substituted Polybenzimidazoles (N-PBI) (A), magnified portion in the region 2500 to 3725 cm^{-1} (B). All spectra recorded from the thin films (~40 μm).*

The representative ^{1}H NMR spectra of N-PBIs along with peak assignments and chemical structures are shown in Figure 3.2. The NMR signal matches perfectly as expected from the chemical structure. The characteristic aromatic C-H protons are appearing at δ ~7.5-9.5 ppm for all the N-PBI.[38]

Signals at $\delta \sim 4.47$ ppm (denoted as g) for the methylene protons attached to imidazolium nitrogen atom. The other alkyl chain proton signals are appeared at $\delta \sim 1.72$, 1.04 and 0.7 ppm for h, i and j as denoted, respectively. The signals h, i for methylene groups and j for methyl group of alkyl chains. A careful analysis and comparison of methylene (4.47 ppm) and aromatic protons signals suggests partial N-alkylation. We estimated % of N-alkylation of N-PBIs from the ^{1}H NMR peaks integral ratio (Table 3.1) which alters from 40% to 65% depending on the size of alkyl chain length. The % of N-alkylation are obtained from the ^{1}H NMR peaks integral ratio of -NCH$_2$ (δ 4.47 ppm) and all aromatic hydrogens (δ 7.5-9.5). Higher % of N-alkylation observed in case of larger chain may be due to the better electrophilic character of long chain alkyl halides. The above estimation and the complicated aromatic protons peak patterns of N-PBIs compared to PBI ascribes the N-PBIs structure as shown in Scheme 3.2 which resembles the copolymer structure.
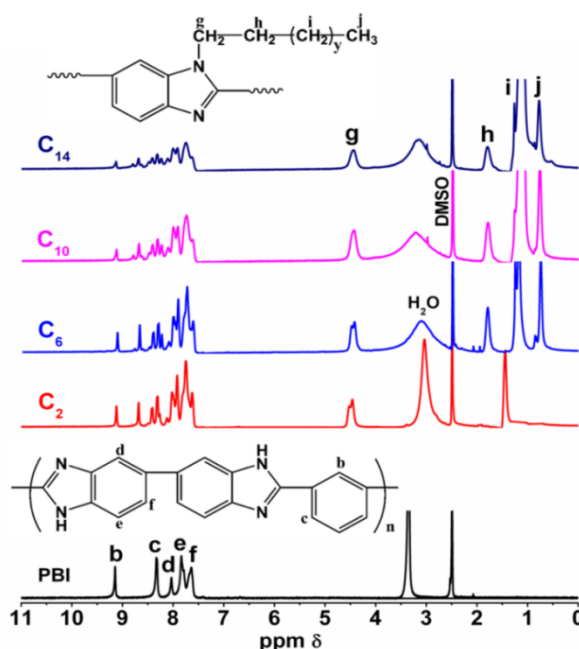
Figure 3.2. *^{1}H NMR spectra of few representative N-substituted PBI along with parent PBI. DMSO-d$_6$ is used as NMR solvent.*

3.4.2. Solubility Test:

The solubility of parent PBI and N-PBIs are checked in several common organic solvents like DMAc, NMP, DCM, THF, formic acid (FA), chloroform etc. and the solubility chart is shown in Table 3.1. It is clearly evident from the solubility chart (Table 3.1) that the PBI and N-PBIs are highly soluble in DMAc and NMP. Interestingly, N-PBIs show very high solubility in formic acid (FA) whereas parent PBI is partially soluble. This enhanced solubility of N-PBI is because after alkyl substitution the PBI backbone becomes less rigid (as seen from the T_g data in the later section) by increasing their face-to-face packing distances

Table 3.1. *Solubility of N-substituted PBI in different organic solvents and % of N-alkylation.*

Polymer	% of N–alkylation[a]	DMAc	NMP	FA	CH_2Cl_2	$CHCl_3$	THF
PBI	–	++	++	+	–	–	–
PBI–C_2	42.25	++	++	++	–	–	–
PBI–C_5	46.25	++	++	++	–	–	–
PBI–C_6	50.25	++	++	++	–	–	–
PBI–C_7	57.75	++	++	++	–	–	–
PBI–C_{10}	60.75	++	++	++	–	–	–
PBI–C_{12}	65.00	++	++	++	–	–	–
PBI–C_{14}	63.50	++	++	++	–	–	–

++ : Soluble at ambient temperature; **+** : Partial solubility; **-** : Insoluble even after heating; solubility was carried out up to 3% (w/v) concentration.

[a] Estimated from the ^{1}H NMR peaks integral ratio of -NCH_2 (δ 4.47 ppm) and aromatic hydrogens.
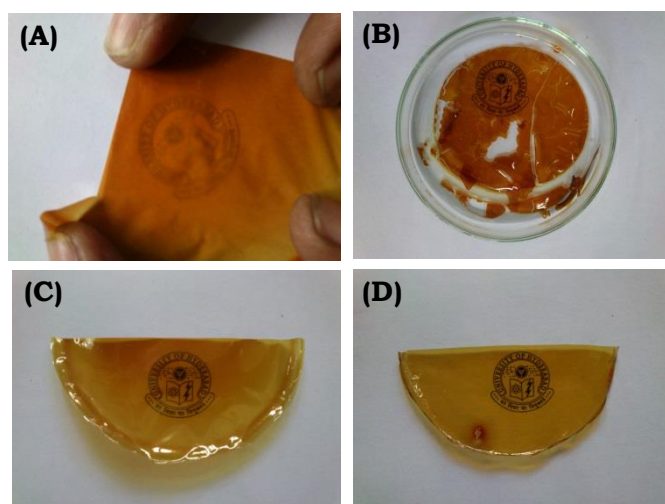
Figure 3.3. *Photographs of membranes casting from (A) DMAc, (B) formic acid solution of PBI and (C) DMAc,(D) formic acid of C_{14} N-PBI samples.*

(discussed in the WAXD section) which helps to decrease the self-association between the chains. FA is a low boiling solvent and hence one can readily remove the solvents to cast the film from the polymer solution. Earlier, we have observed that certain type of PBI structure like [poly(4,4'-diphenylether-5,5'-bibenzimidazole)], an ether linkage present in the polymer backbone, forms very transparent homogeneous films when films were made from FA solution.[39] Therefore the solubility in FA helps easy processability. Table 3.1 clearly shows that N-PBIs have very high solubility compared to parent PBI which makes these modified PBI as easily processable material when FA is used as processing medium. Figure

3.3 compares the photographs of PBI and N-PBI membranes obtained from DMAc and FA. It is very clear from photographs that the N-PBI membranes obtained from FA are very much homogeneous and transparent compared to all other membranes. Also, parent PBI membrane from FA is mechanically weak owing to its low solubility as evident from the photographs. Therefore it can be summarized that N-substitution with alkyl group in the PBI backbone enhances the processability and solubility of rigid PBI.

3.4.3. Structural Prediction of N-PBIs:

3.4.3.1. Thermal Study:

The thermal stability of N-PBI samples obtained from TG-DTA studies under nitrogen atmosphere are presented in Figure 3.4. It is known that approximately 5-15% weight loss occurs for PBI due to its hygroscopic nature at 100 °C. We observed here from TGA that with increasing alkyl chain length the initial weight loss due to hygroscopic nature decreases indicating that N-PBIs are less hydrophilic than PBI, which is also observed from FT-IR studies presented in earlier section. Although N-PBIs are found to be less thermally stable compared to parent PBI, however all the samples show first major degradation above ~300 °C, indicating good and enough thermal stability for the use as thermally stable processable materials.
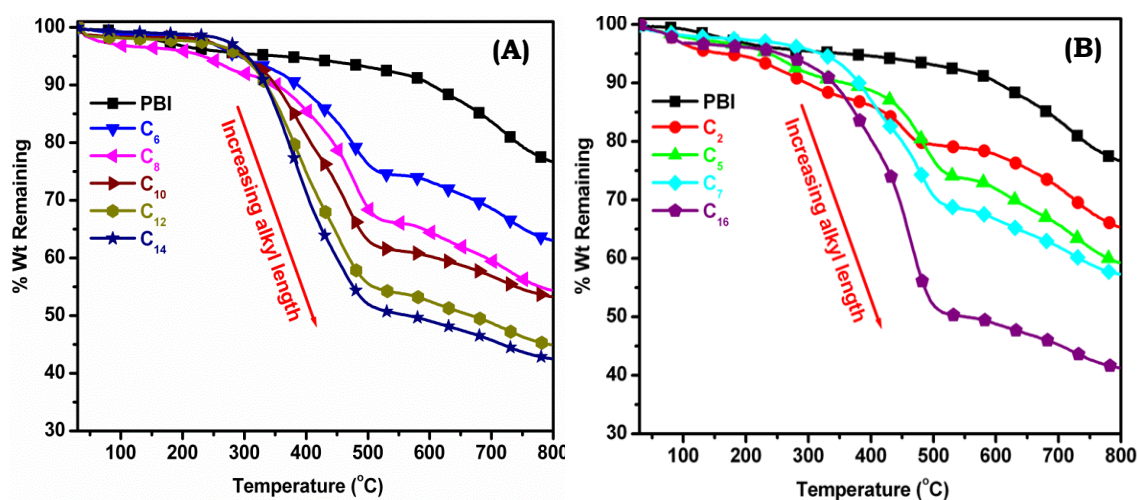
Figure 3.4. TGA curves of N-PBI under N_2 atmosphere. Samples are separated in two figure for the clarity.

All the N-PBIs samples display weight losses in three stages; first one is at ~100 °C due to absorb moisture, the second weight loss is at ~300 °C followed by third weight loss at ~510 °C owing to the degradation of PBI backbone (Figure 3.4A & B). Parent PBI does not exhibit second weight loss at ~300 °C. This attributes that at ~300 °C, the grafted alkyl chains are knocked out form the PBI backbone. The extent of this weight loss for N-PBI samples increases with increasing alkyl chain length attributing the

fact that this weight loss is associated with N-substituted PBI backbone. Hence the second weight loss is due to degradation of grafted alkyl chains. The degradation behaviour of N-PBIs also predicts the partial grafting of alkyl group in the polymer backbone and copolymer type molecular structure as discussed in the previous section from NMR results.

3.4.3.2. Thermo-mechanical Studies:

The effect of alkyl substitution on the glass transition temperature (T_g) and the mechanical properties of the PBI are studied using DMA both in the sub-ambient temperature (-120 °C to 100 °C) as well as in the higher temperature (100-450 °C). DMA data for both the temperature ranges are shown in Figures 3.5 and 3.6. It is known that the peaks appeared in the loss modulus (E'') and tan δ plot corresponds to the thermal transitions of the polymer. Parent PBI exhibits a transition at -78 °C (from E'' plot) [-71 °C from tan δ plot] which corresponds to the rotation of the *m*-phenylene ring.[40] This transition can be called as δ transition and it shifts towards higher temperature with increasing size of alkyl chain length in case of N-PBIs (Figure 3.5, Figure 3.6 and Table 3.2). This indicates that the substituted alkyl group interferes the *m*-phenylene ring rotation resulting the δ transition shift. Parent PBI also displays a transition at ~30 °C which is known as γ transition,[40] but this transition is absent in N-PBI (Figure 3.5). The δ transition and T_g values obtained from loss modulus (E'') and tan δ plots are listed in Table 3.2. The parent PBI shows only one T_g at 350 °C (tan δ, inset of Figure 3.6) which is in agreement with previous results.[36]

DMA studies exhibit peculiar thermomechanical properties for N-PBI samples. The decrease in T_g value compared to parent PBI is expected as flexible alkyl groups are incorporated in the PBI backbone; T_g value of N-PBI decreases with increasing alkyl chain length up to C_7 (Table 3.2). We observed two distinct T_g's from C_8 substitution onwards for all N-PBI (Table 3.2, Figure 3.5 and Figure 3.6); in which one T_g (T_{g1} <300 °C) appears much below than the parent PBI T_g (~350 °C) and other T_g (T_{g2}) appears quite close to T_g of parent PBI. It also must be noted that T_{g1} decreases with increasing alkyl chain length; however T_{g2} remains almost unaltered with size of alkyl chain length. The presence of two T_g's and variation of one T_g with altering the chemical structures clearly attributes the copolymer structure of the N-PBI backbone. The lower T_g (T_{g1}) is the segmental motion of the PBI backbone in which N-substitution has taken place with the alkyl chain and the higher T_g (T_{g2}) is the segmental motion of the unsubstituted PBI backbone. The alteration in T_{g1} with increasing alkyl chain length is due to the increase alkyl size and this result again confirms that T_{g1} is the N-PBI T_g. The other T_g (T_{g2}) does not display the variation much since this is the T_g for unsubstituted PBI, whatever little variation is observed that is because of the effect of T_{g1}. So the above discussion clearly attributed the copolymer nature of N-PBI which consists of alkyl substituted and unsubstituted PBI chains. Our above DMA results are also tally with our TGA observation. The overall decrease of T_g drives the enhanced solubility of N-PBIs.
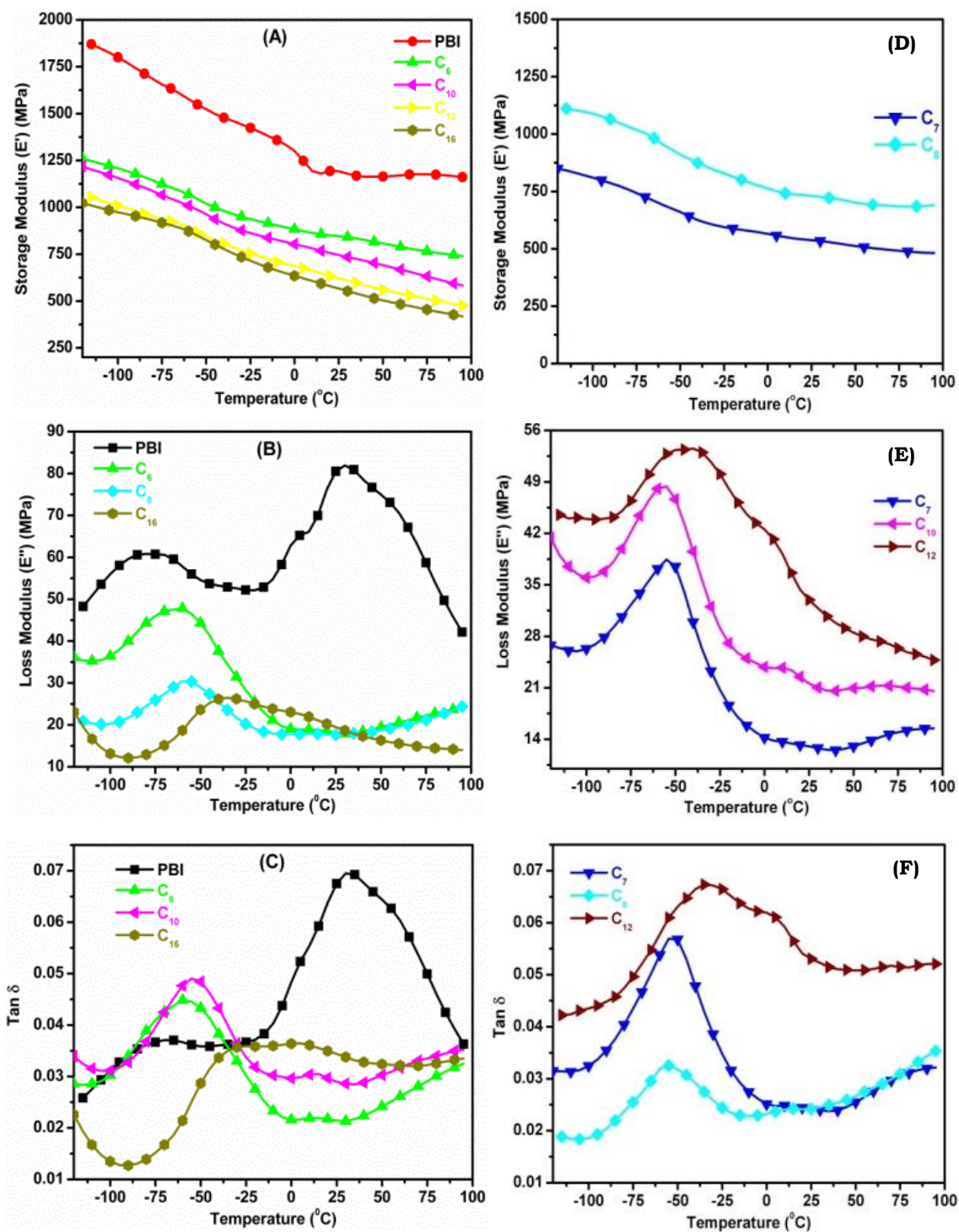
Figure 3.5. *Temperature dependent (-120 to 100 °C) plots of mechanical properties obtained from DMA of N-PBI samples; (A & D) storage modulus (E'), (B & E) loss modulus (E") and (C & F) tan δ. Samples are separated into two figures for the clarity of presentation.*
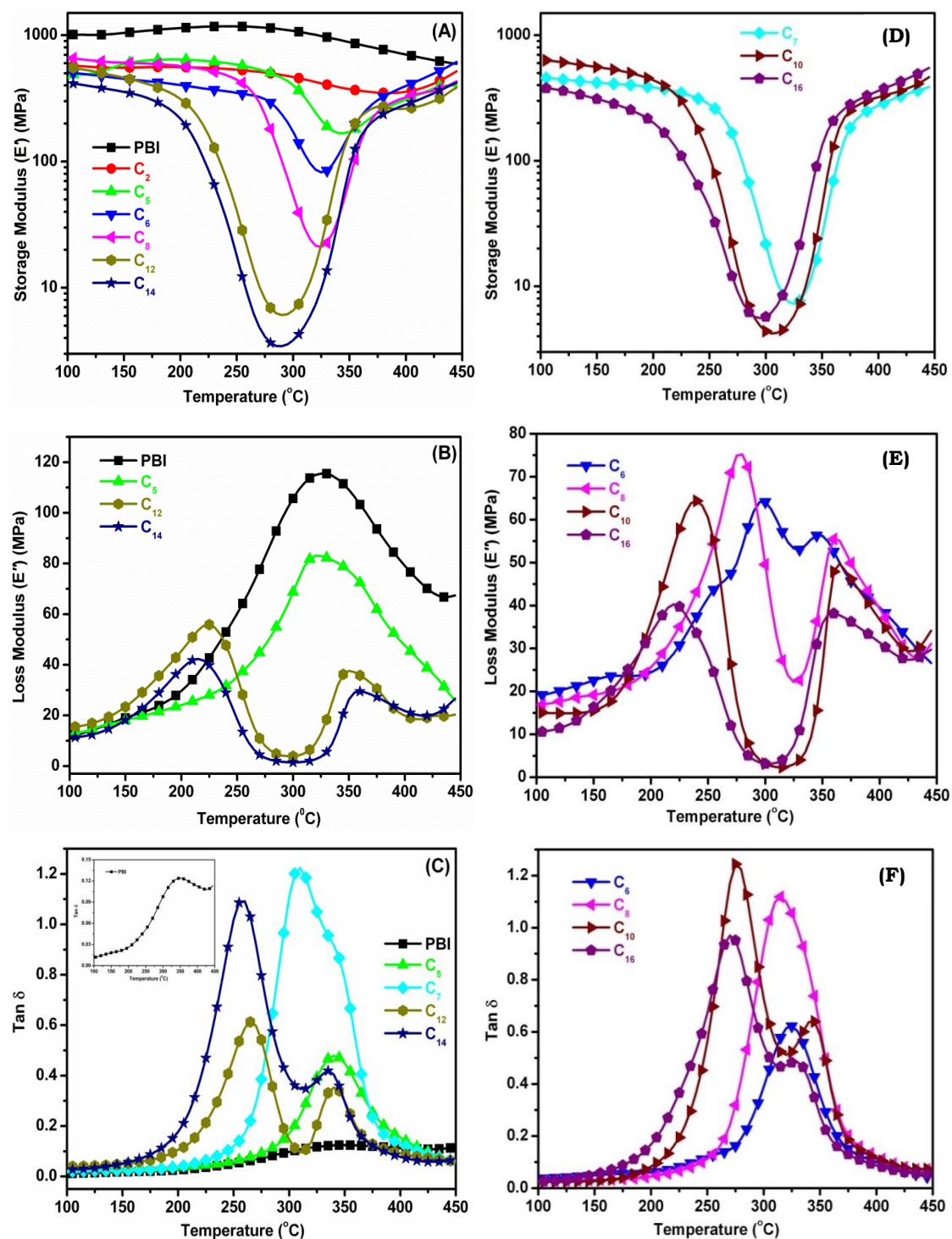
Figure 3.6. *Temperature dependent (100-450 °C) plots of mechanical properties obtained from DMA of N-PBI samples; (A & D) storage modulus (E'), (B & E) loss modulus (E") and (C & F) tan δ. Inset of (C) is the magnified tan δ plot of parent PBI. Samples are separated into two figures for the clarity of presentation.*

Table 3.2. *Various thermal transitions data of N-PBI films obtained from DMA study.*

Polymer	T_g (^{o}C) from E"	T_g (^{o}C) from Tan δ	δ (^{o}C) from E"	δ (^{o}C) from Tan δ
PBI	327	350	−78	−71
C_5	320	341	–	–
C_6	297	324	−62	−58
C_7	275	309	−54	−55
C_8	279, 361	315	−57	−55
C_{10}	240, 366	278, 343	−55	−54
C_{12}	225, 353	264, 340	−41	−32
C_{14}	215, 359	258, 335	–	–
C_{16}	220, 359	270, 330	−36	−27
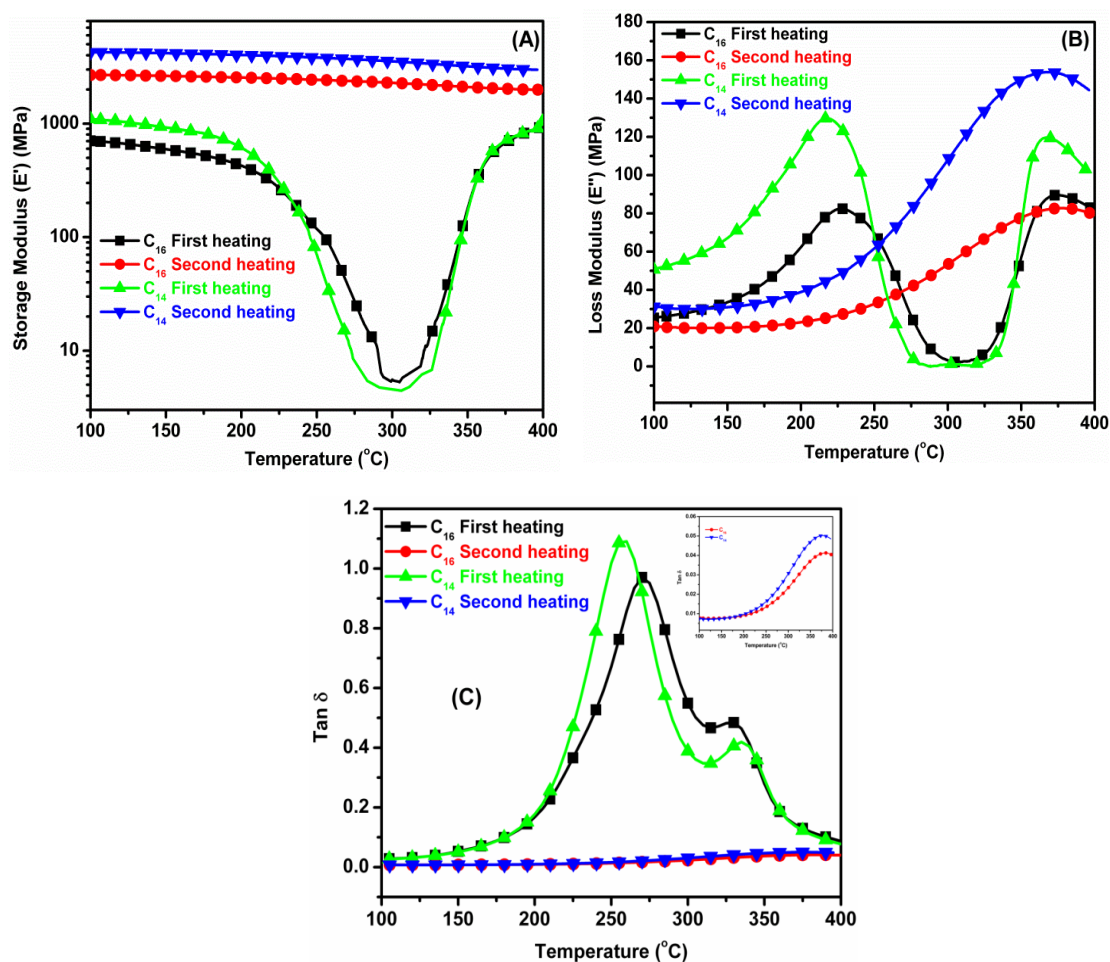
Figure 3.7. *Temperature dependent (first and second heating scans) plots of mechanical properties obtained from DMA of C_{14} and C_{16} N-PBI samples; (A) storage modulus (E'), (B) loss modulus (E") and (C) tan δ. Inset of (C) is the magnified second heating scan plot of C_{14} and C_{16} samples.*
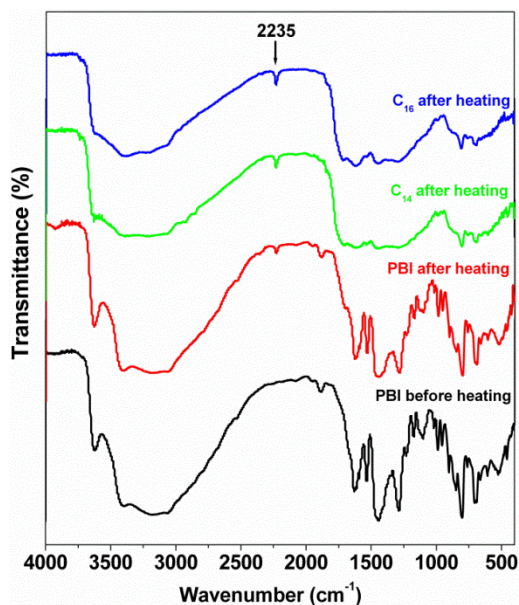
Figure 3.8. *FT-IR spectra of PBI, C$_{14}$ and C$_{16}$ samples after DMA scan and annealing at 400 °C.*
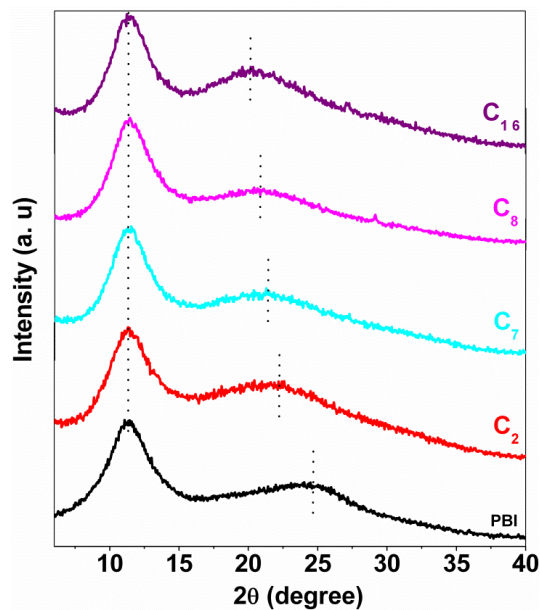
Figure 3.9. *WAXD patterns of N-PBI samples at room temperature. Powder samples are used to record the WAXD pattern.*
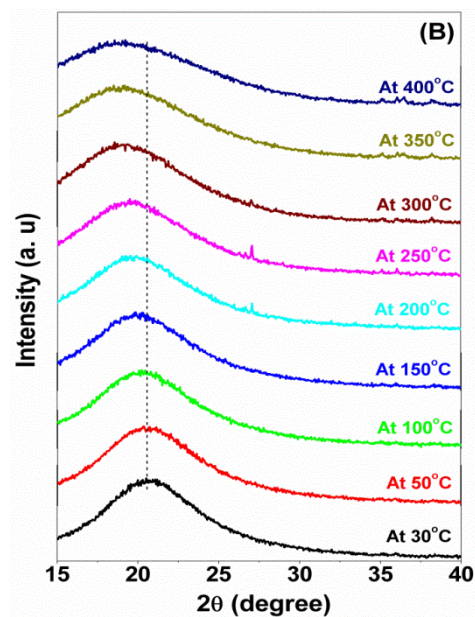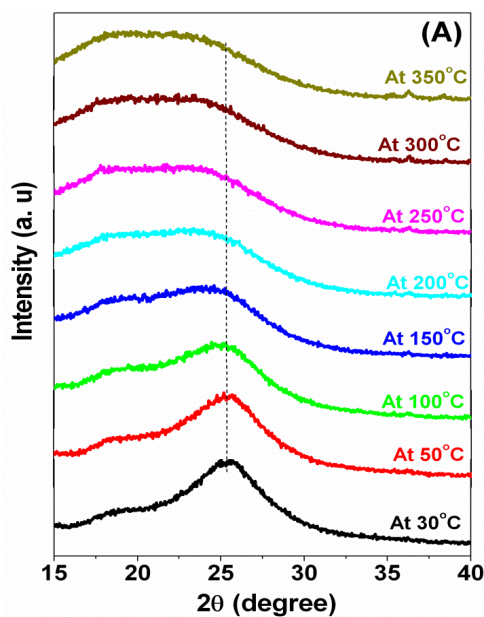
Figure 3.10. *Variable temperature WAXD patterns; (A) PBI and (B) C$_{14}$ N-PBI sample.*

It is interesting to notice that very unusual storage modulus vs temperature dependence in case N-PBI (Figure 3.6A and Figure 3.5A). Storage modulus decreases with increasing temperature as expected, but once the T_g range is crossed the rubber modulus increases sharply with increasing

temperature. This deep rubbery modulus is quite uncommon and very interesting. This kind of observation was observed earlier in case of PVDF/PMMA blend where deep rubbery modulus is explained as the result of non-equilibrium crystalline states of PVDF.[41] But in the current system, no crystallization is observed since all PBI and N-PBI are amorphous in nature (discussed in later section). It is also noticed that (Figure 3.6) the deepness of rubbery modulus increases with increasing size of the alkyl chain length. We believe this deep rubbery modulus may be the result of following; as we increase the temperature the N-PBI shows the T_{g1} (N-substituted chains) at ~ <300 °C (onset of deep is <300 °C), after that with increasing temperature the N-substituted part degrades; as seen in TGA studies where at ~ 300 °C a major weight loss is observed and which varies with alkyl chain length size; and then only unsubstituted PBI exists which has T_g beyond 350 °C (T_{g2}). To display its T_g (T_{g2}), the unsubstitute PBI gains the modulus and exhibits its T_g, therefore we observed the deep rubbery modulus. To confirm our argument that these deep is due to the degradation of N-substituted part, we have carried out DMA experiments (second heating) with the N-PBI samples which are already scanned in DMA from 100 °C to 400 °C and displayed the deep rubbery modulus. In the second heating scan in DMA (Figure 3.7) we observe no such deep in rubbery modulus and the second heating scan is exactly similar to parent PBI indicating that our claim of degradation of N-substitution is indeed correct. To prove it further we have recorded IR spectra of PBI and N-PBI samples after DMA scan and annealing at 400 °C; and results are shown in Figure 3.8. It is clear that the parent PBI does not show any significant changes in the spectrum; however N-PBI spectra after annealing display a peak around ~ 2235 cm^{-1} which corresponds to -C≡N vibration resulting from the degradation of imidazole group; attributing that N-substituted part are degrading after heating at 400 °C.

3.4.3.3. X-ray Study:

The wide angle X-ray diffraction (WAXD) patterns of the parent PBI and representative N-PBI samples are presented in Figure 3.9. Absence of any sharp peak in all the samples suggests the amorphous nature of all N-PBIs. It is known in the literature that PBI is amorphous in nature and our results indicate that substitution did not alter the amorphous nature of the PBI. Earlier several authors[42-44] pointed out two broad peaks at around ~ 25 and 11° 2θ for the PBI. These peaks are correspondence to *d*-spacing 3.64 and 7.29 Å, respectively. The first d-spacing is the characteristic of the planes formed by face to face packing of PBI chain and the latter is due to the length of one repeat unit. Figure 3.8 clearly shows that in case of N-PBI samples the peak corresponding to 7.29 Å *d*-spacing does not alter with increasing alkyl length chain length. However *d*-spacing for face to face packing increases with increasing alkyl chain length size and reaches to maximum value at 4.38 Å (2θ = 20.25°) for C$_{16}$ sample. These observations clearly attributes that with increasing alkyl chain length size the distance between the PBI chains are increasing and as a result the self-association between the PBI chains decreases with increasing alkyl

length. Therefore, substituted alkyl chains in the PBI backbone pushes the PBI chains apart and hence decrease the self-association between the chains. This hinted that the N-PBIs are less tightly packed. Earlier similar observation has been reported in the literature on N substitution of PBI. The increase *d*-spacing of face-to-face packing also helps to increase the solubility of N-PBIs.

We have monitored the *d*-spacing of face-to-face packing as a function of temperature for both parent PBI and N-PBI (C_{14} as a representative) and data are shown in Figure 3.10. Both the cases the *d*-spacing increase (2θ decreases) with increasing temperature indicating the increase in distance between the PBI chains. However in case of parent PBI a significant peak broadening is observed which is not observed in case of C_{14} N-PBI. This attributes that in case of N-PBI, part of the polymer chain has already been separated apart by the long alkyl chain.

In earlier section, we have concluded that the N-PBI samples have copolymer structure, in which one part is N-PBI and other part is unsubstituted PBI, and the N-PBI part degrades upon annealing at 400 °C. Figure 3.11 data reconfirms our claims. The WAXD pattern of N-PBI (C_{14}) samples recorded at room temperature after annealing at 400 °C for 30 min is similar with the parent PBI, indicating that the N-PBI structure is indeed a copolymer in nature and degradable at 400 °C.
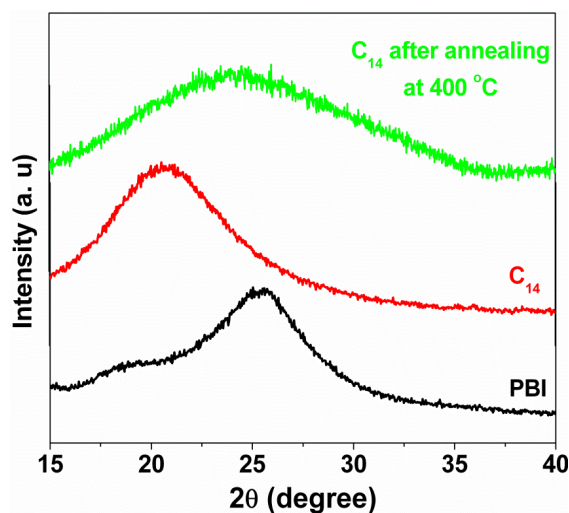
Figure 3.11. *WAXD patterns of PBI, C_{14} samples and C_{14} sample after annealing at 400 °C for 30 min.*

3.4.4. Studies of Crucial PEM Membrane Properties of N-PBIs:

3.4.4.1. Water Uptake, Swelling Ratio and Volume:

It is well known that PBI is hydrophilic and moisture sensitive. Even at room temperature PBI can absorb water up to 15 wt% when dipped into deionized water for several days. This may be due to

hydrogen bonding formation between two nitrogen atoms of amine and imine groups.[45,46] In the imidazole moiety there are two nitrogen atoms one is proton acceptor and one is proton donor and these nitrogen atoms undergo hydrogen bonding readily with H_2O molecule. Figure 3.12 displays that the water absorption capacity gradually decreases with increasing size of the alkyl chain length. In our earlier sections (FT-IR and TGA study), we have seen the exactly similar observation where we demonstrated that the hydrophobic alkyl chain grafting onto the PBI backbone decreases the hydrophilic nature of N-PBI. In the polymer backbone there are two parts, one is nitrogen containing polybenzimidazole which is hygroscopic in nature and another is polymer chain grafted with hydrophobic long alkyl chain. All polymers have the same hydrophilic part but due to different alkyl chain length which is hydrophobic, the hydrophilic nature of whole polymer backbone governed by the size of alkyl length. With increase of alkyl chain length the hydrophobic nature of N-PBI increases resulting lower water absorption by N-PBI. Also since % of N-alkylation increases with increasing alkyl chain length (Table 3.1) hence more hydrophobic character of N-PBIs is expected. Figure 3.13 represents the swelling ratio (SR) and volume (SV) data as a function of number of alkyl carbon atoms substituted in N-PBI. Both SR and SV alter significantly after grafting with the alkyl substitution and decreases with increasing size of alkyl chain length. This is primarily due to the increase hydrophobic nature of N-PBI. Also, we have noticed using X-ray studies that molecular packing (density) decreases with increasing alkyl length, which in turns creates more voids between the chains in case of N-PBI compared to parent PBI. Hence N-PBI has very little chance to swell further upon absorbing water. Therefore it can be concluded that our water uptake and swelling studies data are in agreement with our other results.
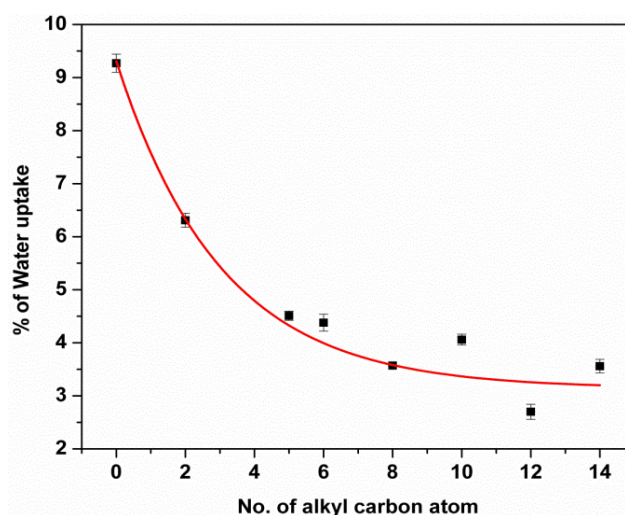
Figure 3.12. *Water uptake of N-PBI samples.*
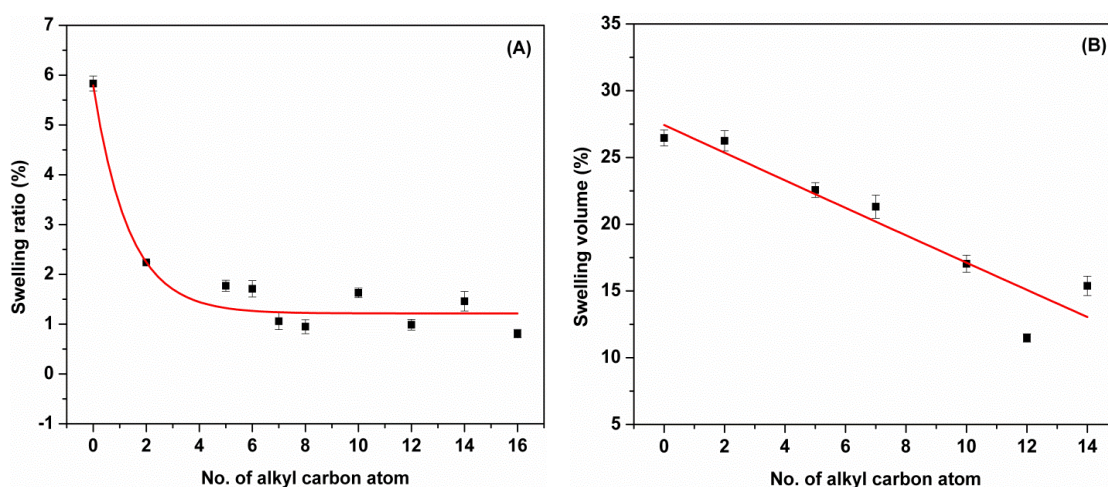
Figure 3.13. *(A) Swelling ratio and (B) swelling volume in water of N-PBI samples.*

3.4.4.2. Acid Doping Level:

It is well known that mechanical properties become poorer for PA doped PBI membrane at high acid doping level although it exhibit higher proton conductivity.[47] Proton conduction occurs in PA doped PBI polymer membranes is because of the presence of amine (-NH-) and imine (-N=) groups which are act as proton donor and proton acceptor, respectively. The amount of acid PBI can consume dictates proton conductivity of the doped PBI and it depends on the concentration of acid and also water uptake capacity of PBI.
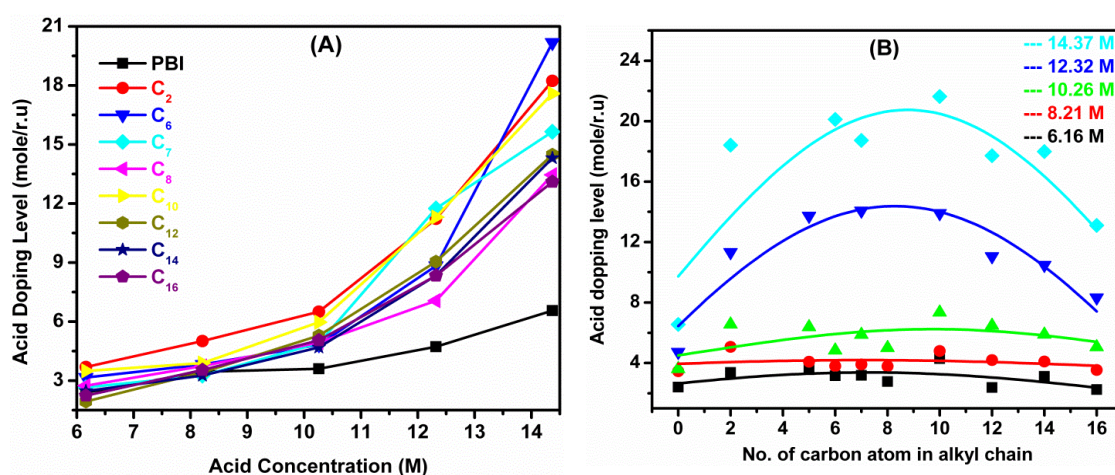
Figure 3.14. *Phosphoric acid (PA) doping level of N-PBI samples; (A) PA loading vs PA concentration and (B) PA loading vs. number of carbon atom in alkyl chain.*

As expected we can see from Figure 3.14 that PA loading of N-PBI membranes increases with increasing acid concentration. It may be noted that there is no definite trend of PA loading of N-PBI with the size of alkyl chain length (Figure 3.14A). To understand it more thoroughly we have plotted PA loading as a function of number of carbon atoms (Figure 3.14B). It has been observed that N-PBI membranes consume the maximum acid when the alkyl chain length is 6-12. We observe a maximum in Figure 3.14B plot and then gradual decrease. Hence among all N-PBI, when the alkyl chain length between 6 and 12, the PA loading is maximum. This could be explained as follows; when alkyl chain length increases the swelling ratio, water uptake, etc. decreases rapidly up to C_6 (as discussed in the previous section) then all these parameters saturate with increasing number of carbon atoms in the alkyl chain, therefore C_6-C_{12} N-PBI can consume more acids.

3.4.4.3. Proton Conductivity Study:

Proton conductivities as a function of temperature from room temperature to 160 °C of all the PA doped N-PBI samples are measured. The proton conductivity data shown here are measured from PA doped N-PBI samples which are doped with 60% PA for seven days. As mention in the experimental section the conductivity data shown here is the second heating scan data. Figure 3.15 shows the plots of proton conductivity against the temperature. As expected in all the cases conductivity increases with increasing temperature and at 160 °C the conductivity of N-PBI samples in the order of ~ 10^{-2} S/cm. Infact, it can be seen that there is no such definite trend of conductivity with alkyl chin length despite the fact that there PA loading is different. Hence it can be said that all N-PBI samples exhibit similar conducting behaviour. The PA loading largely depends on the molecular packing which need not necessarily alter the proton conductivity behaviour.
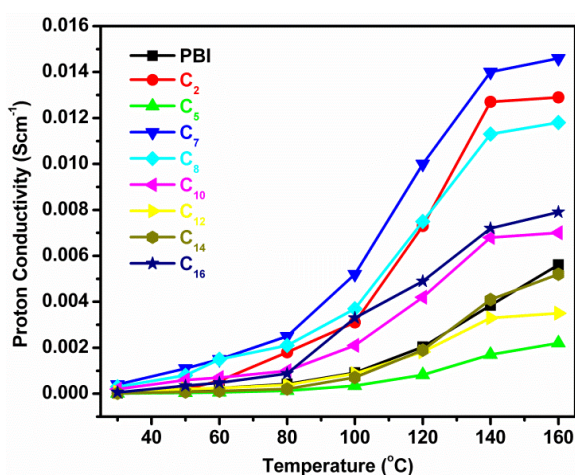
Figure 3.15. *Proton conductivity against temperature plots of N-PBI membranes.*
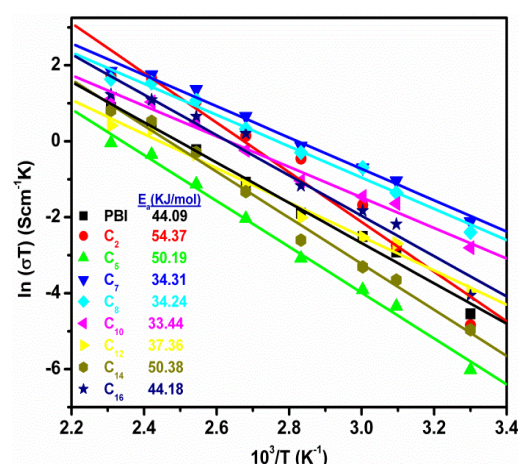
Figure 3.16. *Arrhenius plots for the proton conduction of N-PBI samples.*

Proton conductivity data plotted against temperature using the following Arrhenius type equation (3.1) and presented in Figure 3.16.

$$\ln(\sigma T) = \ln\sigma_o - E_a/RT \qquad \text{---------------} \quad (3.1)$$

Where σ is proton conductivity of the PA doped membrane (S cm^{-1}), T is temperature (K), σ$_o$ is the pre-exponential factor (S K^{-1} cm^{-1}), E_a is the proton conducting activation energy (KJ/mol) and R is the ideal gas constant (J mol^{-1} K^{-1}). All the plots fit well and suggesting Grotthuss mechanism. As it can be seen that; although their conductivity is almost identical, but the calculated E_a value depends on the size of the alkyl length. The E_a value exhibits a decreasing trend as length increases indicating the conductivity path depends on the size of the N-substitution alkyl chain length.

3.5. CONCLUSION:

N-alkyl polybenzimidazoles (N-PBI) of variable alkyl chain lengths are prepared and characterized thoroughly to elucidate the effect of alkyl chain length on the structure and properties of N-PBI. The enhanced solubility of N-PBIs in low boiling solvents like formic acid makes these PBI derivatives as readily processable materials and form homogeneous transparent membranes. TGA and in depth DMA studies suggest the copolymer nature of the N-PBIs chain structure in which one part is substituted PBI and other part is unsubstituted PBI. During the first heating scan in DMA in case of N-PBI samples an unusual deep rubbery modulus in the temperature dependent storage modulus plot is observed owing to the copolymer structure of the N-PBI chains. XRD study shows that the d spacing of face-to-face packing of the amorphous N-PBI chains increases with increasing alkyl chain length. Temperature dependent XRD study reconfirms the copolymer nature of N-PBI chains. N-PBI membranes have significantly lower water uptake, swelling ratio and volume compared to parent PBI. The PA doping level increases with increasing acid concentration and it reaches to maximum when alkyl chain length is 6-12. The conductivities of PA doped NPBI membranes at higher temperature are comparable with the parent PBI. In summary, a series of new PBI derivatives have been developed which are easily processable and possess all the essential characteristics to be an efficient polymer electrolyte membrane (PEM).

REFERENCES:

(1) Doyle, M.; Rajendran, G. *Handbook of Fuel Cells; John Wiley and Sons*: New York, **2003**, Vol. 3.

(2) Mader, J.; Xiao, L.; Schmidt, T. J.; Benicewicz, B. C. *Adv. Polym. Sci.* **2008**, *216*, 63.

(3) Li, Q. F.; Jensen, J. O.; Savinell, R. F.; Bjerrum, N. J. *Prog. Polym. Sci.* **2009**, *34*, 449.

(4) Choe, E. W.; Choe, D. D. In Polymeric Materials Encyclopedia; (Salamone, J. C. *Ed.); CRC Press:* New York, **1996**, Vol. 7, 5619.

(5) Lee, H.; Stoffey, D.; Neville, K. *New Linear Polymers; McGraw–Hill:* New York, **1967**, Chapter 9.

(6) Frazerr, A. H. *High Temperature Resistant Polymers*; *Interscience:* New York, **1968**, 138.

(7) Neuse, E. W.; Loonat, M. S. *Macromolecules* **1983**, *16*, 128.

(8) Brand, R. A.; Bruma, M.; Kellman, R.; Marvel, C. S. *J. Polym. Sci. Polym. Chem. Ed.* **1978**, *16*, 2275.

(9) Higgins, J.; Marvel, C. S. *J. Polym. Sci.* **1970**, *8*, 171.

(10) Asensio, J. N.; Borros, S.; Gomez, R. P. *J. Electrochem. Soc.* **2004**, *151*, A304.

(11) Jouanneau, J.; Mercier, R.; Gonon, L.; Gebel, G. *Macromolecules* **2007**, *40*, 983.

(12) Jouanneau, J.; Gonon, L.; Gebel, G.; Martin, V.; Mercier, R. *J. Polym. Sci. Part A: Polym. Chem.* **2010**, *48*, 1732.

(13) Tan, N.; Xiao, G.; Yan, D.; Sun, G. *J. Membr. Sci.* **2010**, *353*, 51.

(14) Li, Z. X.; Liu, J. H.; Yang, S. Y.; Huang, S. H.; Lu, J. D.; Pu, J. L. *J. Polym. Sci. Part A: Polym. Chem.* **2006**, *44*, 5719.

(15) Lin, H. L.; Chou, Y. C.; Yu, T. L.; Lai, S. W. *International J. Hydrogen Energy* **2012**, *37*, 383.

(16) Xiao, L.; Zhang, H.; Jana, T.; Scanlon, E.; Chen, R.; Cheo, E. W.; Ramanathan, L. S.; Yu, S.; Benicewicz, B. C. *Fuel Cells* **2005***, 5*, 287.

(17) Sansone, M. J. U. S. Patent 4,814,400, Mar 21, 1989.

(18) Sansone, M. J. U. S. Patent 4,868,249, Sept 19, 1989.

(19) Sansone, M. J. U. S. Patent 4,898,917, Feb 6, 1990.

(20) Sansone, M. J.; Kwiatek, M. S. Patent 4,933,397, Jun 12, 1990.

(21) Gieselman, M. B.; Reynolds, J. R. *Macromolecules* **1992**, *25*, 4832.

(22) Gieselman, M. B.; Reynolds, J. R. *Macromolecules* **1993**, *26*, 5633.

(23) Klahen, J. R.; Luther, T. A.; Orme, C. J.; Jones, M. G.; Wertsching, A. K.; Peterson, E. S. *Macromolecules* **2007**, *40*, 7487.

(24) Glipa, X.; Haddad, M. E.; Jones, D. J.; Roziere, J. *Solid State Ionics* **1997**, *97*, 323.

(25) Kumbharkar, S. C.; Kharul, U. K. *J. Membr. Sci.* **2010**, *360*, 418.

(26) Rikukawa, M.; Sanui, K. *Prog. Polym. Sci.* **2000**, *25*, 1463.

(27)   Bae, J. M.; Honma, I.; Murata, M.; Yamamoto, T.; Rikukawa, M.; Ogata, N. *Solid State Ionics* **2002**, *147*, 189.

(28)   Guan, Y. S.; Pu, H. T.; Jin, M.; Chang, Z. H.; Wan, D. C. *Fuel Cells* **2010**, *10*, 973.

(29)   Lina, H. L.; Hua, C. R.; Lai, S. W.; Yua, T. L. *J. Membr. Sci.* **2012**, *389*, 399.

(30)   Pu, H.; Liu, Q.; Liu, G. *J. Membr. Sci.* **2004**, *241*, 169.

(31)   Yamaguchi, I.; Osakada, K.; Yamamoto, T. *Macromolecules* **1997**, *30*, 4288.

(32)   Angioni, S.; Righetti, P. P.; Quartarone, E.; Dilena, E.; Mustarelli, P.; Magistris, A. *International J. Hydrogen Energy* **2011**, *36*, 7174.

(33)   Qian, G.; Smith, D. W.; Benicewicz, B. C. *Polymer* **2009**, *50*, 3911.

(34)   Peron, J.; Ruiz, E.; Jones, D. J.; Roziere, J. *J. Membr. Sci.* **2008**, *314*, 247.

(35)   Sannigrahi, A.; Arunbabu, D.; Jana, T. *Macromol. Rapid. Commun.* **2006**, *27*, 1962.

(36)   Sannigrahi, A.; Arunbabu, D.; Sankar, R. M.; Jana, T. *Macromolecules* **2007**, *40*, 2844.

(37)   Brooks, N. W.; Duckett, R. A.; Rose, J.; Ward, I. M.; Clements, J. *Polymer* **1993**, *34*, 4038.

(38)   Conti, F.; Willbold, S.; Mammi, S.; Korte, C.; Lehnertad, W.; Stoltenad D. *New J. Chem.* **2013**, *37*, 152.

(39)   Sannigrahi, A.; Ghosh, S.; Lalnuntluanga, J.; Jana, T. *J. Appl. Polym. Sci.* **2009**, *111*, 2194.

(40)   Menczel, J. D. *J. Thermal Analysis Calorimetry* **2000**, *59*, 1023.

(41)   Campo, C. J.; Mather, P. T. *Polym. Mater. Sci. & Eng.* **2005**, *93*, 933.

(42)   Venkatasubramanian, N.; Dean, D. R.; Dang, T. D.; Price, G. E.; Arnold, F. E. *Polymer* **2000**, *41*, 3213.

(43)   Staiti, P.; Lufrano, F.; Arico, A. S.; Passalacqua, E.; Antonucci, V. *J. Membr. Sci.* **2001**, *188*, 71.

(44)   Wereta, A.; Gehatia, M. T. *Polym. Eng. Sci.* **1978**, *18,* 204.

(45)   Chung, T. S. *Rev. Macromol. Chem. Phys.* **1997**, *C37*, 277.

(46)   Li, Q.; Jensena, J. O.; Savinell, R. F.; Bjerrum, N. J. *Prog. Polym. Sci.* **2009**, *34*, 449.

(47)   Qingfeng, L.; Hjuler, H. A.; Bjerrum, N. J. *J. Appl. Electrochem.* **2001**, *31*, 773.

CHAPTER 4

Soluble Polybenzimidazoles for PEM: Synthesized from Efficient, Inexpensive, Readily Accessible Alternative Tetraamine Monomer
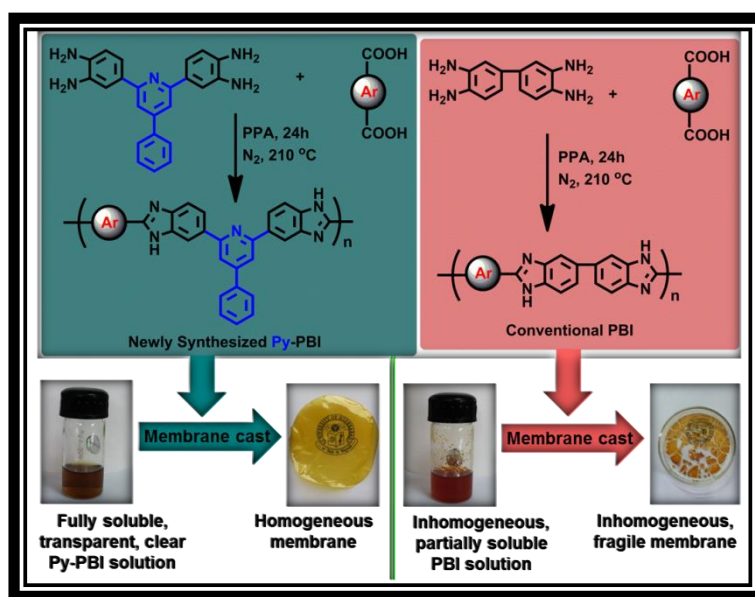
4.1. INTRODUCTION:

Polybenzimidazole (PBI), an amorphous rigid polymer, was first synthesized by Vogel et al.[1] in 1961, and since then, PBIs have been studied enormously and utilized in numerous application areas owing to their superb thermal, mechanical, and chemical stability.[2-6] Excellent film forming capability of PBI makes it an attractive choice to be used as membrane for several applications.[7-12] Since the inception, a myriad number of publications and patents appeared on PBI. SciFinder database search displays ~ 5600 references containing the concept "polybenzimidazole", attributing to the importance of PBI. The profound commercial values and aspects of PBI-based polymers have been discussed in great detail in the patent literature.[3]

A detailed analysis of the above search brings an important fact to our notice. Almost in 90% of cases of the above publications (patents), the PBIs were synthesized by polycondensation of 3,3′,4,4′-tetraaminobiphenyl (TAB) (Scheme 4.1) with several of dicarboxylic acids (DCAs).[13-20] The TAB became the synonymous and "must use" only monomer for PBI chemistry. This observation encourages us to understand "why only TAB" has been used for synthesizing so popular a polymer like PBI, and also, we raised the question "what is so special about TAB?" so that it cannot be replaced with another tetramine monomer. To our surprise, we found that there are only a few efforts that were made in the literature to replace TAB,[21,22] however, those efforts were not successful because the obtained PBIs did not offer better properties than the already known conventional PBI synthesized from TAB. We also found that synthesis of the TAB monomer is very complex process and hence it is not so easily accessible.[23] The TAB is not a very stable monomer, it is carcinogenic and also very expensive (cost of 25 g is 425 USD as per Sigma Aldrich catalogue). It is also noticed that 100% pure TAB is difficult to obtain. These lacunas with the monomer TAB in the PBI synthesis motivated us to look for an alternative, readily accessible, easily synthesizable, extra pure, and cost-effective tetramine monomer, which can replace TAB effectively and PBI can be synthesized with better properties.

In addition to the above drawbacks of the PBI chemistry, most of the PBIs synthesized from TAB with varieties of DCAs are soluble only in high boiling polar solvents like *N,N*-dimethyl acetamide, dimethyl sulfoxide, and so on,[24-26] with few exceptions, like poly(4,4′-diphenylether-5,5′-bibenzimidazole),[19,27] which shows solubility in low boiling solvent. Hence, the solubility of PBIs are DCAs structure dependent. The insolubility in low boiling solvents restricts the large scale convenient use of PBI owing their difficult processability problems. Therefore, many groups have made many efforts to enhance the solubility by altering the DCAs structure or by attaching soluble functionality in the PBI backbone.[24,28-30] Earlier, we demonstrated that synthesis of long alkyl chain dramatically enhance the solubility.[31] However, it is important to note that all these attempts for enhancing the solubility were attempted by playing around DCAs structure. There is not a single effort to change the TAB structure. Therefore, we wish to make an

effort to make soluble PBI by choosing different tetramine monomer than conventional one, so that PBI made with that monomer and any DCAs can produce readily soluble and processable PBI. If success can be achieved then the obtained PBI will be always soluble irrespective of DCAs structure and therefore the scope of PBI utility will further enhance since any kind of DCAs structure can be used depending on the desired applications.

We wish to highlight another important aspect (drawback) of the conventional PBIs and their use. In the last 10 years, PBI became very popular after it was discovered that phosphoric acid (PA) doped PBI membrane is the most suitable candidate as a polymer electrolyte membrane (PEM) for a low cost, high performance, and high temperature PEM fuel cell.[5-7,15-17,32-37] Innumerable reports have come on the PA doped PBI for PEM in recent years. Despite the great success and hope of the PEM, still few tough challenges remain unanswered. Among many of these challenges, one of the most prominent ones is the amount of PA loading into the PBI, because the amount of PA dictates the proton conductivity of the PEM, which in turn decides the fuel cell efficiency. Generally, higher PA loading yields lead to higher proton conductivity and hence, enhance the performance of the fuel cell. Sadly, the conventional PBI loads a moderate amount of PA, which eventually results in low proton conductivity. Although there were some improvements of PA loading by altering DCAs structure,[5,6,14,20,37,38] by making blends,[39] nanocomposites,[40] or by altering membrane formation techniques,[6,7,37,38,41a,b,c] but each of these attempts have advantages and disadvantages, too. Hence, we believe it would be fascinating if PA loading can be enhanced by altering the PBI backbone structure, especially by changing the tetramine structure. Incorporation of hetero atoms in the polymer backbone and increasing the chain to chain distance in the molecular packing by pushing away the chains are believed to be the way forward for enhancing the PA loading. Therefore, we look for a tetramine with heteroatom and bulky structure for this study.

As is evident from the above discussion, in this chapter we develop a new type of PBI by utilizing a new type of pyridine bridged tetramine (Py-TAB, Scheme 4.1) with the 3-fold objectives, which include (I) easily synthesizable cost-effective tetramine monomer and (II) soluble and processable PBI irrespective of DCA structure and (III) PBI, which can hold a large quantity of PA. With these objectives in mind, we have utilized Py-TAB as a new tetramine monomer to make Py-PBI.

4.2. SYNTHESIS:

4.2.1. Monomer synthesis:

2,6-bis(3',4'-diaminophenyl)-4-phenylpyridine (abbreviated as Py-TAB) monomer was synthesized in the laboratory in 100 g scale using previously reported method after some modification (see Chapter 2, Scheme 2.1).[41d] The Py-TAB monomer was characterized by using FT-IR, ^{1}H-NMR and LCMS

spectroscopy as shown in Figure 4.1, Figure 4.2 and Figure 4.3, respectively. The monomer structure was confirmed as expected.
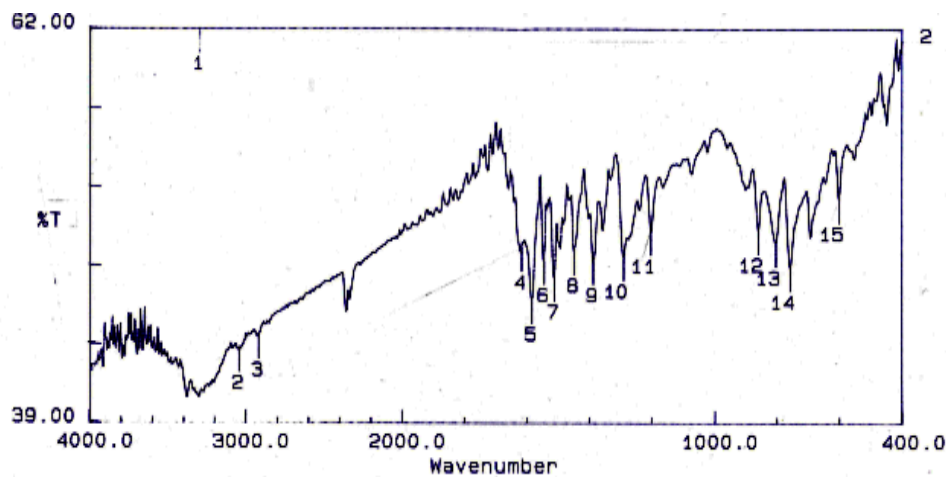
Figure 4.1. *FT-IR spectra of 2,6-bis(3',4'-diaminophenyl)-4-phenylpyridine (Py-TAB) monomer.*

Chemical Shift (δ ppm)
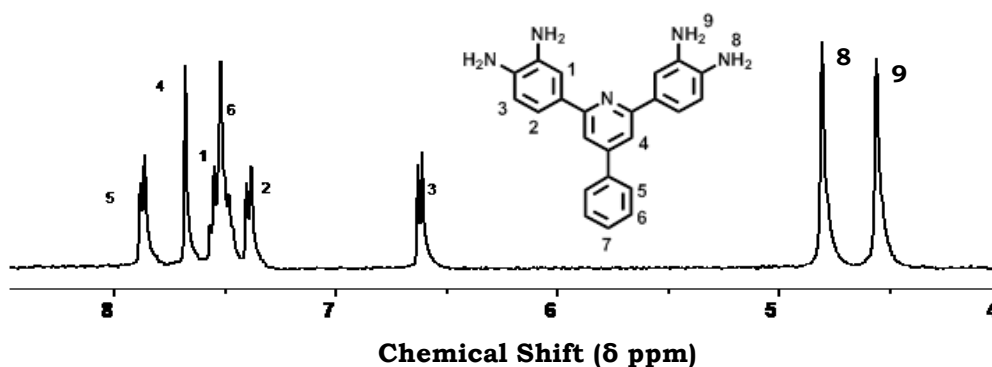
Figure 4.2. *^{1}H-NMR spectra of 2,6-bis(3',4'-diaminophenyl)-4-phenylpyridine (Py-TAB) monomer.*
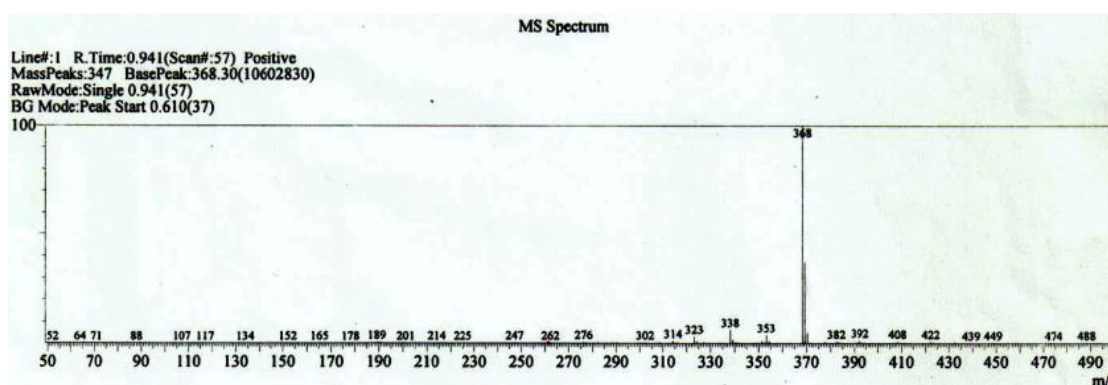
Figure 4.3. *Mass spectra of 2,6-bis(3',4'-diaminophenyl)-4-phenylpyridine (Py-TAB) monomer.*

4.2.2. Polymer (Py-PBI) Synthesis:

Equal mols of different dicarboxylic acids (DCAs) and Py-TAB were taken into a three-neck flask with polyphosphoric acid (PPA) for the synthesis of pyridine bridge PBI (Py-PBI) homopolymers. Six DCAs with different molecular structure were used, and these are isophthalic acid (IPA) and terephthalic acid (TPA), biphenyl 4,4′-dicarboxylic acid (BDA), 4,4′-oxybis(benzoicacid) (OBA), 4,4′-dicarboxy benzophenone (BPDA), and 4,4′-(hexafluoroisopropylidene)bis(benzoicacid) (HFIPA). Monomers were taken along with polyphosphoric acid (PPA) in a 300 ml three-neck mercury sealed flask equipped with mechanical stirrer and nitrogen atmosphere. The reactions were carried in 100 ml PPA for 24 h at 210 °C. The total monomer concentration for each DCA monomers was varied from 1-5% (wt%) to optimize the reaction condition and to obtain high molecular weight Py-PBIs. For each reaction, the reaction time and temperature (which is often in the range of temperature 50 to 210 °C with appropriate ramp and soak times) were optimized. After the complete polymerization, the viscous polymer solutions were slowly poured into the deionized water and neutralized with sodium bicarbonate. The polymers were filtered and washed with deionized water several times and dried in a vacuum oven for 24 h at 100 °C to remove the water completely. The reaction scheme for the synthesis is shown in Scheme 4.1, along with the reaction scheme for conventional PBI.
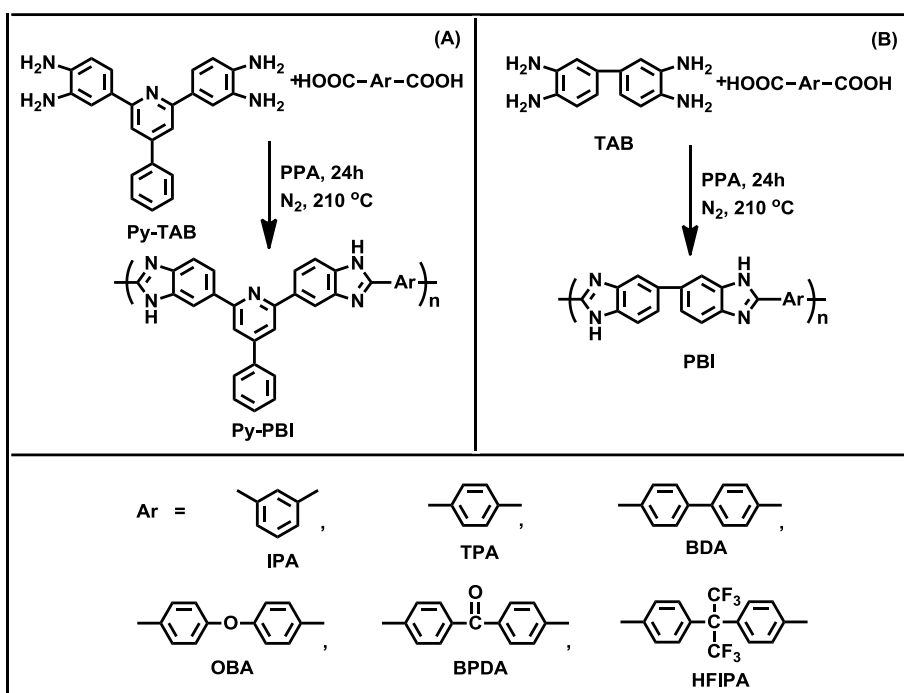
Scheme 4.1. *Synthesis of (A) Pyridine Bridge Polybenzimidazoles (Py-PBI) Polymers from the 2,6-Bis(3',4'-diaminophenyl)-4-phenylpyridine (Py-TAB) Monomer and (B) Conventional PBI from 3,3',4,4'-Tetraaminobiphenyl (TAB) Monomer with Varieties of Dicarboxylic Acid Monomers.*

4.3. CHARACTERISATION:

All the information about the materials used in this study and solubility test, membrane fabrication method from the synthesized Py-PBIs and the experimental methods of all the characterization techniques which include molecular weight measurements by viscosity and gel permeable chromatography (GPC), spectroscopic characterization by Fourier transform infrared spectroscopy (FT-IR) and proton NMR, photophysical studies by UV-visible and fluorescence spectroscopy, X-ray diffraction (WAXD), thermogravimetric analysis (TGA) and dynamic mechanical analysis (DMA) for all the Py-PBI polymers are shown in the Chapter 2. The Py-PBI membranes stability toward oxidation, H_3PO_4 doping level, water uptake, swelling ratio and the proton conductivity measurements are also discussed in the Chapter 2.

4.4. RESULTS AND DISCUSSION:

4.4.1. Polymer Synthesis and Molecular Weight:

A series of pyridine bridged polybenzimidazoles (Py-PBIs) are synthesized by polycondensation of the pyridine base tetramine (Py-TAB) monomer with several dicarboxylic acid (DCA) monomers, as shown in Scheme 4.1. To prove the feasibility of the new Py-TAB monomer as an efficient, inexpensive, and alternative to conventionally used 3,3′,4,4′-tetraaminobiphenyl (TAB); to understand the effect of the presence of bulky phenyl pyridine in the main chain of PBI, it is necessary to make polymers with the most commonly used DCAs. As observed from Scheme 4.1, we have verified the scope of polycondensation of Py-TAB monomer with a large number of commonly used structurally different DCAs. In all the cases, we obtained polymers (Py-PBI) with good yields and molecular weight attributing to the fact that the Py-TAB monomer can be used to prepare PBI type polymers instead of conventional TAB. The molecular weight of the polybenzimidazole polymers are most commonly expressed in terms of their inherent viscosity (IV) in concentrated H_2SO_4 (98%).[2,3,6,37,42] The higher IV of polymers implies the higher molecular weight. The molecular weight (MW) data for all Py-PBI polymers of various DCAs series are presented in Figure 4.4. We also measured the MW of Py-PBI polymers by GPC (Figure 4.5) and listed in Table 4.1. Both Figure 4.4 and Table 4.1 clearly satisfy that the new Py-TAB has produced higher MW Py-PBI readily with several DCAs.

It is well documented in the literature that the total monomer concentration (TMC), concentrations of both tetramine and DCA, plays a crucial role in deciding the course of the polymerization, reaction yield, and most importantly, the molecular weight of the resulting PBI.[14,37,42,43] In fact, it is shown that the DCA structure and TMC has an interrelation. In other words, for certain DCA, low TMC is required for obtaining high MW; on the other hand, higher TMC is required for some DCA to achieve high MW PBI. Hence, the optimization of TMC versus MW dependence for the Py-PBI synthesis in the case of all DCAs structures used here is very essential. Figure 4.4 shows that MW versus TMC plots for several DCAs for the Py-PBI

synthesis. Except HFIPA, in all other cases, MW increases with increasing TMC and reaches a maximum, and after certain TMC, the MW decreases further. It is to be noted that the dependence of TMC and MW, as well as the MW maxima (Figure 4.4), are highly dependent on the DCA structure. The reactivity of monomers truly depends upon their structure owing to the solubility of DCA monomer in PPA. It has been confirmed from earlier reports by several other groups and by us that the high molecular weight para-PBIs can be made if the lower monomer concentration is employed owing to the lower solubility of para oriented dicarboxylic acid.[37,42] In the present work, we observed all the para oriented DCAs result in higher MW Py-PBI in much lower TMC compared to meta-structure DCAs (Figure 4.4). A comparison of MW data for IPA with other DCAs in Figure 4.4 clearly proves the above observation.
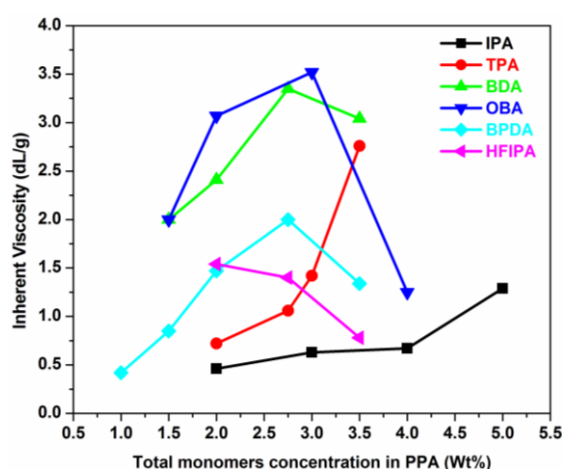
Figure 4.4. *Effect of total monomer concentration (TMC) on the molecular weight of Py-PBIs.*

We observed that in all para-structure-oriented Py-PBIs except HFIPA, the molecular weight increases with increasing TMC and gives the maximum. However, in the case of HFIPA, the MW decreases with increasing TMC. By further decreasing TMC, we did not obtain polymer. When the TMC is less than 1.5% (wt%), then the product (polymer) is suddenly precipitated out and solidified, and it may be due to the formation of higher molecular weight polymers at the early stage, which are not soluble in PPA medium. The odd behaviour of HFIPA may be due to strong electronegativity and bulkiness of the hexafluoroisopropylidene moiety.

We wish to highlight another important aspect that we notice during the course of this study. The TMCs required to achieve highest IV of polymers using conventional TAB and Py-TAB are listed in Table 4.1 for all the DCAs studied here. The conventional TAB data are obtained from the literature.[37,42,43] It can be seen from Table 4.1 that much lower TMC is required for all the DCA cases to achieve higher molecular weight Py-PBI polymers using Py-TAB, rather than conventional TAB. Lower TMC in the polymerization

mixture is advantageous over higher TMC because several concerns like monomer insolubility and viscosity rise during the polymerization are easily evaded.

Table 4.1. *The comparison of TMC and IV of conventional Py-TAB with TAB.*

DCA	IV[a]	M_w	PDI	TMC required	
				Conventional TAB[b]	Py-TAB
IPA	1.29	4.4×10^5	2.86	~ 6.5	5
TPA	2.76	5.4×10^5	3.48	~ 4.5	3.5
BDA	3.35	3.3×10^5	2.38	–	2.75
OBA	3.52	21.2×10^5	4.92	~ 5.5	3
BPDA	2	5.3×10^5	4.09	–	2.75
HFIPA	1.54	9.0×10^5	3.14	> 5	2

[a] Highest IV obtained (from Figure 4.4) in this study is considered.

[b] Data obtained from literature (references 37, 42, 43) for similar IV samples.
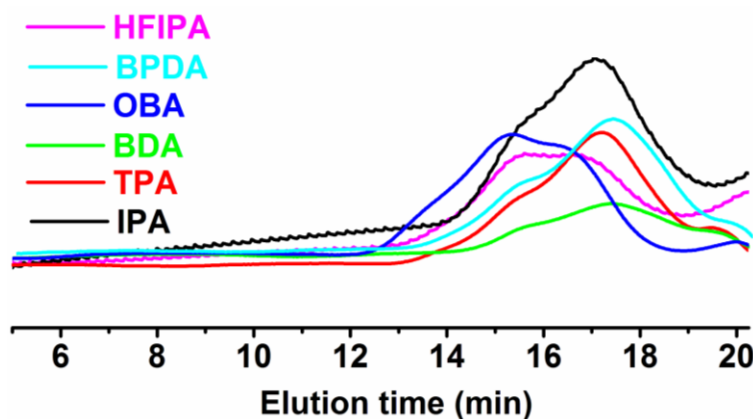
Figure 4.5. *GPC traces of all Py-PBI polymers in DMAc with LiCl at 65 °C.*

4.4.2. FT-IR and ^{1}H NMR Characterization:

FT-IR spectra of all Py-PBI polymers are recorded from 30-40 μm thin film, which were made from the dilute solution (2% w/v) of the polymers in *N,N*-dimethyl acetamide (DMAc). Prior to recording of the IR spectra of all the films are boiled in hot water thoroughly and dried in vacuum oven at 100 °C for two days to remove the water. The IR spectrum of all polymers shows in the Figure 4.6. The IR spectra of all the Py-PBI polymers are similar and the stretching bands are the characteristic bands of PBI. All the important stretching bands shows in the Figure 4.6, by dotted lines, and these are discussed in several literature earlier.[39-42] The IR stretching bands appeared at 3625, 3415, 3175, and 3063 cm^{-1} are due to the O-H of absorbed moisture, free N-H of imidazole, self-associated N-H of imidazole, and C-H of aromatic

ring, respectively.[42] The other characteristic bands of benzimidazole polymers observed at ~1610, 1442, and 840 cm^{-1} are because of C=C/C=N, in-plane benzimidazole ring deformation and C-H stretching vibration of pyridine ring, respectively.[42]
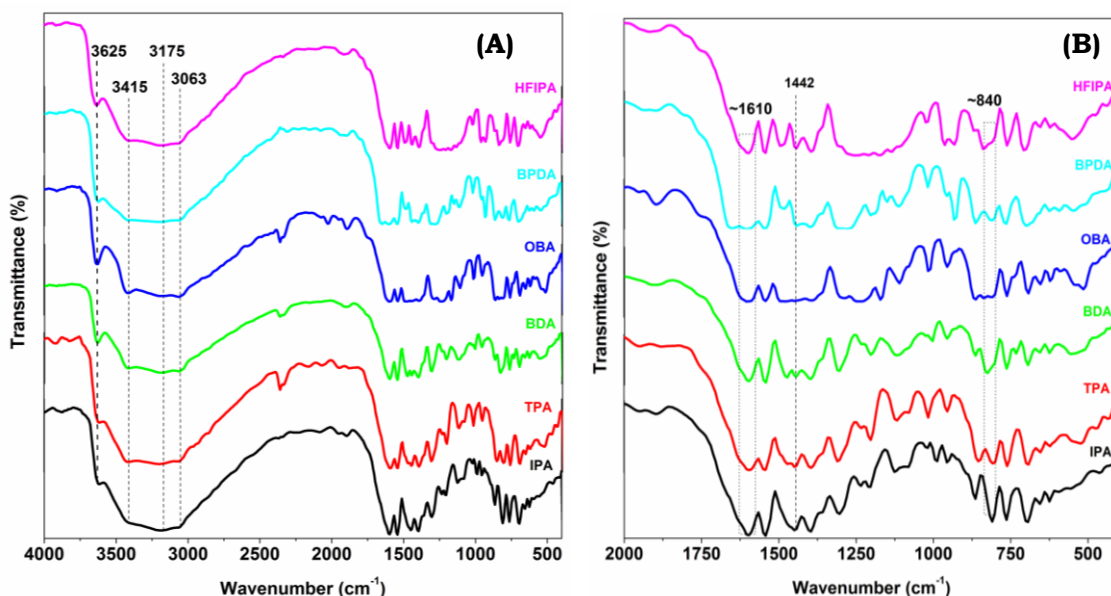
Figure 4.6. *FT-IR spectra of Py-PBI homo polymers (A), magnified portion in the region 2000 to 400 cm^{-1} (B).*

The proton NMR spectra of all the Py-PBI samples are shown in Figure 4.7, along with their structure and the peak assignments. The assigned peaks, as shown in the Figure 4.7, are in good agreement with the anticipated chemical structure of Py-PBIs. The imidazole proton peak positions of Py-PBI polymers are quite different for different DCAs owing to their different chemical environment. The chemical shift of the imidazole N-H proton of Py-PBI polymers are observed at between δ 13.13 and 13.36 ppm. All other chemical shifts of aromatic protons are observed at δ 7.34-9.21 ppm. Aromatic region C-H proton signals are also different from sample to sample due to different DCAs structures, as depicted in peak assignments, shows in Figure 4.7.[13,20,42]

Although a similar type of NMR spectra for PBI polymers are reported earlier by several authors, but we are presenting these spectra in this article to convince the readers that the new Py-TAB monomer can be used successfully to prepare PBI in the same manner like conventional TAB. Therefore, we can replace the TAB with the new Py-PBI, which has many advantages including the cost as described in the following sections.
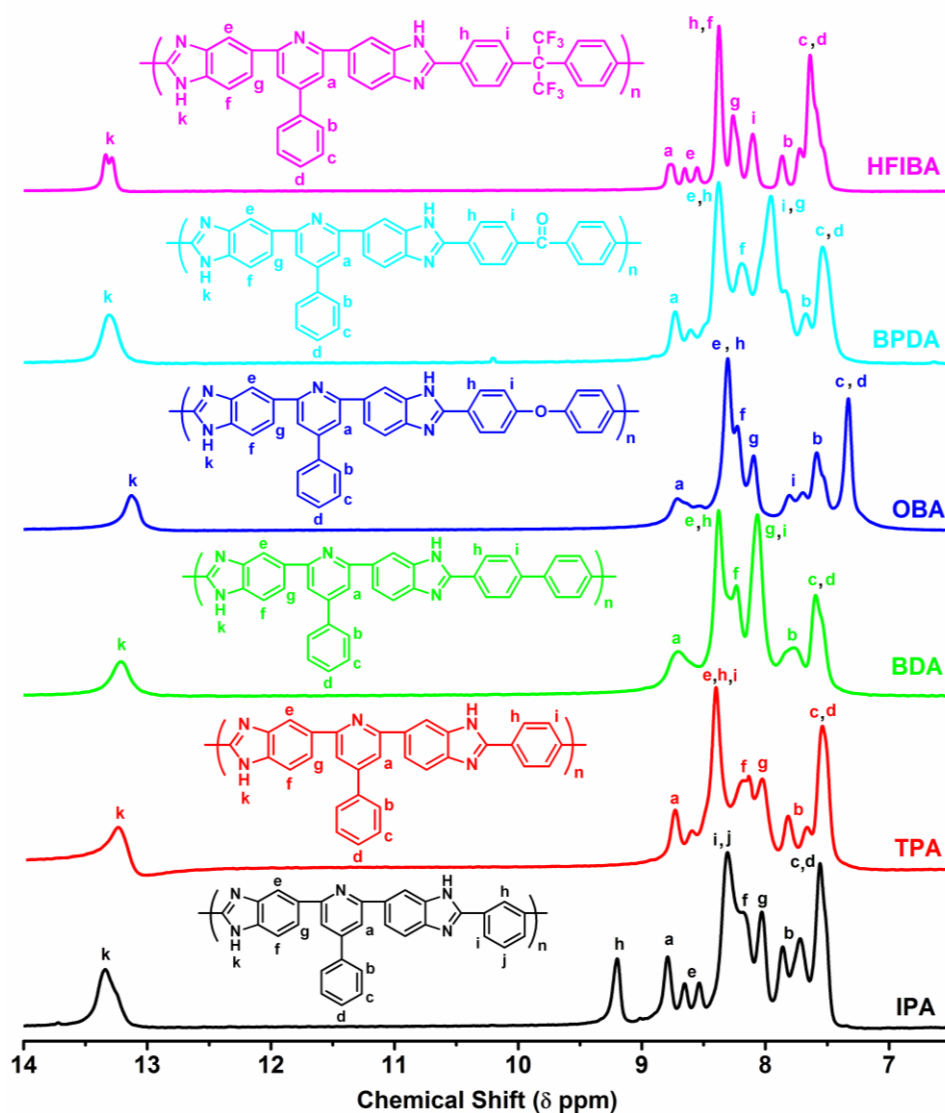
Figure 4.7. ^{1}H-NMR spectra of all Py-PBI polymers recorded in DMSO-d_6 solvent. Peak assignments of all polymers are shown in the figure.

4.4.3. X-ray Diffraction:

The wide-angle X-ray diffraction (WAXD) patterns of all the Py-PBI polymers shown in the Figure 4.8. The broad peak in all the samples indicates the amorphous nature. The peak at ~24° 2θ corresponds to the d-spacing for face to face packing, as noted by several authors earlier.[31,44] Except HFIPA polymer all the chain packing pattern are quite same. But in the case of HFIPA polymer, a relatively intense peak appears at around 14.5° 2θ. This is because of the presence of a bulky hexafluoroisopropylidene group, which influences the different type chain packing of Py-PBI.
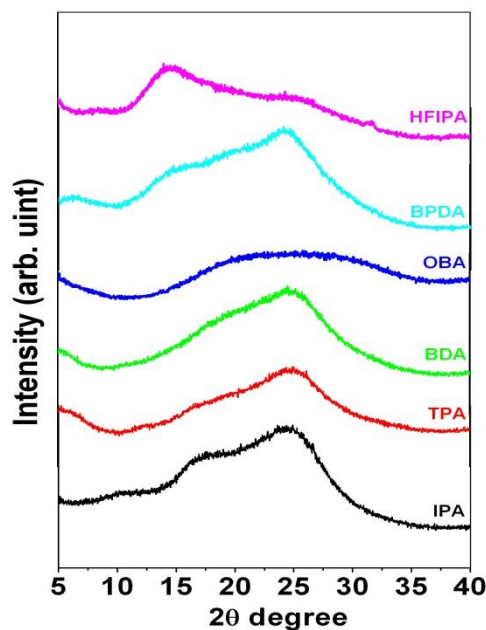
Figure 4.8. *WAXD patterns of Py-PBI polymers.*

4.4.4. Solubility:

One of the major barriers to the extensive use of the rigid-rod PBI is their infusibility, poor solubility, and consequently poor processability. To increase the solubility of PBI polymers, many groups have attempted either modification of main polymer backbone chain or substitution of different groups in imidazole ring.[24,28-31] Almost in all the cases of main PBI backbone chain modification have been carried out by polymerizing conventional TAB with different DCAs. Often incorporation of hetero atoms (oxygen, nitrogen) directly in the polymer backbone is known to enhance the solubility of PBIs.[19,27,42] For example, either linkage containing PBI [poly(4,4′-diphenylether-5,5′-bibenzimidazole), named as OPBI], obtained from the conventional TAB and OBD, is highly soluble in low boiling solvent like formic acid (FA),[27,40] which makes OPBI an interesting type of PBI because the processability and hence film formation become easy. However, the insolubility of other PBI in FA obtained from conventional TAB and other DCAs (Table 4.2, last row) remains as challenging a task for the wider use of PBI materials. Incorporation of a bulky group in the polymer backbone can also enhance the solubility due to disruption of the rigid structure and decreased intermolecular attraction.[45] The solubility of these newly synthesized Py-PBIs in various solvents is listed in Table 4.2. These polymers are easily soluble in polar aprotic solvents such as dimethyl formamide (DMF), DMAc, *N*-methyl-2-pyrrilidinone (NMP), and dimethyl sulfoxide (DMSO) at room temperature. Most importantly they are readily soluble in low boiling acidic solvent like formic acid (FA; Table 4.2, last row). It must be noted that all the Py-PBI, irrespective of DCA structure, are soluble in FA;

hence, this opens up the possibility of easy processability and wider usability of these new Py-PBIs. The enhanced solubility of Py-PBIs is due to the bulky structure of the Py-TAB monomer, which disrupts the rigidity of the PBI structure by breaking the intermolecular interaction and also the incorporation of an extra N atom in the ring helps the solubility. In conclusion, if we use Py-TAB instead of conventional TAB as a tetramine monomer, we can easily make soluble and processable PBIs (Py-PBIs) from any kind of DCAs, whereas with conventional TAB, only OBA results in the soluble PBI in FA.

Table 4.2. *Comparisons of solubility of Py-PBI and PBI polymers in various organic solvents*[a]

Solvent	Polymer	Dicarboxylic acids					
		IPA	TPA	BDA	OBA	BPDA	HFIPA
DMAc	PBI	++	++	++	++	++	++
	Py-PBI	++	++	++	++	++	++
NMP	PBI	+	+	++	++	++	++
	Py-PBI	++	++	++	++	++	++
FA	PBI	−	−	−	++	−	−
	Py-PBI	++	++	++	++	++	++

[a]Solubility is checked up to 3 wt.% (w/v). ++ : Soluble at room temperature; + : soluble on heating; − : insoluble even on heating.

4.4.5. Thermal Stability:

TGA analysis of all the synthesized Py-PBIs were carried out in the temperature range of 30-900 °C with a scanning rate of 10 °C/min in the presence of a nitrogen flow. The TGA curves of all Py-PBI are shown in Figure 4.9, and the important thermal data extracted from the TGA plots for all the samples are presented in Table 4.3. Two distinct weight losses are observed: an initial weight loss at around 100-150 °C and the second weight loss at around > 550 °C. The first weight loss is assigned to the loss of loosely bound absorbed water molecules. The second stage degradation occurred at around > 550 °C because of the decomposition of pyridine groups and the decomposition of benzimidazole groups. The thermal stability results (Figure 4.9 and Table 4.3) indicate the remarkable thermal stability of the polymers and also indicate the DCA monomers structure effect on the Py-PBIs thermal stability. Among the polymers studied here, HFIPA polymer weight loss is less in the lower temperature range, which is responsible for the loss of water molecules, which indicates the low water absorption due to the hydrophobic nature of the hexafluoroisopropylidene group. The differences in the second stage degradation temperatures at around 500 °C among the Py-PBIs are very minimal; the small differences can be attributed to the effect of DCA monomers structures. At higher temperature range, the HFIPA polymer displays slightly higher degradation compared to others. In the case of IPA and TPA polymers, TPA polymer degradation is more

compared to IPA polymer due to the symmetrical structure of TPA. But finally, with the weight loss around 900 °C, degradation increases with increasing the repeat unit molecular weight. Hence, we can summarize that our synthesized new Py-PBI polymers are thermally stable at higher temperature, like conventional PBI structure.

Table 4.3. *Thermal stability data of Py-PBI polymers.*

Py-PBI	$W_{150 °C}$ (%)[a]	$W_{570 °C}$ (%)[b]	$W_{900 °C}$ (%)[c]	$T_{10\%}$[d]
IPA	95.16	89.25	72.65	558.65
TPA	94.84	91.65	74.78	594.45
BDA	92.32	87.91	71.67	408.69
OBA	93.90	90.39	72.03	576.71
BPDA	92.15	86.84	67.50	539.14
HFIPA	95.04	79.00	64.97	518.27

[a,b,c] are the residual weight percent at 150 °C, 570 °C and 900 °C temperature, respectively and [d] is the corresponding temperature where 10% weight loss is observed.
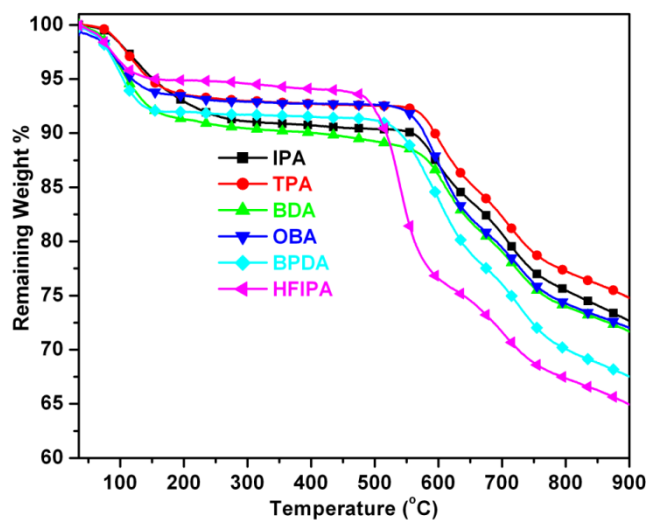
Figure 4.9. *Thermogravimetric plots of Py-PBI polymers in N$_2$ atmosphere. The heating rate was 10 °C /min.*

4.4.6. Thermal Transitions and Mechanical Properties:

The storage modulus (E'), loss modulus (E''), and tan δ as a function of temperature for all the Py-PBIs are represented in Figure 4.10. The glass transition temperature (T_g) and E' at different temperatures extracted from Figure 4.10 are tabulated in Table 4.4. The E′ values of Py-PBIs differ from each other, depending on the DCA structure. The E' values of all the Py-PBI polymers are comparable with the

literature value of PBI.[2,3,40,42] The *E'* decreases with increasing temperature in all cases indicates that mechanical property becomes poorer at higher temperature. However, the change is not very significant proves the fact that these Py-PBIs have good mechanical strength even at very high temperature. In the case of BDA polymer, the storage modulus is less than the other polymers. It could be because of the biphenyl ring of the acid monomer is more flexible due to the larger distance and more symmetrical para connected structure. It must be noticed that TPA polymer is showing better strength compared to that of IPA polymer (Table 4.4 and Figure 4.10). In fact, not only TPA, but it is clear that all para structure Py-PBIs show (except BDA) higher *E'* at all temperatures (Table 4.4) than meta Py-PBI, suggesting meta has inferior mechanical property compare to para structure oriented Py-PBI polymers. The higher modulus of para structure polymer may be due to the different structural packing of para owing to their symmetrical nature.
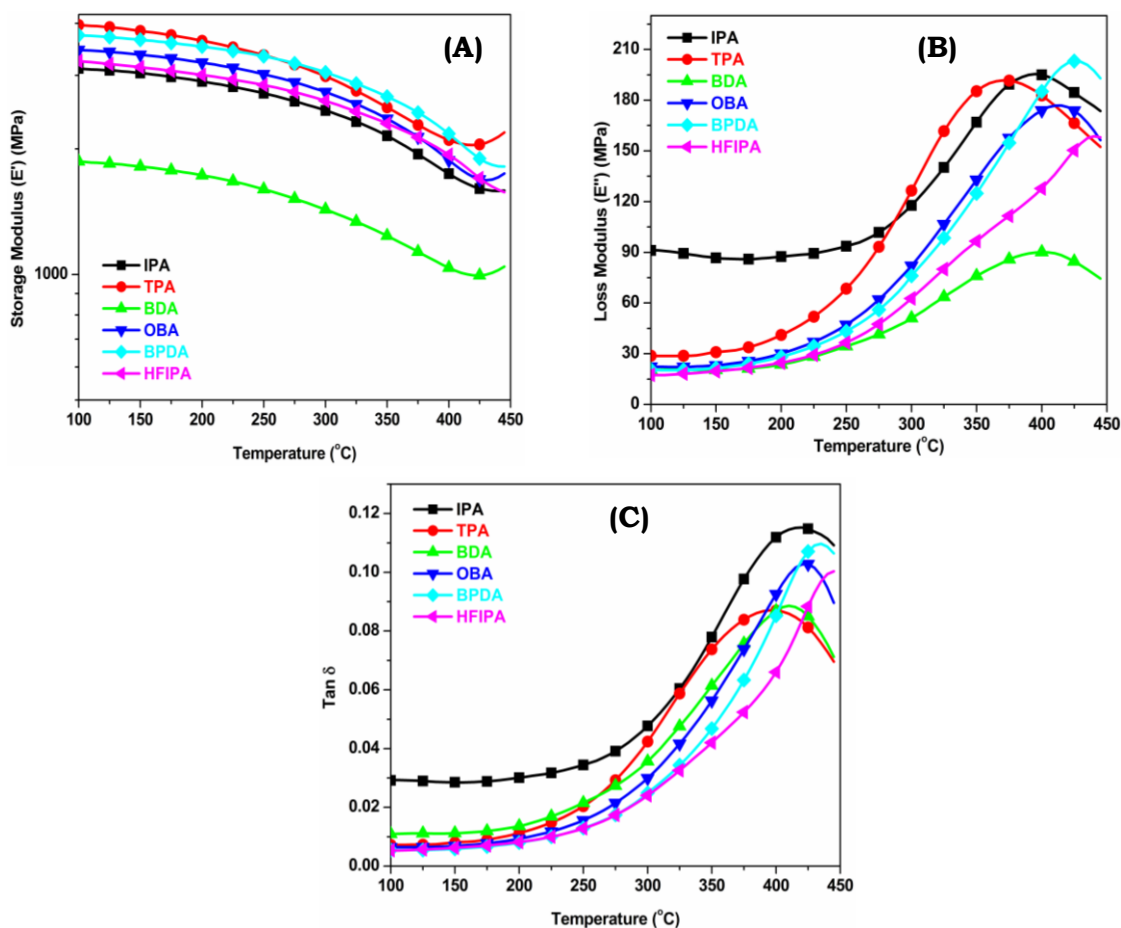
Figure 4.10. *Various thermo-mechanical properties of Py-PBI polymers obtained from DMA. (A), (B) and (C) represent the storage modulus (E'), loss modulus (E") and tan δ, respectively.*

The T_g of PBI polymers are generally very high and varies from 350 to 450 °C depending on the backbone structure.[2,3,42] The T_g obtained in this study for all Py-PBI polymers also fall in this range (Table 4.4 and Figure 4.10) attributing that these are high T_g polymers. Generally the para connected PBI displays lower T_g than the meta PBI.[2,42] The T_g values differ from polymer to polymer depending on the DCA structure used for making the Py-PBI. The T_g of the TPA polymer (397 °C, obtained from tan δ) is lowest among all the polymers. The highest T_g (448 °C, obtained from tan δ) is the hexafluoro containing HFIPA polymer.

Table 4.4. *Various thermo-mechanical data and glass transition temperatures obtained from DMA study.*

Py-PBI	E' (MP$_a$) at 100 °C	E' (MP$_a$) at 425 °C	T_g (°C) from E''	T_g (°C) from tan δ
IPA	3120	1607	394	418
TPA	3961	2049	369	397
BDA	1866	995	400	411
OBA	3454	1691	413	423
BPDA	3747	1896	425	434
HFIPA	3284	1702	439	448

4.4.7. Oxidative Stability:

The oxidative stability was performed by doing the Fenton's test. In the test, the hydroxyl (OH$^•$) and hydroperoxyl (OOH$^•$) radicals attack polymer backbone and degradation takes place. Figure 4.11 shows the oxidative stability of all Py-PBI polymers as a function of time. All the newly synthesized Py-PBIs have significantly higher stability than the conventional PBI. For example, only 60% weight remains after 120 h in case of conventional PBI obtained from IPA, whereas ~80% weight remains in case of Py-PBI made from IPA (Figure 4.11). This may be due to the presence of bulky pyridine groups in the main chain of Py-PBI polymers. Therefore, these new Py-PBIs have better usability than the conventional PBI in an oxidative environment. The heteroatom containing polymers like OBA, BPDA, and HFIPA displays less degradation than the Py-PBIs obtained from other DCAs (TPA, IPA, and BDA). Therefore, the heteroatom in the main chain enhances the oxidative stability. Among all, the HFIPA polymer degradation is the lowest. In the case of HFIPA, owing to the hexafluoro moieties polymer, is less hygroscopic nature and hence retards the attack by OH$^•$ and OOH$^•$ radicals to the polymer backbone.[43a] Therefore, the HFIPA shows the highest stability. Hence, we can conclude that the current pyridine-based PBIs (Py-PBIs) are more chemically stable even after 120 h and the only ~20% (by weight) degradation takes place. After the completion of the Fenton test, membranes are not brittle; it proves that the membranes are stable in a drastic chemical environment.
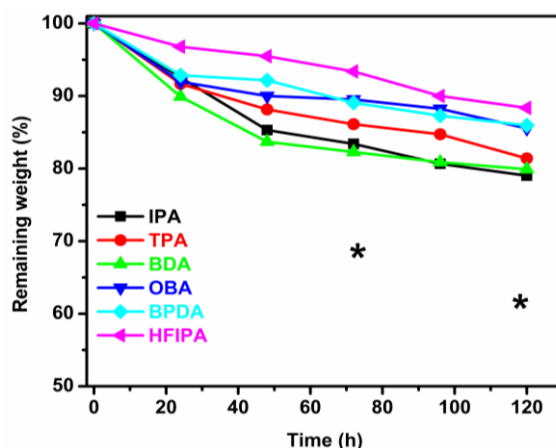
Figure 4.11. *Oxidative stability of Py-PBI polymers. The symbol (*) in the figure shows the stability data of IPA based conventional PBI reported in the literature earlier.[46]*

4.4.8. Water Uptake and Swelling Ratio:

The proton conduction of phosphoric acid (PA) doped PBI membrane depends upon the amount of water molecule associated with the polymer matrix. Hence, the amount of water molecules present in the membrane is an important parameter for proton conduction. Polybenzimidazole is a hygroscopic polymer and can absorb moisture up to 5 wt% from atmosphere due to formation of intermolecular hydrogen bonding between N-H and water molecules. From our experimental measurement, we observe that the amount of water uptake of Py-PBI polymers is between 7.15 to 12.76 wt% (Table 4.5). The hexafluoro containing HFIPA polymer absorbed less amount of water due to the hydrophobic fluorine atoms incorporation to the polymer backbone. Heteroatom containing BPDA and OBA polymers absorbed more amounts of water. It could be that the hydrogen bonding occurs between water molecules and hetero atoms of polymer. The literature reported that water uptakes for the conventional PBIs are ~ 15 to 20% (by weight), depending on the polymer structure.

Table 4.5. *The water uptake and swelling ratio of Py-PBIs polymers after dipping in water for seven days.[a]*

Py-PBI	Water uptake (%)	Swelling Ratio (%)
IPA	8.12 (1.50)	3.16 (0.27)
TPA	8.50 (1.59)	3.36 (0.06)
BDA	10.94 (0.22)	3.43 (0.29)
OBA	12.66 (0.58)	4.20 (0.19)
BPDA	12.76 (0.90)	3.61 (0.06)
HFIPA	7.15 (0.36)	3.04 (0.07)

[a]The standard deviations are shown in the parentheses.

Swelling of the membrane is also a crucial parameter to be checked for in the use of fuel cell when it absorbs solvent. When membrane absorbs solvent, it swells and loses the mechanical strength; therefore, the swelling must be checked to verify the feasibility of the membrane to make membrane electrode assembly. Here we observe that the swelling ratios of Py-PBI polymers are around 3 to 4%. Among all the polymers, hexafluoro containing polymers swell the least amount due to the presence of the hydrophobic fluorine atom, and hence, water molecules cannot go inside the polymer backbone so readily. The water uptake and swelling ratio of these newly synthesized Py-PBIs are comparatively lower than the conventional PBI, making these Py-PBI polymers more useful as PEM in the fuel cell.

4.4.9. Phosphoric Acid Doping Level:

The proton conductivity of PEM membrane depends upon the phosphoric acid (PA) loading of the membrane. According to hopping mechanism, increasing acid loading enhances the proton transfer throughout the membrane and hence increases the proton conductivity. We have doped the Py-PBI membranes by varying the H_3PO_4 concentration of the doping solution from 30 to 60 wt%. We could not dip the Py-PBI membranes more than 60% (by weight) H_3PO_4 since at higher acid concentration most of the membranes are soluble. This may be due to the large intermolecular distance and presence of pyridine ring in the backbone and hence the acid molecules can penetrate inside the polymer chain and easily dissolve the polymers. The acid loading increases with increasing the acid concentration, which in good agreement with literature,[47,48] and also the PA loading, depends on the DCAs structure (Figure 4.12). We found that the Py-PBI polymers load higher PA than the conventional PBIs when doping conditions (PA concentration and doping duration) are kept identical for both types of PBIs. For example, the PA loading of all the Py-PBI polymers studied here are > 9 mole/repeat unit when they were dipped in 60 wt% (12.32 M) H_3PO_4 bath for three days, whereas in the similar condition, PA loading of conventional PBI is much lower, as indicated by symbol * in Figure 4.12.[48] This is because of the extra N atom which is incorporated in the Py-PBIs backbone through the Py-TAB monomer enhances the basic nature of the polymer and hence facilitated absorption of more PA compared to conventional PBI.
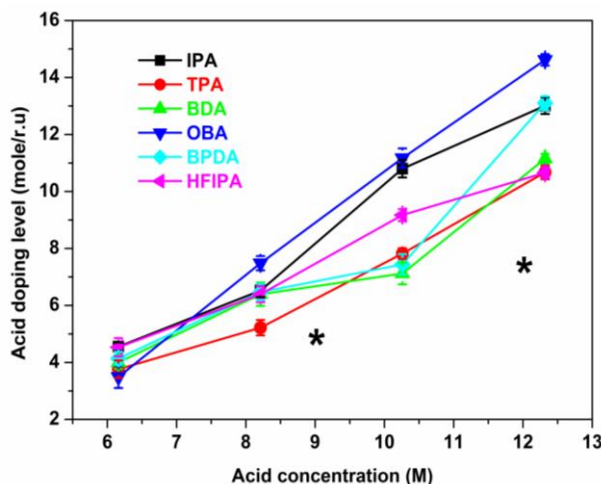
Figure 4.12. *Acid doping level of Py-PBI membranes obtained by dipping in different phosphoric acid concentrations at room temperature. The symbol (*) in the figure shows the PA loading data of IPA based conventional PBI reported in the literature earlier.[48]*

4.4.10. Proton Conductivity:

The temperature-dependent protonconductivity of all acid-doped Py-PBIs are calculated from Nyquist plots. Figure 4.13, shows representative Nyquist plots for all Py-PBIs at various temperatures, as obtained from the conductivity experiment during a second heating scan. Proton conductivity of the membranes are expected to increase with the increasing acid loading of membrane and our results in current studies are in agreement. The conductivity data as a function of temperature (Figure 4.14A) are the results obtained from those membranes that were doped with 60% (wt) H_3PO_4. As expected, the proton conductivity increases with increasing the temperature. The proton conductivity depends on the acid loading, temperature, and humidity, as well as the structure of the polymer backbone. Figure 4.13A clearly demonstrates that the Py-PBI backbone structure largely influences the conductivity. Py-PBIs obtained from heteroatom containing DCA and bigger molecular size DCA show higher conductivity than the IPA and TPA. In the literature for conventional PBI, similar observations have been reported earlier. The transport of proton in acid-doped membranes follows the Grotthuss mechanism and can be influenced by the hydrogen bonding. The diacid containing monomers are largely influenced by the proton conductivity due to their different structure orientation. Although the acid loading is highest in OBA polymer, proton conductivity is highest in HFIPA polymer. From Figure 4.14A we can see that the proton conductivity of acid-doped membranes at 160 °C for HFIPA and BPDA polymers are nearly 0.01 Scm^{-1}. The heteroatom containing polymers are more conducting compared to IPA and TPA polymers. This implies that the heteroatom might be participating in the hydrogen bonding to influence the proton conductance. Another reason for high proton conductivity of HFIPA polymer is the large electronegativity of fluorine atoms that

activates the imidazole ring N-H proton, thus, proton- hopping across the membrane becomes easier.[15] Recently, we have observed a similar effect in the blends of PBI and poly(vinylidene fluoride-co-hexafluoro propylene).[39]
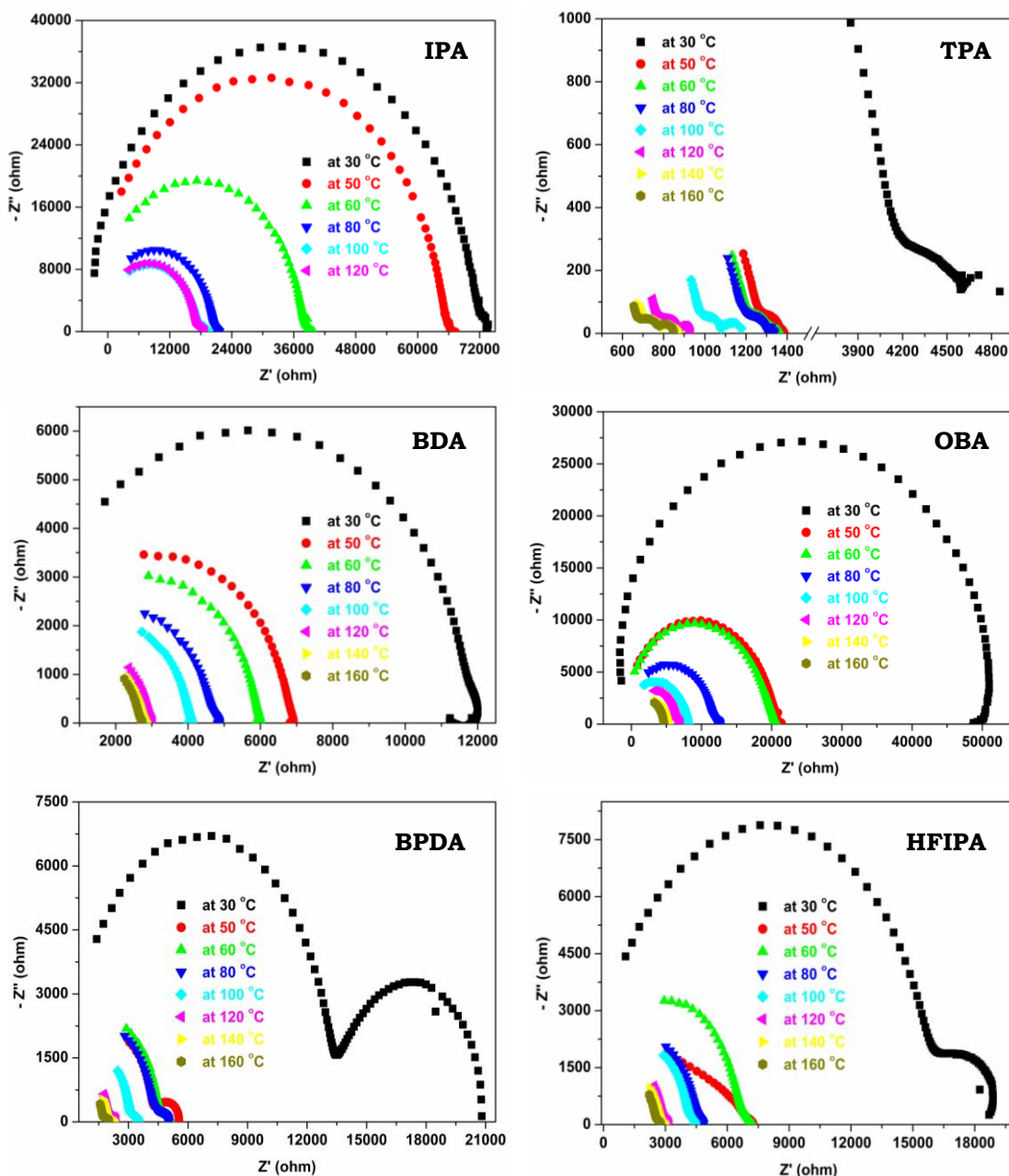
Figure 4.13. *Nyquist plots of various Py-PBI polymers at different temperatures.*

To calculate the activation energy (E_a) of the proton conduction process, the conductivity data plotted in Figure 4.13B using the following equation:

$$\ln(\sigma T) = \ln\sigma_o - Ea/RT \qquad \text{--------------} \quad (4.1)$$

Where σ is the proton conductivity of the PA-doped membranes (Scm^{-1}), T is the temperature (K), σ_o is the pre-exponential factor ($SK^{-1}cm^{-1}$), E_a is the proton conducting activation energy (kJ/mol), and R is the ideal gas constant ($Jmol^{-1}K^{-1}$). The E_a values are obtained by linear fitting the data. E_a values are also highly dependent on the structure of DCA. The E_a values obtained here are smaller than the E_a values of conventional PBI. This may be due to a bulky pyridine group in the main chain of Py-PBI, which facilitated further proton conduction.
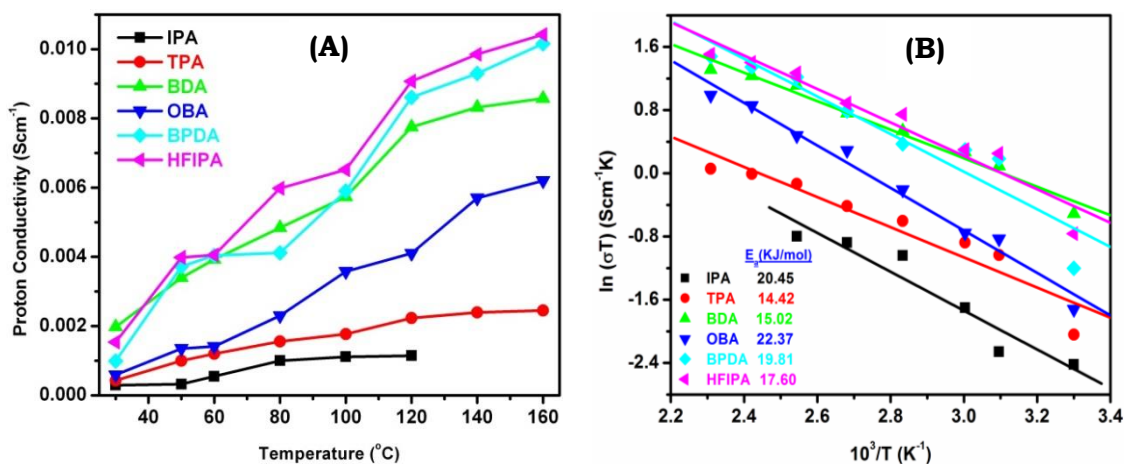
Figure 4.14. *(A) Proton conductivity vs. temperature plots and (B) Arrhenius plot for the proton conduction of PA doped Py-PBI membranes.*

4.3.11. Photophysical Studies:

The photophysical studies of all the Py-PBIs are carried out from dilute solution of polymer in DMAc. The concentration of the solution for all the Py-PBI samples is kept at 2×10^{-5} M, where molarity is calculated by considering repeat unit as 1 mole. The absorption spectra of Py-PBIs in DMAc solutions are presented in Figure 4.15A. The peak positions and the shape of the peaks are varied depending on the structure of Py-PBI, that is, varied from DCA to DCA. Table 4.6 lists all peak positions. Except BDA and BPDA polymer all other DCA polymer display two absorption peaks. From our earlier studies we know that PBI shows λmax at ~ 350 nm (depending on the DCA structure this alters) for π-π* transition.[25,27] However, in case of Py-PBI we obtained two λmax for π-π* transitions. This is because the phenyl group, which is connected with the pyridine moiety of Py-TAB monomeric unit, can exist as two different forms; one is in

plane with the polymer backbone and another one is perpendicular to the polymer backbone, hence, because of the two forms we obtained two π-π* transitions. This observation attributes the clear distinction between conventional PBI and newly synthesized Py-PBI. It is also noted that the λ_{max} peak positions alter from DCA to DCA. As we know from our earlier observation that para connected structure shows λ_{max} at higher wavelength than the meta connected owing to their better conjugation and symmetrical structure.[42] Figure 4.15A clearly shows λ_{max} of TPA, BDA, and BPDA polymers at a higher wavelength than the IPA. Although the other two (OBA and HFIPA) are also a para connected structure, but they display λ_{max} similar to IPA, which may be due to the presence of highly electronegative atoms (O, CF$_3$) in the backbone. It is also to be noted that BDA and BPDA do not show double λ_{max}, this is probably because of their structure effect.
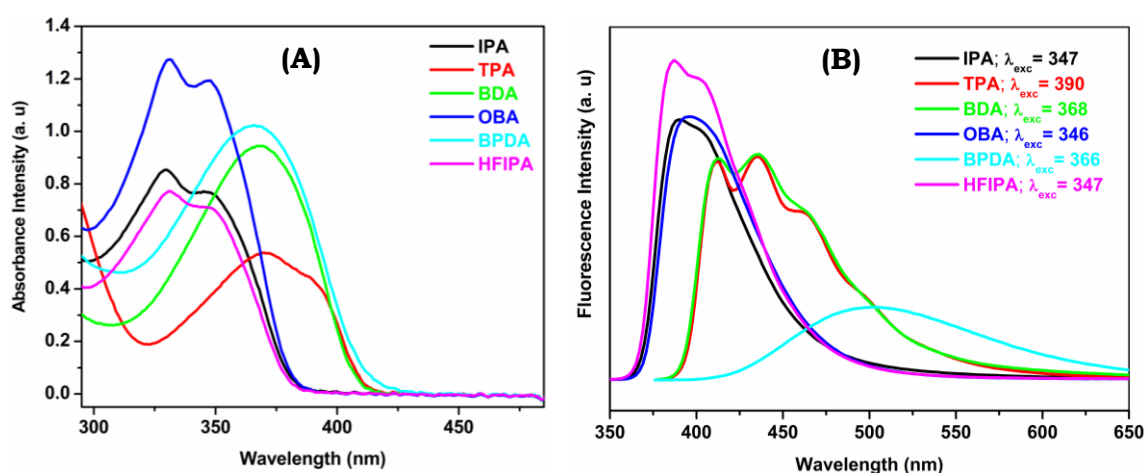
Figure 4.15. *(A) Absorption spectra and (B) Fluorescence emission spectra of Py-PBI polymers in DMAc solution as recorded with a cuvette of 1 cm path length. Concentrations are 2 x 10^{-5} M and excitation wavelengths (λ_{exc}) are indicated in the figure.*

Table 4.6. *Electronic spectroscopy data of Py-PBI polymers.*

PY-PBI	Absorption (λ) peak (nm)	Emission peaks (nm)
IPA	329, 347	389, 403
TPA	370, 390	411, 436, 463
BDA	368	411, 436, 463
OBA	331, 346	395
BPDA	366	502
HFIPA	330, 347	388, 402

Figure 4.15B shows the emission spectra of all the Py-PBIs recorded from DMAc dilute solution. As we know, the emission of PBI comes from ^1L_b state, which has two excitations for 0-0 and 0-1 states, here also we obtained similar results.[25,27,49] All the peak positions are listed in Table 4.6. Except BPDA and OBA, all others show two emission peaks. TPA and BDA polymers also exhibit a broad emission shoulder at ~463 nm. As expected, para structure (TAP, BDA) shows longer wavelength emission than meta structure (IPA). However, despite the para structure, OBA and HFIPA displays an emission similar to IPA as it is seen in absorption spectra (Figure 4.15A) due to the presence of strong electronegativity atoms (O, CF_3) in the backbone.

4.5. CONCLUSION:

A series of novel pyridine bridge polybenzimidazoles (Py-PBIs) are synthesized by polymerizing a large variety of dicarboxylic acids with an efficient, cost-effective, and readily accessible pyridine bridge tetramine (Py-TAB) monomer with an objective to replace the conventionally used tetramine monomer. The polymerization conditions are optimized to obtain high molecular weight Py-PBIs. Spectral characterization confirms the molecular structure of the resulting polymers. Py-PBIs display better stability compared to the conventional PBI; especially remarkably good solubility of all Py-PBIs in low boiling organic solvent like formic acid eliminates the inherent processability problems of PBI type polymers. Thermal, mechanical, and chemical stability studies indicate the thermomechanical and chemical stabilities of Py-PBIs are as good as conventional PBI. These new polymer membranes absorb more phosphoric acid compared to conventional PBI and hence display higher proton conductivity. Photophysical studies confirm the structural aspects of the newly synthesized polymer. Therefore, these newly synthesized Py-PBs satisfy 3-fold objectives: (a) an inexpensive alternative TAB monomer, (b) soluble, readily processable PBI, and (c) higher acid-loaded PEM membranes with higher proton conductivities.

REFERENCES:

(1) Vogel, H. A.; Marvel, C. S. *J. Polym. Sci.* **1961,** *50*, 511.

(2) Neuse, E. W. *Adv. Polym. Sci.* **1982,** *47*, 1.

(3) (a) Dang, T. D.; Narayanan V.; Mark, J. E. *Polyimides and Other High Temperature Polymers*, **2009**, *5*, 145. (b) Dawkins, B. G.; Baker, J. D. US 20080207869, 2008. (c) Choe, E. W.; Conciatori, A. B. EP 115945, 1984.

(4) Chung, T. S. *J. Macromol. Sci., Rev. Macromol. Chem. Phys.* **1997,** *C37*, 277.

(5) Asensio, J. A.; Sánchez, E. M.; Gomez-Romero, P. *Chem. Soc. Rev.* **2010,** *39*, 3210.

(6) Mader, J.; Xiao, L.; Schmidt, T. J.; Benicewicz, B. C. *Adv. Polym. Sci.* **2008,** *216*, 63.

(7) Wainright, J. S.; Wang, J. T.; Weng, D.; Savinell, R. F.; Litt, M. *J. Electrochem. Soc.* **1995**, *142*, L121.

(8) Jung, K. H.; Ferraris, J. P. *Carbon* **2012,** *50*, 5309.

(9) Ng, F.; Peron, J.; Jones, D. J.; Roziere, J. *J. Polym. Sci., Part A: Polym. Chem.* **2011,** *49*, 2107.

(10) Li, Q. F.; Rudbeck, H. C.; Chromik, A.; Jensen, J. O.; Pan, C.; Steenberg, T.; Calverley, M.; Bjerrum, N. J.; Kerres, J. *J. Membr. Sci.* **2010,** *347*, 260.

(11) Shi, G. M.; Chen, H.; Jean, Y. C.; Chung, T. S. *Polymer* **2013**, *54*, 774.

(12) Weber, J.; Antonietti, M.; Thomas, A. *Macromolecules* **2007**, *40*, 1299.

(13) Chuang, S. W.; Hsu, S. L. C. *J. Polym. Sci., Part A: Polym. Chem.* **2006,** *44*, 4508.

(14) Mader, J. A.; Benicewicz, B. C. *Macromolecules* **2010**, *43*, 6706.

(15) Pu, H.; Wang, L.; Pan, H.; Wan, D. *J. Polym. Sci., Part A: Polym. Chem.* **2010**, *48*, 2115.

(16) Kim, S. K.; Choi, S. W.; Jeon, W. S.; Park, J. O.; Ko, T.; Chang, H.; Lee, J. C. *Macromolecules* **2012**, *45*, 1438.

(17) Li, Q.; Jensen, J. O.; Savinell, R. F.; Bjerrum, N. J. *Prog. Polym. Sci.* **2009**, *34*, 449.

(18) Wang, G.; Xiao, G.; Yan, D. *J. Membr. Sci.* **2011**, *369*, 388.

(19) Kang, Y.; Zou, J.; Sun, Z.; Wang, F.; Zhu, H.; Han, K.; Yang, W.; Song, H.; Meng, Q. *Int. J. Hydrogen Energy* **2013**, *38*, 6494.

(20) Qing, S.; Huang, W.; Yan, D. *J. Polym. Sci., Part A: Polym. Chem.* **2005**, *43*, 4363.

(21) Suegusa, Y.; Horikiri, M.; Nakurnura, S. *Macromol. Chem. Phys.* **1997,** *198*, 619425.

(22) Ma, T.; Li, Y. F.; Zhang, S. J.; Yang, F. C.; Gong, C. L.; Zhao, J. *J. Chin. Chem. Lett.* **2010,** *21*, 976.

(23) Maner, A.; Bavikar, S.; Sudalai, A.; Sivaram, S. WO 2005/063679*,* 2005.

(24) Klaehn, J. R.; Luther, T. A.; Orme, C. J.; Jones, M. G.; Wertsching, A. K.; Peterson, E. S. *Macromolecules* **2007,** *40,* 7487.

(25) Sannigrahi, A.; Arunbabu, D.; Sankar, R. M.; Jana, T. *Macromolecules* **2007**, 40, 2844.

(26)   Shogbon, C, B.; Brousseau, J. L.; Zhang, H.; Benicewicz, B. C.; Akpalu, Y. *Macromolecules* **2006**, *39*, 9409.

(27)   Ghosh, S.; Sannigrahi, A.; Maity, S.; Jana, T. *J. Phys. Chem. B* **2010,** *114*, 3122.

(28)   Gieselman, M. B.; J, Reynolds, J. R. *Macromolecules* **1992,** *25*, 4832.

(29)   Pu, H.; Liu, Q.; Liu, G. *J. Membr. Sci.* **2004**, *241,*169.

(30)   Glipa, X.; Haddad, M. E.; Jones, D. J.; Roziere, J*. Solid State Ion.* **1997**, *97*, 323.

(31)   Maity, S.; Sannigrahi, A.; Ghosh, S.; Jana, T. *Euro. Polym. J.* **2013**, *49*, 2280.

(32)   He, R.; Li, Q.; Jensen, J. O.; Bjerrum, N. J. *J. Polym. Sci., Part A: Polym. Chem.* **2007**, *45*, 2989.

(33)   Weber, J.; Kreuer, K. D.; Maier, J.; Thomas, A. *Adv. Mater.* **2008**, *20*, 2595.

(34)   Ma, Y. L.; Wainright, J. S.; Litt, M. H.; Savinell, R. F. *J. Electrochem. Soc.* **2004,** *151*, A8.

(35)   Kim, S. K.; Kim, T. H; Jung, J. W; Lee, J. C. *Polymer* **2009**, *50*, 3495.

(36)   Asensio, J. A.; Borros, S.; Gomez-Romero, P. *J. Membr. Sci.*, **2004**, *241*, 89.

(37)   (a) Xiao, L.; Zhang, H.; Scanlon, E.; Ramanathan, L. S.; Choe, E. W.; Rogers, D.; Apple, T.; Benicewicz, B. C. *Chem. Mater.* **2005**, *17*, 5328. (b) Xiao, L.; Zhang, H.; Jana, T.; Scanlon, E.; Chen, R.; Choe, E. W.; Ramanathan, L. S.; Yu, S.; Benicewicz, B. C. *Fuel Cells* **2005**, *5*, 287.

(38)   Hickner, M. A.; Ghassemi, H.; Kim, S. Y.; Einsla, B. R.; McGrath, J. E. *Chem. Rev.* **2004**, *104*, 4587.

(39)   (a) Deimede, V.; Voyiatzis, G. A.; Kallitsis, J. K.; Qingfeng, L.; Bjerrum, J. N. *Macromolecules* **2000**, *33*, 7609. (b) Arunbabu, D.; Sannigrahi, A.; Jana, T. *J. Phys. Chem. B* **2008**, *112*, 5305. (c) Hazarika, M.; Jana, T. *ACS Appl. Mater. Interfaces* **2012**, *4*, 5256. (d) Hazarika, M.; Jana, T. *Euro. Polym. J.* **2013,** *49,* 1564.

(40)   (a) Ghosh, S.; Sannigrahi, A.; Maity, S.; Jana, T. *J. Phys. Chem. C* **2011,** *115*, 11474. (b) Ghosh, S.; Sannigrahi, A.; Maity, S.; Jana, T. *J. Mater. Chem.* **2011**, *21,* 14897. (c) Kannan, R.; Kagaiwale, H. N.; Chaudhari, H. D.; Kharul, U. K.; Kurungot, S.; Pillai, V. K. *J. Mater. Chem.* **2011**, *21*, 7223. (d) Chung, S. W.; Hsu, S. L. C.; Liu, Y. H. *J. Membr. Sci.* **2007**, *305*, 353.

(41)   (a) Sannigrahi, A.; Arunbabu, D.; Jana, T. *Macromol. Rapid Commun*. **2006,** *27*, 1962. (b) Sannigrahi, A.; Ghosh, S.; Maity, S.; Jana, T. *Polymer* **2011**, *52*, 4319. (c) Mecerreyes, D.; Grande, H.; Miguel, O.; Ochoteco, E.; Marcilla, R.; Cantero, I. *Chem. Mater.* **2004,** *16*, 604. (d) Liu, J. G.; Wang, L. F.; Yang, H. X.; Li, H. S.; Li, Y. F.; Fan, L.; Yang, S. Y. *J. Polym. Sci., Part A: Polym. Chem.* **2004,** *42*, 1845.

(42)   (a) Sannigrahi, A.; Ghosh, S.; Maity, S.; Jana, T. *Polymer* **2010,** *51*, 5929. (b) Sannigrahi, A.; Ghosh, S.; Lalnuntluanga, J.; Jana, T. *J. Appl. Polym. Sci.* **2009,** *111*, 2194. (c) Sannigrahi, A.; Arunbabu, D.; Sankar, R. M.; Jana, T. *J. Phys. Chem. B* **2007,** *111*, 12124.

(43)   (a) Qian, G.; Benicewicz, B. C. *J. Polym. Sci., Part A: Polym. Chem.* **2009,** *47*, 4064. (b) Yu, S.; Zhang, H.; Xiao, L.; Choe, E. W.; Benicewicz, B. C. *Fuell Cells* **2009**, *4*, 318.

(44)   Staiti, P.; Lufrano, F.; Arico, A. S.; Passalacqua, E.; Antonucci, V. *J. Membr. Sci.* **2001,** *188*, 71.

(45)   Ma, T.; Li, Y. F.; Zhang, S. J.; Yang, F. C.; Gong, C. L.; Zhao, J. *J. Chin. Chem. Lett.* **2010,** *21*, 976.

(46)   Li, Q.; Pan, C.; Jensen, J. O.; Noye, P.; Bjerrum, N. J. *Chem. Mater.* **2007**, *19*, 350.

(47)   He, R.; Che, Q.; Sun, B. *Fibers Polym.* **2008,** *9*, 679.

(48)   Li, Q.; Hjuler, H. J.; Bjerrum, N. J. *J. Appl. Electrochem.* **2001,** *31*, 773.

(49)   Kojima, T. *J. Polym. Sci.: Polym. Phys. Ed.* **1980,** *18*, 1685.

CHAPTER 5

Polycondensation of Structurally Dissimilar Tetraamine Monomers with Dicarboxylic Acids to Synthesize Polybenzimidazole Copolymers for PEM
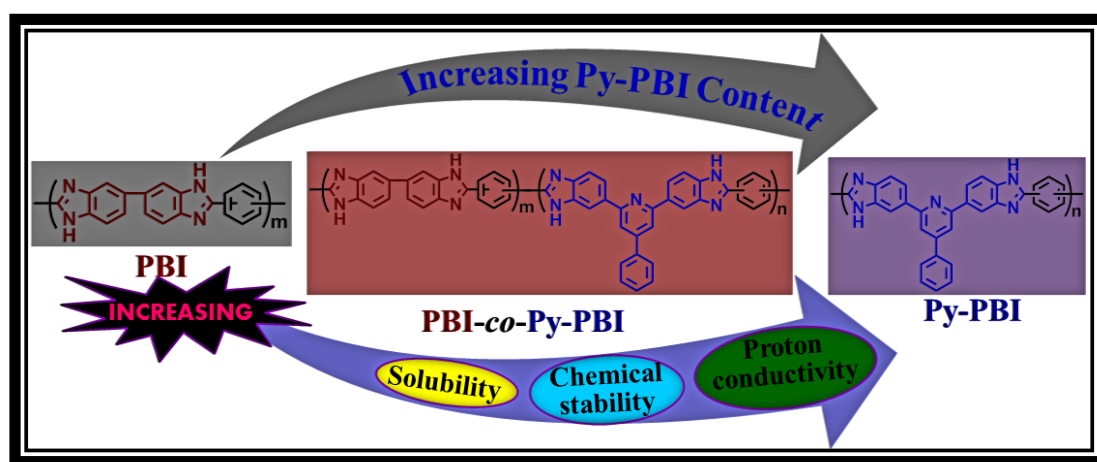
5.1. INTRODUCTION:

Since the discovery of polybenzimidazoles (PBIs), heterocyclic rigid high performance polymers, the interests and importance of this class of polymers are growing exponentially because of tremendous applications potentials in numerous areas owing to very high thermal, mechanical and chemical stabilities.[1-6] Naturally, huge scope of studies on PBIs have been generated to meet the growing demand. PBIs usability ranges from fire retarding polymer, chemically resistant polymer and other high performances applications; however the most important areas of application is as a thermo-mechanical and chemically stable membrane used in areas like reverse osmosis, water purification etc. since PBI forms membrane readily.[7-10] The discovery of phosphoric acid (PA) doped PBI membranes as a promising polymer electrolyte membrane (PEM) for high performance fuel cell in 1990's by Case Waster University research group led to an important breakthrough in the areas of PBI.[11]

To meet the application booms as described above, synthesis of PBIs with varieties of structures so that the properties can be readily manipulated became the prime objective for the researchers working in this area.[12-17] Polycondensation of a tetramine with dicarboxylic acid (DCA) yields PBI; in literature 3,3',4,4'-tetraaminobiphenyl (TAB) is polymerized with varieties of DCA structures to modulate the PBI properties. Huge numbers of DCAs with varieties of structures have been used to make PBIs. The primary objectives of the structural variation of DCAs were mainly two folds: firstly make soluble and hence easily processable PBI since otherwise PBI is difficult to process and secondly controls the PBI properties like rigidity, thermal stability, basicity, chains folding, etc.[12-18] The most common PBI structures known in the literature are *meta*-PBI (*m*-PBI), *para*-PBI (*p*-PBI), sulfonated PBI, pyridine based PBI, oxy-PBI, etc. It must be noted that in all these cases, only TAB used as tetramine source. There are only few literature reports where tetramines structures other than TAB have been used. Among these, AB type PBI is the most common.[19] Recently, we demonstrated tetramine 2,6-bis(3′,4′-diaminophenyl)-4-phenylpyridine (Py-TAB) is the most effective tetramine monomer as an alternative to TAB and the resulting PBIs (Py-PBIs) have showed many fold improvements in properties especially processability than the conventional PBIs Chapter 4).[20]

At this moment, the most important use of PBI is as PEM when it is doped with PA. The biggest dilemma in the use of PA doped PBI as PEM is the balancing of thermo-mechanical stability and the acid loading which in turns control the proton conductivity and hence the cell performance. Several techniques have been developed to tackle this problem and among them the most prominents are: (a) synthesis of new PBI structures[12-18] (b) development of new membrane fabrication method[11,21-23] (c) preparations of blends and nanocomposites, etc.[24-26]

Researchers have put lot of efforts to build new type of PBIs backbone either by polymerizing the TAB with varieties of DCA structure or by post polymerization modifications. The other synthetic design

which allows the introduction and modulation of varieties of properties in the PBI chain is to construct the novel PBI backbone by copolymerization of TAB (tetramine) with two different DCAs. For example only *m*-PBI is not very strong because of low molecular weight, therefore synthesis of *m*PBI-*co-p*PBI can increase the molecular weight hence the mechanical strength, however this compromises the processability and hence the composition of DCAs (meta and para component) in the final PBI structure can be controlled readily during the copolymerization to achieve the desire properties of the resulting polymer. Several literature reports are available where one DCA is the sulfonated DCA so that it enhances the conductivity of the PEM. Therefore, always the DCAs are used with TAB to prepare copolymers with structural variation.[3,6,27] However; we noticed that there is not a single attempt has been made where one DCA is used with two tetramines to prepare the copolymers. This is perhaps due to the non-availability of suitable tetramines except TAB. Since recently we showed that Py-TAB can be the best alternative of TAB, hence we proposed to make copolymer varying TAB and Py-TAB as source of tetramines with DCAs. Therefore, in this article we made two sets of copolymers with isophthalic acid (IPA) and terephthalic acid (TPA) by altering TAB and Py-TAB monomers mole ratio in the polymerization. Our earlier studies revealed that Py-TAB can enhance several important properties of PBI such as solubility and processability and PEM made from Py-PBI displayed higher conductivity, oxidative stability.[20] Therefore, we wish to demonstrate the feasibility of Py-PBI in the formation of copolymer, where we can tailor the properties of polymer as per our desire in between conventional and Py-PBI.

In the present work, we have synthesized two series of *meta* and *para* connected random copolymers by polymerizing TAB and Py-TAB with one DCA. IPA and TPA are used as DCAs to prepare two sets of copolymers. The synthesized polymers are characterized by different techniques like FT-IR, ^{1}H NMR and WAXD for structural elucidation. Molecular weight measurements, thermogravimetric analysis (TGA), dynamic mechanical analysis (DMA), oxidative stability studies have been carried out to prove the formation of thermally, mechanically and chemically stable PBI polymers. We have also measured the absorption and fluorescence for the photophysical properties studies. Proton conductivity studies are carried out to understand the influence of copolymers structure.

5.2. SYNTHESIS:

5.2.1 Monomer (Py-TAB) Synthesis:

The detail information about the synthesis and characterization of 2,6-bis(3',4'-diaminophenyl)-4-phenylpyridine (abbreviated as Py-TAB) monomer are shown in the Chapter 2 & 4.

5.2.2. Copolymer (PBI-co-Py-PBI) Synthesis:

Two series of random copolymers of PBI were prepared by altering the amount (compositions) of TAB and Py-TAB for fixed content of dicarboxylic acids. In Series I, isophthalic acid (IPA) was polymerized

with varying content of TAB and Py-PBI to prepare *meta* (*m*) structured random copolymers of PBI and Py-PBI. These copolymers are referred as *m*PBI-*co-m*Py-PBI. Similarly in Series II, terephthalic acid (TPA) was used to synthesize *para* (*p*) structured random copolymers of PBI and Py-PBI (Scheme 5.1). These series of copolymers are referred as *p*PBI-*co-p*Py-PBI. In both the cases equal moles of dicarboxylic acid and tetramines were taken. The number of mols of TAB and Py-TAB were varied from 10 to 90%; however total moles of tetramines were always equal to total mols of dicarboxylic acids. All the polymerization were carried out in the polyphosphoric acid (PPA) medium in 100 g scale in a three neck mercury sealed flask equipped with mechanical stirrer and nitrogen atmosphere. Typically reactions were carried out for 24 hours using a fixed ramp and soak temperature profile from 50 °C to 210 °C. The final reaction temperature was always 210 °C. In case of Series I, total monomer concentration (TMC) was 5% (by weight) and Series II, TMC was 3.5%. These respective TMCs were kept constant for all the copolymers synthesized in this article. After the complete polymerization the viscous polymer solution was slowly poured into deionized water and neutralized with sodium bicarbonate solution. The polymers were filtered and washed with deionized water for several times to remove the excess bicarbonate and dried in vacuum oven for 24 h at 100 °C to remove the water completely. The reaction scheme is shown in the Scheme 5.1.
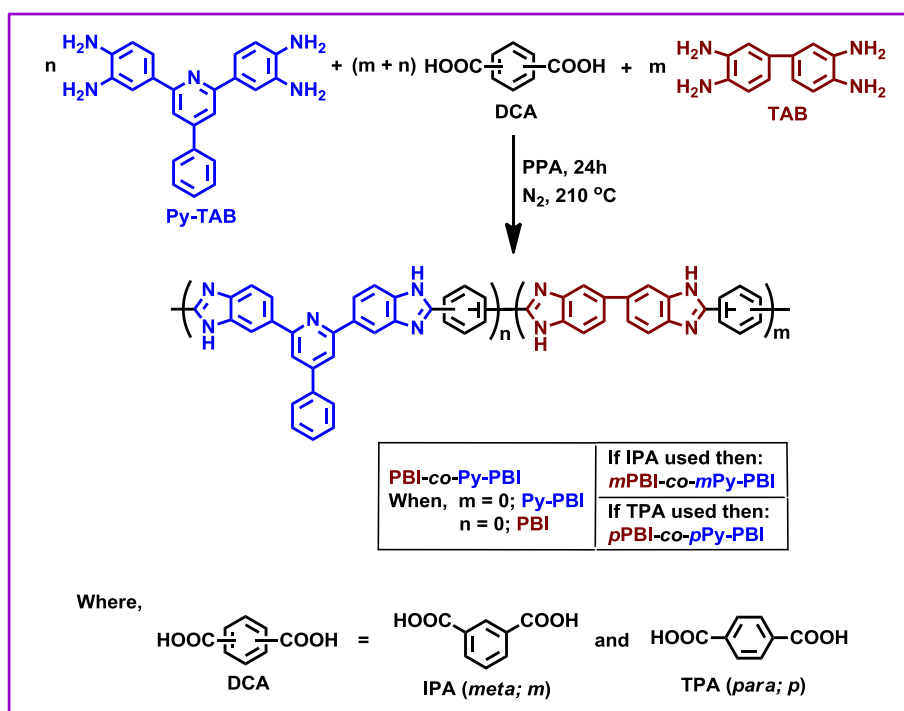
Scheme 5.1. *Polycondensation of two structurally different tetramines namely 3,3',4,4'-tetraaminobiphenyl (TAB) and 2,6-bis(3',4'-diaminophenyl)-4-phenylpyridine (Py-TAB) with dicarboxylic acids such as isophthalic acid (IPA) and terephthalic acid (TPA) for the synthesis of two sets of polybenzimidazole (PBI) random copolymers (PBI-co-Py-PBI).*

5.3. CHARACTERISATION:

All the information about materials used in this study and detail experimental procedures and characterizations which include molecular weight measurements by viscosity and gel permeation chromatography (GPC), X-ray diffraction (WAXD), thermal and mechanical studies by thermogravimertic analysis (TGA) and dynamic mechanical analysis (DMA) respectively, spectroscopic characterization by FT-IR, ^{1}H NMR, photophysical studies of copolymers solution by UV-visible and fluorescence spectroscopy are described in the Chapter 2. The solubility test, membrane fabrication, oxidative stability, acid loading and proton conductivities measurements are also discussed in the Chapter 2.

5.4. RESULTS AND DISCUSSION:

5.4.1. Copolymer Synthesis and Molecular Weight:

We have synthesized two sets of polybenzimidazole-co-pyridine polybenzimidazole random copolymers (PBI-*co*-Py-PBI), in which one series is *meta* and another is *para* connected structures. The polymerization scheme and the random copolymers structures are shown in Scheme 5.1. In Chapter 4, we have proved that Py-TAB can be used as a very effective, successful and efficient alternative tetramine source to replace TAB; hence we wanted to test the feasibility of Py-TAB in making of copolymers.[20] Generally, in the literature PBI copolymers were synthesized by polymerizing tetramine (such as TAB) with two dicarboxylic acid (DCAs) and the mols ratio (composition) of DCAs were varied in the reaction feed to make copolymers with altered DCAs content in the final structure.[27] Hence, to test the feasibility of Py-TAB in making of copolymers and as well as to prepare the copolymers by varying the tetramine moles ratio rather than DCAs mols ratio in the polymerization feed for the fixed DCA mol. Therefore, in this study we have made copolymers by altering the tetramines moles ratio (composition) instead of conventional DCA composition variation method.

We have used conventional TAB and new Py-TAB as tetramines source. We have tested our objective with two most commonly used DCAs namely IPA which produces *meta* oriented structure and TPA which results *para* oriented structure. Therefore, two sets of PBI-*co*-Py-PBI random copolymers designated as *m*PBI-*co*-*m*Py-PBI (produced using IPA as DCA) and *p*PBI-*co*-*p*Py-PBI (obtained using TPA as DCA) are produced as shown in Scheme 5.1. We have altered tetramine mols ratio in the feed from 10% to 90% to produce the variety of random copolymers structures and also to understand the effect of tetramine relative content on the properties of copolymers.

As mentioned by us and several other authors in the past that the total monomer concentration (TMC)[3,12,20,21a,27a,b] plays a crucial role in the polymerization and the molecular weight of resulting polymer, hence it is important to monitor this aspect of polymerization very carefully during the course of reaction. Earlier, we have observed that the best possible TMCs are 5 and 3.5% for *meta* and *para* structure Py-

PBI, respectively.[20] In this work for *meta* series copolymer (*m*PBI-*co-m*Py-PBI) we kept the TMC fixed at 5% to all mole variation, similarly 3.5% TMC where maintained for *para* series. We did not altered the TMC in a series since by altering that we won't be able to see the effect tetramine structure on the polymerization and the resulting molecular weight. The all other reaction condition were kept constant for all polymerization. Table 5.1 represents the molecular weight data of both the sets of copolymers. As we know higher IV of polymer attributes the higher molecular weight of polymer; the current data shows that with increasing PBI content, the molecular weights are increasing in both the sets. However, only Py-PBIs (both *meta* and *para*) have higher IV than the copolymers with higher Py-PBI content. Although we have kept the reaction conditions and total monomer concentration constant, but the monomer structures have huge effect in controlling the molecular weight of polymer as seen from Table 5.1. The possible reason could be more reaction of Py-TAB monomer than the normal TAB monomer due to presence of pyridine phenylene ring in the structure. The other reason could be the higher solubility of Py-TAB monomer in PPA. Because of higher solubility of Py-TAB, the monomer will react faster with the DCA than the TAB, which will end cut short the growth of bigger polymer chain since as we know the slower and heterogeneous reaction pathway allows bigger polymer chain to grow, which we have demonstrated earlier in case *m-p* random PBI copolymer obtained from TAB.

Table 5.1. *Molecular weight data of both meta and para structured PBI-co-Py-PBI random copolymers as obtained from GPC and viscosity measurements. Total monomer concentrations (TMC) are 5 and 3.5 wt% for mPBI-co-mPy-PBI and pPBI-co-pPy-PBI structure, respectively. The TMCs are kept constants for all the copolymers composition studied here.*

Copolymer	mPBI-co-mPy-PBI			pPBI-co-pPy-PBI		
	M_W	PDI	IV (dL/g)	M_W	PDI	IV (dL/g)
Py-PBI 100	4.10×10^5	2.06	1.29	5.73×10^5	2.47	2.76
Py-PBI 90	3.60×10^5	2.26	0.91	4.64×10^5	2.38	1.63
Py-PBI 75	5.00×10^5	2.64	0.98	4.30×10^5	2.34	2.83
Py-PBI 50	3.05×10^5	2.24	1.01	6.05×10^5	2.97	2.95
Py-PBI 25	3.57×10^5	2.53	1.09	1.74×10^5	1.97	3.07
Py-PBI 10	3.26×10^5	2.49	1.13	2.62×10^5	1.60	3.29
PBI 100	3.64×10^5	2.77	1.21	–	–	3.72

The other observation from Table 5.1 is that always TPA (*para* structure DCA) producing higher molecular weight polymer than IPA (*meta* structure DCA). This is a well-known phenomenon in PBI polymerization that always *para* structure polymers are higher IV polymer than *meta*.[3,21a,27a,b] GPC plots are shown in Figure 5.1A and B. GPC data is not completely agreement with IV data, it may be due to the over estimation of molecular weight by GPC owing to the solubility issues of PBI type polymers. However,

we want to stress upon one factor that the new tetramine monomer Py-PBI can produce copolymers and it is also possible to prepare copolymers by altering the tetramine structures instead of only DCA structures.
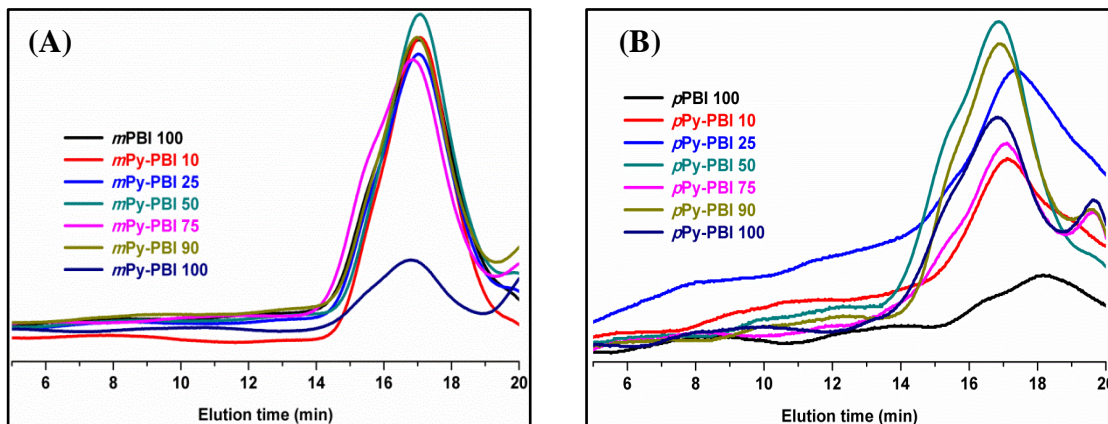
Figure 5.1. *GPC traces of (A) mPBI-co-mPy-PBI random copolymers and (B) pPBI-co-pPy-PBI random copolymers in DMAc with LiCl at 65 °C.*

5.4.2. FT-IR and ^{1}H NMR Spectroscopic Characterization:

The FT-IR spectra of all random copolymers were recorded from dried 30-40 µm thin films and shows in Figure 5.2A and B. The absence of C-H stretching frequency at 2940 cm^{-1} due to -CH$_3$ group of DMAc in FT-IR spectra indicate that all the DMAc solvent has been removed during drying process. Due to hygroscopic nature, O-H stretching frequency of water is observed at 3615 cm^{-1} in all the copolymers. However, this O-H peak is less intense in *para* directed copolymer (*p*PBI-*co*-*p*Py-PBI) (Figure 5.2B) indicating less hygroscopic character compare to its meta directed counterparts.[27a,b] This may be due to the structural difference between those two sets of polymers. Most of the important characteristic stretching frequencies in both the cases are marked by dotted line in the Figure 5.2. These peaks are in well agreement with the literature reports. The characteristic absorption at 3415 and 3175 cm^{-1} attributes the corresponding free N-H and self-associated hydrogen bonding of imidazole protons. The characteristic low absorption at 3063 cm^{-1} attributes the stretching frequency of aromatic C-H bond. Absorption at 1625 cm^{-1} attributes the stretching frequency of C=C and C=N of benzimidazole ring. Stretching frequency at 1625 cm^{-1} gradually shifted to ~ 1600 cm^{-1} in both 100% *meta* and *para* structure Py-PBI samples. Another peak is gradually increases in both *meta* and *para* at ~ 860 cm^{-1} with increasing the Py-PBI content which is the corresponding C-H stretching frequency of pyridine ring of Py-TAB.[20]

Proton NMR spectra of all the random copolymers are shown in Figure 5.3A and B along with their structures and peaks assignments.[28] Similar structure elucidations have been reported by us in the literature earlier[20] and the current spectra are in well agreement with the expected chemical structures of

the random copolymers. The imidazolium N-H chemical shift of *meta* and *para* structure PBI are observed at 13.26 and 13.18 ppm, respectively. In case of *meta* connected homo polymer of Py-PBI, N-H chemical
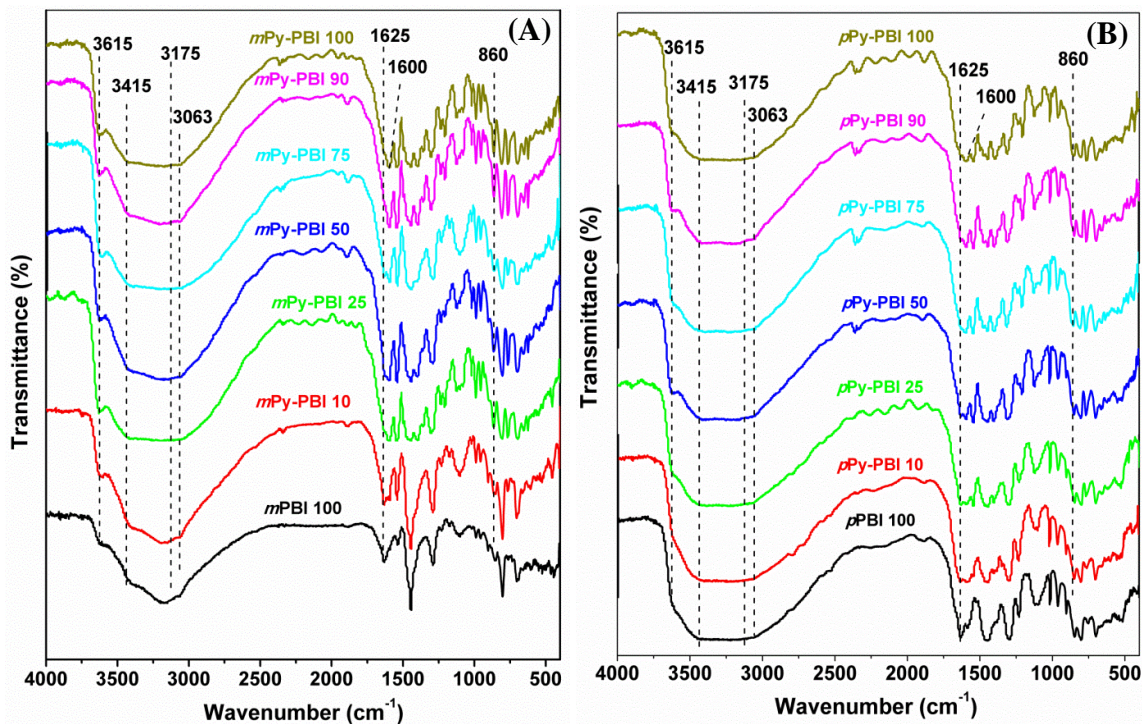
Figure 5.2. FT-IR spectra of (A) mPBI-co-mPy-PBI and (B) pPBI-co-pPy-PBI random copolymers.
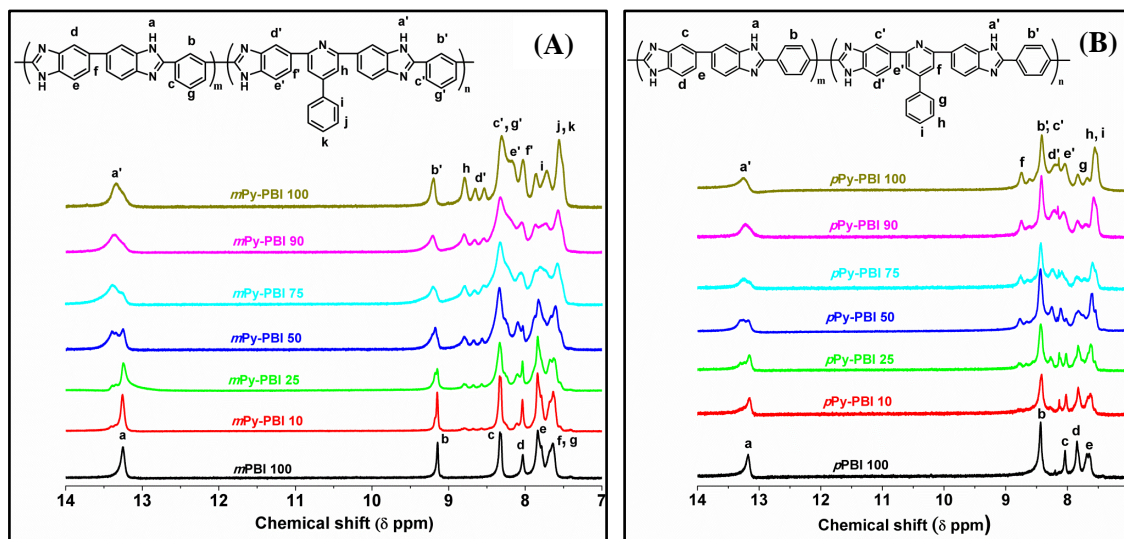
Figure 5.3. ^{1}H NMR spectra of all random copolymers (A) mPBI-co-mPy-PBI and (B) pPBI-co-pPy-PBI. Spectra were recorded in DMSO-d$_6$ solvent. Peak assignments are shown in the figure.

shift shifted to lower field at 13.37 ppm and in case of *para* connected Py-PBI, it is shifted to lower field at 13.27 ppm. The shift of both *meta* and *para* homo polymer of Py-PBI compare to PBI is due to the different structure of Py-TAB and extra electronegative N atoms present in the polymers backbone. Both sets of copolymers show the N-H peak having character of both PBI and Py-PBI. Quantitative splitting of N-H peaks are observed in case of all random copolymers for both the sets. In case of *meta* copolymer, the aromatic proton chemical shifts appear between 7.4 to 9.4 ppm and in case of *para* copolymers it is 7.4 to 9 ppm. However, the all aromatic signals vary from copolymer to copolymer owing to their different chemical environments.

5.4.3. Solubility:

The solubility of all random copolymers are checked in several common organic solvents like *N,N*-dimethyl acetamide (DMAc), *N*-methyl-2-pyrrolidone (NMP), dimethyl sulfoxide (DMSO), formic acid (FA), etc. It is clearly evident from the solubility chart (Table 5.2) that there is a significant difference in solubility depending on the copolymers structures. All the copolymers are soluble in DMAc and DMSO except that the *para* structures are soluble in DMAc only after heating. This is in agreement with reported data which showed that *para* structure always has relatively less solubility than *meta* structure. The most striking observation to be noted from Table 5.2 is that all the copolymers (both *meta* and *para*) are readily soluble in formic acid at room temperature whereas polymers obtained from only TAB monomer (i.e. PBI 100) are insoluble even after heating (1st column in the Table 5.2). Therefore, introduction of Py-PBI part in the copolymer enhances the solubility dramatically. It is to be noted that even only 10% of Py-PBI is enough to make the polymer soluble in low boiling solvent like FA. This enhanced solubility is because of pyridine bridged phenyl group in the backbone which makes the polymer more flexible owing to the presence of bulky pyridine group which also increases the d-spacing between the polymer chains which in turn allows the solvent molecules to enter the polymer chains and make it soluble in low boiling solvent like formic acid.[20] Earlier, in literature we have observed that due to presence of an ether linkage in the polymer backbone, certain type of PBI structure like poly(4,4′-diphenylether-5,5′-bibenzimidazole) [OPBI] soluble in formic acid and forms very transparent homogeneous films.[29] Similarly, recently we demonstrated that Py-TAB monomer always produces soluble Py-PBI because of the reason as stated above.[20] However, what is most important in this study is that the introduction of Py-PBI part even in very little amount in copolymers chains greatly influences the polymers solubility. The solubility in low boiling solvent allows the easy processability of this copolymers which is otherwise impossible. As a result of that, we are able to fabricate very strong, transparent membrane from all copolymers very readily.

Table 5.2. *Solubility chart of PBI-co-Py-PBI random copolymers in different organic solvents.*

Solvents	*PBI 100*	*Py-PBI 10*	*Py-PBI 25*	*Py-PBI 50*	*Py-PBI 75*	*Py-PBI 90*	*Py-PBI 100*
				mPBI-co-mPy-PBI			
DMSO	++	++	++	++	++	++	++
DMAc	++	++	++	++	++	++	++
NMP	+	+	+	+	+	+	++
FA	−	++	++	++	++	++	++
				pPBI-co-pPy-PBI			
DMSO	++	++	++	++	++	++	++
DMAc	+	+	+	+	+	++	+
NMP	+	+	+	+	+	+	++
FA	−	++	++	++	++	++	−

++ : soluble at room temperature; + : soluble after heating; − : insoluble after heating. Solubility checked up to 2% (W/V).

5.4.4. Thermal Stability:

The thermal stability of all *para* and *meta* series random copolymers were studied in TGA under N_2 atmosphere with heating scan rate 10 °C/min and the results are presented in Figure 5.4 and Table 5.3. All the samples display two degradations: first one is around ~ 150 °C and second one is around 550 °C. The first degradation is due to the removal of loosely bound moisture from the samples and second degradation is due to the polymer backbone. It is to be noted that, all the polymer having almost similar stability and all of them can withstand temperature as high as upto ~ 600 °C.

Table 5.3. *The thermal stability data (TGA) of PBI-co-Py-PBI random copolymers.*

Copolymer	*mPBI-co-mPy-PBI*		*pPBI-co-pPy-PBI*	
	$T_{10\%}$ $(^oC)^a$	$W_{550 ^oC}$ $(\%)^b$	$T_{10\%}$ $(^oC)^a$	$W_{550 ^oC}$ $(\%)^b$
PBI 1000	166	87.40	275	85.84
Py-PBI 10	–	–	332	87.43
Py-PBI 25	270	88.02	573	88.46
Py-PBI 50	474	89.27	590	89.08
Py-PBI 75	566	90.39	595	89.58
Py-PBI 90	573	90.70	–	–
Py-PBI 100	579	91.89	615	91.76

[a] Corresponding temperature at which 10% weight loss is observed.
[b] Residual weight percent at 550 ºC.

In our earlier report we have shown that the *para* series copolymers have higher stability than the *meta* series especially at higher temperature range.[20] Here, also the same trend is present at higher temperature. The thermal stability of polymer depends upon the chemical structure of polymer backbone. In both the cases with increasing the Py-PBI content; the thermal stability gradually increases. From the Table 5.3, it can easily observable that the temperature at which 10% weight loss is occurred increases gradually with increasing Py-PBI content in the copolymers. The weight loss at 550 °C gradually decreases with increasing Py-PBI content in the polymer for both the cases. This is probability due the bulky hetero phenylene pyridine group present in the polymer backbone.
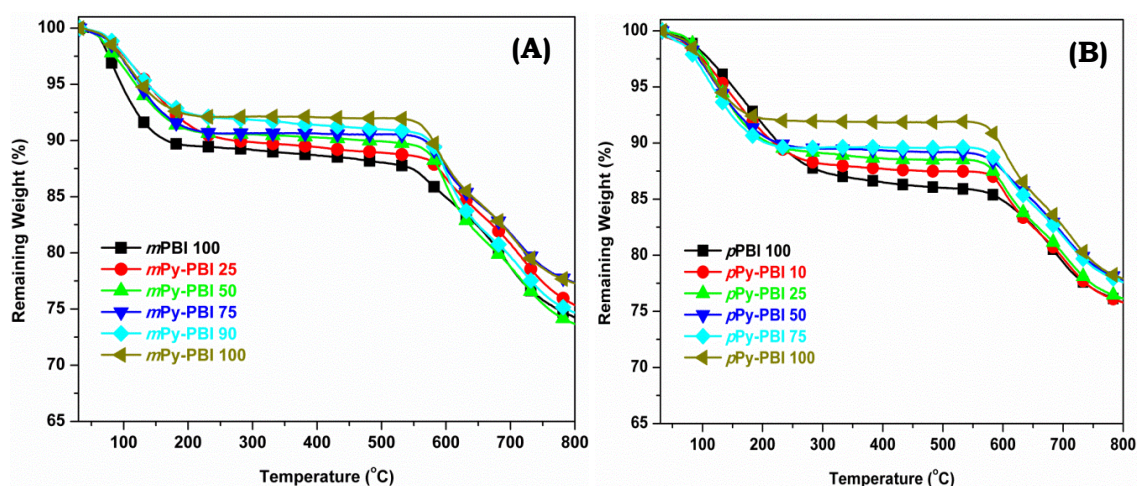
Figure 5.4. *The thermogravimetric plots of random PBI-co-Py-PBI copolymers (A) meta and (B) para series. The TGA experiments were carried out in N_2 atmosphere at a heating rate 10 °C/min.*

5.4.5. X-ray Studies:

Wide angle X-ray diffraction (WAXD) patterns (Figure 5.5) of all copolymers were recorded to understand the amorphous nature. From the Figure 5.5, it is easily observe that all polymers are amorphous in nature, because of absence at any crystalline sharp peaks. Only one broad peak is present at 2θ ~ 25° in all samples. Despite the structural alteration, there is no structural peaking and hence the polymers remain amorphous. The similar type diffraction data reported in the literature.[27,29] Hence the results shown in thermal stability and X-ray studies clearly prove that copolymerization by altering tetramine composition produces PBI based copolymer with basic characteristics which are similar to already reported PBI copolymers.
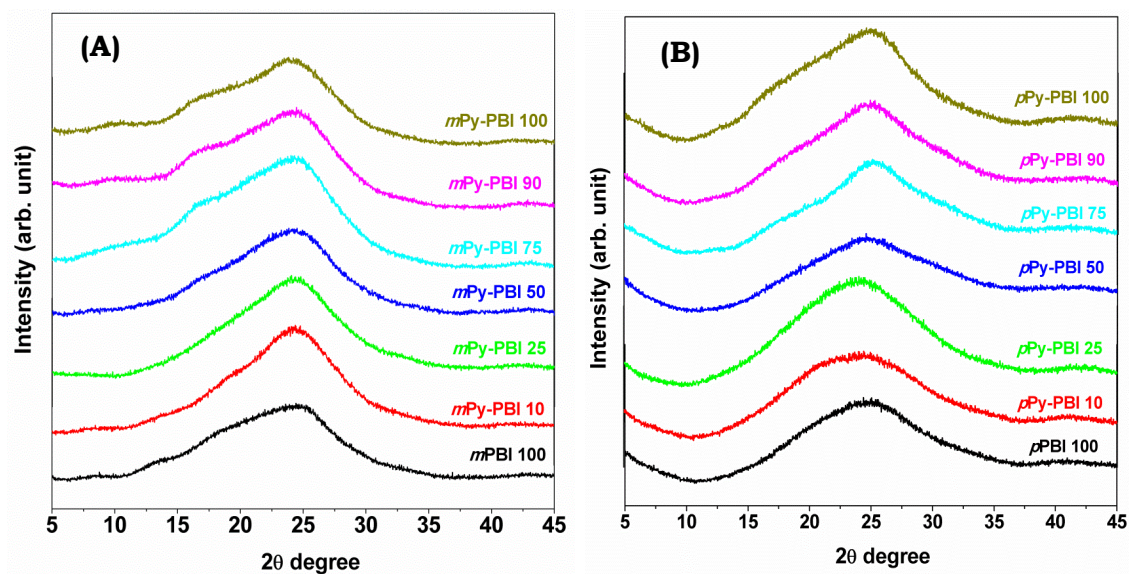
Figure 5.5. *The WAXD diffraction patterns of PBI-co-Py-PBI random copolymers; (A) meta and (B) para series.*

5.4.6. Thermo-mechanical Studies:

Various thermo-mechanical properties like storage modulus (E'), loss modulus (E'') and tan δ as a function of temperature for both sets of copolymers are presented in Figure 5.6. All the data were collected in DMA after annealing the sample at 100 °C for 30 min to avoid the effect of residual moisture on the thermal transitions. The glass transition temperature of both sets of copolymers obtained from temperature dependent tan δ and E'' are tabulated in Table 5.4. All the T_g values obtained in this study are ≥ 350 °C, is in well agreement with PBI literature. It has been shown earlier that the polymer backbone structure of PBI based polymers has significant impact on the T_g values and also higher IV (higher molecular weight) PBI polymer generally exhibits higher T_g.[20,27a,b,29] Table 5.4 data clearly shows that 100% Py-PBIs (both *meta* and *para*) have higher T_g that 100% PBI (both *meta* and *para*). Therefore, it is expected that with increasing PBI (a decreasing Py-PBI) content in the copolymer, the T_g will decrease and indeed the Table 5.4 results match the expected trend. However, it must be kept in mind that with increasing PBI content the IV value increases in both *meta* and *para* series (Table 5.1) and hence the variation of T_g might have affected by increasing molecular weight. Therefore, it can be said that the greater degree of decrease in T_g with increasing PBI content in the polymer would have been observed if all the polymer would have similar molecular weight. Hence, the above discussion clearly attributes the effect of copolymer structure on the T_g values.
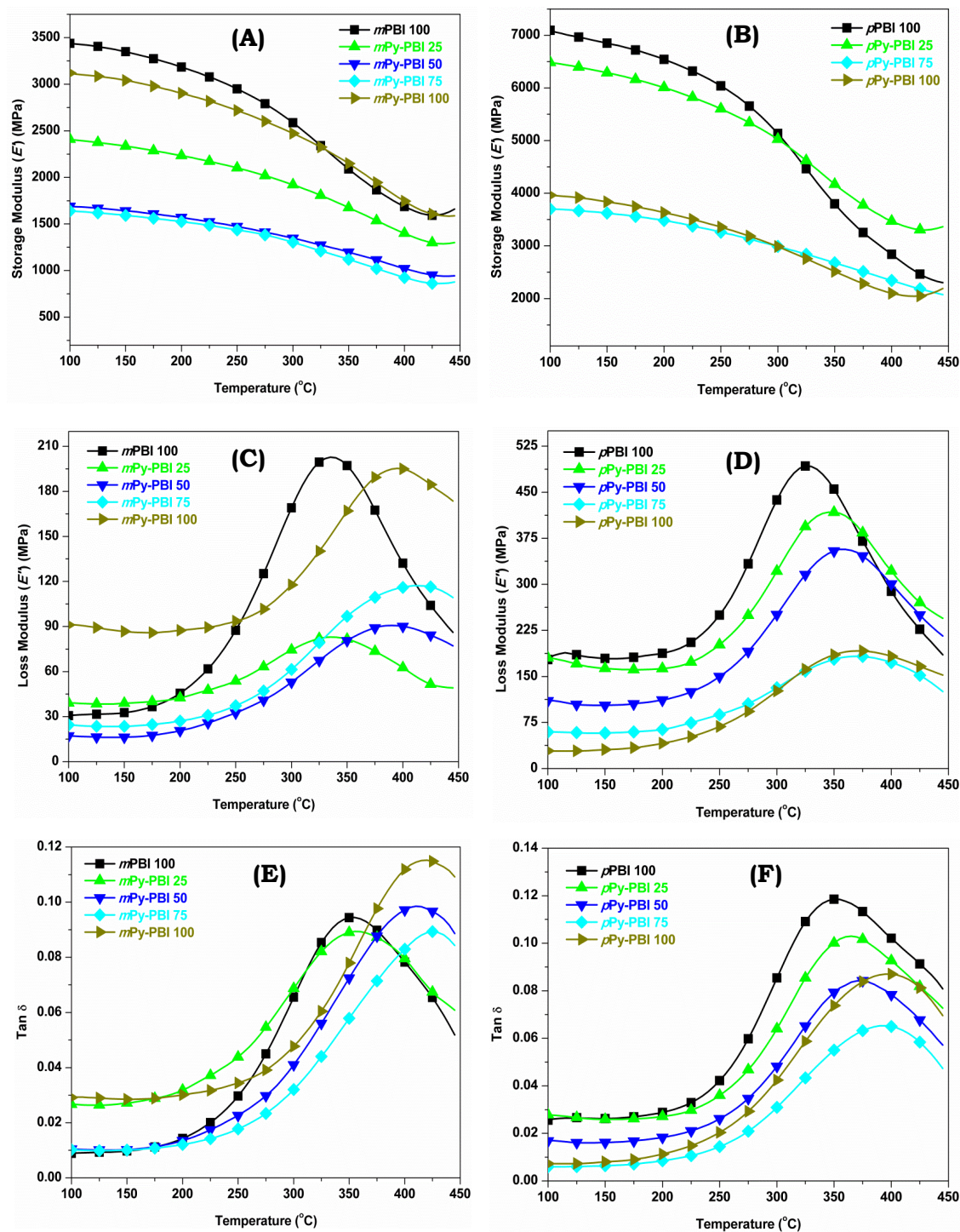
Figure 5.6. *Temperature dependent (100 to 450 °C) plots of various thermomechanical properties of PBI-co-Py-PBI copolymers obtained from DMA. Storage modulus (E') plot of meta (A) and para (B) series; loss modulus (E") plot of meta (C) and para (D) series and tan δ plot of meta (E) and para (F) series.*

Table 5.4. *Various temperature dependent thermomechanical data and glass transition temperatures of representative PBI-co-Py-PBI random copolymers obtained from DMA study.*

Copolymer	E' (MPa) at 100 °C	E' (MPa) at 425 °C	T_g (ºC) from tan δ	T_g (ºC) from E"
mPBI-co-mPy-PBI				
Py-PBI 100	3120	1607	418	394
Py-PBI 75	1641	864	422	413
Py-PBI 50	1690	952	412	391
Py-PBI 25	2408	1299	357	339
PBI 100	3438	1593	349	335
pPBI-co-pPy-PBI				
Py-PBI 100	3961	2049	397	369
Py-PBI 75	3701	2184	390	369
Py-PBI 50	–	–	372	357
Py-PBI 25	6483	3306	364	348
PBI 100	7093	2463	348	325

The difference in T_g values between *meta* and *para* series is because of DCA structure. As it has been shown earlier by us several times that the *para* connected PBI displays lower T_g than *meta* connected owing to the symmetrical structure of *para* PBI.[27a,b] The variation in T_g values obtained from E" versus temperature and tan δ versus temperature is also a known phenomenon of several type of polymer including PBIs.

Temperature dependent storage modulus (*E'*) values (Figure 5.6 and Table 5.4) indicate that with increasing temperature the *E'* values decreases and this decrease depends on the copolymer structure. However, the decreases are not very significant indicating strong mechanical characteristics of all the copolymers. In case of *meta* series copolymers both 100% Py-PBI and PBI (homopolymers) have almost similar *E'* all over the temperature range. However, *meta* series copolymer *E'* values (throughout the temperature range) decrease with increasing Py-PBI content. This may be due to the structural effect as well as the molecular weight effect which decreases with increasing Py-TAB content till 90% Py-TAB in the copolymer (Table 5.1). On the other hand in case of *para* series copolymer the mechanical properties are quite different than *meta* series. *Para* PBI (100% PBI) shows significantly higher *E'* than the *para* Py-PBI homo polymer (Figure 5.6B). Copolymers with higher PBI content (e.g. Py-PBI 25) also display higher *E'* all the temperature than 100% Py-PBI. Remaining copolymer *E'* values are lower than 100% *para* Py-PBI. The difference in *E'* values in copolymers can be explained using their IV (molecular weight) values. Since 100% PBI and higher PBI content copolymers having higher IV (Table 5.1) than 100% Py-PBI, hence they displays better mechanical strength than the later one.

5.4.7. Oxidative Stability:

The well-known Fenton's test was preferred to study the oxidative stability of the samples. In the test, the freshly generated hydroxyl ($OH^•$) and hydroperoxyl ($OOH^•$) radicals attack the polymer backbone and degradation of polymer chain takes place. Figure 5.7 displays the oxidative stability plots as a function of time for few representative copolymers from both the sets. Figure 5.7 data clearly proves that Py-PBIs have higher oxidative stability than the PBIs for both in case of *meta* and *para* structure polymers and this result is in agreement with our previous observation. We believe the higher oxidative stability of Py-PBIs is due to the presence of pyridine ring in the polymer backbone which protects the polymer chain from the attack of free radicals.[20] As expected oxidative stability of copolymers gradually increases with increasing the Py-PBI content in the copolymer in both the *meta* and *para* series. It is clearly observed from the Figure 5.7 that only ~ 60% weight remains after 120 h in case of *m*PBI and *p*PBI polymers (homopolymers), whereas ~ 80% weight remains in case of both *m*Py-PBI and *p*Py-PBI polymers. All the copolymers oxidative stability is in between two homopolymers and the stability alters as we alter the copolymer composition. Hence, it is clearly prove that copolymer structure plays the crucial role for the stability of the polymers in the drastic chemical environment.
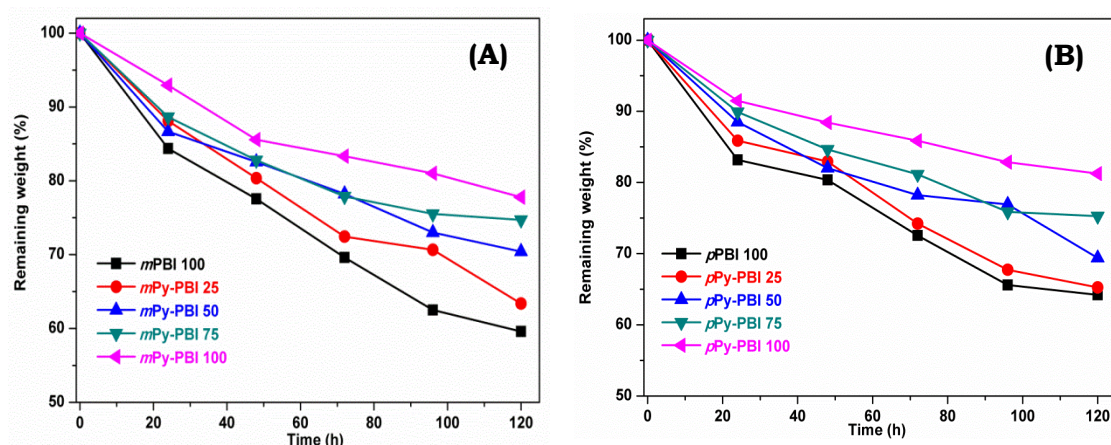
Figure 5.7. Oxidative stability of random PBI-co-Py-PBI copolymers: (A) meta and (B) para series.

5.4.8. Phosphoric Acid Doping Level:

Since the phosphoric acid (PA) doping level is one of the major factor which dictates the proton conducting character of PEM, hence studies of PA doping level are carried out for all copolymer samples to validate their suitability as PEM. All the copolymer membranes were doped by dipping the membrane in 50% (10.26M) H_3PO_4 solutions, we have chosen this low concentration of H_3PO_4 instead of conventionally used 85% H_3PO_4 since beyond this low concentration of H_3PO_4 *meta* Py-PBI samples becomes unstable at temperature above 120 °C during conductivity measurement.[20] As observed from Figure 5.8, it is clearly

evident that with increasing Py-TAB concentration in the copolymer, the PA doping level increases in both sets of copolymers. This is because of the more basic character of the copolymer with increasing Py-PBI content in the polymer owing to pyridine ring of Py-TAB monomer. However, we do not observe much difference between the *meta* and *para* structures. This attributes that the nature and characteristics of the copolymers are mostly governed by the tetramine structure.
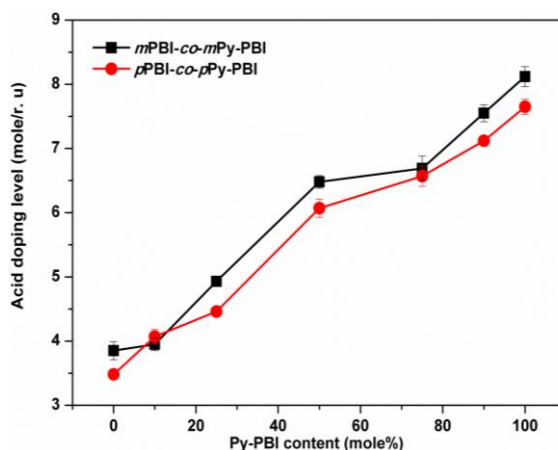
Figure 5.8. *Phosphoric acid (PA) doping level of all the random copolymers. The copolymer membranes were dipped into the 50% (10.26M) H_3PO_4 for three days at room temperature.*

5.4.9. Conductivity Study:

The proton conductivity of all acid doped *meta* and *para* series copolymers were measured in the temperature range from 30 ⁰C to 160 ⁰C without any extra humidity condition. It is well known in the literature that the proton conduction largely depends upon the water molecules associated with the membrane.[1-3] Here, we made effort to measure the proton conduction without any humidification to check the suitability of the current membrane. All the conductivity data shown here are obtained from the second heating scan to ensure that the data are collected without the presence of water since during first hearting scan all water molecules go away from the acid doped membrane. The conductivity values are collected from the Nyquist plots; several representative Nyquist plots are shown in Figure 5.9. The temperature dependent conductivity data of both sets of copolymer membranes those were doped with 10.26M H_3PO_4 for three days are shown in Figure 5.10. In all the cases proton conductivities increase with increasing temperature as per the expectation. Proton conductivities of Py-PBIs are higher than the conventional PBIs in both the cases and this is due to higher acid loading owing to the more basic character in polymers backbone because of pyridine ring.

Since acid loading increases with increasing Py-PBI content (Figure 5.8), hence conductivity increases with increasing Py-PBI content in the polymer (Figure 5.10). Hence, clearly the copolymer

backbone structures and content of Py-PBI in the copolymers dictate the PA loading which in turns influences the proton conductivity of the samples. Therefore, we can argue that for any given DCAs structure, we can tailor the proton conductivity by altering the tetramine mole percent in the copolymer, which is not known and discussed in the literature earlier.
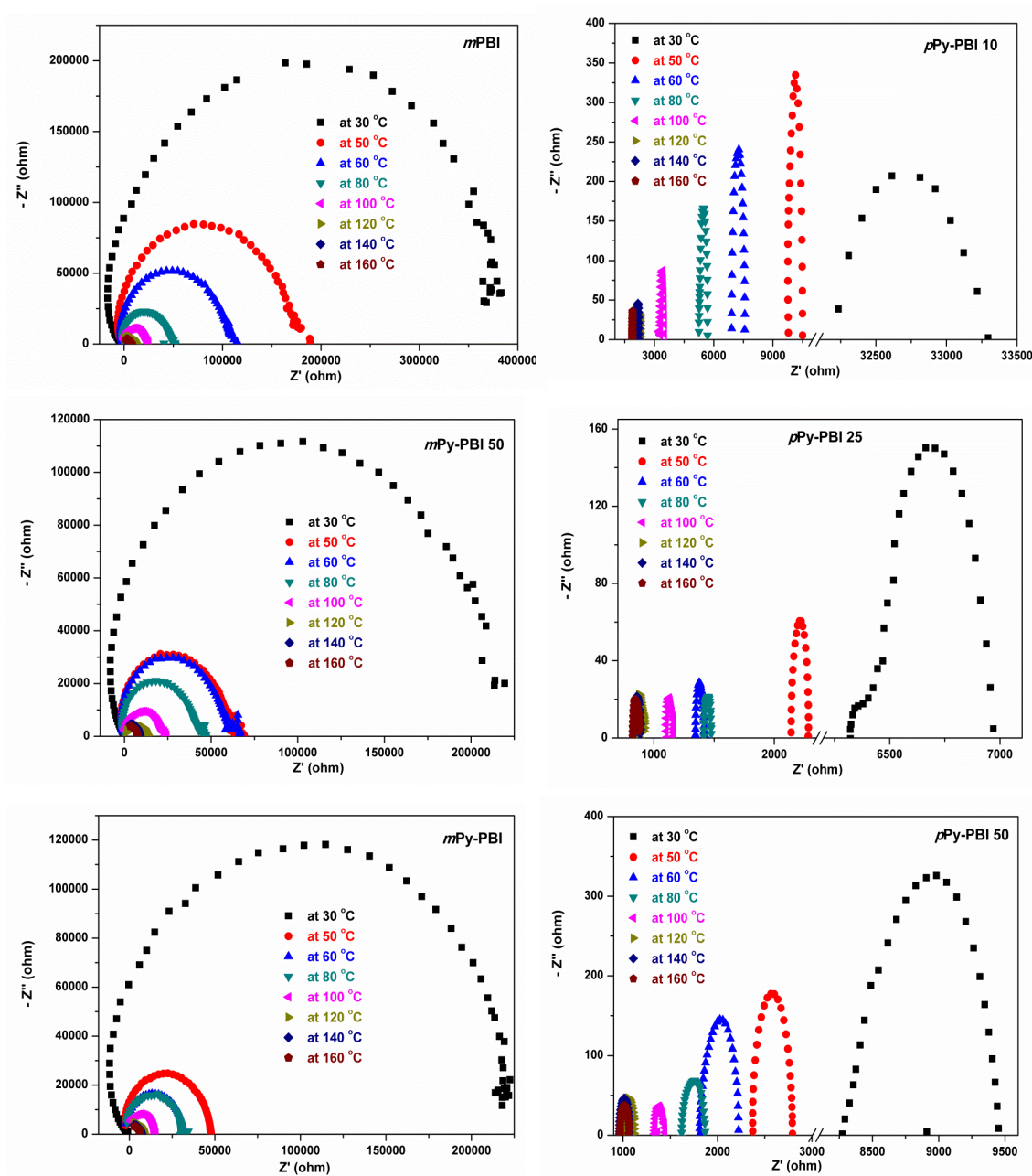
Figure 5.9. *Few representative Nyquist plots of both meta and para series PBI-co-Py-PBI random copolymers at different temperatures during the second heating scans.*

To understand and calculate the activation energy (E_a) of proton conduction process, the conductivity data are plotted using Arrhenius equation and shown in Figure 5.10C and D for *meta* and *para* series copolymers, respectively. Since all the data are fitting well with the Arrhenius model, hence it can be said that the conductivity of all these acid doped membranes follow Grotthuss mechanism. The E_a value calculated from the linear fitting of the data are shown in Figure. It is evident that E_a values decreases with increasing Py-PBI content in both the cases attributing the influence of polymer backbone structure in the proton conductivity process.
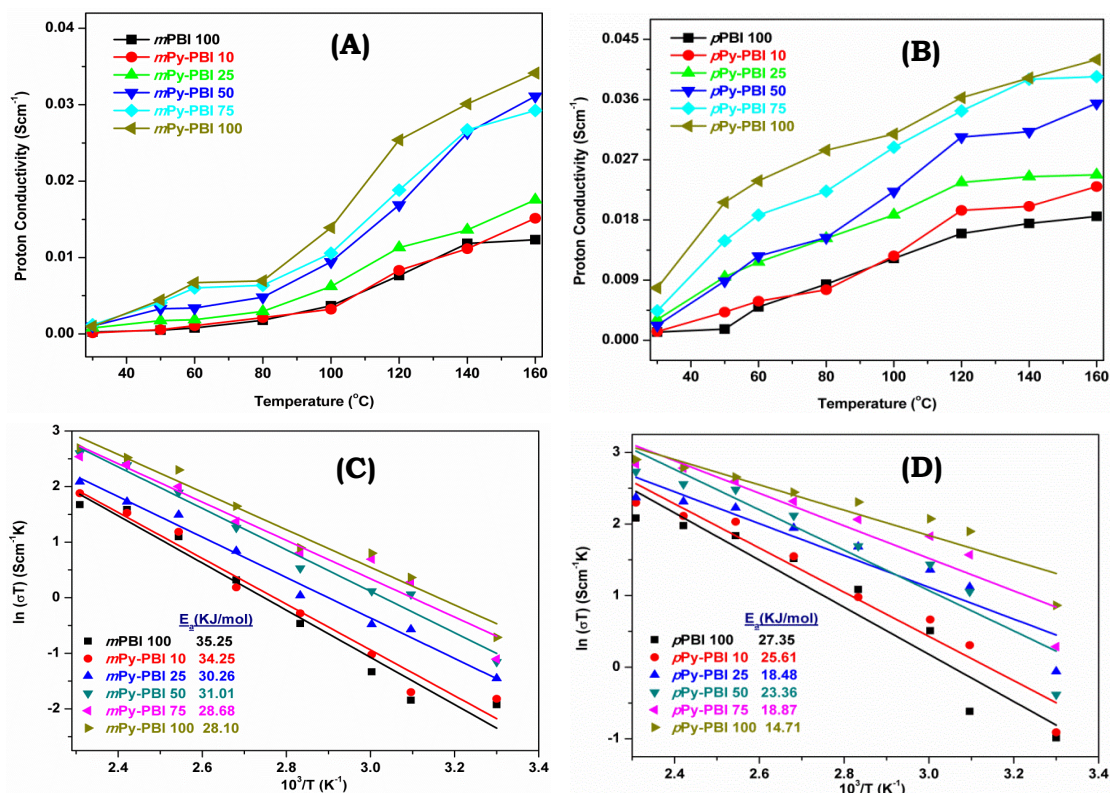
Figure 5.10. *Temperature dependent conductivity of PA doped random PBI-co-Py-PBI copolymers membranes (A) meta and (B) para series. Arrhenius plot of proton conductivity of the PA doped copolymers membranes (C) meta and (D) para series for the calculation of activation energy (E$_a$) values.*

5.4.10. Spectroscopy Study:

The absorption and the fluorescence emission spectra of all the copolymers are recorded from dilute solutions of copolymers in dimethylacetamide (DMAc) solvent and the concentration of the solution for all the case are 10^{-5} M. The absorbance spectra are shown in Figure 5.11. The 100% PBI samples show only one λ_{max} at 347 and 394 nm for *meta* and *para* PBI, respectively.[30] These λ_{max} is due to the π-π* transition. On the other hand 100% Py-PBI sample display two λ_{max} for π-π* transition: *m*Py-PBI has absorption peaks at 329 and 347 nm and *p*Py-PBI has peaks at 370 and 394 nm. All these peaks are due

to the π-π* transitions. Therefore in both the cases (*meta* and *para*) of 100% Py-PBI as extra lower wavelength π-π* transition is observed. We have explained the reason behind this lower wavelength π-π* peak as a result of existence of two different forms of pyridine phenyl group which are in plane with the polymer backbone and other one is out of plane.[20] From Figure 5.11, it is clear that the lower wavelength peak grows gradually with increasing Py-PBI content in the copolymer in case of both *meta* and *para* series.
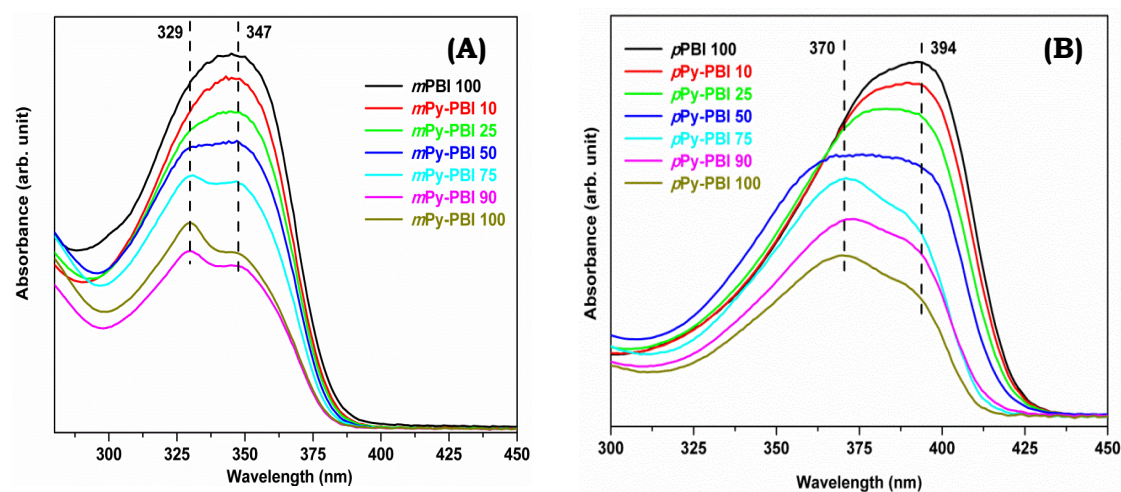
Figure 5.11. *Absorption spectra of all random PBI-co-Py-PBI copolymers in DMAc solution (A) meta series and (B) para series, as recorded with a cuvette of 1 cm path length. Concentrations are 2×10^{-5} M.*

The emission spectra of all polymers are shown in Figure 5.12. The excitations of polymer solution were chosen from their corresponding π→π* transition maximum absorption. The emission spectra of *meta* PBI in DMAc solution are already reported in the literature. The two emission bands observed at 398 and 416 nm which are responsible for the excited state ^1L_b transition of benzimidazole ring and are assigned to the transition of 0-0 and 0-1.[30] Here, we also observed the same kind of transition in excited state. In our earlier repot we have shown that the emission peaks gradually shifted to higher wavelength with increasing content of *para* structure in the copolymer backbone due to the higher conjugation and in case of *para* PBI the emission peaks appear at 430 and 452 nm (Figure 5.12B). Here we also observed the same kind of transition. However, in case of both *meta* and *para* Py-PBI series the peaks are gradually shifted to the lower wavelength region (Figure 5.12). This may be the due to presence of more electronegative extra nitrogen atoms in the priding ring of Py-PBI which may hinder the conjugation of the copolymer chains.
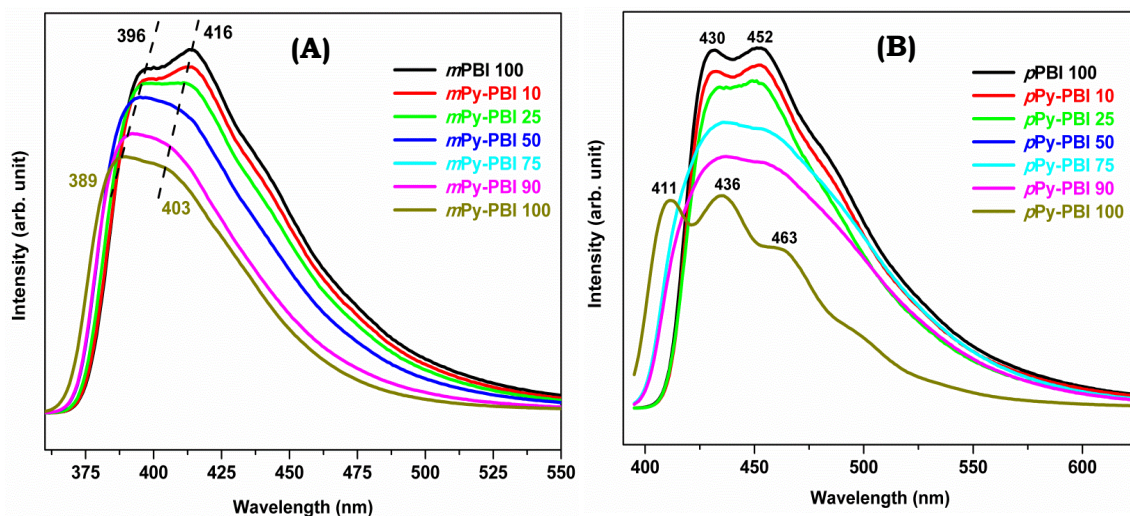
Figure 5.12. *Emission spectra of all random PBI-co-Py-PBI copolymers in DMAc solution (A) meta series and (B) para series. The excitation wavelength (λ$_{exc}$) for meta and para series are 347 and 392 nm, respectively and concentrations are 2 × 10^{-5} M.*

5.5. CONCLUSION:

Random copolymers of polybenzimidazole have been synthesized successfully by tetramines compositions variations instead of dicarboxylic acids compositions, which is often used, in the polymerization feed for the first time in the literature. Two series of copolymers (PBI-*co*-Py-PBI) are synthesized by polycondensation of recently developed alternative pyridine bridged tetramine (Py-TAB) and conventional tetramine (e.g. TAB) monomers with isophthalic acid (IPA) to produce *meta* structure copolymers, and with terephthalic acid (TPA) to synthesize *para* structure copolymers. The copolymers compositions are varied by altering the relative mole ratio of TAB and Py-TAB. Molecular weight and spectral characterizations confirm the formation of desired copolymer structures. Both the *meta* and *para* series random copolymers are readily soluble in low boiling solvent like formic acid (FA) which in turn helps to fabricate the homogeneous transparent membranes readily. All the random copolymers have high thermal and chemically stabilities than the conventional polybenzimidazole (PBI). The synthesized random copolymers absorbed more phosphoric acid compare to the conventional PBI which influences the proton conductivity. The photo physical studies also confirm the copolymers structure and demonstrate the influences of copolymers composition. In conclusion, the new types of PBI based copolymer system have been developed and studied to prove the following facts: (a) Py-TAB is a viable alternative to produce copolymer structure, (b) the PBI based copolymer can be made not only by tuning the dicarboxylic acid content in feed, it is also possible by varying the tetramine content.

REFERENCES:

(1) (a) Li, Q.; Jensen, J. O.; Savinell, R. F.; Bjerrum, N. J. *Prog. Polym. Sci.* **2009**, *34*, 449. (b) Li, Q.; Aili, D.; Yang, J.; Rudbeck, H. C.; Jensen, J. O.; Bjerrum, N. J. *Mater. Sci. Res. J.* **2012**, *6*, 219.

(2) Asensio, J. A.; Sánchez, E. M.; Gomez-Romero, P. *Chem. Soc. Rev.* **2010**, *39*, 3210.

(3) Mader, J.; Xiao, L.; Schmidt, T. J.; Benicewicz, B. C. *Adv. Polym. Sci.* **2008**, *216*, 63.

(4) Chung, T. S. *J. Macromol. Sci., Rev. Macromol. Chem. Phys.* **1997**, *C37*, 277.

(5) Wang, Y.; Chung, T. S.; Gruender, M. *J. Membr. Sci.* **2012**, *415-416*, 486.

(6) Zhang H.; Shen, P. K. *Chem. Rev.* **2012**, *112*, 2780.

(7) Shi, G. M.; Chen, H.; Jean, Y. C.; Chung, T. S. *Polymer* **2013**, *54*, 774.

(8) Jung, K. H.; Ferraris, J. P. *Carbon* **2012**, *50*, 5309.

(9) Kim, H. J.; Ham, H. C.; Yoon, C. W.; Choi, D. G.; Hwang, S. J.; Kim, Y. M.; Nam, S. U. KR 2013097441 A 20130903, 2013.

(10) Hopkins, J. B. Jr.; Hudson, K. M.; Copeland, G. S.; Gruender, M. U. S. Patent US 20110189484 A1 20110804, 2011.

(11) (a) Wainright, J. S.; Wang, J. T.; Weng, D.; Savinell, R. F.; Litt, M. *J. Electrochem. Soc.* **1995**, *142*, L121. (b) Savinell, R. F.; Litt, M. H. PCT Int. Appl. WO 9613872 A1 19960509, 1996. (c) Schechter, A.; Savinell, R. F. *Solid State Ionics* **2002**, *147*, 181.

(12) (a) Xiao, L.; Zhang, H.; Jana, T.; Scanlon, E.; Chen, R.; Cheo, E. W.; Ramanathan, L.S.; Yu, S.; Benicewicz, B. C. *Fuel Cells* **2005**, *5*, 287. (b) Yu, S.; Benicewicz, B. C. *Macromolecules* **2009**, *42*, 8640. (c) Gulledge, A. L.; Gu, B.; Benicewicz, B. C. *J. Polym. Sci., Part A: Polym. Chem.* **2012**, *50*, 306 (d) Mader, J. A.; Benicewicz, B. C. *Macromolecules* **2010**, *43*, 6706.

(13) Asensio, J. A.; Borros, S.; GoMez-Romero, P. *J. Polym. Sci.: Part A: Polym. Chem.* **2002**, *40*, 3703.

(14) (a) Pu, H.; Wang, L.; Pan, H.; Wan, D. *J. Polym. Sci.: Part A: Polym. Chem.* **2010**, *48*, 2115. (b) Guan, Y.; Pu, H.; Wan, D. *Polym. Chem.* **2011**, *2*, 1287.

(15) Chuang, S. W.; Hsu, S. L. C. *J. Polym. Sci.: Part A: Polym. Chem.* **2006**, *44*, 4508.

(16) (a) Kim, T. H; Lim, T. W; Lee, J. C *J. Power Sources* **2007**, *172*, 172. (b) Kim, S. K.; Kim, T. H.; Jung, J. W.; Lee, J. C. *Polymer* **2009**, *50*, 3495. (c) Kim, S. K.; Choi, S. W.; Jeon, W. S.; Park, J. O.; Ko, T.; Chang, H.; Lee, J. C. *Macromolecules* **2012**, *45*, 1438. (d) Choi, S. W.; Park, J. O.; Pak, C.; Choi, K. H.; Lee, J. C.; Chang, H. *Polymer* **2013**, *5*, 77.

(17) (a) Yang, J.; He, R.; Che, Q.; Gao, X.; Shi, L. *Polym. Int.* **2010**, *59*, 1695. (b) Yang, J.; Xu, Y.; Zhou, L.; Che, Q.; He, R.; Li, Q. *J. Membr. Sci.* **2013**, *446*, 318. (c) Yang, J.; Aili, D.; Li, Q.; Xu, Y.; Liu, P.; Che, Q.; Jensen, J. O.; Bjerrum, N. J.; He, R. *Polym. Chem.* **2013**, *4*, 4768.

(18)   (a) Bhadra, S.; Ranganathaiah, C.; Kim, N. H.; Kim, S.; Lee, J. H. *J. Appl. Polym. Sci.* **2011**, *121*, 923-929. (b) Bhadra, S.; Kim, N. H.; Lee, J. H. *J. Membr. Sci.* **2010**, *349*, 304.

(19)   (a) Conti, F.; Majerus, A.; Noto, V. D.; Korte, C.; Lehnert, W.; Stolten D. *Phys. Chem. Chem. Phys.* **2012**, *14*, 10022. (b) Lineras, J. J.; Sanches, C.; Paganin, V. A.; Ganzalez, E. R. *J. Electrochem. Soc.* **2012**, *159*, F194. (c) Asensio, J. A.; Borros, S.; Gomez-Romero, P. *J. Electrochem. Soc.* **2004**, *151*, A304.

(20)   Maity, S.; Jana, T. *Macromolecules*, **2013**, *46*, 6814.

(21)   (a) Xiao, L.; Zhang, H.; Scanlon, E.; Ramanathan, L. S.; Choe, E. W.; Rogers, D.; Apple, T.; Benicewicz, B. C. *Chem. Mater.* **2005,** *17,* 5328. (b) Hickner, M. A.; Ghassemi, H.; Kim, S. Y.; Einsla, B. R.; McGrath, J. E. *Chem. Rev.* **2004**, *104*, 4587.

(22)   (a) Sannigrahi, A.; Arunbabu, D.; Jana, T. *Macromol. Rapid Commun.* **2006**, *27*, 1962. (b) Sannigrahi, A.; Ghosh, S.; Maity, S.; Jana, T. *Polymer* **2011**, *52*, 4319.

(23)   (a) Mecerreyes, D.; Grande, H.; Miguel, O.; Ochoteco, E.; Marcilla, R.; Cantero, I. *Chem. Mater.* **2004**, *16*, 604. (b) Weber, J.; Kreuer, K. D.; Maier, J.; Thomas, A. *Adv. Mater.* **2008**, *20*, 2595.

(24)   (a) Deimede, V.; Voyiatzis, G. A.; Kallitsis, J. K.; Qingfeng, L.; Bjerrum, J. N. *Macromolecules* **2000**, *33*, 7609. (b) Arunbabu, D.; Sannigrahi, A.; Jana, T. *J. Phys. Chem. B* **2008**, *112*, 5305. (c) Hazarika, M.; Jana, T. *ACS Appl. Mater. Interfaces* **2012**, *4*, 5256. (d) Hazarika, M.; Jana, T. *Eur. Polym. J.* **2013**, *49*, 1564. (e) Katzfub, A.; Krajinovic, K.; Chromik, A.; Kerres, J. *J. Polym. Sci. Part A: Polym. Chem.* **2011**, *49*, 1919.

(25)   (a) Ghosh, S.; Sannigrahi, A.; Maity, S.; Jana, T. *J. Phys. Chem. C* **2011**, *115*, 11474. (b) Ghosh, S.; Sannigrahi, A.; Maity, S.; Jana, T. *J. Mater. Chem.* **2011**, *21*, 14897. (c) Kannan, R.; Kagaiwale, H. N.; Chaudhari, H. D.; Kharul, U. K.; Kurungot, S.; Pillai, V. K. *J. Mater. Chem.* **2011**, *21*, 7223. (d) Chung, S. W.; Hsu, S. L. C.; Liu, Y. H. *J. Membr. Sci.* **2007**, *305*, 353.

(26)   (a) Liu, Y.; Shi, Z.; Xu, H.; Fang, J.; Ma, X.; Yin, J. *Macromolecules* **2010**, *43*, 6731. (b) Suryani; Chang, C. M.; Liu, Y. L.; Lee, Y. M. *J. Mater. Chem.* **2011**, *21*, 7480. (c) Wang, Y.; Shi, Z.; Fang, J.; Xu, H.; Ma X.; Yin J. *J. Mater. Chem.* **2011**, *21*, 5050. (d) Xu, C.; Wu, X.; Wang, X.; Mamlouk M.; Scott K. *J. Mater. Chem.* **2011**, *21*, 6014.

(27)   (a) Sannigrahi, A.; Ghosh, S.; Maity, S.; Jana, T. *Polymer* **2010**, *51*, 5929. (b) Sannigrahi, A.; Arunbabu, D.; Sankar, R. M.; Jana, T. *J. Phys. Chem. B* **2007**, *111*, 12124. (c) Jouanneau, J.; Mercier, R.; Gonon, L.; Gebel, G.; *Macromolecules* **2007**, *40*, 983. (d) Ng, F.; PeRon, J.; Jones, D. J.; RozieRe, J. *J. Polym. Sci., Part A: Polym. Chem.* **2011**, 49, 2107. (e) Qing, S.; Huang, W.; Yan, D. *Euro. Polym. J.* **2005**, *411*, 589.

(28)   Conti, F.; Willbold, S.; Mammi, S.; Korte, C.; Lehnert, W.; Stolten, D. *New J. Chem.* **2013**, *37*, 152.

(29)   Sannigrahi, A.; Ghosh, S.; Lalnuntluanga, J.; Jana, T. *J. Appl. Polym. Sci.* **2009**, *111*, 2194.

(30)   (a) Sannigrahi, A.; Arunbabu, D.; Sankar, R. M.; Jana, T. *Macromolecules* **2007**, *40*, 2844. (b) Ghosh, S.; Sannigrahi, A.; Maity, S.; Jana, T. *J. Phys. Chem. B* **2010**, *114*, 3122.

CHAPTER 6

Polybenzimidazole Diblock Copolymers for PEM Fuel Cell: Synthesis and Studies of Block Length Effect on Nanophase Separation, Mechanical Properties and Proton Conductivity of PEM
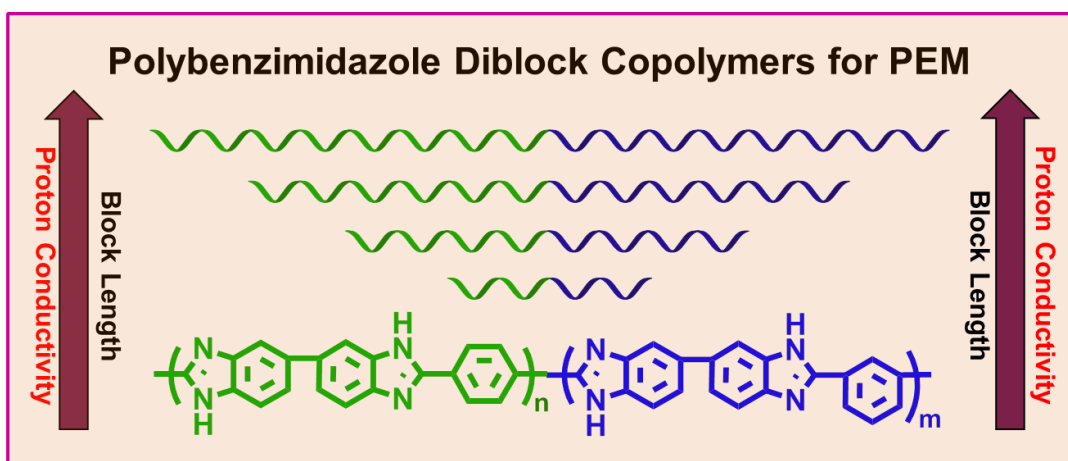
Maity, S.; Jana, T. Communicated to *Macromolecules.*

6.1. INTRODUCTION:

For extensively huge polluting civilization because of industrial growth; demand of energy for mobile as well as stationary purposes need a clean environmentally and eco-friendly energy conversion device.[1] In this connection, from last two decades research towards the development of polymeric membrane which can be used as high temperature polymer electrolyte membrane (PEM) in fuel cell has gained considerable interests in the scientific community owing to its several advantages compared to traditional perfluorinated sulfonic acid containing polymer membrane such as Nafion.[2-4] Among large number of polymeric systems which have been developed for this purpose, phosphoric acid (PA) doped polybenzimidazole (PBI) has been found to be the most attractive because of their very high thermo-mechanical stability, resistance to chemical and long term durability.[5-10]

With regard to the use of PBI as PEM, several aspects of PBI chemistry have been studied thoroughly in the last ten years.[11-13] Few aspects among these which are often highlighted in the literature are solubility and hence processability issues of PBI, thermal, mechanical stability of PBI, acid loading capability, proton conductivity and especially the thermo-mechanical stability of PA doped PBI membrane in particular when PA loading is high.[14-20] Another important drawback which is also pointed out to be as one of the bottlenecks for the use in PEM is the durability of PA doped membrane since PA can readily leach out from the membrane and thereby reducing the membrane proton conducting character.[21,22]

To address the solubility problem, several varieties of PBI structures have been suggested.[23-28] However, many of them failed to enhance the solubility or even it improves, resulting membranes obtained from these new structures display inferior properties compared to traditional PBI as PEM. Recently, we have reported (Chapter-4) a new type of PBI called pyridine based PBI (Py-PBI),[13] which was synthesised from an alternative, inexpensive monomer called Py-TAB, which has very high solubility and as well as enhanced proton conducting character compared to traditional PBI. Other synthetic methods, which have been adapted very often to increase the processability, are grafting the alkyl[23] or functionalized alkyl chain in the PBI backbone[29,30] by substituting in the imidazole ring. However these approaches also have many disadvantages.

In regard to the development and fabrication of PA doped PBI membrane with workable thermo-mechanical stability and high PA loading, hence high proton conductivity several approaches have been explored in literature, recently several reviews have summarized them.[1,4,9,16] In general following four methods are adapted and these are: (1) synthesis of new PBI structures which include structural varieties in homopolymers and copolymers,[23-28] (2) development of novel fabrication method which addresses all the issues raised above, (3) preparation of nanocomposites of PBI with inorganic fillers such as clay,[31] silica particles,[32] nanotubes,[33] graphene[34] etc. and (4) making blend with another polymer which helps to obtain the desired property as mentioned above. All these approaches of making PA doped PBI

membrane with high PA loading and conductivity without comprising thermo mechanical properties are extensively studied by us and other groups.

Recently, synthesis of PBI copolymers increasingly becoming important since copolymer structure offers opportunities to improve the properties and especially the PA doped PBI properties.[24,25,28,35-39] Majority of the literature reports are on the random copolymer of two or three different types of PBI. Among these random copolymer of *meta* connected PBI and *para* connected PBI is very significant since chemical structure-wise they are same, however their linkage with imidazole are different which makes them isomeric structure.[40] It has been pointed out that PA doped *para* PBI shows higher conductivity than *meta* PBI.[13] However, *para* PBI has very low solubility and hence processability. Therefore a combination of *meta* and *para* PBI can result into processable material and as well as good proton conducting PEM can be fabricated.[16,41,42] With this background, earlier we had synthesised *meta/para* random copolymer. However, we found that the conductivity did not improve as per our expectations. Hence, it became necessary for us to come up with new structural strategies.

It has been reported that the blocks of multi block structure can easily phase separate into two domains which enhances the internal connectivity within the block and hence resulting in higher conductivity.[43-45] In literature only two reports are available on multi block copolymers of PBI with poly(aryleneethersulfone)[44] and Benicewicz *et al.*[45] reported segmented block copolymer of sulfonated PBI with para PBI. All of these reports highlighted increase in proton conductivity and argued that the nanophase segregation of blocks as the cause for higher conductivity. Keeping this background of nanophase separation of block structure and absence of *meta para* block copolymer in the literature, we planned to synthesize *meta*-PBI-*block*-*para*-PBI diblock copolymer and study the effect of each block length on the phase separation and hence on the proton conductivities. We also attempted to build several structural varieties (motifs) of diblock copolymers and study their influences on the properties of PEM obtained from these diblock copolymers.

6.2. SYNTHESIS:

6.2.1. Synthesis of Diamine Terminated Polybenzimidazole Oligomers:

Diammine terminated poly[2,2'-(*m*-phenylene)-5,5'-benzimidazole] oligomers (abbreviated as *m*-PBI-Am) were synthesized from the polycondensation of the TAB and IPA monomers in PPA medium. We have carried out total five sets of reactions and all the reactions were in 100 g scale. In all the cases total monomer concentration (TMC) at the beginning of the reaction was kept at 5 wt%. The mole ratio of TAB and IPA were altered to get the variable molecular weight of the resulting oligomers. We have kept the fixed IPA mole ratio at 1 and systematically varied the TAB mole ratios from 1.06 to 1.25 as seen in Table 6.1. The reactions were carried out as follows: all reactions of different mols of TAB and IPA were taken

into a three neck flask with 100 g PPA for diamine terminated oligomers synthesis and the reactions were carried out for 12 h at 190 °C. After the polymerization, the viscous oligomer solutions were slowly poured into the de-ionized water and washed with de-ionized water several times. Then dilute solution of ammonium hydroxide solution added to neutralize the excess phosphoric acid. The oligomer were filtered and washed with ethanol several times and dried in vacuum oven for three days at 60 °C to remove the solvents completely. This reaction scheme is shown in the Scheme 6.1.

Diamine terminated *meta*-polybenzimidazole oligomer (*m*-PBI-Am)
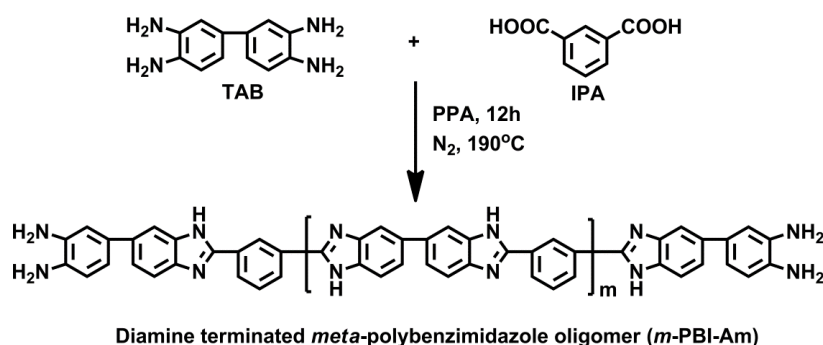
Scheme 6.1. *Synthesis of meta oriented diamine terminated polybenzimidazole oligomer.*

6.2.2. Synthesis of Diacid Terminated Polybenzimidazole Oligomers:

Diacid terminated poly[2,2'-(*p*-phenylene)-5,5'-benzimidazole] oligomers (abbreviated as *p*-PBI-Ac) were synthesized using the condensation of TAB and TPA monomers in PPA medium. Here also we have done total five sets of reactions and all are in 100 g scale and the total monomer concentrations (TMC) were kept at 5 wt%. We have varied the mole ratio of TAB and TPA to alter the molecular weight of oligomers. We have kept the fixed TAB mole ratio at 1 and varied the TPA mole ratio from 1.06 to 1.25 as seen in Table 6.1. All reactions of different mols of TAB and TPA were taken into a three neck flask with 100 g PPA for acid terminated oligomers synthesis and the reaction were carried out for 6-8 hours at 190 °C. After the polymerization the viscous oligomer solutions were slowly poured in to the deionized water and washed with deionized water several times. Then dilute solution of ammonium hydroxide was added to neutralize the excess phosphoric acid. The oligomers were filtered and washed with ethanol several times and dried in vacuum oven for three days at 60 °C to remove the solvents completely. This reaction scheme is shown in the Scheme 6.2.

Acid terminated *para*-polybenzimidazole oligomer (*p*-PBI-Ac)
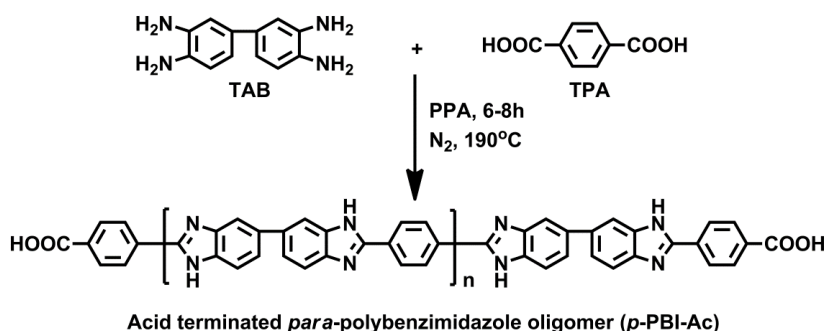
Scheme 6.2. *Synthesis of para oriented acid terminated polybenzimidazole oligomer.*

6.2.3. Synthesis of Diblock Copolymers of Polybenzimidazole:

Diblock copolymers of PBI were synthesized by polycondensation (coupling) reactions of diamine (*m*-PBI-Am) and acid (*p*-PBI-Ac) terminated oligomers in PPA medium, which resulted in block polymer of the following structure *meta*-polybenzimidazole-*block*-*para*-polybenzimidazole; abbreviated as *m*-PBI-*b*-*p*-PBI. Three different types of diblock copolymers were synthesized and these are: (I) (Am$_{fix}$-*b*-Ac$_{vary}$), in this we varied the block length of acid terminated oligomer with the fixed diamine terminated oligomer, (II) (Am$_{vary}$-*b*-Ac$_{fix}$), in this case, we varied the diamine terminated oligomer with the fixed acid terminated oligomer and (III) (Am$_{equal}$-*b*-Ac$_{equal}$) where we took equal block length of diamine terminated and acid terminate oligomers. In case of block copolymer of Am$_{fix}$-*b*-Ac$_{vary}$ *(Case I)*, we have chosen the highest molecular weight of diamine terminated oligomer (IV = 0.59 dL/g, Table 6.3) and in case of Am$_{vary}$-*b*-Ac$_{fix}$, we have chosen the highest molecular weight of acid terminated oligomer (IV = 0.54 dL/g), Table 6.3). The detail reactions recipes are summarised in results and discussion section (Table 6.3). We have taken the ammine and acid terminated PBI oligomers weight according to their end group analysis to maintain their stoichiometric balance. End group analysis technique by ^{1}H NMR was used to calculate the molecular weight of the oligomers. All diblock copolymers synthesis were carried in 100 g scale and total monomer concentrations were kept at 4 wt%. Polymerizations were carried out as follows: the synthesized oligomers with appropriate stoichiometry were taken in a three neck flask and connect with sealed over headed mechanical stirrer and the reaction was kept at 210 °C for 24-26 h with continuous nitrogen purging. After the complete polymerization the viscous polymer solutions were slowly poured into the de-ionized water and washed several times. Then ammonium hydroxide solution was added to neutralize the excess phosphoric acid. The polymers were filtered and washed with deionized water several times and dried in vacuum oven for three days at 100 °C to remove the solvents completely. The synthesis of diblock copolymer of PBI is represented in Scheme 6.3.

Diamine terminated *meta*-polybenzimidazole oligomer (*m*-PBI-Am)

+

Acid terminated *para*-polybenzimidazole oligomer (*p*-PBI-Ac)

PPA, 24-26h
N$_2$, 210°C

***meta*-polybenzimidazole-*block-para*-polybenzimidazole (*m*-PBI-*b-p*-PBI)**
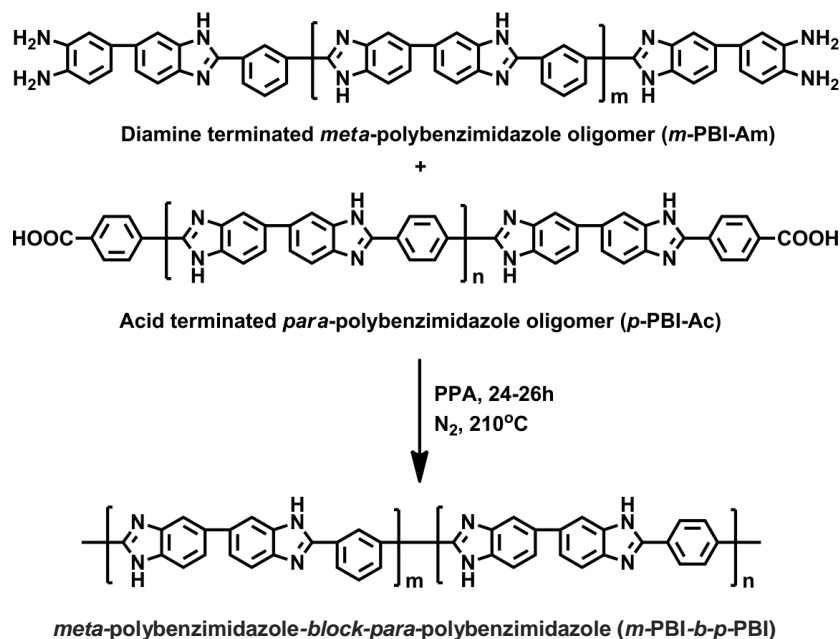
Scheme 6.3. *Synthesis of diblock copolymer of polybenzimidazole.*

6.3. CHARACTERIZATION:

All the information about the materials used in this study, membrane fabrication method from the synthesized *m*-PBI-*b-p*-PBIs and the experimental methods of all the characterization techniques which include molecular weight measurements by viscosity and proton NMR analysis, thermogravimetric analysis (TGA) and dynamic mechanical analysis (DMA) for all the *m*-PBI-*b-p*-PBIs polymers are described in the Chapter 2. The *m*-PBI-*b-p*-PBIs membranes H$_3$PO$_4$ doping level and the proton conductivity measurements are also discussed in the Chapter 2.

6.4. RESULTS AND DISCUSSION:

6.4.1. Synthesis of Polybenzimidazole Oligomers:

Since in this work, we wish to prepare PBI block copolymers hence firstly we need to synthesize oligomeric blocks, which further can be connected by condensation (coupling) to build the block copolymer structure. To get the block copolymer structure of PBI, we need to have diamine terminated PBI oligomeric structure and acid terminated PBI oligomeric structure which upon condensing can produce block PBI structure. As shown in Scheme 1 & 2, we have prepared diamine terminated *meta* polybenzimidazole (*m*-PBI-Am) oligomer and acid terminated *para* polybenzimidazole (*p*-PB-Ac) oligomer by the condensation reaction TAB with IPA and TPA, respectively in PPA. It is expected that further condensation of these two oligomers structure will produce block PBI structure in which one block would be *meta* connected

structure and other would be para connected structure. To get the terminal functionalities in oligomers we have used stoichiometric imbalance method in the reaction mixture as shown in Table 6.1. For diamine termination higher amount TAB was taken and similarly for acid termination higher amount of acid was taken. Since we also would like to see the effect of block lengths in the final properties of PBI block copolymers, therefore it is necessary to build different chain length oligomeric structures. To do so, we have varied the mole ratio of IPA and TPA with the TAB. For *meta* diamine terminated PBI oligomers we have varied the mole ratio of TAB 1 to 1.25 with a fixed 1 mole ratio of IPA and for *para* acid terminated oligomer we have varied TPA mole ratio 1 to 1.25 with a fixed 1 mole ratio of TAB. From Table 6.1 it is clear that with increasing the stoichiometric imbalances; the molecular weight (inherent viscosity, IV) of both the diamine and acid terminated oligomer gradually decrease.

Table 6.1. *Monomer mole ratios and molecular weights of synthesized diamine (meta) and acid terminated (para) PBI oligomers.*

Diamine terminated oligomer (m-PBI-Am)			Acid terminated oligomer (p-PBI-Ac)		
TAB:IPA (mole ratio)	*IV (dL/g)^a*	*M_n (g/mole)^b*	*TAB:TPA (mole ratio)*	*IV (dL/g)^a*	*M_n (g/mole)^b*
1.06 : 1	0.59	5500	1 : 1.06	0.54	5200
1.09 : 1	0.47	4300	1 : 1.09	0.43	4100
1.14 : 1	0.32	3100	1 : 1.14	0.35	3300
1.20 : 1	0.22	2100	1 : 1.20	0.23	2200
1.25 : 1	0.12	1000	1 : 1.25	0.11	1100

^{a}Determined from 0.2 g/dL oligomers solution in conc. H_2SO_4 (98%) at 30 °C.

^{b}Determined by ^1H NMR end group analysis.

The proton NMR structure of representative oligomeric structure for both *m*-PBI-Am and *p*-PBI-Ac are shown in Figure 6.1 with their peak assignments. The structures match very well with the spectral data. In both the oligomers, the terminal peaks are assigned as shown in Figure 6.1. In case of *m*-PBI-Am (Figure 61.A), the terminal peaks of oligomers are assigned by a', b', d', e', f', g and h. The other peaks are assigned as nonterminal peaks. The terminal imidazole proton peaks are appeared at 13.08 ppm designated as a', terminal aromatic proton appears in between 6.56-7.46 ppm assigned as d', e', f', g and terminal amine peak appear at 4.61 ppm numbered as h[44]. Similarly in case of *p*-PBI-Ac (Figure 6.1B), in addition to nonterminal peaks, all terminal peaks are assigned as d', e', f', g, i', j, k' and l. In which d', e', f', g represented the terminal aromatic protons as shown in Figure 6.1A. The i' peak at ~ 13.12 ppm represents the imidazole proton and j at ~ 13.12 ppm is assigned as terminal carboxylic proton. It must be noted that the peaks at ~ 13.12 ppm (denoted as i', i, j) is broad in nature and this is due to overlap of carboxylic and imidazole proton peaks.
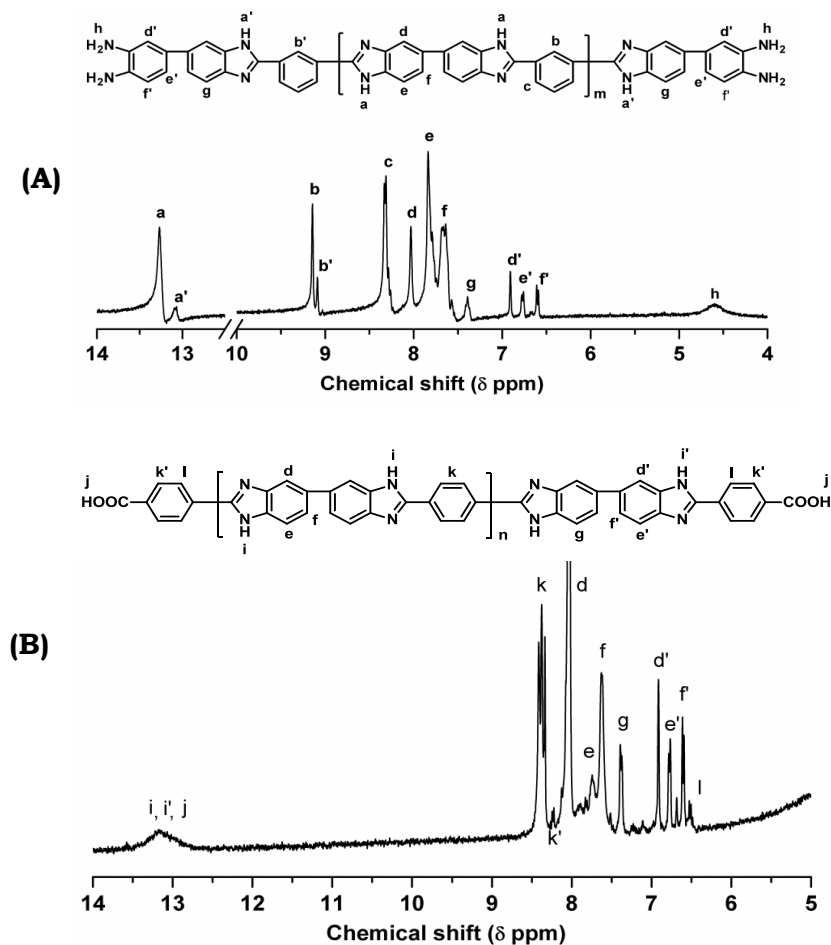
Figure 6.1. *^{1}H-NMR spectra of (A) diamine terminated meta-polybenzimidazole oligomer (m-PBI-Am) (B) acid terminated para-polybenzimidazole oligomer (p-PBI-Ac). Peaks assignments and chemical structure of oligomers are also shown in the figure. All spectra were recorded using DMSO-d_6 as NMR solvent.*

The number average molecular weights (M_n) of diamine and acid terminated oligomers are calculated from the end group analysis by peak integration of ^{1}H NMR spectra using technique similar to method reported earlier.[44] The molecular weights (MW) of diamine terminated oligomers are varied from 1000 to 5500 and for acid terminated oligomers 1100 to 5200 (Table 6.1). M_n values also follow the similar trend as IV values in both the cases; with increasing stoichiometric imbalance MW decreases. The MW increases with increasing IV values as per the expectation both the cases. Linear ships between IV and MW are observed for both the cases (*m*-PBI-Am & *p*-PBI-Ac) when a log-log plot was drawn between IV and MW (Figure 6.2), which in turn confirmed the successful control of MW for both the blocks.
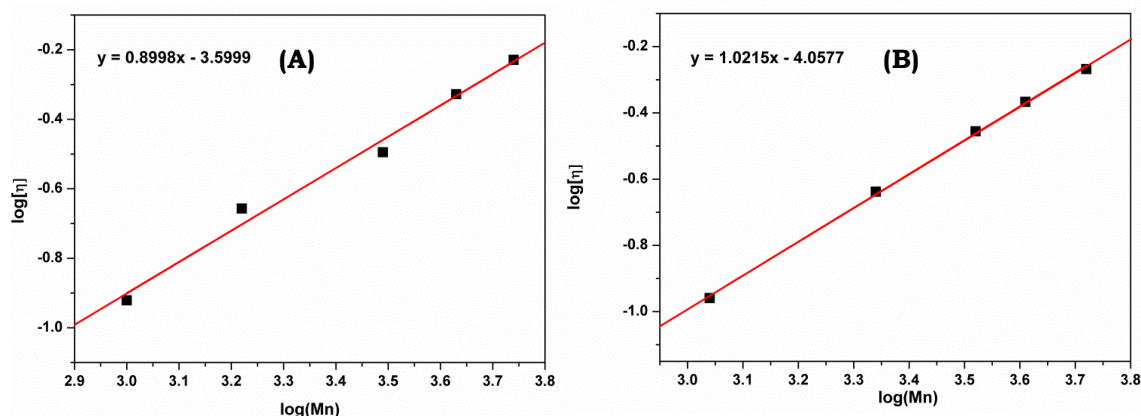
Figure 6.2. *Double logarithmic plot of IV vs* M_n *of [A] diamine terminated PBI oligomer (m-PBI-Am) and (B) acid terminated PBI oligomer (p-PBI-Ac).*

It is important to note that, we have prepared diamine terminated oligomer using IPA with TAB and acid terminated oligomer using TPA with TAB (Scheme 6.1 & 6.2 and Table 6.1). The question can be asked why not vice versa i.e. TPA for diamine termination and IPA for acid termination and why we are so particular about it? Infact this should have been a natural choice since our earlier studies indicated formation of diamine terminated oligomeric species as a major intermediate when TPA and TAB condensation takes place owing to the low solubility of TPA in PPA. We also attributed this as a cause for formation of high MW PBI whenever a para connected diacid (such as TPA) is used. In this study, initially we indeed attempted to make diamine oligomer using TPA and acid oligomer using IPA and the results are shown in Table 6.2. However, we observe that MW (IV values) for diamine terminated are always quite high than acid terminated (Table 6.2) even though stoichiometric imbalance are quite similar. This is quite obvious as the reaction stated above and as per our earlier observation. Therefore, we do not have good control over the MW (chain size) of both the oligomers, which will not allow to build the final block structure with several varieties. Hence, we opted the reverse i.e. IPA for diamine and TPA for acid terminated as discussed and shown in Scheme 6.1, 6.2 and Table 6.1, where we have very good control over both oligomers MW and hence we can build blocky PBI structure of several varieties which will be discussed in next section. The reason why TPA produced relatively lower MW acid terminated oligomer compare to diamine terminated (Table 6.1) using IPA is that since it is favoured to go via acid termination instead of diamine termination owing to high acid stoichiometry.

Table 6.2. *Monomer mole ratios and inherent viscosity of synthesized diamine (para) and acid (meta) terminated PBI oligomers.*

Acid terminated oligomer (Am)		Amine terminated oligomer (Ac)	
TAB:IPA (mole ratio)	IV (dL/g)^a	TAB:TPA (mole ratio)	IV (dL/g)^a
1 : 1.014	0.71	1.014 : 1	3.01
1 : 1.065	0.21	1.065 : 1	0.81
1 : 1.114	0.03	1.114 : 1	0.61

^{a}Determined from 0.2 g/dL oligomers solution in conc. H_2SO_4 (98%) at 30 °C.

6.4.2. Synthesis of Diblock Copolymer of Polybenzimidazoles:

meta-polybenzimidazole-*block-para*-polybenzimidazole (*m*-PBI-*block-p*-PBI) are synesized by condensing equal moles of diamine terminated *meta* PBI and acid terminated *para* PBI in PPA medium for 24 hours as shown in Scheme 6.3. The stoichiometric balance (1:1 moles) of *p*-PBI-Ac and *m*-PBI-Am in the polybenzimidazole feed are maintained in all the block copolymer synthesis based on the calculated stoichiometry of oligomer obtained from end group analysis using ^{1}H-NMR spectra. It is expected that this condensation of oligomers will yield blocky structure of PBI. A careful analysis of 1H-NMR spectra further clarified the formation of diblock PBI. ^{1}H-NMR spectra of one representative diblock PBI is shown in Figure 6.3 along with diblock structure. The peak assignments of the diblock structures are also represented in the figure. A comparison of Figure 6.3 spectra with oligomeric spectra shown in Figure 6.1 clearly proves the formation of block structure. In case of *m*-PBI-Am oligomer (Figure 6.1A), the peaks of terminal diamine protons (h) appears at 4.61 ppm and terminal imidazole peak is seen at 13.08 ppm (a'). Similarly all the aromatic peaks (b', d', e', f', g) are also clearly distinguish all the oligomeric proton signal (Figure 6.1A). Similarly in case of *p*-PBI-Ac oligomer (Figure 6.1B) the terminal acid (J), and imidazole peaks (i') are identified as broad peaks along with regular peak. The remaining terminal aromatic (d', e', f', g, k', l) peaks are seen as in case of *m*-PBI-Am. The block copolymer *m*-PBI-*block-p*-PBI, ^{1}H-NMR spectra matches well with the expected structure as shown in Figure 6.3. The complete disappearance of terminal protons signals of both oligomers [imidazole (a', i'), amine (h), acid (j) and aromatic (b', d', e', f', g, k', l)] as shown by the arrow in the Figure 6.3 clearly indicates the formation and ring closer of the condensation polymerization and hence the formation of block copolymer of PBI. The all other peaks are indicated in the figure clearly attributes and agrees with block PBI structure as shown in Scheme 6.3.
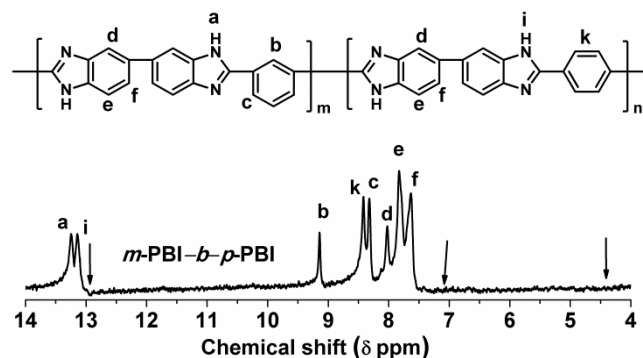
Figure 6.3. ^{1}H-NMR spectra of meta-PBI-block-para-PBI block copolymer. Peaks assignments and chemical structure of block copolymer is shown in the figure. Spectra was recorded using DMSO-d_6 as NMR solvent. Arrow indicating the disappearance of terminal peaks of oligomer due to formation of block PBI.

The above discussion and Figure 6.1 clearly prove the formation of diblock PBI copolymer structure upon condensation of diamine and acid terminated PBI oligomers. It is to be noted, from Table 6.1 that, we have synthesized both types of PBI oligomers with variable chain length (molecular weight). Therefore, we can utilized the various combination of these variable chain length oligomers to build the different types of diblock PBI structures as shown in Table 6.3. The schematic structures of blocks are shown in last column of Table 6.3. There varieties of block PBI structures are prepared and these are: (I) fixed diamine-block-variable acids (Am$_{fix}$-b-Ac$_{vary}$), (II) variable diamine-block-fixed acid (Am$_{vary}$-b-Ac$_{fix}$) and (III) equal diamine-block-equal acid (Am$_{equal}$-b-Ac$_{equal}$). In case of (I) (Am$_{fix}$-b-Ac$_{vary}$); we have chosen the highest molecular weight of diamine terminated m-PBI oligomer and varied the acid terminated p-PBI oligomers molecular weight. Similarly, in case of (II) (Am$_{vary}$-b-Ac$_{fix}$); we have chosen the highest molecular weight of acid terminated p-PBI oligomer and varied the molecular weight of diamine terminated m-PBI oligomers. But in case of (III) (Am$_{equal}$-b-Ac$_{equal}$); similar molecular weight of both oligomer are chosen, however, their size are vary equally from one polymer to another.

In both cases of fixed amine and acid terminated diblock copolymer of PBI; the molecular weight gradually decreases with the increasing of counter oligomers molecular weight (Table 6.3). This could be due to the reactivity of counter oligomers which gradually decreases with the increasing the molecular weight of the oligomers due the different chain length of oligomers which do not allow the longer chain length to react readily. But in case of the equal ammine and acid terminate diblock (case III) copolymer, due to the equal length of molecular weight; they have the same reactivity and the condensation reaction takes place readily.

Table 6.3. Oligomers combinations and molecular weights of synthesized diblock copolymer of polybenzimidazoles and the schematic structures of block copolymers.

Oligomers IV (dL/g) m-PBI-Am:p-PBI-Ac	Block copolymer IV (dL/g)[a]	Copolymer composition (meta/para)[b]	Schematic structure[c]
Fixed diamine-block-variable acids copolymer (Am_{fix}-b-Ac_{vary})			
0.59 : 0.11	2.01	-	
0.59 : 0.23	1.42	63.60/36.40	
0.59 : 0.35	0.87	60.44/39.56	
0.59 : 0.43	0.87	52.75/47.25	
Variable diamine-block-fixed acid copolymer (Am_{vary}-b-Ac_{fix})			
0.12 : 0.54	1.62	-	
0.22 : 0.54	1.08	37.18/62.82	
0.32 : 0.54	1.06	-	
0.47 : 0.54	0.97	43.75/56.25	
Equal diamine-block-equal acid copolymer (Am_{equal}-b-Ac_{equal})			
0.12 : 0.11	0.47	-	
0.22 : 0.23	1.28	49.95/50.05	
0.32 : 0.35	0.75	-	
0.47 : 0.43	1.33	51.79/48.21	
0.59 : 0.54	1.37	52.90/47.10	

[a]Determined from 0.2 g/dL polymers solution in conc. H_2SO_4 (98%) at 30 °C.

[b]Determined by ^{1}H NMR peak integration using equation 6.1.

[c] ∿∿ = *m*-PBI-Am and ∿∿ = *p*-PBI-Ac

The proton NMR spectra of all the three types of diblock PBI structures with variable chain length of *meta* and *para* blocks are shown in the Figure 6.4. The several peaks assignments are also shown in the figure with the diblock structure and schematic colour coding. It must be carefully noted that the peaks at designated by a, b, c are for the *meta* structure and similarly the peaks which are appear at designated by I, k are for the *para* structure of PBI.[40] As it can be seen, in case of Am_{fix}-b-Ac_{vary} (Figure 6.4A), the peaks due to the *para* structure becomes stronger with increasing IV (molecular weight and chain length) of *para* block in the diblock structure. Similarly, *meta* structure peaks (a, b, c) becomes more and more prominent in case of Am_{vary}-b-Ac_{fix} (Figure 6.4B) with increasing IV of *meta* PBI oligomer. However, in case of Am_{equal}-b-Ac_{equal} (Figure 6.4C), relative intensity of both *meta* and *para* peaks remain same, but peaks become more intense as we increase the chain length.
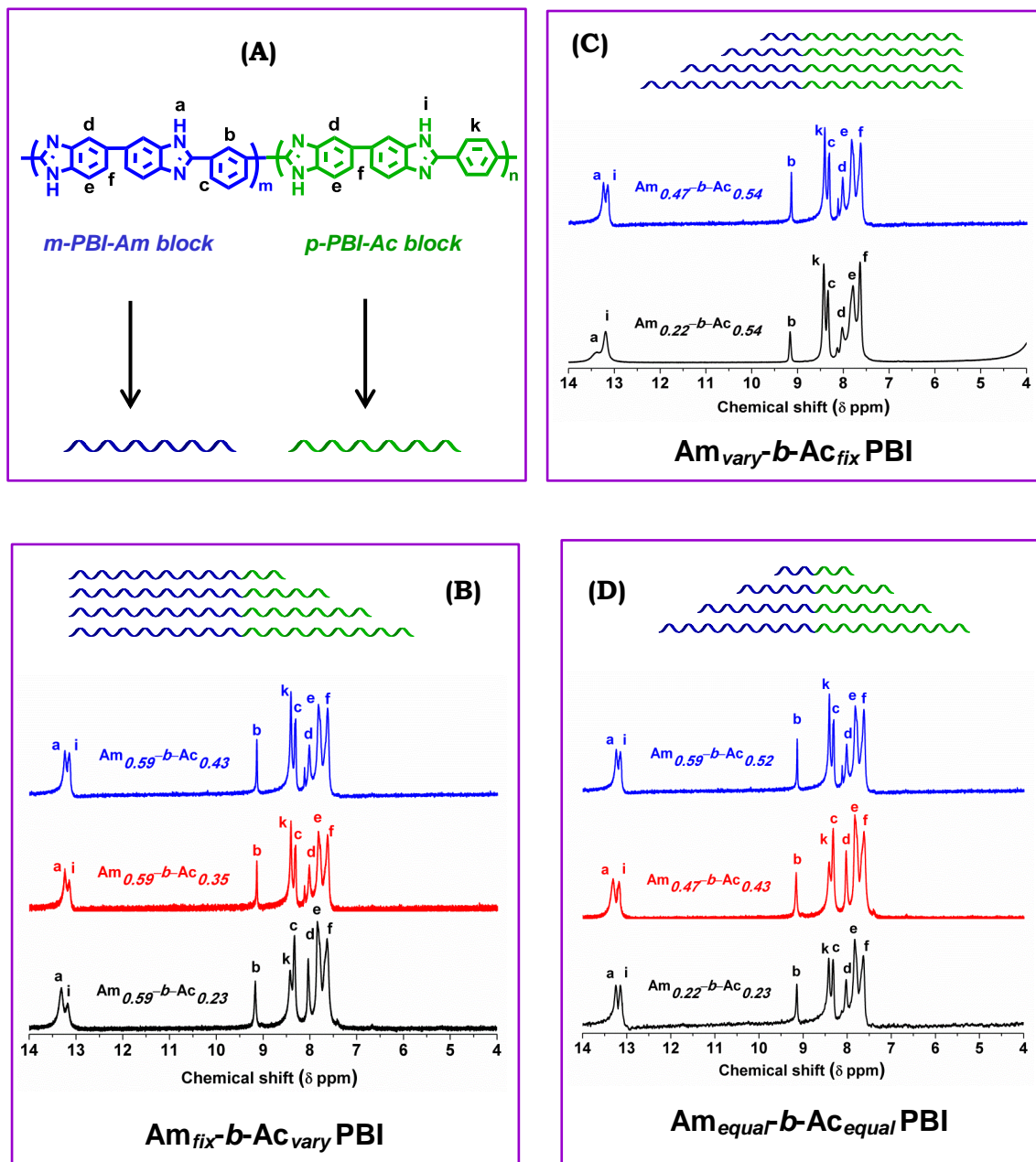
Figure 6.4. ^{1}H-NMR spectra of PBI diblock copolymer of varieties of structures (as shown in Table 6.3): (A) a general block structure with peak assignments and schematic colour coding for each block. (B) Am$_{fix}$-b-Ac$_{vary}$, (C) Am$_{vary}$-b-Ac$_{fix}$ and (D) Am$_{equal}$-b-Ac$_{equal}$. The data are recorded from DMSO-d$_6$. Schematic diblock structure along with colour coding are shown in each cases with their spectra.

$$\% \ of \ para \ mole \ fraction \ in \ the \ copolymer = \frac{I_i + I_k}{I_a + I_b + I_c + I_i + I_k} \qquad --------(6.1)$$

The *para* copolymer compositions (*meta/para*) in the diblock structure are calculated from the integral ratio of proton peaks (a, b, c, i, k) intensities with help of following equation (6.1) and listed in Table 6.3. In case of Am_{equal}-*b*-Ac_{equal} samples the meta/para compositions are always approximately 50/50 irrespective of block length, which is in agreement with the feed *meta/para* composition (50/50). On the other hand, *meta/para* composition alters in other two types of block; the % of *para* increases with increasing block length (MW) of *para* connected acid terminated oligomer in case of Am_{fix}-*b*-Ac_{vary}; where as % of *para* decreases with increasing block length of amine terminated oligomer in case of Am_{vary}-*b*-Ac_{fixd}. These are simply due to the effect of corresponding block length which changes as we alter the molecular weight of oligomers.

6.4.3. Thermal Stability:

We have carried out TGA analysis for all diamine and acid terminated oligomers, and the three sets of diblock copolymers of PBI under continuous nitrogen flow from room temperature to 800 °C. Figure 6.5 & 6.6 show the thermal degradation of the oligomers and block copolymers, respectively. It is clearly visible that all synthesized oligomers and block copolymers are highly thermally stable as per the expectation for PBI type polymers. The weight loss at the initial stage near 150 °C is occurring due to the loss of loosely hydrogen bonded water molecules which are associated to the polymer backbone.[45] The weight loss after 600 °C is due to the degradation of the benzimidazole group of the polymer backbone.[1,40] Both in case of diamine and acid terminated oligomers; the thermal stability gradually increases with increasing the molecular weight of oligomers (Figure 6.5).
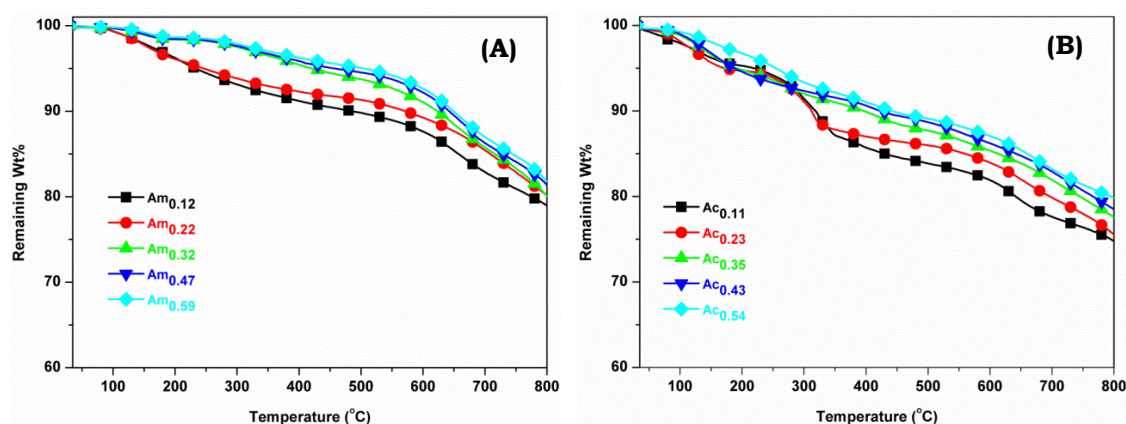
Figure 6.5. Thermogravimetric plots of (A) meta oriented diamine terminated oligomers and (B) para oriented acid terminated oligomers in a N_2 atmosphere at the heating rate of 10 °C/min.

The thermal stability of block copolymers shown in Figure 6.6 display the dependence on the copolymer structure for example in case of Am_{fix}-*b*-Ac_{vary}, the thermal stability decreases with increasing

MW (chain length) of *para* connected acid terminated block (Figure 6.6A). We have found similar trend in case of Am$_{vary}$-*b*-Ac$_{fix}$, where thermal stability decreases with increasing MW of *meta* connected block (Figure 6.6B). Therefore, it can be said that although block lengths are increasing in these two cases, however their thermal stability decrease and this is probably due to the decrease of the molecular weight (IV) of diblock copolymer with increasing block length as showed in Table 6.3. But in case of the equal amine and acid terminated block copolymer we got the reverse results; thermal stability increases with increasing block length (Figure 6.6C). The molecular weight of the resulting block copolymer gradually increases with increasing both molecular weight of acid and amine terminated oligomers. The thermal stability of equal amine and acid terminated block coplolyemr thermal stablity gradually increasing with the inceasing the block lengths (Figure 6.6C). This is due to the fact that the molecular wight of the block copolymers increases with increasing the block length of both oligomers.
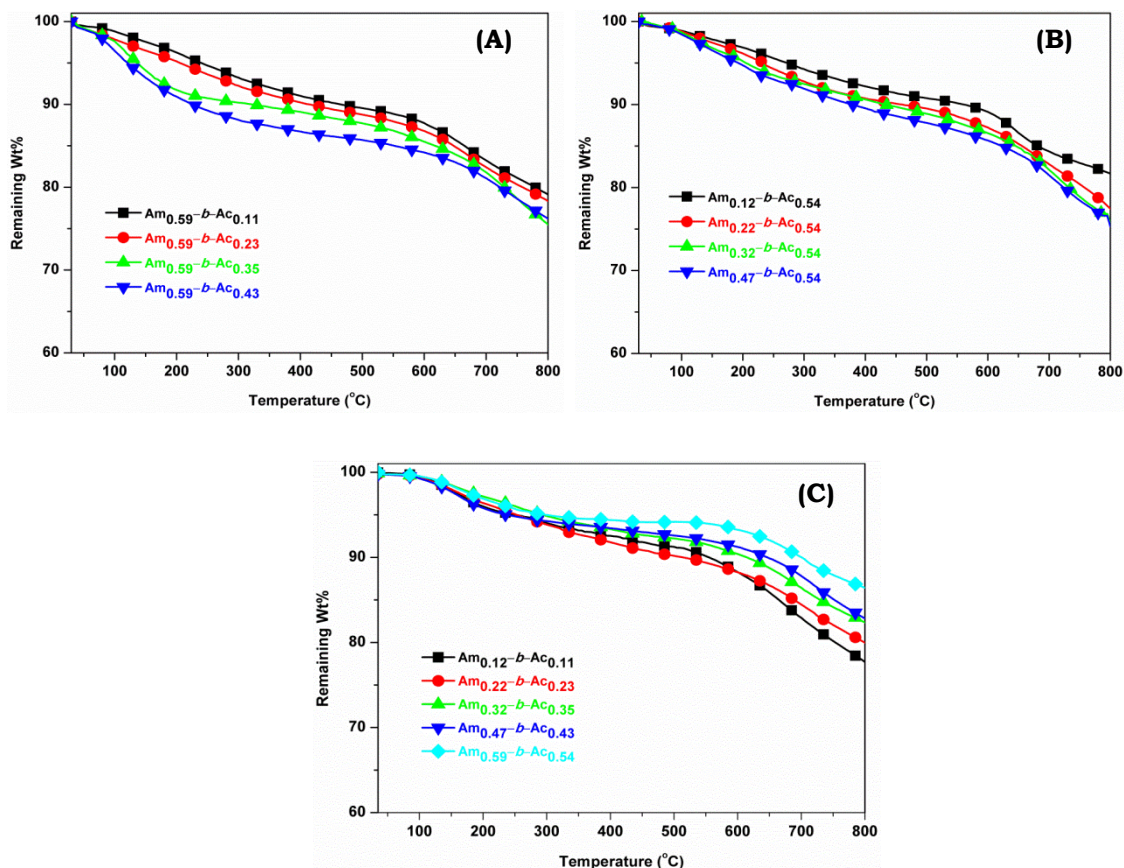
Figure 6.6. *Thermogravimetric plots of (A) Am$_{fix}$-b-Ac$_{vary}$ PBI, (B) Am$_{vary}$-b-Ac$_{fix}$ PBI and (C) Am$_{equal}$-b-Ac$_{equal}$ PBI block copolymer in a N$_2$ atmosphere at the heating rate of 10 °C/min.*

6.4.4. Dynamic Mechanical Properties:

The temperature dependent various thermo-mechanical properties such as storage modulus (E'), loss modulus (E'') and tan δ of PBI diblock copolymers are studied in DMA instrument. The glass transition temperature (T_g) of all types of diblock PBIs are obtained from temperature dependent plots of both E'' and tan δ as shown in Figures 6.7 and 6.8, respectively. All the samples display two distinct glass transition temperatures, attributing the formation of diblock copolymer structures. All the T_g values for all samples are tabulated in Table 6.4. It has been reported by us and several other authors earlier that *para*-PBI T_g is lower than *meta*-PBI T_g owing to the symmetrical structure of *para*-PBI. Based on this experience we have identified the higher temperature transitions as T_g for *para* block (acid terminated) and lower temperature transition as T_g of *meta* block (diamine terminated).
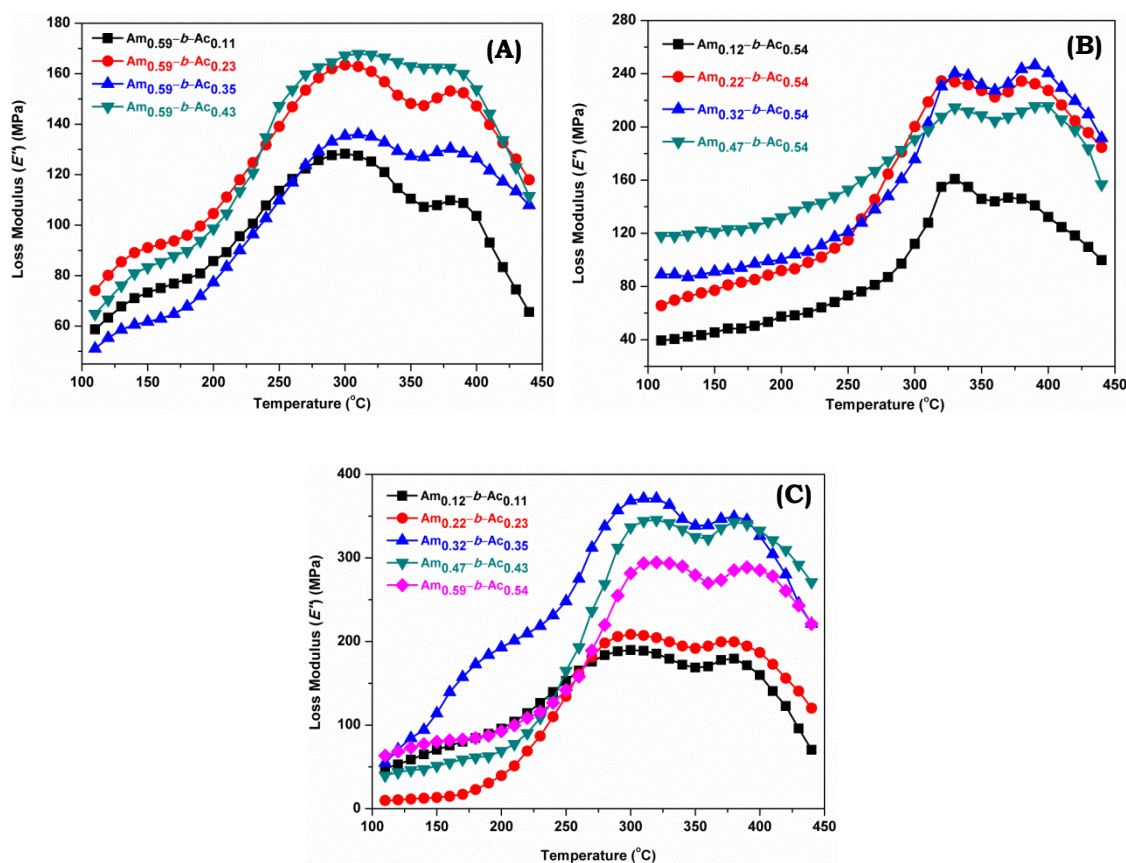
Figure 6.7. *Loss modulus (E'') plots against temperature obtained from DMA study. (A) Fixed diamine terminated with varied acid terminated (Am$_{fix}$-b-Ac$_{vary}$), (B) fixed acid terminated with varied diamine terminated (Am$_{vary}$-b-Ac$_{fix}$) and (C) equal diamine and acid terminated (Am$_{equal}$-b-Ac$_{equal}$) block copolymer at the heating rate of 4 °C/min.*
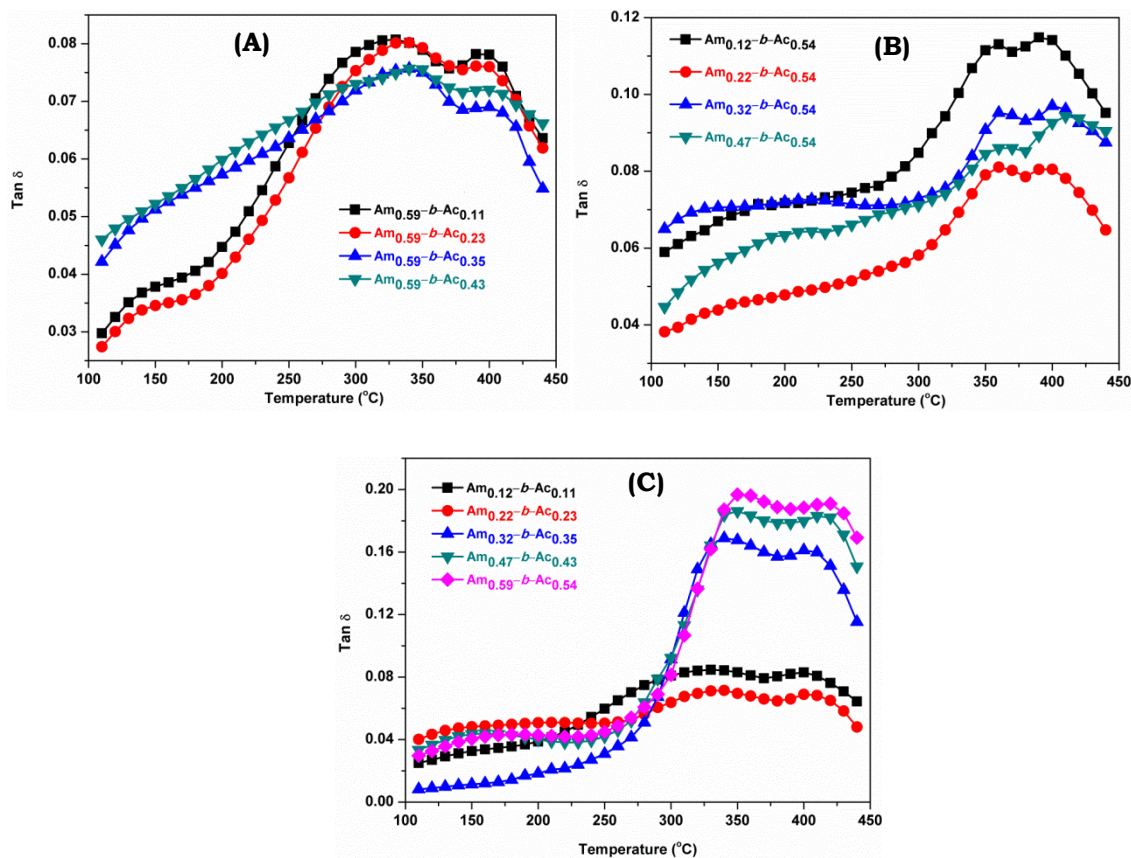
Figure 6.8. *Tan δ plots against temperature obtained from DMA study. (A) Fixed diamine terminated with varied acid terminated (Am$_{fix}$-b-Ac$_{vary}$), (B) fixed acid terminated with varied diamine terminated (Am$_{vary}$-b-Ac$_{fix}$) and (C) equal diamine and acid terminated (Am$_{equal}$-b-Ac$_{equal}$) block copolymer at the heating rate of 4 °C/min.*

In case of fixed diamine terminated diblock copolymer (Am$_{fix}$-b-Ac$_{vary}$); the T_g of fixed *meta* block length does not change that much it is only 5 to 7 °C [395 to 402 °C (tan δ plot) and 380-385 °C (E″ plot)], but increasing the chain length of *para* acid block part T_g increases significantly (20 to 30 °C) from 329 to 349 °C (tan δ plot) and 298-317 °C (E″ plot) shown in Figure 6.7A, 6.8B and Table 6.4. Similarly, in case of fixed acid terminated block copolymer (Am$_{vary}$-b-Ac$_{fix}$); the T_g of fixed *para* block length does not change that much, but increasing the chain length of *meta* diamine block part T_g increases significantly as shown in Figure 6.7A, 6.8B and Table 6.4. But in case of equal acid and equal diamine terminated block copolymers (Am$_{equal}$-b-Ac$_{equal}$) we have got two T_g and both are increasing with increasing *meta* and *para* block length [(Figure 6.7C, 6.8C and Table 6.4)]. This is due to both *meta* and *para* have similar size block chain length and hence with increasing size (chain length) their T_g increases in same manner. It is reported in the literature that with increasing the block lengths the glass transition temperature gradually increases.[44] Here we also found the same trend. From the above discussion of DMA study, it is clear that the T_g variations

depend on the block length and the type of the block structure. Since the molecular weight of block copolymer varies depending on the block length and the structure, hence there could be some effect of MW on T_g as well. However, the trend of T_g variations as shown in Table 6.4 does not seem to reflect the MW dependence on T_g. From the above discussion it is confirmed that the copolymer structure in diblock stricture and the T_g values varies with nature of block and especially on the block length.

Table 6.4. *Glass transition temperatures (T_g) obtained from DMA study of m-PBI-b-p-PBI.*

Block polymer	T_g from E″ (°C)		T_g from tan δ (°C)	
	Amine block (meta)	Acid block (para)	Amine block (meta)	Acid block (para)
Fixed diamine-block-variable acid block copolymer (Am$_{fix}$-b-Ac$_{vary}$)				
Am$_{0.59}$–*b*–Ac$_{0.11}$	383	298	395	329
Am$_{0.59}$–*b*–Ac$_{0.23}$	385	306	398	338
Am$_{0.59}$–*b*–Ac$_{0.35}$	380	311	397	342
Am$_{0.59}$–*b*–Ac$_{0.43}$	382	317	402	349
Variable diamine-block-fixed acid block copolymer (Am$_{vary}$-b-Ac$_{fix}$)				
Am$_{0.12}$–*b*–Ac$_{0.54}$	375	330	393	359
Am$_{0.22}$–*b*–Ac$_{0.54}$	381	326	397	360
Am$_{0.32}$–*b*–Ac$_{0.54}$	390	334	405	365
Am$_{0.47}$–*b*–Ac$_{0.54}$	399	331	417	364
Equal diamine-block-equal acid block copolymer (Am$_{equal}$-b-Ac$_{equal}$)				
Am$_{0.12}$–*b*–Ac$_{0.11}$	377	300	400	326
Am$_{0.22}$–*b*–Ac$_{0.23}$	381	306	408	336
Am$_{0.32}$–*b*–Ac$_{0.35}$	385	314	403	344
Am$_{0.47}$–*b*–Ac$_{0.43}$	391	319	417	351
Am$_{0.59}$–*b*–Ac$_{0.54}$	399	327	420	354

It must be noted that with increasing block length, the two T_g peaks which are assigned to two separate blocks (*meta* and *para*) become increasingly distinct and prominent in all the three sets of samples in both *E′* and tan δ plots as shown in Figure 6.7 and 6.8. This attributes that with increasing block length the degree of mixing between the two blocks decreases and hence resulted into higher degree of phase separation. Hence, at higher block length nano phase segregation of two blocks are more prominent. This nano phase separation is most distinct in case of Am$_{equal}$-*b*-Ac$_{equal}$ block and they are different in nature for other two blocks as well.

Figure 6.9 displays the E' variation as a function of temperature for all types of samples. In all the cases with increasing block length E' values are increasing in the entire temperature range even though in case of Am_{fix}-b-Ac_{vary} and Am_{vary}-b-Ac_{fix} MW decreases with increasing block length as shown in Table 6.3 in earlier section. It also interesting to note that, the % of increase in E' values is not only depends on the block length but it also significantly relys on the block structure as seen from Figure 6.9 plots.
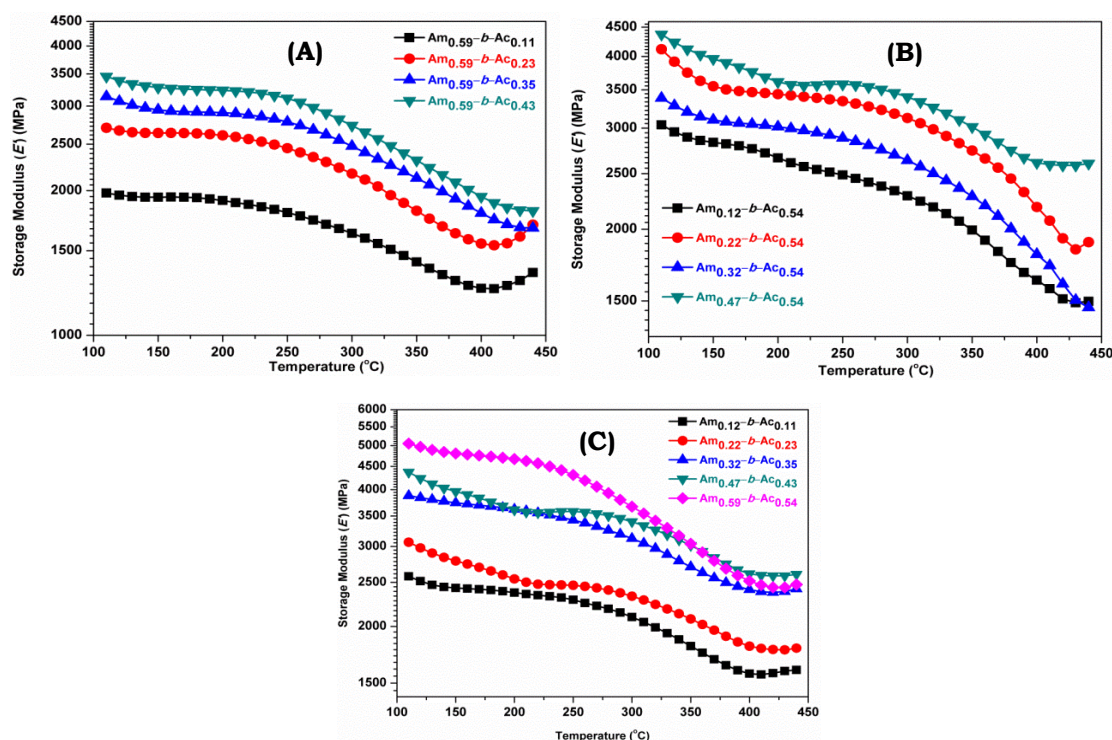
Figure 6.9. Storage modulus (E') plots against temperature obtained from DMA study. (A) Fixed diamine terminated with varied acid terminated (Am_{fix}-b-Ac_{vary}), (B) fixed acid terminated with varied diamine terminated (Am_{vary}-b-Ac_{fix})and (C) equal diamine and acid terminated (Am_{equal}-b-Ac_{equal}) block copolymer at the heating rate of 4 °C/min.

6.4.5. Phosphoric Acid Loading:

Table 6.5 tabulated the phosphoric acid (PA) doping level for all three types of diblock copolymers when the membranes are doped in 85% (14.6M) H_3PO_4 for seven days. The PA doping level for all the samples varies between 8-11 moles per PBI repeat unit. We do not observe any definite conclusive trend with increasing block length, molecular weight of the polymer and the type of diblock structures. The little variations are may be due to the *meta/para* composition variation from one copolymer to another. These measured doping levels of diblock copolymer are comparable with the literature reported doping level of *meta* and *para* PBI polymers when doped into 85% PA.[12,46] It has been reported earlier also that membranes of meta and para PBI obtained from solvent casting method do not display much difference in

acid loading. However, the *meta* and *para* PBI membranes obtained from PPA process exhibits significant difference in PA loading. We also made *meta-para* random PBI copolymer in which *meta/para* composition is 50/50 and measured PA loading of this sample, which is ~ 10 moles/PBI repeat unit. Hence, it is clear that block structure of PBI not influence the PA loading character of the membrane which is justifiable since PA molecule will interact with all the imidazole groups in a same manner irrespective of their nano phase separation or segregation.

Table 6.5. Phosphoric acid (PA) doping level data for all three types of diblock PBI copolymers.

Am_{fix}-b-Ac_{vary}	PA(mols/PBI repeat unit)	Am_{vary}-b-Ac_{fix}	PA(mols/PBI repeat unit)	Am_{equal}-b-c_{equal}	PA(mols/PBI repeat unit)
$Am_{0.59}$–b–$Ac_{0.11}$	7.77	$Am_{0.12}$–b–$Ac_{0.54}$	8.19	$Am_{0.12}$–b–$Ac_{0.11}$	8.42
$Am_{0.59}$–b–$Ac_{0.23}$	8.66	$Am_{0.22}$–b–$Ac_{0.54}$	9.05	$Am_{0.22}$–b–$Ac_{0.23}$	8.81
$Am_{0.59}$–b–$Ac_{0.35}$	8.97	$Am_{0.32}$–b–$Ac_{0.54}$	10.43	$Am_{0.32}$–b–$Ac_{0.35}$	10.81
$Am_{0.59}$–b–$Ac_{0.43}$	9.88	$Am_{0.47}$–b–$Ac_{0.54}$	9.55	$Am_{0.47}$–b–$Ac_{0.43}$	10.72
-	-	-	-	$Am_{0.59}$–b–$Ac_{0.54}$	11.64

Although it might be argued that with increasing block length more PA loading should have taken place which indeed true to some extent in all the cases. However, it must be noted that especially in case of Am_{fix}-b-Ac_{vary} and Am_{vary}-b-Ac_{fix} the MW (IV) of copolymers decrease with increasing block length (Table 6.3) which in turn can decrease the PA loading, but observed PA loading for these two copolymers do not decrease indicating that blocks structure might have facilitated the absorption of PA owing to their phase separated morphology. However, in case of Am_{equal}-b-Ac_{equal} the increase in PA loading is more prominent than other two block structure since MW in this case does not decrease with increasing block length like other two cases.

6.4.6. Proton Conductivity:

The proton conductivity as a function of temperature of all the diblock copolymer membranes are obtained from Nyquist plots from the second heating measurement as discussed in the experimental section. All experiments have been carried out in fully non humid condition. The representative Nyquist plots obtained from the impedance measurements are shown in Figure 6.10. The proton conductivity of acid doped membranes is the key property of high temperature polymer electrolyte membrane since PEM fuel cell efficiency directly related to the proton conductivity. The proton conductivity measurements were carried out from room temperature to 160 °C. Figure 6.11 represents, the proton conductivity vs temperature plots for all three types of block copolymers. As mentioned in the previous section, all these membranes were doped with 85% PA (H_3PO_4) for seven days and their PA loading are not dramatically different as seen from Table 6.5.
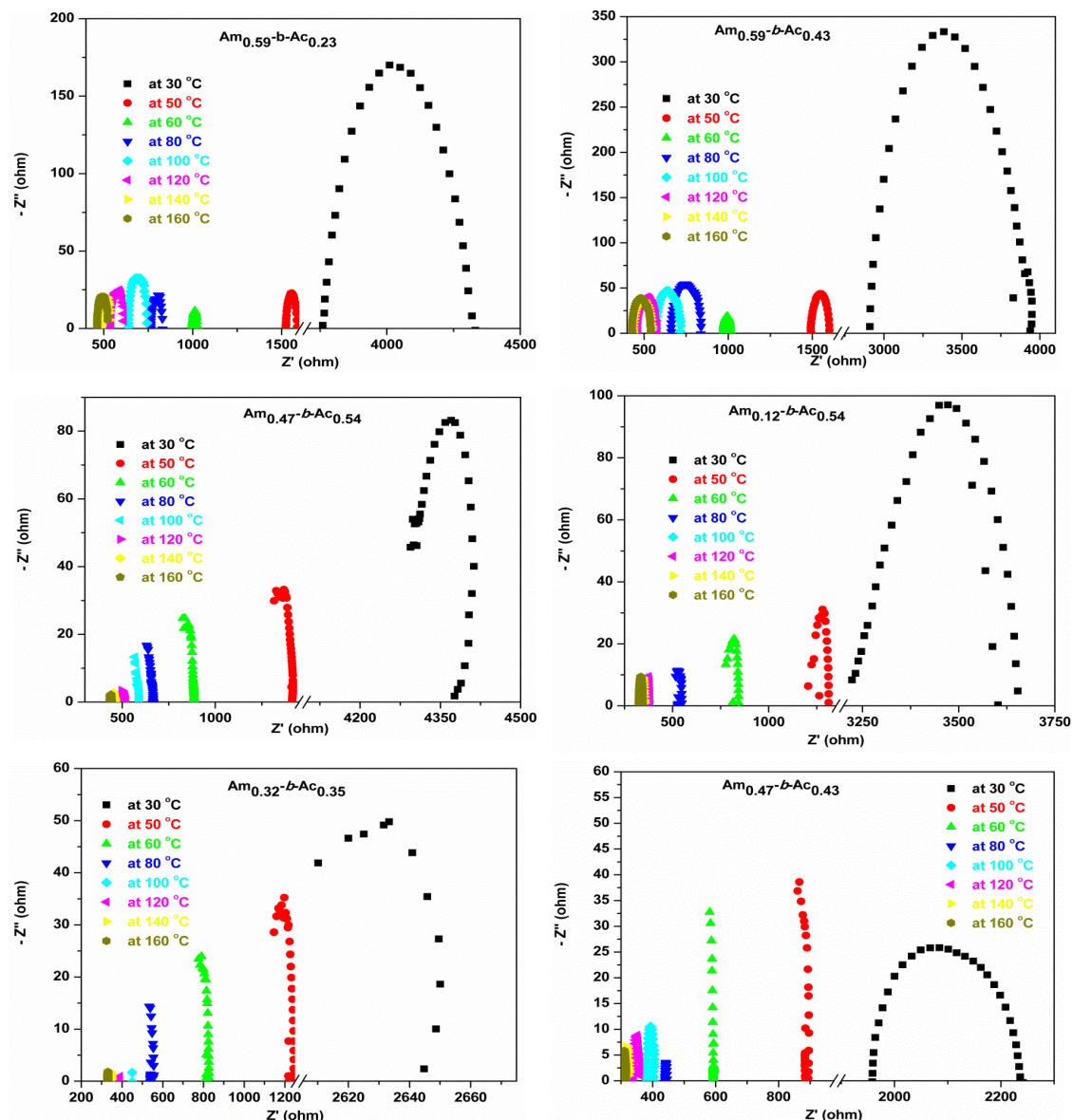
Figure 6.10. *Few representative Nyquist plots of three sets of PBI block copolymers at different temperatures during the second heating scans.*

In all three cases of block copolymers proton conductivities increases with increasing temperature which are in good agreement with the behaviour of PA doped PBI membrane as reported in the literature. From the Figure 6.11, it is clearly evident that in all the three cases proton conductivities in the entire temperature range increase with increasing block length. Also, it must be noted that the increase in conductivity with block length is most prominent in case of Am_{equal}-b-Ac_{equal} copolymers (Figure 6.11C). Generally, proton conductivity of PBI based membrane increases with increasing PA loadings. In the current diblock copolymers, PA loadings are almost similar, then question can be asked why proton

conductivity varying from copolymer to copolymer. The other interesting observation that, in case of random *meta/para* copolymer where *meta/para* composition is 50/50, and also the acid loading is ~ 10 mols/PBI repeat unit, the conductivity is much lower than the other 50/50 block copolymer as shown in Figure 6.11D. At 160 °C random *meta/para* copolymer coductivity is 0.04 S/cm whereas diblock meta/para coplymer conductivity is much higher. Even the smallest block length sample conductivity is 0.05 S/cm which is higher than the random copolymer.
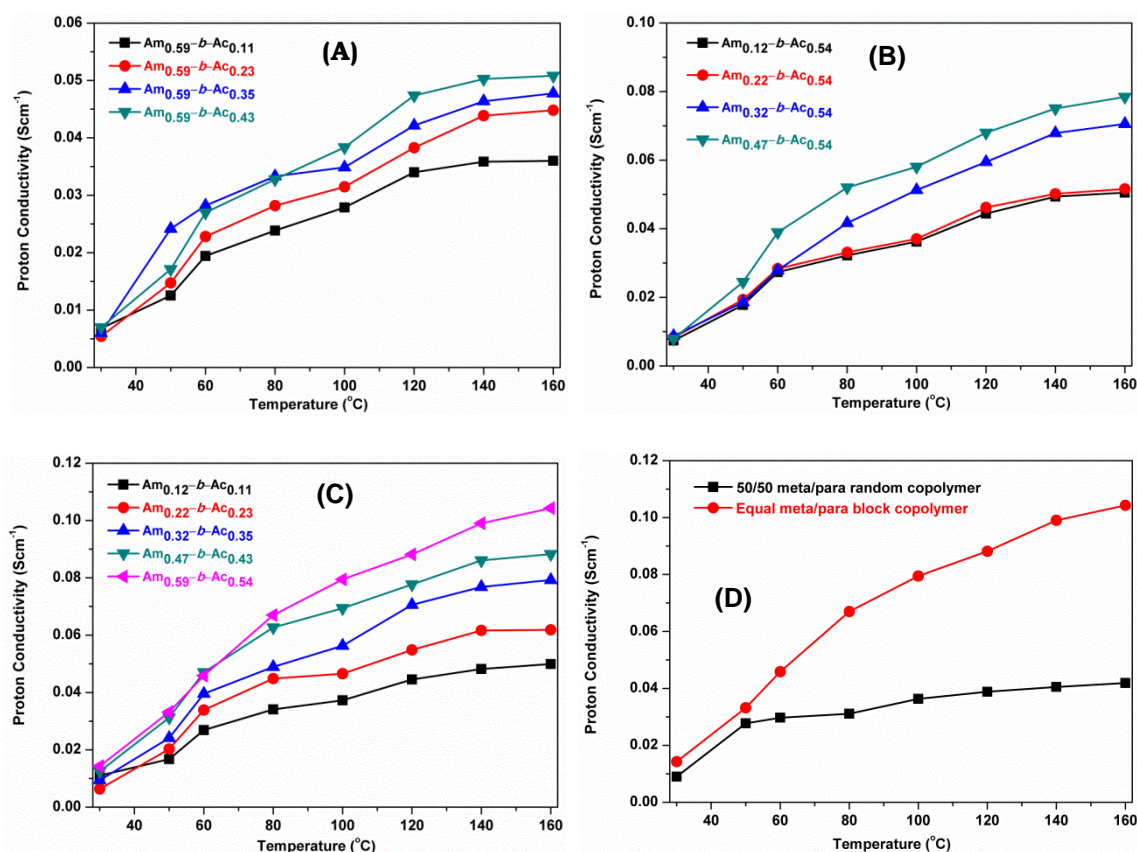
Figure 6.11. *Proton conductivity plots of acid doped diblock PBI membranes against temperature without any external humidification supply; (A) Fixed diamine terminated with varied acid terminated (Am$_{fix}$-b-Ac$_{vary}$), (B) fixed acid terminated with varied diamine terminated (Am$_{vary}$-b-Ac$_{fix}$), (C) equal diamine and acid terminated (Am$_{equal}$-b-Ac$_{equal}$) block copolymer and (D) comparison of diblock and random copolymers. These membranes were obtained by doping the copolymer membranes in 85% (14.6M) H$_3$PO$_4$ for 7 days.*

The higher proton conductivity of diblock copolymer than random copolymer despite the similar PA loading, increase of proton conductivity with increasing block length although PA loading are same can be attributed to the formation of phase separated morphology with increasing block length[43-45] as observed from the DMA study (earlier section). It is known that *para* structured PBI display higher proton conductivity than *meta* structured PBI owing to its symmetrical nature. In case of random *meta/para* (50/50) copolymer

this symmetrical influence of *para* is completely disturbed by *meta* and hence conductivity of 50/50 *meta/para* random copolymer decreases. However, in case of blocky structure, since phase separated morphology of *meta* and *para* structures are resulted and hence the interference by the *meta* to *para* is reduced which resulted in increased conductivity within *para* PBI units. This connnectivity between the *para* increases with increasing block length which in turn lowered the morphological barrier between the *para* segments resulting higher conductivity despite the similar PA loading. On the other hand in case of random copolymer because of phase mixing the high morphological barrier sets in which in turn reduces the proton conductivity.

It must be noted that there are significant difference in the increase in proton conductivity from one type block structure to another, this may be due to the structural effect which influences the nanophase separation of these block copolymers.

6.5. CONCLUSION:

A series of polybenzimidazole (PBI) diblock copolymers namely *meta*-polybenzimidazole-*block*-*para*-polybenzimidazole (*m*-PBI-*b*-*p*-PBI) of three different structural varieties are synthesized with an aim to develop new type of PBI based polymer electrolyte membrane (PEM). The diblock copolymers of PBI are synthesized by condensing diamine terminated *meta* oriented polybenzimidazole (*m*-PBI-Am) and acid terminated *para* oriented polybenzimidazole (*p*-PBI-Ac) oligomers. The block length and the structural motifs of the diblock copolymers are diversified by choosing and optimizing the appropriate pairs of oligomers with targeted molecular weight. Extensive NMR studies confirmed the formation of diblock copolymers of varieties of structures which also supported by DMA studies. Thermally and mechanically stable membrane prepared by solvent casting from MSA solution displayed two T_g's in DMA studies confirming the formation of diblock copolymer structure. The existence of nanophase separation between two blocks is confirmed from the DMA studies. Increase in block length decreases the phase mixing between two blocks, which in turn facilitated the nanophase segregation of two blocks - this is confirmed from the observation of DMA studies that T_g peaks for higher block length copolymers increasingly become more distinct. Phosphoric acid loading of the diblock copolymers does not follow any trends as a function of block length or the copolymer structural motifs. On the other hand, proton conductivities for all the copolymers increase with increasing block length because of the increased phase separation which improved the connectivity within the same block and hence increase the conductivity. The block structural motif also influences the proton conductivity. A comparison of diblock copolymers with random *meta/para* copolymers clearly indicates that the former exhibit much higher proton conductivity in the similar H_3PO_4 loading, attributing that new block copolymers are much better alternative as PBI based PEM.

REFERENCES:

(1) Li, Q.; Jensen, J. O.; Savinell, R. F.; Bjerrum, N. J. *Prog. Polym. Sci.* **2009**, *34*, 449.

(2) Costamagna, P.; Srinivasan, S. *J. Power Sources* **2001**, *102*, 253.

(3) Wang, J. T. W.; Hsu, S. L. C. *Electrochim. Acta* **2011**, *56*, 2842.

(4) Kreuer, K.; Paddison, S.; Spohr, E.; Schuster, M. *Chem. Rev.* **2004**, *104*, 4637.

(5) Bouchet. R.; Siebert, E. *Solid State Ion.* **1999**, *118*, 287.

(6) Glipa, X.; Bonnet, B.; Mula, B.; Jones, D. J.; Roziere, J. *J. Mater. Chem.* **1999**, *9*, 3045.

(7) Kawahara, M.; Morita, J.; Rikukawa, M.; Sanui, K.; Ogata, N. *Electrochim. Acta* **2000**, *45*, 1395.

(8) Ma, Y. L.; Wainright, J. S.; Litt, M. H.; Savinell, R. F. *J. Electrochem. Soc.* **2004**,*151*, A8.

(9) Asensio, J. A.; Sanchez, E. M.; Gomez-Romero, P. *Chem. Soc. Rev.* **2010**, *39*, 3210.

(10) Mader, J.; Xiao, L.; Schmidt, T. J.; Benicewicz, B. C. *Adv. Polym. Sci.* **2008**, *216*, 63.

(11) Linkous, C. A.; Anderson, H. R.; Kopitzke, R. W.; Nelson, G. L. *Int. J. Hydrogen Energy* **1998**, *23*, 525.

(12) Xing, B. Z.; Savadogo, O. *J. New. Mater. Electrochem. Syst.* **1999**, *2*, 95.

(13) Maity, S.; Jana, T. *Macromolecules* **2013**, *46*, 6814.

(14) Samms, S. R.; Wasmus, S.; Savinell, R. F. *J. Electrochem. Soc.* **1996** *143*, 1225.

(15) Kerres, J.; Ullrich, A.; Meier, F.; Haring, T. *Solid State Ion.* **1999**, *125*, 243.

(16) Cassidy, P. E. *Marcel Dekker, Inc.,* New York, Sect. 6.10, **1980**.

(17) Wang, S.; Zhao, C.; Ma, W.; Zhang, N.; Zhang, Y.; Zhang, G.; Liu, Z.; Na, H. *J. Mater. Chem. A* **2013**, *1*, 621.

(18) Serad, G. A. *J. Polym. Sci.; A: Polym. Chem.* **1996**, *34*, 1123.

(19) Banihashemi, A.; Atabaki, F. *Eur. Polym. J.* **2002**, *38*, 2119.

(20) Chung, T. S. *J. Macromol. Sci. Rev. Macromol. Chem. Phys.* **1997**, *C37*, 277.

(21) Mustarelli, P.; Quartarone, E.; Grandi, S.; Carollo, A.; Magistris, A. *Adv. Mater.* **2008**, *20*, 1339.

(22) Berber, M. R.; Fujigaya, T.; Sasaki, K.; Nakashima, *N. Scientific Reports* **2013**, *3*, 1764.

(23) Maity, S.; Jana, T. *Eur. Polym. J.* **2013**, *49*, 2280.

(24) Sannigrahi, A.; Ghosh, S.; Maity, S.; Jana, T. *Polymer* **2010**, *51*, 5929.

(25) Li, X. Z.; Liu, J.H.; Yang, S. Y.; Huang, S. H.; Lu, J. D.; Pu, J. L. *J. Polym. Sci.; Part A: Polym. Chem.* **2006**, *44*, 5729.

(26) Chen, C. C.; Wang, L. F.; Wang, J. J.; Hsu, T. C.; Chen, C. F. *J. Mater. Sci.* **2002**, *37*, 4109.

(27) Pu, H.; Wang, L.; Pan, H.; Wan, D. *J. Polym. Sci.; Part A: Polym. Chem.* **2010**, *48*, 2115.

(28) Qing, S.; Huang, W.; Yan, D. *Eur. Polym. J.* **2005**, *41*, 1589.

(29) Bae, J. M.; Honma, I.; Murata, M.; Yamamoto, T.; Rikukawa, M.; Ogata, N. *Solid State Ion.* **2002**, *147*, 189.

(30) Klahen, J. R.; Luther, T. A.; Orme, C. J.; Jones, M. G.; Wertsching, A. K.; Peterson, E. S. *Macromolecules* **2007**, *40*, 7487.

(31) (a) Ghosh, S.; Sannigrahi, A.; Maity, S.; Jana, T. *J. Phys. Chem. C* **2011**, *115*, 11474. (b) Chung, S. W.; Hsu, S. L. C.; Hsu, C. L. *J. Power Sources* **2007**, *168*, 172.

(32) (a) Ghosh, S.; Maity, S.; Jana, T. *J. Mater. Chem*. **2011**, *21*, 14897. (b) Pu, H.; Liu, L.; Chang, Z.; Yuan, *J. Electrochim. Acta* **2009**, *54*, 7536.

(33) (a) Fijigaya, T.; Okamaoto, M.; Nakashima, N. *Carbon* **2009**, *47*, 3227. (b) Shao, H.; Shi, Z.; Fans, J.; Yin, J. *Polymer* **2009**, *50*, 5987. (c) Kannan, R.; Kagaiwale, H. N.; Chaudhari, H. D.; Kharul, U. K.; Kurungot, S.; Pillai, V. K. *J. Mater. Chem*. **2011**, *21*, 7223.

(34) (a) Wang, Y.; Shi, Z.; Fang, J.; Yin, J. *Carbon* **2011**, *49*, 1199. (b) Wang, Y.; Shi, Z.; Famg, J.; Hu, H.; Ma, X.; Yin, J. *J. Mater. Chem*. **2011**, *21*, 505.

(35) Jouanneau, J.; Mercier, R.; Gonon, L.; Gebel, G. *Macromolecules* **2007**, *40*, 983.

(36) Yang, J.; He, R.; Che, Q.; Gao, X.; Shi, L. *Polym. Int.* **2010**, *59*, 1695.

(37) Yu, S.; Benicewicz, B. C. *Macromolecules* **2009**, *42*, 8640.

(38) Seel, D. C.; Benicewicz, B. C. *J. Membr. Sci.* **2012** *405*, 57.

(39) Bai, H.; Ho, W. S. W. *J. Taiwan Inst. Chem. Eng.* **2009**, *40*, 260.

(40) Sannigrahi, A.; Arunbabu, D.; Sankar, R. M.; Jana, T. *J. Phys. Chem. B* **2007**, *111*, 12124.

(41) Xiao. L.; Zhang, H.; Jana, T.; Scanlon, E.; Chen, R.; Choe, E. W.; Ramanathan, L. S.; Yu, S.; Benicewz, B. C. *Fuel Cells* **2005**, *5*, 287.

(42) Kovar, R, F.; Arnold, F. E. *J. Polym. Sci. Polym. Chem.* **1976**, *14*, 2807.

(43) Ng, F.; Bae, B.; Miyatake, K.; Watanabe, M. *Chem. Commun.* **2011**, *47*, 8895.

(44) Lee, H. S.; Roy, A.; Lane, O.; McGrath, J. E. *Polymer* **2008**, *49*, 5387.

(45) Mader, J. A.; Benicewicz, B. C. *Fuel Cells* **2011**, *11*, 222.

(46) Asensio, J. A.; Borros, S.; Gomez-Romero, P. *J. Electrochem. Soc.* **2004**, *151*, A304.

CHAPTER 7

Summary & Conclusions

7.1. SUMMARY:

Thesis entitled ***"Synthesis and Studies of Novel Polybenzimidazoles with Improved Properties for Proton Exchange Membrane"*** describes the synthesis and characterization of several structurally different polybenzimidazole from conventional 3,3',4,4'-tetraaminobiphenyl (TAB) and unconventional 2,6-bis(3',4'-diaminophenyl)-4-phenylpyridine (Py-TAB) tetraamines monomers. We have carried out the structural variation of PBI by (a) post polymerization to synthesize N-alkyl substituted PBIs, (b) by tetraamine and diacid monomer structure variation to synthesize a series of pyridine based PBI (Py-PBIs), (c) a series of *meta* and *para* random Py-PBI copolymers and (d) the *meta-para* PBI block copolymers by using ammine and acid terminated PBI oligomers. The synthesized PBIs are fully characterized and proton exchange membranes are fabricated from these polymers which are finally examined for their potential as PEM. The thesis consists of seven chapters. The summary of the contents of each chapter is given below.

CHAPTER 1:

This Chapter 1 described a brief introduction of various types of polybenzimidazoles (PBIs) types of polymers, history of PBI, describes their different synthetic procedure of preparation, different types PBI, brief discussion on physical and chemical properties. This chapter also discussed common and advanced application for membrane formation and phosphoric acid (PA) doped polybenzimidazole in high temperature polymer electrolyte membrane fuel cell (HT-PEMFC). A brief introduction about fuel cell, types of fuel cells and challenges involved in PEM fuel cell research were also included. Finally the aims of the current work were presented.

CHAPTER 2:

Chapter 2 described the details of materials which were used for all the working chapters and the details of experimental procedures, instrumentation techniques for characterization and properties evaluation of the synthesized different types of PBIs.

CHAPTER 3:

Despite the presence of bulk literature on polybenzimidazole (PBI), unavailability of readily soluble and processable PBI remains as the tallest challenge for the end-use. N-alkyl PBIs (N-PBIs) were synthesized by grafting the alkyl chain in the imidazole backbone to resolve this key constrain. The chain length of substituted alkyl groups was varied to evaluate the influence of chain size on the structures and properties of N-PBIs. Significant enhancement of solubility of N-PBIs compared to parent PBI in formic acid offered the opportunity to fabricate the homogeneous mechanically tough membranes with minimal

efforts. The substituted long alkyl chains pushes apart the PBI chains and hence increases the face-to-face packing distance by breaking the self-association between the chains; resulted into less rigid highly soluble N-PBIs. Alkyl chain length dependent weight loss at ~300 °C, presence of two glass transition temperatures and peculiar deep rubbery modulus in storage modulus vs. temperature plots resembled the copolymer molecular structure of N-PBIs. Hydrophobic character of alkyl chains and loosely packed structure of N-PBIs facilitated decrease in water uptake and swelling of the N-PBI membranes compared to parent PBI membrane. The temperature dependent proton conductivity of PA loaded N-PBIs membranes were found to be satisfactory.

CHAPTER 4:

Tetraamine 2,6-bis(3′,4′-diaminophenyl)-4-phenylpyridine (Py-TAB) was found to be an efficient, readily accessible, inexpensive monomer for synthesizing pyridine bridge polybenzimidazoles (Py-PBIs). The Py-TAB monomer replaced the frequently and conventionally used 3,3′,4,4′-tetraaminobiphenyl (TAB) monomer for synthesizing polybenzimidazoles (PBIs) structure. Py-TAB monomer showed wider scope for synthesis of PBIs with various dicarboxylic acids. Py-PBIs displayed superior solubility in low boiling solvent and hence eliminated the processability issues of PBIs which often restricted the large scale use. Comparable and in some instances superior thermal, mechanical and oxidative stability of Py-PBI proved that the Py-TAB is the most attractive alternative tetraamine monomer to TAB for synthesis of PBIs. The membranes obtained from Py-PBIs displayed significantly lower water uptake and swelling than the conventional PBIs due to the presence of bulky Py-TAB monomer. The presence of pyridine moiety in Py-PBIs helped to load larger amount of phosphoric acid (PA) compare to conventional PBIs. The proton conductivity of PA doped Py-PBI membranes were higher than the conventional PBI membranes owing to the higher PA loading and the complex bulky structure. Photophysical studies demonstrated the complexity of Py-PBIs structure. In summary, 3-fold objectives, namely, (I) alternative tetraamine monomer, (II) soluble PBI, and (III) higher proton conducting PBI based PEM, were achieved in this study.

CHAPTER 5:

In our effort to promote 2,6-bis(3,4-diaminophenyl)-4-phenylpyridine (Py-TAB) as an alternative tetraamine monomer to conventionally used 3,3',4,4'-tetraaminobiphenyl (TAB) for synthesizing readily processable pyridine bridged polybenzimidazoles (Py-PBIs), two series of random copolymers (PBI-*co*-Py-PBI) were synthesized by polymerizing Py-TAB and TAB with isophthalic acid (IPA), and terephthalic acid (TPA) to produce *meta* (*m*PBI-*co*-*m*Py-PBI) and *para* (*p*PBI-*co*-*p*Py-PBI) connected copolymers, respectively. For the first time in the PBIs literature, copolymers were synthesized by varying the relative compositions of tetraamines (TAB and Py-TAB) in the polymerization feed with a single dicarboxylic acid

(DCA) instead of traditionally used method where two DCAs with variable compositions are polymerized with single tetraamine. The solubility and hence the processability of the copolymers were improved significantly upon introduction of Py-PBI in the copolymer chain. The detailed characterizations of both *meta* and *para* series copolymers compellingly established that thermal, chemical and mechanical stabilities can be easily modulated as per the need by altering the relative compositions of PBI and Py-PBI. The phosphoric acid (PA) loading of copolymers were increased gradually with increasing Py-PBI content in the copolymer chain since bulky pyridine moiety facilitated the absorption of PA. The presence of pyridine functionality and larger PA loading caused the higher proton conductivity of PA doped copolymer membranes and the conductivity at 160 °C steadily increased with increasing Py-PBI. In summary, two age-old notions in the PBI chemistry, namely, (1) copolymers can be prepared only by altering DCAs compositions and (2) PBIs properties can be tuned only by DCAs structure, were replaced in this study by synthesizing copolymers from TAB and Py-TAB with different DCAs.

CHAPTER 6:

A series of *meta*-polybenzimidazole-*block-para*-polybenzimidazole (*m*-PBI-*b-p*-PBI), diblock copolymers of PBI, were synthesized with various structural motifs and block lengths by condensing the diamine terminated *meta* PBI and acid terminated *para* PBI oligomers. NMR studies and existence of two T_g's, obtained from DMA results, unequivocally confirmed the formation of diblock copolymer structure through the current polymerization methodology. Appropriates and careful selection of oligomers chain length enabled us to tailor the block length of diblock copolymers and also to make varieties of structural motifs. Increasingly distinct T_g peaks obtained from DMA studies with higher block length of diblock structure attributed the decrease in phase mixing between the *meta* and *para* PBI blocks which in turn resulted into naophase segregated domains. The diblock structure and the block length did not display any significant trend on the phosphoric acid loading of membrane obtained from these diblock copolymers. The proton conductivities of H_3PO_4 doped diblock copolymer membranes were found to be increasing substantially with increasing block length because of the nanophase separation and thereby less morphological barrier within the block and hence better conductivity in the same block. The structural varieties also influenced the phase separation and proton conductivity. In comparison to *meta-para* random copolymers, the current *meta-para* diblock copolymers were found to be more suitable for PBI based PEM.

7.2. CONCLUTIONS:

From the above discussion in the Chapter 3 to 6 on the topic *"Synthesis and Studies of Novel Polybenzimidazoles with Improved Properties for Proton Exchange Membrane,"* the following conclusions are drawn

1.   A series of N-alkyl substituted polybenzimidazole has been synthesized and their properties are studied.

2.   The storage modulus and water uptake and swelling volume of the N-PBIs gradually decreases with increasing of alkyl chain length.

3.   We have synthesized 2,6-bis(3,4-diaminophenyl)-4-phenylpyridine (Py-TAB) as an alternative tetraamine monomer to conventionally used 3,3',4,4'-tetraaminobiphenyl (TAB) for synthesizing readily processable pyridine bridged polybenzimidazoles (Py-PBIs) which is cost effective, readily available and easy to synthesis.

4.   We have synthesized a series of pyridine based polybenzimidazole (Py-PBIs) which shows the grater thermal and chemical stability and more soluble in low boiling solvent formic acid (FA) and proton conductivity than the conventional polybenzimidazole.

5.   All the Py-PBIs can be an alternative to the PBI for the use in fuel cell.

6.   Py-TAB and TAB are used to synthesize readily processable *meta* and *para* series pyridine bridged polybenzimidazoles random copolymers (PBI-*co*-Py-PBI)

7.   Both *meta* and *para* series random copolymer are mechanically and chemically stable than normal PBI.

8.   The phosphoric acid (PA) loading increases with increasing in both *meta* and *para* series random copolymers (PBI-*co*-Py-PBI) with increasing the Py-TAB contents.

8.   Both *meta* and *para* series polybenzimidazoles random copolymers (PBI-*co*-Py-PBI) are more proton conducting than the normal PBI which can be used in high temperature polymer electrolyte membrane fuel cell (HT-PEMFC).

9.   Acid and diamine terminated PBI oligomers can be easily synthesize by changing the mole ratio of tetramines and diacids monomer.

10.   We have synthesized three different type of *meta* and *para* connected diblock polybenzimidazole by using varying block length of oligomers.

11.   The proton conductivity of the block copolymer displayed dependency on block length due to the nanophase segregation of individual blocks.

7.3. SCOPE OF FUTURE WORK:

The present thesis has addressed three important aspects of polybenzimidazoles random copolymerization, block copolymerization and monomer structure variation. We believe the findings of this thesis will have great impact on the future development of polybenzimidazole (PBI) chemistry in general, especially the use of PBI in PEMFC application. The thesis put forward and establish novel concept in the PBI chemistry research. The potential and scope of future work of this thesis are enormous. Few of these are listed below

1. Structure variation of PBI by post polymerization technique can be developed.

2. Pyridine based different structured PBIs have enough potentially enough to be used in PEMFC.

3. Efforts can be made to make new PBI structure using Py-TAB.

4. The Py-PBIs show higher proton conductivity compare to the conventional m-PBI, efforts should be made to study more details.

5. Synthesis of block copolymers from Py-PBI can be tried.

6. More systematic efforts must be made to understand the usefulness of newly synthesized Py-PBIs.

7. Varieties of block copolymer can be made using the methods established in this thesis.

8. Finally, all these newly developed PBIs can be tested as PEM in working fuel cell so that the potential of these polymers are explored.

Publications
&
Presentations
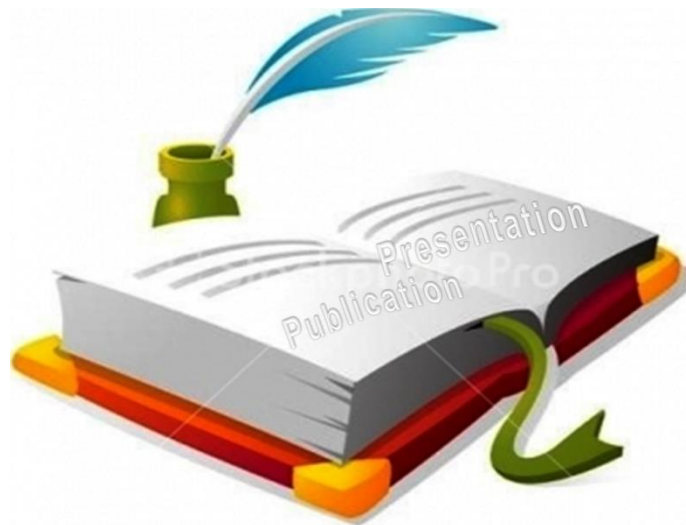
PUBLICATIONS

(1) *Role of Solvents Protic Character on the Aggregation Behavior of Polybenzimidazole in Solution.* Sandip Ghosh, Arindam Sannigrahi, <u>Sudhanshu Maity</u> and Tushar Jana. *J. Phys. Chem. B* **2010**, 114, 3122.

(2) *Monomer Structural Isomer Directed Polybenzimidazole Copolymerization and Their Properties.* Arindam Sannigrahi, Sandip Ghosh, <u>Sudhangshu Maity</u> and Tushar Jana. *Polymer* **2010**, 51, 5929.

(3) *Role of Clays Structures on the Polybenzimidazole Nanocomposites: Potential Membranes for the Use in Polymer Electrolyte Membrane Fuel Cell.* Sandip Ghosh, Arindam Sannigrahi, <u>Sudhanshu Maity</u> and Tushar Jana. *J. Phys. Chem. C* **2011**, 115, 11474.

(4) *Polybenzimidazole/Silica Nanocomposites: Organic-Inorganic Hybrid Membranes for Polymer Electrolyte Membrane Fuel Cell.* Sandip Ghosh, <u>Sudhanshu Maity</u> and Tushar Jana. *J. Mater. Chem.* **2011**, 21, 14897.

(5) *Polybenzimidazole Gel Membrane for the Use in Fuel Cell.* Arindam Sannigrahi, Sandip Ghosh, <u>Sudhangshu Maity</u> and Tushar Jana. *Polymer* **2011**, 52, 4319.

(6) *N-Alkyl Polybenzimidazole: Effect of Alkyl Chain Length.* <u>Sudhangshu Maity</u>, Arindam Sannigrahi Sandip Ghosh and Tushar Jana. *Euro. Polym. J.* **2013**, 49, 2280.

(7) *Soluble Polybenzimidazoles for PEM: Synthesized from Efficient, Inexpensive, Readily Accessible Alternative Tetraamine Monomer.* <u>Sudhangshu Maity</u> and Tushar Jana. *Macromolecules* **2013**, 46, 6814.

(8) *Polycondensation of Structurally Dissimilar Tetraamine Monomers with Dicarboxylic Acids to Synthesize Polybenzimidazole Copolymers for PEM.* <u>Sudhangshu Maity</u> and Tushar Jana *(Communicated to Polymer)*.

(9) *Polybenzimidazole Diblock Copolymers for PEM Fuel Cell: Synthesis and Studies of Block Length Effect on Nanophase Separation, Mechanical Properties and Proton Conductivity of PEM.* <u>Sudhangshu Maity</u> and Tushar Jana *(Comunnicated to Macromolecules)*.

(10) *Protic Ionic Liquid Based Potentially Enfolded Organic/Inorganic Hybrid Silica Nanomaterials Composite with Ether Linked Polybenzimidazole for the Application in HT-PEMFC.* <u>Sudhangshu Maity</u>, Shuvra Singha and Tushar Jana *(Manuscript under preparation)*.

(11) *Solvent Induced Porous Polybenzimidazole Membrane: A Facile Route to Enhance Proton Conductivity* Sandip Ghosh, Arindam Sannigrahi, <u>Sudhangshu Maity</u> and Tushar Jana. *(Manuscript under preparation)*.

(12) *Investigation of Polyelectrolyte Nature of Polybenzimidazole in Various Acidic Solvents Using the Isoionic Dilution Mthod.* Sandip Ghosh, Arindam Sannigrahi, <u>Sudhangshu Maity</u> and Tushar Jana *(Manuscript under preparation)*.

(13) *Aggregation of meta-Polybenzimidazole in Phosphoric Acid.* Arindam Sannigrahi, Sandip Ghosh, <u>Sudhangshu Maity</u> and Tushar Jana *(Manuscript under preparation)*.

Note: Only publication numbers 6, 7, 8 and 9 are included in this thesis as Chapter 3, 4, 5 and 6, respectively.

CONFERENCE & PRESENTATIONS

(1) Poster Presented on *"Synthesis, Characterization and Photophysical Study of N- alkyl Substituted Polybenzimidazole,"* **6th Annual in-house Symposium: CHEMFEST 2009**; March 7-8, 2009, School of Chemistry, University of Hyderabad, Hyderabad, India.

(2) Poster Presented on *"Synthesis and Characterization of N-substituted Polybenzimidazole,"* **7th Annual in-house Symposium: CHEMFEST 2010**; January 8-9, 2010, School of Chemistry, University of Hyderabad, Hyderabad, India.

(3) Poster Presented on *"Synthesis, Characterization and Photophysical Study of N-substituted Polybenzimidazole,"* **Frontiers of Polymers & Advanced Materials: MACRO 2010**; December 15-17, 2010, Indian Institute of Technology, New Delhi, India.

(4) Poster Presented on *"Synthesis, Characterization and Photophysical Study of N-substituted Polybenzimidazole,"* **Colloquium on Perspectives in Polymer Science & Technology**; November 27, 2010, Indian Association for the Cultivation of Science, Jadavpur, Kolkata, India.

(5) Poster Presented on *"Synthesis and Characterization of N-substituted Polybenzimidazole,"* **8th Annual in-house Symposium: CHEMFEST 2011**; School of Chemistry, University of Hyderabad, Hyderabad, India.

(6) Poster Presented on *"Pyridine Bridged Polybenzimidazole for HT-PEMFC Application,"* **9th Annual in-house Symposium: CHEMFEST 2012**; February 24-25, 2012, School of Chemistry, University of Hyderabad, Hyderabad, India.

(7) Oral Presented on *"Soluble and Processable Polybenzimidazoles: Synthesis and Properties Evaluation,"* **10th Annual in-house Symposium: CHEMFEST 2013;** February 15-16, 2013, School of Chemistry, University of Hyderabad, Hyderabad, India.

(8) Poster Presented on *"Synthesis of Pyridine Bridge Random Copolymers of Polybenzimidazoles for the Application in fuel Cell,"* **Polymers on the Frontiers of Science and Technology: APA 2013**; February 21-23, 2013, Punjab University, Chandigarh, India.

(9) Poster Presented on *"Proton Exchange Membrane for Fuel Cell Fabricated from Pyridine Bridge Polybenzimidazole Copolymers,"* **3rd FAPS Polymer Congress and MACRO-2013**; May 15-18, 2013, Indian Institute of Science, Bangalore, India.